UNIVERSITY OF LONDON THESIS

Degree PhD Year 2007 Name of Author MEADOWS, John Cecil

Regulation of mitotic progression by factors that influence spindle position and stability in fission yeast

John Cecil Meadows

A thesis submitted to the University of London in fulfilment of the requirements for the degree: Doctor of Philosophy

May 2007

Division of Stem Cell Biology and Developmental Genetics,
National Institute for Medical Research.
The Ridgeway,
Mill Hill,
London,
NW7 1AA

ProQuest LLC
789 East Eisenhower Parkway
P.O. Box 1346
Ann Arbor, MI 48106-1346

I, John Cecil Meadows, confirm that the work presented in this thesis is my own and was completed within the National Institute for Medical Research between September 2003 and May 2007. Where information has been derived from other sources, I confirm that this has been indicated in the thesis.

John Cecil Meadows
May 2007

Acknowledgements

I would like to thank Jonathan Millar for giving me the opportunity to carry out my PhD in his lab. and for his intellectual input, advice and humour. Within the lab. I particularly thank Vicky Buck not only for her critical reading of this manuscript, her problem solving and her unparalleled molecular biology skills but also for her friendship and lifts down the hill. I acknowledge Isabel Sanchez-Perez and Steven Renwick for showing me the ropes on the microscope and Alejandro Franco-Sanchez for his unerring and inspirational work ethic. In the division I acknowledge Tony Johnson whose knowledge of computers and equipment is only surpassed by his knowledge and love of music. Within the Institute I thank Alex Gould, Steve Sedgwick, Rita Cha and Marco Geymonat for their constructive criticisms and encouragement throughout this work. In particular Marco whose enthusiasm and attitude towards science is infectious. I also thank Kate Sullivan for maintaining the microscopes so diligently and for her helpful advice and trouble-shooting.

I thank the rest of the division for their camaraderie and enthusiasm. In particular James Cauwood, Margaret Migocki and Gaelle Marinoni who rarely turned down the opportunity for a drink and Nadeem Shaikh who provided much needed comic relief.

I thank Rhona Borts, Eva Hoffmann and Craig Griffin for showing me just how rewarding a career in science can be and for allowing me to take the first steps into such a career.

I acknowledge my parents and grandparents whose unconditional love and support has been particularly appreciated over the course of this work.

Lastly, I thank my wife, Abigail, who ventured that I might be correct when no-one else would (let alone myself), who has put up with all the late nights and weekends spent at work with good grace, and who understands all those things about life that I probably never will.

Abstract

It has previously been proposed that in fission yeast mitotic spindle position is monitored by a checkpoint that controls the timing of anaphase onset. This checkpoint is activated by treatment of cells with Latrunculin A (Lat A), an inhibitor of actin polymerisation. It was previously thought that Lat A imposes an anaphase delay by preventing interaction of astral microtubules with the cortical actin cytoskeleton and that this interaction was required for correct spindle orientation.

By contrast I show that cells lacking Mto1, a centrosomin-like protein, have mis-orientated spindles but are not delayed in the timing of sister chromatid separation.

Secondly, I show that astral microtubules are only nucleated after sister chromatids separate and that mitotic spindle orientation is instead determined by the position of the spindle pole body during interphase. Spindle pole position is controlled by interphase microtubules, which also position the nucleus in the centre of the cell. Since the position of the nucleus determines the site of septation, I propose that interphase microtubules ensure perpendicular alignment of the spindle and the axis of cell division.

Thirdly, in contrast to previous findings, I find that Lat A causes an anaphase delay and mitotic spindle collapse in a proportion of cells. These results suggest that Lat A delays the onset of anaphase by disrupting mitotic spindle stability rather than by causing spindle mis-orientation. Importantly, this effect is abolished in a Lat A-insensitive actin mutant, implicating a role for actin in mitotic spindle stability.

Lastly, I demonstrate that the effect of Lat A is exacerbated in cells lacking Ase1, which binds and stabilises the spindle midzone. I have uncovered two factors, Mal3, and a novel kinesin, Klp9, which are required for viability in the absence of Ase1. I present a preliminary characterisation of the role of Klp9 in the mitotic cell cycle.

Table of Contents

TITLE.....1
DECLARATION.....2
ACKNOWLEDGEMENTS.....3
ABSTRACT.....4
TABLE OF CONTENTS.....5
TABLE OF FIGURES.....11
TABLE OF TABLES.....14
TABLE OF MOVIES.....14
LIST OF ABBREVIATIONS.....15

* * *

Chapter 1

GENERAL INTRODUCTION

1.1 Fission yeast as a model organism to study the cell cycle.....17
1.1.1 G2-M transition.....20
1.1.2 Mitotic progression.....21
1.2 Organisation of the *S.pombe* cytoskeleton.....25
1.2.1 Microtubules.....25
1.2.1.1 Interphase microtubule organising centres (iMTOCs).....27
1.2.1.2 Nuclear face of spindle pole bodies.....28
1.2.1.3 Cytoplasmic face of spindle pole bodies.....32
1.2.1.4 Equatorial microtubule organising centres (eMTOCs).....33
1.2.1.5 Mto1: a universal cytoplasmic γ-TURC-MTOC tethering protein.....33
1.2.2 Actin.....36
1.3 Checkpoints controlling mitotic entry and progression.....39
1.3.1 Checkpoints acting over the G2-M transition.....39
1.3.1.1 Cell size checkpoint.....39
1.3.2 Checkpoints acting over mitotic progression.....40
1.3.2.1 The spindle assembly checkpoint (SAC).....38
1.3.2.2 The spindle orientation checkpoint (SOC).....44

1.3.2.2.1 SOC in budding yeast.....44
1.3.2.2.2 SOC in fission yeast.....45
1.4 Aims of my project.....**49**

Chapter 2

MATERIALS AND METHODS

2.1 Yeast Techniques.....**51**
2.1.1 Yeast strains.....51
2.1.2 Yeast media.....51
2.1.3 Yeast growth conditions.....55
2.1.4 Yeast storage conditions.....55
2.1.5 Cell cycle synchronisation.....55
2.1.6 Yeast transformation by lithium acetate.....55
2.1.7 Isolation of yeast genomic DNA.....56
2.1.8 Mating.....57
2.1.8.1 Random spore analysis.....57
2.1.8.2 *Tetrad dissection*.....57
2.2 Microscopy.....**57**
2.2.1 (4'6-diamino-2-phenylindole) DAPI and calcofluor staining.....57
2.2.2 Fixation of cells expressing green fluorescent protein (GFP) and cyan fluorescent protein (CFP).....58
2.2.3 Image acquisition.....58
2.2.3.1 Fixed cells.....58
2.2.3.2 *Live cells*.....58
2.3 Nucleic acid manipulation.....**59**
2.3.1 Polymerase chain reaction (PCR).....59
2.3.2 Agarose gel electrophoresis.....60
2.3.3 Recovery of DNA fragments from agarose gels.....60
2.3.4 Restriction endonuclease digestion and DNA modification.....60
2.3.5 DNA sequencing.....63
2.4 Bacterial techniques.....**63**
2.4.1 Bacterial strain.....63
2.4.2 Bacterial media.....63
2.4.3 Bacterial growth conditions.....63

2.4.4 Bacterial storage conditions....63
2.4.5 Bacterial transformation....64
2.4.5.1 Preparation of competent E.coli cells....64
2.4.5.2 Transformation of E.coli cells....64
2.4.6 Isolation of plasmid DNA....64
2.5 Strain construction....64
2.5.1 Deletion of genomic loci....64
2.5.2 C-terminal tagging of genomic loci....66
2.5.3 Latrunculin A-insensitive actin strain construction....67
2.6 Bioinformatics....68
2.6.1 BLAST searches....68
2.6.2 Sequence alignment....69

Chapter 3

RELATIONSHIP BETWEEN SPINDLE ANGLE AND THE TIMING OF ANAPHASE ONSET IN FISSION YEAST

3.1 Introduction....71
3.2 Results....74
3.2.1 Mis-orientation of the mitotic spindle does not delay the onset of anaphase....74
3.2.2 Astral microtubules do not effect the rate of spindle elongation....82
3.2.3 A proportion of cells lacking Mto1 have unclustered kinetochores....82
3.2.4 Asymmetry of SIN activation is independent of astral microtubule contact with the cell cortex....85
3.3 Discussion....89
3.3.1 Re-assessing the evidence for a spindle orientation checkpoint....89
3.3.2 Mitotic spindle dynamics in the absence of Mto1....90
3.3.3 Unclustering of kinetochores in cells lacking Mto1....91
3.3.4 Astral microtubules do not impose the asymmetry of SIN activation....92
3.4 Conclusions....93

Chapter 4

MECHANISM CONTROLLING MITOTIC SPINDLE ORIENTATION IN FISSION YEAST

4.1 Introduction.....94

4.2 Results.....95

4.2.1 Spindle orientation during prometaphase and metaphase.....95

4.2.2 Astral microtubules control spindle alignment during anaphase B.....98

4.2.3 Role of astral microtubules and the post-anaphase array in determining SPB position.....100

4.2.4 Interphase SPB position determines initial spindle angle in mitosis.....103

4.3 Discussion.....105

4.3.1 Mechanism controlling spindle orientation: previous hypotheses.....105

4.3.2 Mechanism controlling spindle orientation: a new model.....106

4.3.3 Cell shape and a more important role for astral microtubules?.....109

4.4 Conclusions.....110

Chapter 5

ACTIN IS REQUIRED FOR PRE-ANAPHASE MITOTIC SPINDLE STABILITY

5.1 Introduction.....111

5.2 Results.....111

5.2.1 Lat A delays anaphase onset and causes pre-anaphase spindle collapse.....111

5.2.2 In the presence of Lat A a proportion of cells lacking Mto1 undergo phase 2 delay and pre-anaphase spindle collapse.....116

5.2.3 Construction of a Lat A-insensitive mutant.....119

5.2.4 Lat A delays anaphase onset and causes mitotic spindle collapse by preventing actin polymerisation.....122

5.3 Discussion.....125

5.3.1 The target of Lat A: previous assumptions.....125

5.3.2 Why is the pre-anaphase collapse only seen in a proportion of cells?.....125

5.3.3 What is the real target of Lat A?.....126

5.4 Conclusions.....128

Chapter 6

ASE1 CONTROLS PRE-ANAPHASE SPINDLE STABILITY AND THE TIMING OF ANAPHASE ONSET

6.1 Introduction.....129

6.2 Results.....129

6.2.1 Ase1 localises to the spindle midzone prior to anaphase onset.....129

6.2.2 Cells lacking Ase1 are delayed in anaphase onset and undergo frequent pre-anaphase spindle collapses.....130

6.2.3 Abnormal kinetochore behaviour in the absence of Ase1.....133

6.2.4 Actin and Ase1 co-ordinately control spindle elongation.....133

6.3 Discussion.....137

6.3.1 Re-assessing the cell cycle role of Ase1.....137

6.3.2 Cell-to-cell variation.....137

6.4 Conclusions.....138

Chapter 7

THE KINESIN KLP9 IS A NOVEL REGULATOR OF MITOTIC SPINDLE STABILITY

7.1 Introduction.....139

7.2 Results.....139

7.2.1 Mal3 is essential for viability in the absence of Ase1.....139

7.2.2 Klp9 is essential for viability in the absence of Ase1.....140

7.2.3 Klp9 localises to the spindle midzone.....143

7.2.4 Effect of loss of Klp9 on mitotic progression.....143

7.2.5 Effect of Lat A in the absence of Klp9.....146

7.3 Discussion.....150

7.3.1 Role of Klp9 at the metaphase to anaphase transition.....150

7.3.2 Does fission yeast possess genetically separable attachment and tension checkpoints?.....151

7.3.3 Role of Klp9 during anaphase B.....151

7.3.4 Do Klp9 and actin lie on the same pathway controlling pre-anaphase spindle stability?.....152

7.4 **Conclusions.....152**

Chapter 8

GENERAL DISCUSSION

8.1 **Summary**.....153

8.2 **Why do spindles collapse in only a proportion of cells?**.....154

8.3 **Spindle checkpoint(s) affecting mitotic progression in fission yeast**.....156

8.4 **The spindle integrity checkpoint: a spatial model monitoring tension *via* chromatid congression**.....159

REFERENCES.....162

APPENDIX - MOVIE LEGENDS.....186

Table of Figures

1.1 The fission yeast cell cycle....19

1.2 *S.pombe* divides by medial fission following the segregation of the genetic material....23

1.3 Cell cycle dependent localisation of actin and tubulin....24

1.4 Cell cycle and Microtubule Organizing Centre (MTOC) overview....26

1.5 Mto1 is required for microtubule nucleation from the cytoplasmic, but not nuclear, face of the spindle pole body....34

1.6 Mto1 is required for microtubule nucleation from all cytoplasmic MTOCs....35

1.7 A 3-dimensional representation of the actin monomer....37

1.8 The spindle assembly checkpoint (SAC) in fission yeast....41

1.9 The spindle orientation checkpoint (SOC) in fission yeast....46

2.1 *act1*, *act1-R183A,D184A* and *act1-D157E* rescue *act1-188*^{ts} at restrictive temperature....70

3.1 Profile of mitotic spindle dynamics....72

3.2 Positioning of spindle pole bodies and kinetochores throughout the cell cycle....73

3.3 Phase 2 is variable whereas phases 1 and 3 are invariant....75

3.4 *lys1:nmt1-atb2-gfp* cells lacking Mto1 show no mitotic delay....77

3.5 *lys1:nmt1-atb2-gfp* cells lacking Mto1 show severe mis-orientation of the mitotic spindle....78

3.6 *mto1D ndc80-gfp cdc11-cfp* cells show severe mis-orientation, but no delay over anaphase onset....79

3.7 *ndc80-gfp cdc11-cfp* cells lacking Mto1 show no mitotic delay....80

3.8 *ndc80-gfp cdc11-cfp* cells lacking Mto1 show severe mis-orientation of the mitotic spindle....81

3.9 *mto1D* cells exhibit significant mis-orientation of the mitotic spindle but no difference in the timing of mitosis at 26°C....83

3.10 Spindle elongation rates remain unchanged in cells lacking Mto1....84

3.11 A small proportion of cells lacking Mto1 have unclustered kinetochores....85

3.12 *mto1D* cells with unclustered kinetochores have an extended phase 2....87

3.13 Asymmetry of SIN component loading is maintained in *mto1D* cells....88

4.1 There is no corrective orientation of the mitotic spindle during phase 2.....96

4.2 The average spindle angle of both *mto1D* and control cells remains constant prior to anaphase.....97

4.3 Microtubule contact with the ring occurs after sisters have separated.....99

4.4 SPB repositioning post-mitosis is deficient in cells lacking Mto1.....101

4.5 SPB repositioning post-mitosis is dependent on astrals and the PAA.....102

4.6 Cells lacking Mto1 have mis-positioned SPBs in interphase.....104

4.7 A model for orientation of the mitotic spindle being dependent on initial spindle pole body position and orientation.....107

5.1 Latrunculin A treatment causes a concentration dependent pre-anaphase delay.....112

5.2 Latrunculin A treatment results in a proportion of cells that undergo an extended phase 2 and a subsequent pre-anaphase spindle collapse.....113

5.3 Spindle mis-orientation is not significantly elevated by Latrunculin A treatment.....115

5.4 Latrunculin A treatment results in a proportion of *mto1D* cells with an extended phase 2 and a subsequent pre-anaphase spindle collapse.....117

5.5 Latrunculin A treatment does not increase spindle mis-orientation in cells lacking Mto1.....118

5.6 Actin sequence alignments between *S.pombe* (S.p.), *S.cerevisae* (S.c.), mouse (M.m.) and man (H.s.).....120

5.7 *act1-R183A,D184A* is resistant to Lat A.....121

5.8 *act1-R183A,D184A* cells do not undergo a pre-anaphase delay or collapse in the presence of Lat A.....123

5.9 Latrunculin A has no effect on the length of phase 2 or spindle stability in an *act1-R183A,D184A* mutant.....124

6.1 Ase1 localisation.....131

6.2 Cells lacking Ase1 are delayed in phase 2 and undergo frequent spindle collapse both before and after anaphase onset.....132

6.3 Kinetochore dynamics are perturbed in cells lacking Ase1.....134

6.4 Latrunculin treatment does not extend the length of phase 2 in cells lacking Ase1.....135

6.5 Latrunculin treatment decreases the percentage of bi-nucleate cells following mitosis in cells lacking Ase1.....136

7.1 Mal3 is required for viability in cells lacking Ase1.....141
7.2 Klp9 is required for viability in cells lacking Ase1.....142
7.3 Klp9 localisation.....144
7.4 Cells lacking Klp9 are delayed in phase 2 and undergo frequent pre-anaphase spindle collapse.....145
7.5 Spindle elongation rate in anaphase B is reduced in cells lacking Klp9.....147
7.6 Latrunculin treatment does not extend phase 2 in cells lacking Klp9.....148
7.7 Latrunculin treatment does not increase collapse frequency in cells lacking Klp9.....149

8.1 Actin acts as a spindle matrix protein in another organism.....155
8.2 The localisation of Fin1 reveals two distinct lineage-dependent populations of fission yeast cells.....157
8.3 Re-defining the checkpoints acting over mitotic progression in fission yeast.....158
8.4 Is the midzone involved in a tension-sensing pathway that ensures spindle integrity?.....160

Table of Tables

2.1 Strains used in this study.....52

2.2 Oligonucleotides used in this study.....61

* * *

Table of Movies

3.1 Kinetochore and spindle pole body dynamics in a mitotic control cell.....on disc

3.2 Kinetochore and spindle pole body dynamics in a mitotic *mto1D* cell.....on disc

3.3 Retrieval of unclustered kinetochores in an *mto1D* cell.....on disc

5.1 Pre-anaphase spindle collapse in a control cell in the presence of Lat A.....on disc

6.1 Mitotic localisation of Ase1.....on disc

6.2 Kinetochore and spindle pole body dynamics in a mitotic *ase1D* cell.....on disc

6.3 Mitotic spindle fates in *ase1D* cells are independent of light exposure.....on disc

7.1 Mitotic localisation of Klp9.....on disc

List of Abbreviations

AMIZ – astral microtubule interaction zone

APC – anaphase promoting complex

CAR – cortical actomyosin ring

cdc – cell division cycle

Cdk – cyclin dependent kinase

CFP – cyan fluorescent protein

DAPI – 4'6-diamino-2-phenylindole

EMM – Edinburgh minimal medium

eMTOC – equatorial microtubule organising centre

F-actin – filamentous-actin

G1 – gap phase 1

G2 – gap phase 2

G-actin – globular-actin

GEF – guanine exchange factor

GFP – green fluorescent protein

iMTOC – interphase microtubule organising centre

INA – intra-nuclear astral

k-fibre – kinetochore-fibre

Lat – latrunculin

LB – Luria-Bertani

M – mitosis

MAP – microtubule associated protein

MEN – mitotic exit network

MT – microtubule

MTOC – microtubule organising centre

NETO – new end take-off

ORF – open reading frame

PAA – post-anaphase array

RADA – R183A,D184A

S – synthesis phase

SAC – spindle assembly checkpoint

SEM – standard error of the mean

SIC – spindle integrity checkpoint

SIN – septation initiation network

SOC – spindle orientation checkpoint

SPB – spindle pole body

TBZ – thiabendazole

ts – temperature sensitive

YES – yeast extract plus supplements

γ-TURC – gamma-tubulin ring complex

Chapter 1

General Introduction

The cell cycle ensures the correct segregation of replicated genetic material from mother cell to daughter cells. To increase its fidelity this process is tightly regulated by a series of checkpoints. In the absence of such checks, chromosome instability can arise. Indeed, many checkpoint-defective tumour cells display an abnormal number of chromosomes, a phenomenon known as aneuploidy. Analysis of the cell cycle and its regulatory elements provides an understanding of what can go wrong in an unchecked cell cycle and potentially offers long-term therapeutic tools. Due to the high level of homology between eukaryotes, components of the cell cycle machinery are often evolutionarily conserved. As a result, the fission yeast, *Schizosaccharomyces pombe*, and the budding yeast, *Saccharomyces cerevisae*, have proved instrumental in understanding how the cell cycle progresses not only in yeast but also in higher eukaryotes, including man.

1.1 Fission yeast as a model organism to study the cell cycle

S.pombe provides an excellent model organism for cell cycle studies for several reasons. Firstly, it undergoes a more rapid cell cycle than mammalian cells, meaning that the events of a whole cycle can be studied and a large amount of cells can be generated in a relatively short time. Additionally, genetic manipulation of fission yeast is straightforward when compared to mammalian systems. Gene "tags" and deletions can be performed easily and quickly. Aiding this, the entire genome of *S.pom*be has been sequenced (Wood *et al.*, 2002). Fission yeast can also undergo both a haploid and diploid cell cycle, meaning that heterozygous strains deleted for essential genes can be made. Mating between haploid mutants followed by sporulation means that the generation of novel mutant combinations is straightforward. Due to its history as a model organism there is a wide and dedicated community, a wealth of techniques and an array of reagents available for use in *S.pombe*. Fission yeast cells are particularly suited to cell cycle studies as they are rod-shaped and grow by

apical extension so cell cycle stage can be easily estimated. Furthermore, they divide by medial fission as do the majority of mammalian cells but in contrast to budding yeast cells, which undergo an asymmetrical division.

Fission yeast has a rich history of use in cell cycle studies. The seminal cyclin dependent kinase (Cdk) Cdc2 was first identified in fission yeast as a positive regulator of the cell cycle (Nurse and Thuriaux, 1980). Subsequently, the human homologue of Cdc2 was found to complement a fission yeast *cdc2* mutant (Lee and Nurse, 1987), illustrating the degree of conservation between systems. Since this pioneering work multiple cell division cycle (*cdc*) mutants have been identified in fission yeast, which has facilitated further investigation of the eukaryotic cell cycle.

The cell cycle in all eukaryotic cells can be split into four stages, G1, S, G2 and M. The *S.pombe* cell cycle is illustrated in figure 1.1. G1 (gap 1) phase separates M and S phase and is the shortest phase in the fission yeast cycle. Cells in G1 are binucleate following mitosis but have not initiated genome replication, which occurs in S (synthesis) phase immediately following G1. Septum position is defined at the onset of M (mitosis) (Daga and Chang, 2005; Tolic-Norrelykke *et al.*, 2005), however, cytokinesis does not occur until after S phase. The fission yeast cell cycle is therefore unusual since G1 and S phase occur prior to cytokinesis, which results in haploid cells having a 4C DNA content during S phase. The next phase is G2 (gap 2), which accounts for the largest portion of the fission yeast cell cycle and consists of the growth of the recently divided cells. Cells first extend only at the old end, but later, growth switches to bipolar in an event known as new end take-off (NETO; Mitchison and Nurse, 1985). Following growth to a critical size threshold, the cell undergoes M (mitosis) phase when the replicated genome is physically separated within the mother cell.

Several of the checkpoints (Hartwell and Weinert, 1989) that operate to increase the fidelity of the cell cycle (section 1.3) function during mitosis itself or at the G2-M transition, one of the two most important regulatory points in the fission yeast cell cycle.

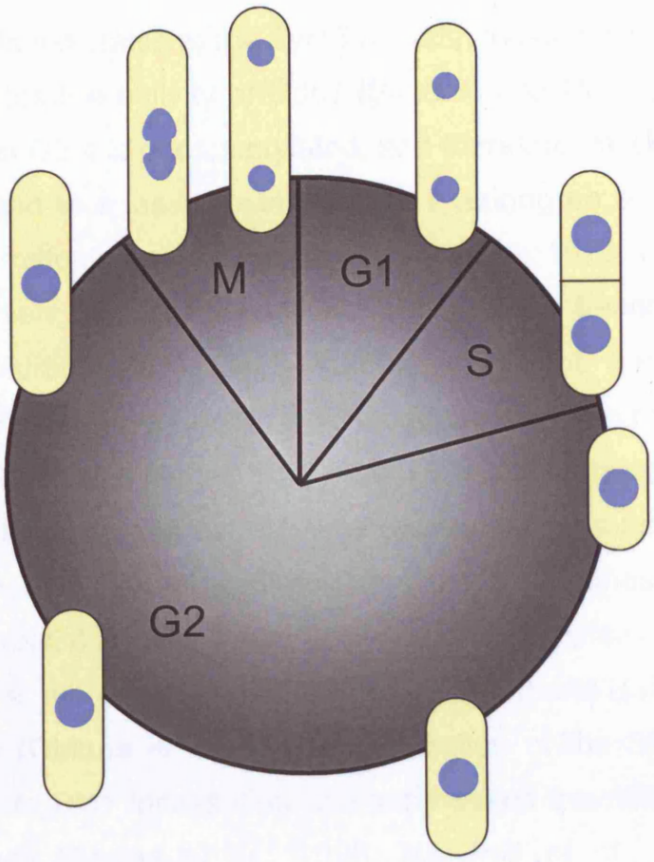

Figure 1.1 The fission yeast cell cycle

Schematic diagram showing the growth of fission yeast during a replicative cell cycle. Abbreviations: M, mitosis; S, DNA synthesis; G1 and G2, gap phases. Nuclear material shown in blue.

1.1.1 G2-M transition

The Cdc2 kinase (section 1.1) is the master regulator of the cell cycle and its switch from inactive to active is responsible for driving cells from G2 to mitosis (Nurse, 1990). The activity of Cdc2 is regulated in three ways, by cyclin binding partner, localisation and by phosphorylation. I describe these mechanisms in brief below.

The phosphorylation status of the Tyr15 residue, located within the ATP binding domain, regulates the activity of Cdc2 (Simanis and Nurse, 1986; Gould and Nurse, 1989). In G2 it is phosphorylated, and therefore inhibited, by the protein kinase Wee1 and to a lesser extent by Mik1 (Lundgren *et al.*, 1991). In cells lacking Wee1, mitosis occurs prematurely (Nurse, 1975; Fantes and Nurse, 1978). Conversely, if Wee1 is overexpressed, cells become blocked in G2 (Russell and Nurse, 1987). Cdc2 is activated via the dephosphorylation of Tyr15 by the phosphatase Cdc25, which triggers entry into mitosis (Russell and Nurse, 1986; Gould and Nurse, 1989). Cdc25 accumulates throughout G2 until cells attain a critical size threshold, whereupon Cdc25 is activated (Moreno *et al.*, 1990). There is some evidence that the Polo kinase (Plo1) may co-ordinately control Cdc25 and Wee1 activities. Plo1 localises to the spindle pole bodies (SPBs) at mitotic onset (Mulvihill *et al.*, 1999) and is necessary to form a mitotic spindle (Ohkura *et al.*, 1995). A mutation of the SPB protein, Cut12, allows premature Plo1 localisation and suppresses the mitotic entry defect of *cdc25-22* cells (Bridge *et al.*, 1998; Mulvihill *et al.*, 1999). Similarly, overexpression of Fin1, the NIMA-related kinase, drives association of Plo1 to the poles and bypasses the requirement for Cdc25 (Grallert and Hagan, 2002).

As well as Tyr15 phosphorylation, the cyclin partner associated with Cdc2 provides a second level of regulation. The essential mitotic cyclin in *S.pombe* is Cdc13, a homologue of human cyclin B (Hagan *et al.*, 1988). This, like Cdc25, accumulates steadily throughout G2, before levels peak in metaphase and then sharply reduce in anaphase (Creanor and Mitchison, 1996). The reason for the rapid reduction in the amount of Cdc13 protein post-anaphase is due to proteolysis carried out by the anaphase promoting complex (APC). This is a necessary regulatory step in limiting the mitotic activity of Cdc2, as

indestructible *cdc13* mutants arrest in anaphase with high Cdc2 activity (Yamano *et al.*, 1996).

A third form of regulation is achieved by localisation. Studies of fluorescently tagged Cdc13 (Decottignies *et al.*, 2001; Tatebe *et al.*, 2001) show that it localises to the spindle poles and the spindle in mitosis. Once sister chromatids separate at anaphase onset Cdc13 is degraded and disappears from the spindle. Antibodies against Cdc2 show that it follows a similar localisation pattern (Alfa *et al.*, 1990). In this way the activity of Cdc2 in mitosis is spatially restricted to the mitotic machinery.

1.1.2 Mitotic progression

The onset of mitosis requires the activation of Cdc2 (section 1.1.1). Upon entry to mitosis chromosomes undergo chromatin condensation (reviewed in Stunnikov, 2003). At the same time SPBs, which duplicate in late G2, enter a fenestra in the nuclear envelope (Ding *et al.*, 1997). This process requires Cut11, a protein that contains membrane spanning domains, is found in the nuclear envelope throughout the cell cycle and localises to SPBs as they enter the envelope (West *et al.*, 1998). Cells entering mitosis also undergo a conformational re-arrangement of their cytoskeletal elements (described in detail in the following section). In brief, actin relocalises from the cell tips to the middle (Marks *et al.*, 1986) and the microtubules of the interphase array are depolymerised and specialised mitotic microtubules are nucleated (Hagan and Hyams, 1988).

The mitotic spindle, composed of tubulin, is responsible for the physical separation of the replicated chromosomes. Tagging tubulin with the green fluorescent protein (GFP) has allowed spindle dynamics to be studied in fission yeast (Tatebe *et al.*, 2001). During mitosis, the spindle elongates in a characteristic three step process (Nabeshima *et al.*, 1998). In phase 1, pro-metaphase, the replicated poles separate and are positioned by microtubules to opposite sides of the nuclear envelope. In this way the spindle rapidly elongates to a length of approximately two microns, the diameter of the fission yeast nucleus. This spindle length is maintained during phase 2, metaphase, during

which sister chromatids are observed to bounce between poles. The duration of phase 2 is presumably dependent on meeting the conditions of the spindle assembly and spindle orientation checkpoints (SAC and SOC, described in section 1.3.2). These mitotic progression checkpoints work by delaying the onset of anaphase by inhibiting the anaphase promoting complex (APC). At anaphase onset cohesin is destroyed, which allows the spindle to undergo anaphase A, where sister chromatids are resected back to opposite SPBs, and anaphase B, where the spindle rapidly elongates to further separate genetic material ready for cytokinesis. This rapid elongation of the spindle has been termed phase 3.

Cohesin is a conserved multi-subunit complex that acts as a "molecular glue" physically holding sister chromatids together and opposing the forces pulling on the spindle microtubules. Cohesion is established in S phase and must be lost in anaphase to allow sister chromatids to separate. Work in budding yeast first described the cohesin complex and its components, Smc1, Smc3, Scc1 and Scc3 (Guacci *et al.*, 1997; Michaelis *et al.*, 1997; Toth *et al.*, 1999). Defects in any of these proteins results in premature chromatid separation. At anaphase onset, targeted proteolysis of cohesin occurs. The APC cleaves Pds1 (securin), which inhibits the protease Esp1 (separase) (Uhlmann *et al.*, 1999). Without its inhibitory element, Esp1 cleaves Scc1 and cohesin is inactivated (Ciosk *et al.*, 1998; Uhlmann *et al.*, 1999). The homologues of both the cohesin complex and its inhibitory elements are conserved in fission yeast. Psm1, Psm3, Psc3 and Rad21 form the cohesin complex (Birkenbihl and Subramani, 1992, 1995; Tatebayashi *et al.*, 1998; Tomonaga *et al.*, 2000) whilst Cut1 is separase and Cut2 is securin (Funabiki *et al.*, 1996a; Kumada *et al.*, 1998).

The APC, a highly conserved multi-subunit E3 ubiquitin ligase, acts by facilitating the destruction of both the mitotic cyclin Cdc13 and securin (Funabiki *et al.*, 1996b, 1997; Yamano *et al.*, 1996, 1998). Targets of the APC contain a conserved 9-residue destruction box motif. Ubiquitin molecules are transferred to a lysine side chain of such target proteins by the APC, which leads to their identification and degradation by the 26S proteosome in M or G1 phase (Wilkinson *et al.*, 1999). In addition the APC associates with adaptor molecules to confer substrate specificity. At anaphase this is Slp1 (Matsumoto, 1997; Kim

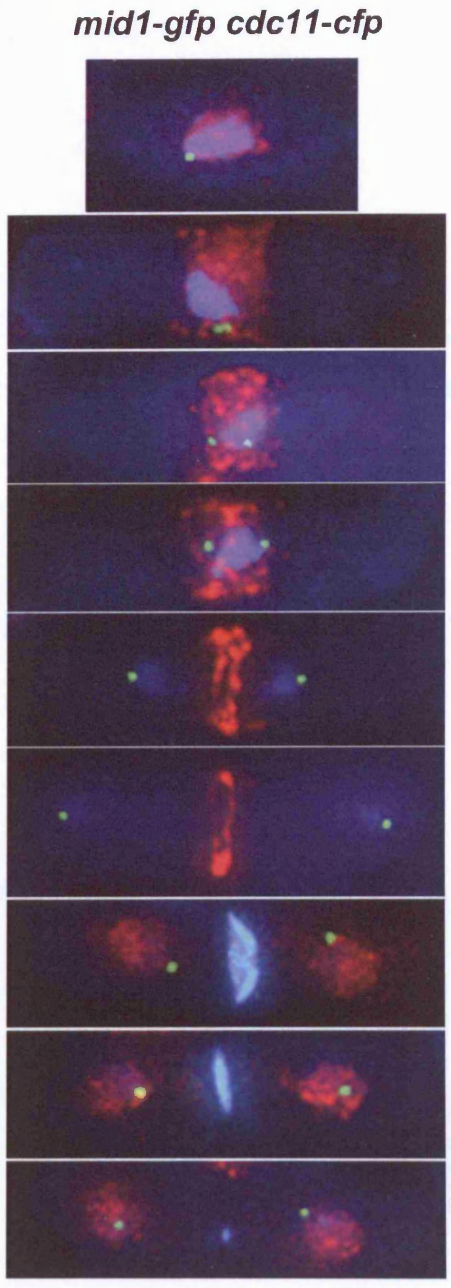

Figure 1.2 *S.pombe* divides by medial fission following segregation of the genetic material

Images through the cell cycle of fixed *mid1-gfp cdc11-cfp* cells expressing Mid1-GFP (red), the earliest known marker for division ring placement, and Cdc11-CFP (green), which marks the spindle pole bodies. DNA and septa are stained blue by DAPI and calcofluor respectively.

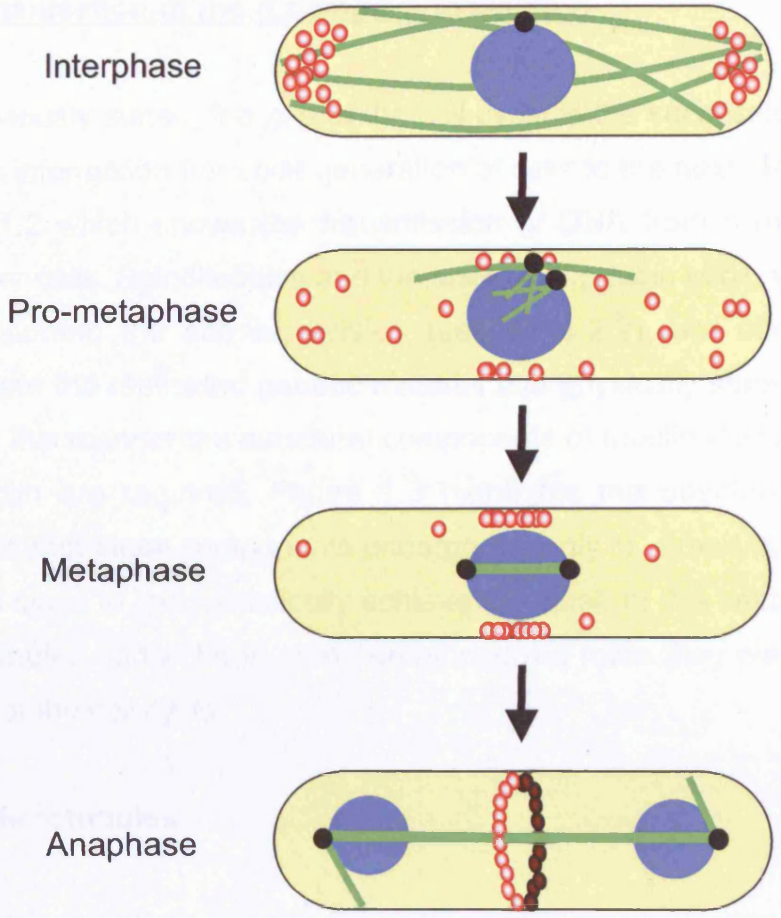

Figure 1.3 Cell cycle dependent localisation of actin and tubulin

Schematic diagram showing both the re-localisation of actin patches (red) from the cell tips to the middle of the cell and the changes the microtubule (green) cytoskeleton undergoes upon entry into mitosis. Nuclei are shown in blue and spindle pole bodies in black.

et al., 1998; Yamada *et al.*, 2000), the fission yeast homologue of Cdc20 in budding yeast (Sethi *et al.*, 1991; Hilioti *et al.*, 2001; Pfleger *et al.*, 2001; Schwab *et al.*, 2001) this acts to target securin. At mitotic exit and G1 the activator Ste9 (Kitamura *et al.*, 1998; Kominami *et al.*, 1998; Blanco *et al.*, 2000), the fission yeast homologue of budding yeast Cdh1 (Visintin *et al.*, 1997), is recruited to confer specificity for mitotic cyclin.

1.2 Organisation of the *S.pombe* cytoskeleton

As previously stated, the aim of the cell cycle is the successful transmission of genetic information from one generation of cells to the next. This is illustrated in figure 1.2 which shows the transmission of DNA from a mother cell to two daughter cells. Spindle poles and the anillin-like protein Mid1, which plays a role in positioning the site of division (section 1.2.2), are shown. In order to segregate the replicated genetic material and physically separate the daughter cells in this manner the structural components of tubulin (forming microtubules) and actin are required. Figure 1.3 highlights the positional and structural changes that these components undergo not only in mitosis but also throughout the cell cycle to mechanistically achieve this goal. In this section I will describe microtubules and actin in some detail and the roles they play in ensuring the fidelity of the cell cycle.

1.2.1 Microtubules

Microtubules in *S.pombe* are formed from the polymerisation of α (*nda2, atb2*) and β (*nda3*) tubulin heterodimers (Yanagida, 1987). These nucleate to a template determined by γ-tubulin (*gtb1*) (Horio *et al.*, 1991; Stearns *et al.*, 1991) and assemble as linear protofilaments that are arranged adjacent to each other forming hollow tube-like structures. Microtubules exhibit dynamic instability at the "plus" end where subunits are added or lost to allow growth and shrinkage respectively (Mitchison and Kirschner, 1984). Polymerisation is dependent on the hydrolysis of GTP bound to the β-tubulin subunit (Weisenberg *et al.*, 1976; Desai and Mitchison, 1997). Microtubules are nucleated from a γ-tubulin ring complex (γ-TURC) (Moritz and Agard, 2001; Janson *et al.*, 2005), so named as it contains γ-tubulin to which the "minus" end of the microtubule is anchored.

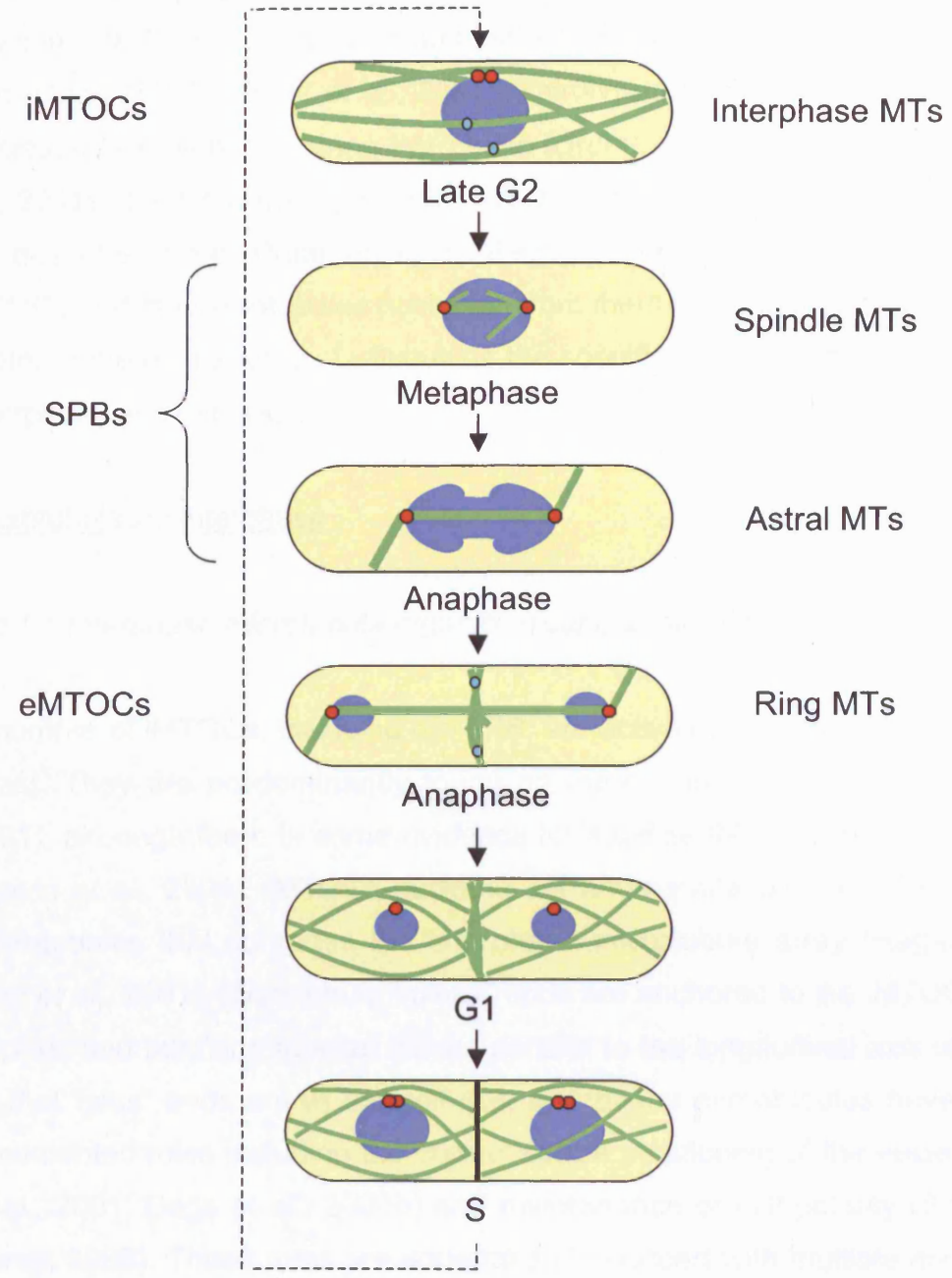

Figure 1.4 Cell cycle and Microtubule Organizing Centre (MTOC) overview

A diagrammatic representation of the three MTOCs (shown in cyan except the SPBs, which are red) present in *S. pombe* and the classes of microtubule (MT, green) nucleated from each during the cell cycle. Nuclei are shown in blue.

These structures are known as microtubule organising centres (MTOCs). There are 4 types of MTOC in fission yeast. Firstly, the SPBs, which are functionally similar to centrosomes in mammalian cells, act as MTOCs during mitosis (Hagan, 1998). Secondly, an equatorial MTOC (eMTOC) forms during mitotic exit (Hagan, 1998; Heitz *et al.*, 2001). Thirdly, an interphase MTOC (iMTOC) nucleates microtubules during interphase (Drummond and Cross, 2000; Tran *et al.*, 2001). Lastly, a mating specific MTOC also exists in *S.pombe* but will not be described here (Petersen *et al.*, 1998). Figure 1.4 illustrates the various MTOCs and the microtubules nucleated from them in the course of a mitotic cell cycle. In the next section, I will outline the specific roles of microtubules during interphase and mitosis.

Microtubules in interphase

1.2.1.1 Interphase microtubule organising centres (iMTOCs)

A number of iMTOCs, including the SPB, are active during interphase in fission yeast. They are predominantly found on the nuclear periphery (Tran *et al.*, 2001), although there is some evidence for satellite iMTOCs in the cytoplasm (Sawin *et al.*, 2004). iMTOCs nucleate 3-4 anti-parallel bundles of interphase microtubules that comprise the interphase microtubule array (Hagan, 1998; Tran *et al.*, 2001). Microtubule "minus" ends are anchored to the iMTOCs at the nucleus and the microtubules extend parallel to the longitudinal axis of the cell so that "plus" ends are at the cell tips. Interphase microtubules have several documented roles including the correct centre positioning of the nucleus (Tran *et al.*, 2001; Daga *et al.*, 2006b) and maintenance of cell polarity (Sawin and Nurse, 1998). These roles are undertaken in concert with multiple microtubule associated proteins (MAPs). So, for example the central position of the nucleus is dependent on Ase1 and Klp2, which act to organise interphase microtubules (Carazo-Salas and Nurse, 2006; Daga *et al.*, 2006a; Janson *et al.*, 2007). Ase1, a member of the ASE1/PRC/MAP65 family, bundles anti-parallel microtubules at zones of overlap, primarily at the nuclear periphery (Loiodice *et al.*, 2005; Yamashita *et al.*, 2005). The kinesin Klp2 is the motor protein responsible for force generation in interphase microtubule sliding (Troxell *et al.*, 2001; Carazo-Salas *et al.*, 2005). Recently it has been shown that these components can

assemble the interphase microtubule array even in the absence of a nucleus (Daga *et al.*, 2006a). Mutants in factors determining polarity have defective cell shapes such as spherical, curved and t-shaped (Verde *et al.*, 1995; Sawin and Nurse, 1998). Polarity is generated and maintained by interphase microtubules, which deposit Tea1-complex at the cell tips (Mata and Nurse, 1997), where it is anchored by the plasma membrane protein Mod5 (Snaith *et al.*, 2005). Tea1 is also required for the localisation of other cell polarity factors including the kinase Pom1, which plays a role in defining the cell tips as a growth site (Bahler and Pringle, 1998). Additionally, localisation at the cell tips of Bub6, an actin-binding protein (Glynn and Chang, 2001), and the formin, For3, required for actin cable formation (Feierbach and Chang, 2001; Feierbach *et al.*, 2004), are both dependent on Tea1. In this way Tea1 establishes a link between the microtubule interphase array and the actin cytoskeleton that is necessary for cell growth (reviewed in La Carbona *et al.*, 2006). Cells lacking either Mal3, the fission yeast EB1 homologue, Tip1, a CLIP170-like protein, or the kinesin Tea2 all suffer polarity defects due to their effects on interphase microtubules (Beinhauer *et al.*, 1997; Brunner and Nurse, 2000; Browning *et al.*, 2000). Mal3 binds to the "plus" end of polymerising microtubules and increases stability (Busch and Brunner, 2004; Sandblad *et al.*, 2006) whereas Tip1 prevents microtubule catastrophe before reaching the cell tips (Brunner and Nurse, 2000).

Microtubules in mitosis

The molecular mechanisms controlling the switch from interphase to mitotic microtubule nucleation are not well understood. After nucleation from iMTOCs is terminated, two types of mitotic MTOCs operate in fission yeast. Firstly, the SPBs, which nucleate microtubules from both their nuclear and cytoplasmic faces. Later in mitosis, an equatorial MTOC nucleates microtubules (figure 1.4).

1.2.1.2 Nuclear face of spindle pole bodies

The microtubules nucleated from the nuclear face of the SPBs are collectively termed spindle microtubules. However, they can be further sub-divided into three groups, k-fibres, pole-to-pole and intra-nuclear astral microtubules.

(i) k-fibres

The "minus" end of these microtubules is anchored to the SPB and the "plus" end is captured and attaches to a kinetochore. Electron microscopy shows that there are 2-4 k-fibres attached to each kinetochore (Ding *et al.*, 1993). To ensure accurate segregation of the genome, one sister chromatid from each pair should be attached to k-fibres nucleated from one of the SPBs while its sister should be similarly attached to the opposing SPB, an arrangement termed amphitelic attachment. The SAC monitors bi-polar chromosome attachment and is described in section 1.3.2.1. At anaphase A, when cohesin is destroyed chromatids retract to opposite spindle poles. Broadly speaking there are two possible mechanisms for this retraction that have been studied in higher eukaryotes. Firstly, the so-called "pacman" model whereby chromatids induce the depolymerisation of "plus" ends of k-fibres enabling the chromatids to be "chewed" poleward (Gorbsky *et al.*, 1987, 1988). Secondly, a model involving poleward microtubule flux whereby chromatids are "reeled" in by continual depolymerisation of the "minus" ends of k-fibres (Margolis and Wilson ,1981; Mitchison, 1989; Mitchison and Salmon, 1992). As there is no microtubule flux in fission yeast (Mallavarapu *et al.*, 1999) the former model seems the most applicable. However, this raises the question of how this retraction is mechanistically achieved. The DASH complex is involved in chromosome bi-orientation and in correcting improper chromosome attachments (Cheeseman *et al.*, 2002; Li *et al.*, 2002; Janke *et al.*, 2002; section 1.3.2.1). The DASH complex contains ten proteins, which connect to kinetochores at the "plus" ends of k-fibres (Cheeseman *et al.*, 2001a, 2001b; Sanchez-Perez *et al.*, 2005; Tanaka *et al.*, 2007). Data from *in vitro* studies shows that the DASH complex forms rings around microtubules and moves progressively at the "plus" ends (Miranda *et al.*, 2005; Westermann *et al.*, 2005; Asbury *et al.*, 2006). Therefore, it is possible that this ring couples the depolymerisation of the "plus" end of the k-fibre with the kinetochore after anaphase A. Whilst the DASH complex is essential for pre-anaphase retrieval of chromatids to the pole in *S.pombe* (Franco *et al.*, 2007) it is not essential for poleward transport in anaphase A (Sanchez-Perez *et al.*, 2005). However, when coupled with deletions of the fission yeast kinesin-8 family members Klp5 and Klp6, which have problems in undergoing timely anaphase A (West *et al.*, 2001), cells are inviable and die

with formed spindles but problems in chromosome segregation (Sanchez-Perez *et al.*, 2005). This suggests that these components may play an overlapping role in the processivity of the chromatids to the poles. Interestingly, in budding yeast displaced chromatids prior to anaphase can be retrieved by both the use of lateral attachments to stabilised microtubules in a Kar3 mediated manner (Tanaka *et al.*, 2005, 2007) and *via* end-on attachments in a DASH-dependent manner (Tanaka et al., 2007). However, in fission yeast lateral attachments do not result in chromatids retracting to the pole (Franco *et al.*, 2007) and the deletion of all "minus" end directed motor proteins does not effect retrieval (Grishchuk and McIntosh, 2006). Therefore the current model is that depolymerisation of the "plus" ends of k-fibres drives poleward chromosome movements in *S.pombe* (Grishchuk *et al.*, 2005; Grischuk and McIntosh, 2006). Interestingly however, dynein has been shown to have a role in mitotic delay (Courtheoux *et al.*, 2007) and cells lacking Klp2 have a slower processivity of retrieval (Grishchuk and McIntosh, 2006). Therefore, it remains conceivable that lateral movement on pole-to-pole microtubules could aid chromatid retraction to the poles.

(ii) Pole-to-pole microtubules

This second class of microtubules extends from a "minus" end tethered at the SPB to a "plus" end located at some point between the SPBs. This allows interdigitation with the "plus" ends of microtubules nucleated from the opposing SPB. The region where anti-parallel microtubules overlap is termed the spindle midzone. Electron microscopy shows that in metaphase the packaging of these pole-to-pole microtubules is loosely hexagonal, whereas after anaphase onset the packaging switches to a tight square formation (Ding *et al.*, 1993). This arrangement ensures that each microtubule is surrounded by 4 anti-parallel microtubules that each originate from the opposite pole. It is unclear which proteins are required for this change in formation, although it is known that multiple proteins localise to the spindle midzone. For example, Ase1 localises to the overlapping anti-parallel microtubules found at the midzone and stabilises them (Loiodice *et al.*, 2005; Yamashita *et al.*, 2005). These authors show that fission yeast cells lacking Ase1 undergo frequent spindle collapses in phase 3. Ase1 has been observed at the fission yeast spindle midzone prior to anaphase

onset (Loiodice *et al.*, 2005; Yamashita *et al.*, 2005). However to date, only a minor role (Loiodice *et al.*, 2005) and no role (Yamashita *et al.*, 2005) in pre-anaphase spindle dynamics has been observed for Ase1. In addition to structural proteins such as Ase1, the chromosome passenger complex protein Bir1 (survivin), which is conserved from yeast to man, also binds to the midzone after having previously bound to the kinetochores (Rajagopalan and Balasubramanian, 1999, 2002; Morishita *et al.*, 2001; Rajagopalan *et al.*, 2006). Bir1 and the *S.pombe* INCENP homologue Pic1 (Leverson *et al.*, 2002) form a complex with the fission yeast Aurora kinase homologue (Ark1), and are required for the localisation of Ark1 to the spindle midzone after anaphase (Morishita *et al.*, 2001; Petersen *et al.*, 2001). This pattern of localisation is similar to that seen in the Aurora B complex in higher organisms where INCENP and survivin are also required (Adams *et al.*, 2000; Wheatley *et al.*, 2001; Bolton *et al.*, 2002). Ark1 is responsible for correcting deleterious kinetochore-microtubule attachments (section 1.3.2.1). During spindle elongation in phase 3 the force required is generated at the midzone. Various MAPs are implicated in this process including the kinesin Cut7, which is required in anaphase B (Hagan and Yanagida, 1990, 1992). Pole-to-pole microtubules are therefore responsible for further elongating the spindle following the retraction of k-fibres in anaphase A, resulting in further separation of daughter genomes.

(iii) Intra-nuclear astrals

The third class of microtubules emanating from the SPBs are termed intra-nuclear astrals (INAs). INAs, like pole-to-pole and k-fibre microtubules, nucleate from the nuclear face of the SPB whilst the "plus" ends are seen within the nucleoplasm. First observed very recently by the use of fluorescently tagged tubulin coupled with a nuclear envelope marker (Zimmerman *et al.*, 2004), they had presumably been mistaken for cytoplasmic microtubules by earlier investigators. INAs are highly dynamic and have been observed in phases 1 and 2. However, upon entry into phase 3, INA nucleation is terminated and instead cytoplasmic astrals are nucleated. This data is reported relative to spindle length and has not been defined relative to anaphase onset. Zimmerman *et al.* (2004) conclude that INAs are nucleated exclusively in

phases 1 and 2 whereas astral microtubules are nucleated exclusively in phase 3. This is in stark contrast to other investigators who state that astrals are nucleated in phases 1, 2 and 3 (Gachet *et al.*, 2001, 2004; Oliferenko and Balasubramanian, 2002; Tolic-Norrelykke *et al.*, 2004). More recently, Gachet *et al.* (2006) have presented evidence to indicate that astrals and INAs can be nucleated at the same time. Clearly, the role of INAs is not fully understood at this time. One possibility, suggested by Zimmerman *et al.* (2004), is that INAs are responsible for corrective spindle orientation prior to anaphase. This could be dependent on the shape of the nucleus or other as yet undescribed nuclear cues. Another possibility is that INAs are naïve spindle microtubules that could either become k-fibres or pole-to-pole microtubules depending on their initial contact. Evidence supporting this hypothesis is that the DASH complex, which plays a role, though not an essential one, in chromatid attachment, caps INAs (Sanchez-Perez *et al.*, 2005).

1.2.1.3 Cytoplasmic face of spindle pole bodies

(iv) Astral microtubules

Another class of microtubules emanates from the SPBs in mitosis, however these are nucleated from the cytoplasmic face and are termed astral microtubules. Astral microtubules were first described by Hagan and Hyams (1988) as being nucleated in a parallel or divergent conformation in cells that that have presumably undergone anaphase A. However, as described above (section 1.2.1.2) the timing of cytoplasmic astral microtubule nucleation is a contentious issue with several groups describing pre-anaphase astrals which may in fact have been INAs. This is an important point as Gachet *et al.* (2001, 2004) concluded that astral microtubules are responsible for orientating the mitotic spindle both before and after anaphase onset. They propose that corrective orientation towards the longitudinal axis of the cell occurs *via* astral interaction with a specialised area of the cortex termed the astral microtubule interaction zone (AMIZ). They further suggest that this interaction can be disrupted by actin depolymerisation, resulting in spindle mis-orientation prior to sister separation and a subsequent delay over anaphase onset, termed the SOC (spindle orientation checkpoint; described in section 1.3.2.2). This infers

that astral microtubules require the polymerised actin band, which localises to a band around the nucleus in mitosis (Marks *et al.*, 1986; Arai *et al.*, 1998; Arai and Mabuchi, 2002), to effect a corrective orientation of the spindle. Interestingly, these authors also suggest that astrals are involved in triggering anaphase onset itself *via* an asymmetrical contact with the cortical actomyosin ring (CAR). It is possible that instead of astral microtubules, INAs are the structures affecting orientation, although it is harder to understand how actin depolymerisation would affect this since direct INA contact with the CAR would require penetration of the nuclear envelope. There is consensus agreement that astral microtubules are present post-anaphase, where their role is again in the orientation of the spindle towards the longitudinal axis of the cell. However, there is still a discrepancy as to whether astral microtubules contribute to the rate of spindle elongation in anaphase B. Using both pharmacological agents and genetic mutations Gachet *et al.* (2004) and Venkatram *et al.* (2004) conclude that astrals increase the rate of elongation, whereas Sawin *et al.* (2004); Tolic-Norrelykke *et al.* (2004) and Zimmerman and Chang (2005) using genetic mutants and laser ablation studies, disagree.

1.2.1.4 Equatorial microtubule organising centres (eMTOCs)

During anaphase B eMTOCs nucleate a microtubule ring from the middle of the cell, which gives rise to the post-anaphase array (PAA) of microtubules (figure 1.4). eMTOC nucleation requires the activity of both the septation initiation network (SIN), that regulates the onset of cytokinesis, and the APC (section 1.1.2) (Heitz *et al.*, 2001). The PAA contributes to nuclear repositioning following mitosis (Hagan and Yanagida, 1997). Recently, Pardo and Nurse (2003) have shown that the microtubule ring maintains the position of the CAR. Additionally, these authors show that actin depolymerisation prevents PAA formation.

1.2.1.5 Mto1: a universal cytoplasmic γ-TURC-MTOC tethering protein

Mto1/Mbo1/Mod20 (hereafter called Mto1) is a centrosomin-like protein responsible for tethering the γ-TURC (section 1.2.1) to all cytoplasmic MTOCs (Sawin *et al.*, 2004; Venkatram *et al.*, 2004). The nuclear face of the SPB is

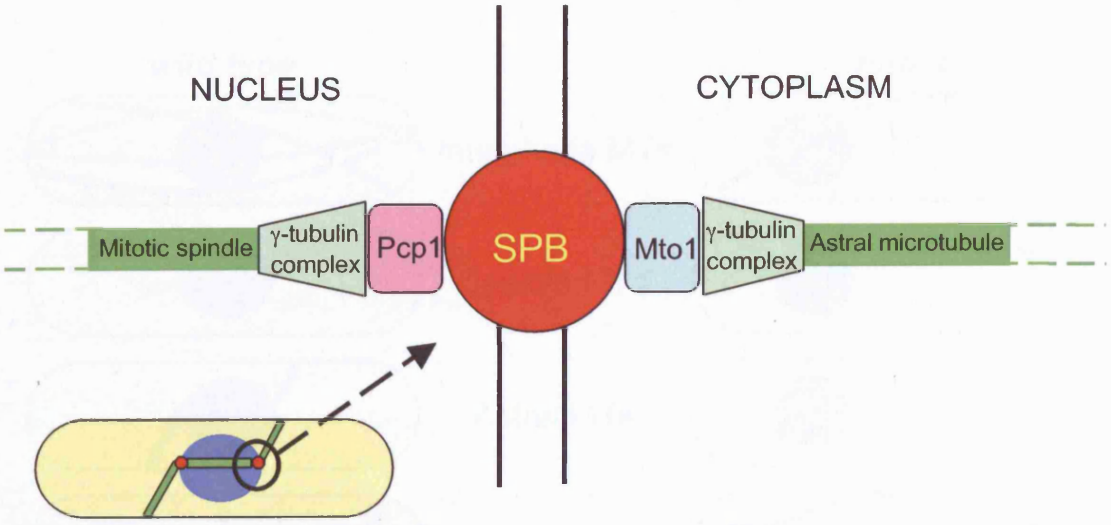

Figure 1.5 Mto1 is required for microtubule nucleation from the cytoplasmic, but not nuclear, face of the spindle pole body

A diagram illustrating the hypothesis that Pcp1 tethers the γ-tubulin complex to the inner face of the SPB whereas Mto1 carries out the same role at the cytoplasmic face.

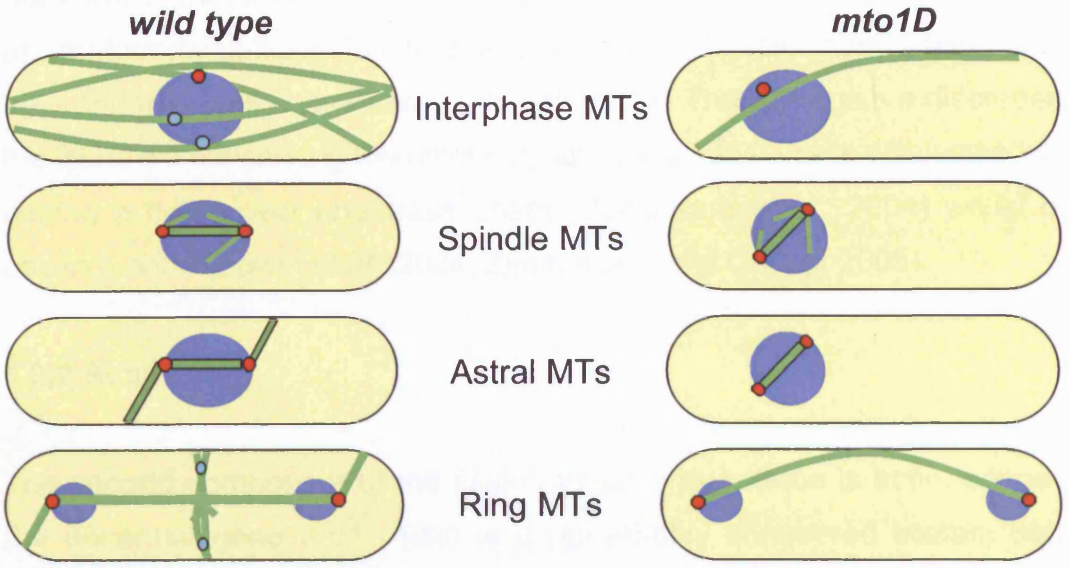

Figure 1.6 Mto1 is required for microtubule nucleation from all cytoplasmic MTOCs

Loss of Mto1 (*mto1D*) affects microtubules (MTs, green) emanating from the iMTOCs, the outer face of the SPBs and eMTOCs. MTOCs are shown in cyan except the SPB, which is shown in red. *mto1D* is depicted with a characteristically mis-positioned nucleus (blue) and a mis-orientated mitotic spindle. The *wild type* microtubule profile is shown for comparison.

tethered to the γ-TURC by the essential protein Pcp1 (figure 1.5), showing that only spindle microtubules are required for cell viability (Flory *et al.*, 2002). Cells lacking Mto1 retain spindle microtubules but are deficient in all cytoplasmic microtubules and thus lack interphase, astral and PAA microtubules (shown in figure 1.6) (Sawin *et al.*, 2004; Venkatram *et al.*, 2004). Occasionally, in *mto1D* cells a single interphase microtubule remains. Evidence from Zimmerman and Chang (2005) shows that this remaining microtubule is in fact nucleated at the inner face of the SPB and has penetrated the nuclear envelope. However it is not known whether it can then attach to an iMTOC. Nevertheless, since they are profoundly deficient in interphase microtubules, cells lacking Mto1 are often bent and frequently have mis-positioned nuclei. There is again a discrepancy in the literature concerning the mitotic dynamics of *mto1D* cells with some workers seeing a delay over anaphase onset (Venkatram *et al.*, 2004) whilst others observe none (Sawin *et al.*, 2004; Zimmerman and Chang, 2005).

1.2.2 Actin

The second component of the fission yeast cytoskeleton is actin, encoded by the essential gene *act1*. Actin is a remarkably conserved protein between species and in fission yeast it exists in two forms: monomeric actin (termed globular or G-actin) and polymeric actin (termed filamentous or F-actin). F-actin is much more prevalent than G-actin and makes up actin cables, actin patches and the cell division ring in *S.pombe* (Marks *et al.*, 1986; Arai *et al.*, 1998; Arai and Mabuchi, 2002). The pharmacological agent latrunculin (Lat) causes rapid depolymerisation of actin by binding to monomers and preventing polymerisation (actin structure is shown in figure 1.7) (Spector *et al.*, 1989; Ayscough *et al.*, 1997; Morton *et al.*, 2000).

Like tubulin (microtubules), actin localisation is cell cycle dependent (Marks *et al.*, 1986; Arai *et al.*, 1998), as illustrated in figure 1.3. After septation, actin patches concentrate at the old end of the daughter cell the site where monopolar growth begins. At NETO, actin patches relocalise to both tips and growth becomes bipolar (Marks *et al.*, 1986). This localisation is influenced by Bud6 and For3 (section 1.2.1.1), which localise to the cell tips in a Tea1, and therefore interphase microtubule, dependent manner. In interphase, actin

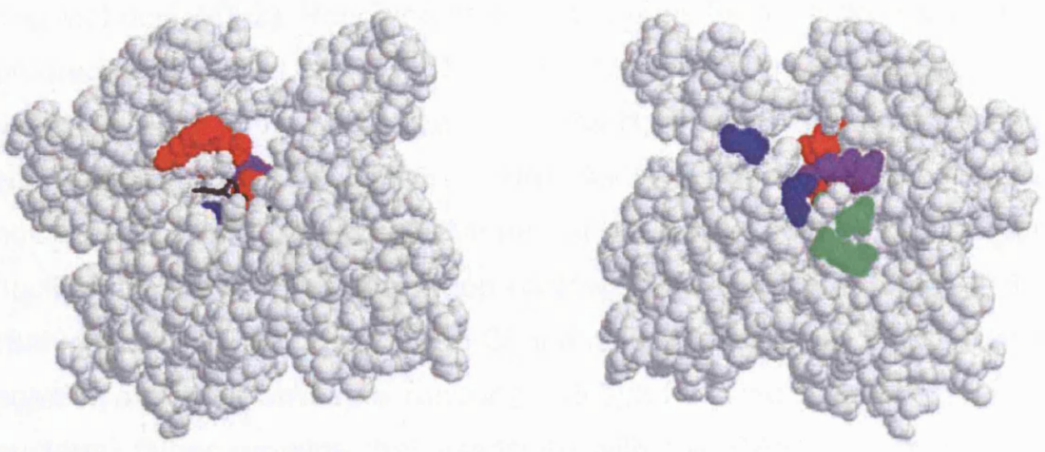

Figure 1.7 A 3-dimensional representation of the actin monomer

The actin monomer seen from the front and reverse. Sites of binding of various compounds are highlighted in colours which correlate to the key. Reproduced from Belmont *et al.* (1999).

cables extend along the longitudinal axis of the cell with the barbed ends facing the tips. This conformation is thought to aid the transport of material to the growing ends of the cell (Kamasaki *et al.*, 2005).

At mitotic entry, actin cables re-orientate so that barbed ends face into the cell middle (Kamasaki *et al.*, 2005). As mitosis proceeds, the actin patches relocalise to a broad band around the middle of the cell and in anaphase, this band concentrates into a tight ring (Marks *et al.*, 1986; Arai *et al.*, 1998; Arai and Mabuchi, 2002). Recruitment of components to this actin ring occurs in an ordered fashion (Wu *et al.*, 2003, 2006). The earliest known marker for division ring placement is the anillin-like protein Mid1, shown in figure 1.2 (Chang and Nurse, 1996; Sohrmann *et al.*, 1996). As SPBs separate, Mid1 leaves the nucleus, in a Plo1-dependent manner, and localises at the cortex around the nucleus in a broad band that then narrows in anaphase to form a tight band (Bahler *et al.*, 1998a; Paoletti and Chang, 2000). Importantly, cells lacking Mid1 position the division septa randomly, despite having a correctly positioned nucleus. Other proteins that associate with the CAR include Myo2, which interacts directly with Mid1, Cdc12, the Arp2/3 complex and Cdc15 (Motegi *et al.*, 2004; Wu *et al.*, 2003; Arai and Mabuchi, 2002; Pollard, 2007). Timing of division ring positioning has recently been investigated. It was found that position is set shortly after mitotic entry, correlating to the timing of Mid1 release from the nucleus (Daga and Chang, 2005; Tolic-Norrelykke *et al.*, 2005). In this way, the position of the mitotic nucleus and the ring site overlap, increasing the efficiency of correctly placing the division plane between the segregated sister genomes. As previously mentioned the CAR is required for eMTOC formation and is then itself spatially maintained by the microtubules nucleated from the eMTOC (section 1.2.1.3). In cytokinesis, the CAR constricts and the daughter cells are physically separated.

Recently, several groups have observed a role for actin in higher organisms in modifying transcriptional complexes in the nucleus (reviewed in Pederson and Aebi, 2005) and in yeast as a chromatin remodelling factor (reviewed in Blessing *et al.*, 2004). Additionally, there is some evidence from other organisms of actin being an extra-spindle matrix (Fabian and Forer, 2005). To date, actin has not been observed in the nucleus in fission yeast. However,

visualisation of actin primarily relies on phalloidin staining which only detects F-actin. Therefore, it is conceivable that actin also exists in the fission yeast nucleus as monomers or short filaments and that conclusions regarding the role of actin will be re-assessed as imaging capabilities improve.

1.3 Checkpoints controlling mitotic entry and progression

In the previous sections, I have described the events of the G2-M transition and mitotic progression together with a summary of the cytoskeletal re-organisation that fission yeast undergoes during these stages. In this section I will describe some of the checkpoints which act to ensure fidelity of the cell cycle at both the G2-M transition and during mitotic progression.

1.3.1 Checkpoints acting over the G2-M transition

Firstly, several checkpoints act over the G2-M transition including those relating to DNA damage, DNA repair and environmental stress. I will not describe these here but will instead summarise the cell size checkpoint as it pertains directly to this work.

1.3.1.1 Cell size checkpoint

The cell size checkpoint acts at the G2-M transition to prevent mitotic entry if cells are too small. This checkpoint works by preventing entry into mitosis by inhibiting the mitotic activity of Cdc2 (section 1.1.1). In brief, Cdc2 is kept phosphorylated and inactive by the kinase Wee1 (Nurse, 1990). This is shown in cells that lack Wee1 where the checkpoint is inactivate, Cdc2 activation is not inhibited and therefore small ("wee") cells progress to mitosis (Nurse 1975; Fantes and Nurse, 1978). In an unperturbed cell cycle the level of the phosphatase Cdc25 that acts antagonistically to Wee1 to dephosphorylate and activate Cdc2 accumulates during G2 (Russell and Nurse, 1986; Gould and Nurse, 1989; Moreno *et al.*, 1990). Likewise, the mitotic cyclin Cdc13 increases during G2 (Hagan *et al.*, 1988; Creanor and Mitchison, 1996). Additionally, the fission yeast polo kinase, Plo1, binding to the poles drives activation of Cdc2 perhaps through an auto-amplification loop of Cdc2 as seen in other eukaryotes

(Kumagai and Dunphy, 1996). A mutation of the SPB component Cut12 and overexpression of the NIMA-related kinase, Fin1, cause premature Plo1 pole localisation and bypass the requirement for Cdc25 for mitotic entry (Bridge *et al.*, 1998; Mulvihill *et al.*, 1999; Grallert and Hagan, 2002). Meaning that the recruitment of Plo1 to the poles influences the balance between Wee1 and Cdc25.

This checkpoint provides a useful tool for synchronising cells at the G2-M transition. Cells containing the *cdc25-22* temperature sensitive mutation can be blocked at a restrictive temperature and released into mitosis at a permissive temperature (Fantes, 1979). The addition of high concentrations of the actin depolymerisation agent latrunculin arrests cells at the G2-M transition due to a failure to reach the critical cell size threshold (Rupes *et al.*, 2001).

1.3.2 Checkpoints acting over mitotic progression

In addition to the checkpoints acting at the G2-M transition there are a number which govern mitotic progression to ensure accurate segregation of the genetic material to daughter cells. In the following section I will describe the spindle assembly and spindle orientation checkpoints (reviewed in Lew and Burke, 2003).

1.3.2.1 The Spindle Assembly Checkpoint (SAC)

In mitosis, the SAC monitors the bi-polar attachment of chromosomes to ensure the correct segregation of the duplicated genome to each daughter cell. This checkpoint, whose function and components are highly conserved in all eukaryotes, acts, *via* APC inactivation, to delay anaphase onset allowing time for the cell to correct deleterious attachments (figure 1.8). Individual SAC components, namely Mad1, Mad2, Mad3, Bub1 and Bub3, were first identified in budding yeast by screening for mutants that died following microtubule destabilising treatment (Li and Murray, 1991; Hoyt *et al.*, 1991). Similarly, Mps1 was also identified as a SAC component with an additional role in SPB duplication (Weiss and Winey, 1996).

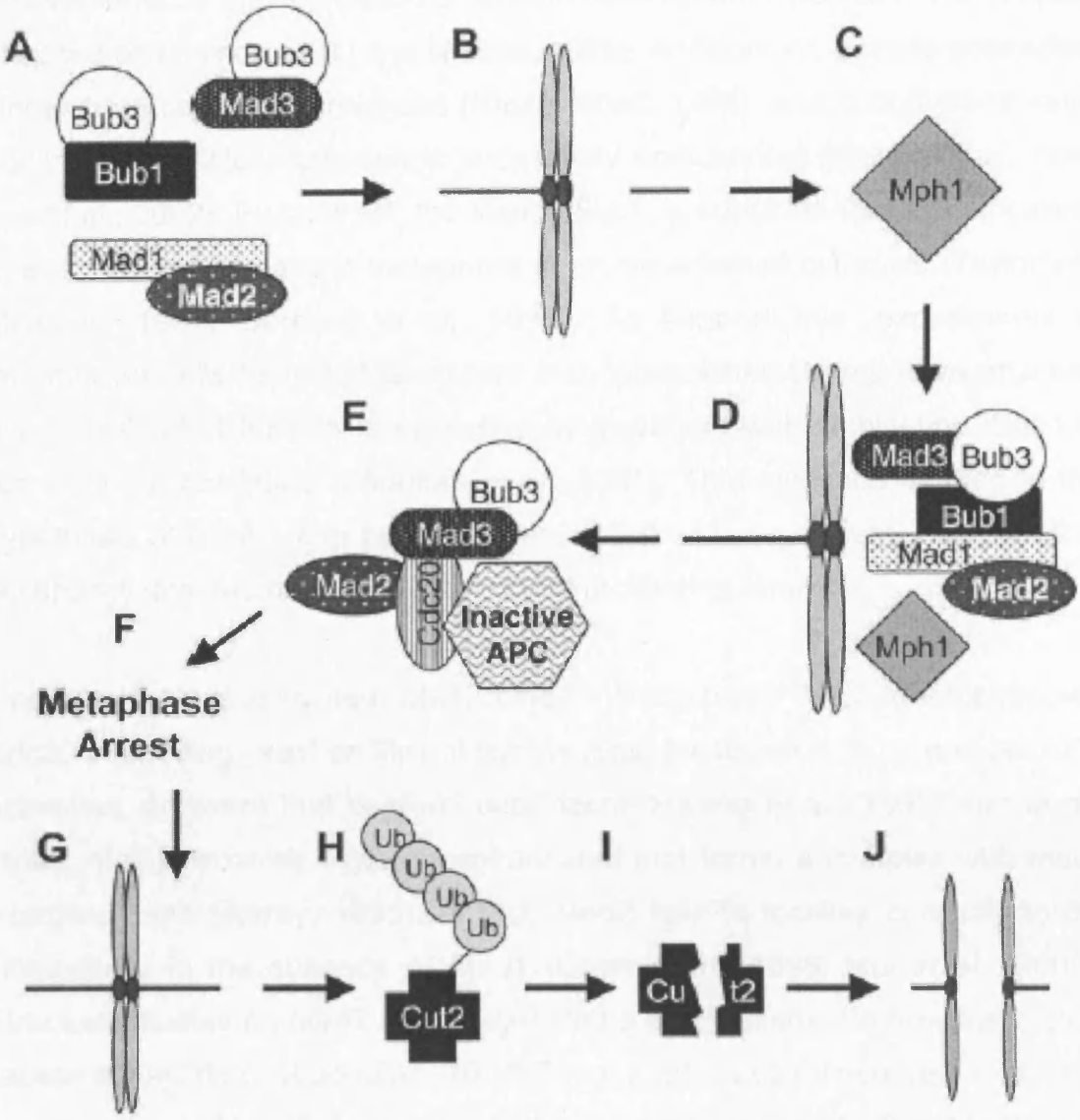

Figure 1.8 The spindle assembly checkpoint (SAC) in fission yeast

In the absence of bipolar spindle attachment (B) components of the SAC (A and C) are loaded to the vacant kinetochore binding site (D) and serve to inactivate the anaphase promoting complex (APC) leading to a metaphase arrest (E and F). In the presence of bipolar spindle attachment (G) APC is active and degrades securin (Cut2) (H and I) leading to cohesin destruction and chromatid separation (J). Reproduced from Kadura and Sazer (2005).

Whilst the SAC is known to monitor the correct bi-polar attachment of sister chromatids to k-fibres the actual mechanism responsible for this has not been straightforward to assess. The SAC could be monitoring either microtubule occupancy of the kinetochore, tension across the spindle or a combination of both of these. Evidence from vertebrates shows that a SAC mediated delay can be overcome by the application of tension, *via* micromanipulation, to improperly attached chromosomes (Li and Nicklas, 1995). Additionally, a single unattached kinetochore can delay anaphase (Rieder *et al.*, 1994), and in both vertebrates and yeast, Mad2 localises only to such empty kinetochores (Waters *et al.*, 1998; Ikui *et al.*, 2002). By contrast, the kinase Bub1, a substrate for Cdc2, localises to all kinetochores early in metaphase in an unperturbed cell cycle (Taylor and McKeon, 1997; Bernard *et al.*, 1998). To support this, experiments in mammalian cells have further shown that, when kinetochores have attached microtubules but tension is abolished by treatment with vinblastine, Bub1 is recruited but not Mad2 (Skoufias *et al.*, 2001). This evidence has led to the hypothesis of a SAC with two branches, one (Mad2-dependent) that monitors occupancy and another (Bub1-dependent) monitoring tension.

Once the SAC is activated, Mad2 binds directly to an APC adaptor protein, Cdc20 in budding yeast or Slp1 in fission yeast (section 1.1.2), to prevent APC activation, an event that is Mad1 dependent (Hwang *et al.*, 1998; Kim *et al.*, 1998). Mad1 becomes hyperphosphorylated and forms a complex with Mad2 (Hardwick and Murray, 1995). In fact, Mad2 fails to localise correctly to the kinetochore in the absence of Mad1 (Chen *et al.*, 1998; Ikui *et al.*, 2002). Structural studies on Mad2 have suggested a mechanism into how the protein causes a SAC delay (Luo *et al.*, 2000; Sironi *et al.*, 2002). There are in fact two conformations of Mad2 (Luo *et al.*, 2004). Recruitment of Mad2 to Mad1 at an unattached kinetochore results in a conformational change in Mad2 that allows it to bind to Mad1 (Luo *et al.*, 2002). As the binding site for Mad2 is similar in Mad1 and Cdc20 (Luo *et al.*, 2002; Sironi *et al.*, 2002) this conformational shift allows Mad2 to then bind to Cdc20 and inhibit the APC. In this way the unattached kinetochore acts to catalyse a conformational change to Mad2 that acts to inhibit the APC *via* Mad2 association to Cdc20 (reviewed in Nasmyth 2005). A complex that comprises the Cdc20 adaptor protein together with Mad2, Mad3 and Bub3 has been identified in human cells (Sudakin *et al.*, 2001)

and yeast cells (Hardwick *et al.*, 2000; Millband and Hardwick, 2002) that, *in vitro*, inhibits the APC up to 3000 times more than Mad2 alone. Other proteins are then recruited to the kinetochore. There is evidence that in fission yeast Bub1 may act with Bub3 to form a scaffold to recruit more Bub1, Bub3 and Mad3 protein to the kinetochore (Vanoosthuyse *et al.*, 2004).

During mitosis in budding yeast, each kinetochore attaches a single k-fibre (Byers and Goetsch, 1975; Peterson and Ris, 1976; Winey *et al.*, 1995). This is in contrast to the situation in fission yeast and mammalian cells where each kinetochore attaches to multiple k-fibres, 2-4 in the case of *S.pombe* (Ding *et al.*, 1993) and approximately 20 in the case of mammalian cells at multiple locations (Cassimeris *et al.*, 1990). Due to the multiple docking sites for k-fibres on each kinetochore, in the same way as mammalian cells, fission yeast can have several attachment conformations. Correct attachment, where an equal number of k-fibres from each SPB are attached exclusively to one of each of the two sister kinetochores, results in balanced tension and is termed amphitelic attachment. Funabiki and colleagues (1993) showed the formation of a metaphase plate of aligned kinetochores in fixed *S.pombe* cells for the first time indicating that balanced tension, and therefore amphitelic attachment, is established prior to anaphase onset. This observation was later confirmed in live cell analyses by Tournier *et al.* (2004). In fission yeast there are three incorrect attachment conformations, namely: monotelic, where only one kinetochore is attached to k-fibres from a single SPB; syntelic, where both kinetochores are attached to k-fibres from the same SPB; merotelic, where one kinetochore is attached to microtubules from both SPBs. Left uncorrected, all these arrangements could potentially cause mis-segregation.

Correction of inappropriate attachments in budding yeast is achieved by the action of the Aurora kinase homolgue Ipl1 (Biggins *et al.*, 1999; Tanaka *et al.*, 2002). The consequent lack of tension induces Ipl1 to activate the SAC and to phosphorylate kinetochore proteins including Dam1 (Kang *et al.*, 2001), which allows uncoupling of the kinetochore and the k-fibre. Dephosphorylation of Dam1 by Glc7 allows re-attachment of the kinetochore and this phosphorylation/dephosphotylation process repeats until the correct attachment is achieved (Pinsky *et al.*, 2006). The fission yeast Aurora kinase, Ark1, is also

involved in regulating chromosome attachment (Petersen *et al.*, 2001). Ark1 is recruited to the mitotic spindle by the chromosome passenger protein Bir1 (survivin) (section 1.2.1.2). Interestingly, cells lacking Ark1 and Bir1 mutants are unable to recruit Mad2 to kinetochores in the presence of microtubule destabilising agents, whereas Bub1 and Mad3 localisation is unaffected (Petersen and Hagan, 2003). This indicates that Ark1 is involved in the predicted occupancy-sensing branch of the SAC. The mitotic fission yeast Shugoshin-like protein Sgo2, is required for Bir1, and therefore Ark1, localisation and activity (Kawashima *et al.*, 2007; Vanoosthuyse *et al.*, 2007). In fission yeast, unlike budding yeast, Dam1 is not essential. However, cells lacking Dam1 undergo a SAC-mediated delay, showing that this protein plays a role in attachment (Sanchez-Perez *et al.*, 2005). In fact, cells lacking both Dam1 and Klp5 are inviable, suggesting that these proteins can substitute for one another. Furthermore, cells lacking Klp5 and Klp6, kinesin-8 family members that destabilise microtubules, are synthetically lethal with cells lacking Bub1 but not Mad2 (West *et al.*, 2002). The localisation of Klp5/6 to the outer repeats of centromeres in metaphase indicates that controlled destabilisation here may be important for generating tension in mitosis (Garcia *et al.*, 2002).

1.3.2.2 The Spindle Orientation Checkpoint (SOC)

The SOC was first described in *S.cerevisae* but has more recently also been described in *S.pombe*.

1.3.2.2.1 SOC in budding yeast

In this organism, a checkpoint exists, known as the SOC, to prevent anaphase onset until the spindle is correctly positioned (reviewed in Lew and Burke, 2003). This is necessary because of the unusual mitotic programme of *S.cerevisae*, whereby it forms a mitotic spindle before the G1-S transition, meaning that both the nucleus and the mitotic spindle have to be physically transported to the bud neck before mitosis. This is achieved by astral microtubule interaction with the actin cytoskeleton at the cell cortex (Palmer *et al.*, 1992). Disruption of any part of this process in mutants with defects in astral microtubules, microtubule motor proteins or cortical proteins leads to a mis-

positioned spindle and an activated SOC (Beach *et al.*, 2000; Schuyler and Pellman, 2001; Segal and Bloom, 2001). The SOC delays anaphase by preventing mitotic exit network (MEN) activation (reviewed in McCollum and Gould, 2001), which in turn controls the release of Cdc14 required for Cdk inactivation (reviewed in Jensen *et al.*, 2002). As the mitotic spindle forms components of the MEN localise to SPBs. Several of these, including Bub2-Bfa1 and Tem1, localise asymmetrically to the pole that will enter the daughter cell (Bardin *et al.*, 2000; Pereira *et al.*, 2000). The only MEN component not to bind at either pole, Lte1, binds instead to the cortex of the daughter cell, providing an appealing model of spatial regulation whereby activation of the MEN, and therefore anaphase onset, can only occur when the pole enters the daughter cell allowing Lte1 to interact with Tem1 (Bardin *et al.*, 2000; Pereira *et al.*, 2000). However, Lte1 is not essential for MEN activation except at low temperature, meaning that there must be other regulatory steps to the SOC that are as yet undescribed and that at least at elevated temperatures Lte1 is not acting as a guanine exchange factor (GEF) for Tem1 (Adames *et al.*, 2001). Another putative target of the GEF activity of Lte1 could be Ras2, however, whilst Ras2 is essential for Lte1 localisation Lte1 preferentially binds to Ras2-GTP (Yoshida *et al.*, 2003; Seshan and Amon, 2005). Whilst this interaction does require the GEF domain of Lte1 it appears to be functioning here not as an exchange factor domain but as a binding motif. Furthermore, the MEN inhibitor Kin4 which localises primarily in the mother cell provides more evidence of particular asymmetric spatial cues (D'Aquino *et al.*, 2005; Pereira and Schiebel, 2005). Interestingly, in an unperturbed cell cycle, it is always the old pole that enters the daughter cell and has the asymmetrically distributed MEN components localised to it. This asymmetry is disrupted by treatment with the microtubule poison nocodazole, meaning that MEN loading becomes symmetrical and either pole enters the daughter randomly (Pereira *et al.*, 2001).

1.3.2.2.2 SOC in fission yeast

The SOC in fission yeast was first described by Gachet *et al.* (2001) as a checkpoint that delays the onset of anaphase if the mitotic spindle is mis-orientated by more than 30° from the longitudinal axis of the cell (figure 1.9). The rationale behind the proposal was that sister chromatid separation along an

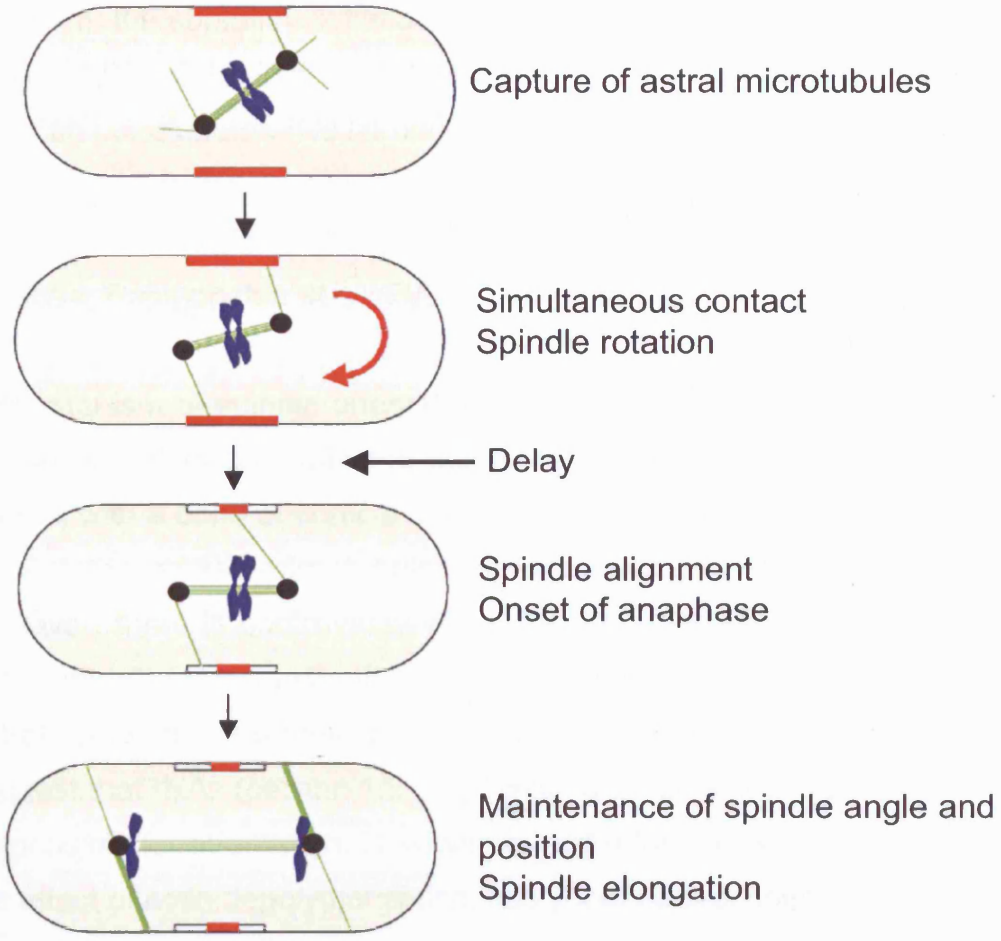

Figure 1.9 The spindle orientation checkpoint (SOC) in fission yeast

A model of the SOC adapted from Gachet *et al*. (2004). Microtubules are shown in green, chromatids in blue, SPBs in black and the astral microtubule interaction zone (AMIZ) in red.

axis that is not approximately perpendicular to the axis of cell division could lead to mis-segregation of the replicated genome. Unlike in budding yeast, mis-positioning of the spindle in *S.pombe* results in a delay over anaphase onset that is mediated by the APC rather than by the MEN equivalent in this organism, the septation initiation network (SIN) (reviewed in Krapp *et al.*, 2004). However, like in budding yeast, the SOC can be activated by the disruption of the actin cytoskeleton (*via* latrunculin treatment or the use of *act1-188* mutants), in mutants defective in actin organisation (*myo5D* and *for3D*) or in mutants with astral microtubule instability (*cdc11-123*) (Gachet *et al.*, 2001, 2004; Tournier *et al.*, 2004; Rajagopalan *et al.*, 2004).

A mechanism of spindle orientation in fission yeast proposed by Gachet *et al.* (2004) is that to orientate the spindle prior to anaphase astral microtubules interact with a band of cortical actin that localises around the nucleus in mitosis, termed the astral microtubule interaction zone (AMIZ) (section 1.2.1.3). However, there is controversy within the literature about the precise timing of astral microtubule nucleation (section 1.2.1.2) meaning that orientation by astrals prior to anaphase onset is now disputed. Zimmerman *et al.* (2004) suggest that INAs (section 1.2.1.2), which are nucleated in phases 1 and 2, are responsible for orientation. However, a model for such orientation, incorporating the effect of actin depolymerisation, has yet to be proposed.

Regardless of the mechanism of spindle orientation it is generally agreed upon that mis-orientation is monitored by a subset of SAC components, which are required for a SOC-mediated delay. However, the exact components required for the SOC are disputed. Tournier *et al.* (2004) state that Bub1, Bub3 and Mad3 are required whereas Mad1 and Mad2 are not. Mph1, the fission yeast homologue of Mps1, is partially required for the delay, perhaps reflecting its partial role in the recruitment of Bub1 to kinetochores (Vanoosthuyse *et al.*, 2004). Recently it has been shown that the exact same subset of SAC components is required to impose a delay on cells lacking Mal3 (Asakawa *et al.*, 2005), the fission yeast EB1 homologue which stabilises polymerising microtubules (Sandblad *et al.*, 2006). By contrast, other groups working on the SOC have found that only Bub1 and Mph1 are required to activate it (Rajagopalan *et al.*, 2004). Interestingly, both groups report a role for Bub1,

which has been implicated in tension sensing but not Mad2, which is thought to be involved in sensing kinetochore occupancy (section 1.3.2.1). Therefore it seems the SOC is monitoring tension across the kinetochores. This may be particularly important in fission yeast, which can have microtubule occupancy at all kinetochore sites but may nevertheless be syntelically or merotelically attached (section 1.3.2.1). In addition to being required to impose the SOC delay, Tournier *et al.* (2004) show that Bub1 localises to kinetochores in the presence of latrunculin and in *cdc11-123* cells, whereas Mad2 does not. In several ways the results of Rajagopalan *et al.* (2004) that Bub3 and Mad3 are not required for the SOC are surprising as both are required in *S.cerevisae* for Mps1 to impose an arrest in response to microtubule damage. Also, Bub3 is required for recruitment of Bub1 to kinetochores and for the SAC function of Bub1 in fission yeast (Vanoosthuyse *et al.*, 2004).

There are several differences in experimental approaches between groups that could have resulted in their differing conclusions as to which SAC components are required. These include the amount of drug used to activate the SOC, the method of visualisation employed and the strains used to activate the SOC. Tournier *et al.* (2004) use a concentration of Lat A that depolymerises actin cables but not patches. In this way the cell size checkpoint (section 1.3.1.1) is not activated and cells enter mitosis. Rajagopalan *et al.* (2004) however, use a *cdc25-22* background to arrest cells after the cell size checkpoint at the G2-M transition meaning that the actin cytoskeleton can be completely depolymerised before mitosis. However, their use of 50μM Lat A has previously been shown to prevent Polo kinase localisation to the SPBs, a necessary step in spindle formation (Tournier *et al.*, 2004). Therefore the fidelity of the spindle at this dose of Lat A may be effected, altering the SAC components needed to impose a SOC delay. Alternatively, the use of DAPI staining to determine mononucleates versus binucleates and the percentage of short spindles in a population used by Rajagopalan and colleagues (2004) to determine whether cells have a delay over anaphase onset may be too crude. By contrast Tournier *et al.* (2004) use fluorescently tagged kinetochores and SPBs to determine the percentage of cells in prometaphase and metaphase. This may contribute to the discrepancies between findings in these groups. In addition, the field has further been complicated by the use of cells lacking Mia1/Alp7 to activate a SOC delay

(Oliferenko and Balasubramanian, 2002), as this deletion was subsequently shown to activate the SAC (Sato *et al.*, 2003).

In addition to the disparity between which SAC components are involved in mediating the SOC delay there are different prevailing theories about where mitotic spindle angle is monitored. Rajagopalan *et al.* (2004) propose that the essential gene Pcp1, which tethers the γ-TURC to the nuclear face of the SPB in mitosis (section 1.2.1.5) monitors tension across the spindle. Thus *pcp1(400-900D)* cells have been described as activating the SOC due to an impairment of the tension-sensing ability of Pcp1 despite no observable mis-orientation of the spindle. However, Tournier *et al.* (2004) favour the hypothesis that spindle orientation is measured at the kinetochores and that this is shown by the localisation of Bub1 to kinetochores, and not the poles, in SOC activation.

In a separate point, unlike the asymmetrically dividing budding yeast, fission yeast divides symmetrically at the middle of the cell. However, asymmetry of the loading of the SIN components, similar to that of the MEN, is observed (reviewed in Bardin and Amon, 2001). Whilst there is no correlation between whether the old or new pole is distributed to the old or new end of the cell in *S.pombe*, the SIN is always activated on the new pole (Grallert *et al.*, 2004). Therefore despite the lack of specific spatial cues, the maturity of the pole determines its role in cytokinesis. It is unknown whether the specific destabilisation of astral microtubules will result in symmetrical loading of SIN components as it does with MEN components in budding yeast.

1.4 Aims of my project

The aim of this thesis is to provide an in depth re-evaluation of the mechanisms controlling mitotic spindle orientation and the SOC in fission yeast, with a view to solving the discrepancies presented in the literature and summarised in this introduction. To do this, I have used highly accurate, single cell time-lapse microscopy that has enabled me to follow minutely the spindle dynamics of a variety of mutant strains as well as those in which the SOC has been activated *via* drug-induced actin depolymerisation. This approach was made possible by specific labelling of individual components of the mitotic machinery (spindle,

SPBs and kinetochores), allowing me to visualise and accurately measure spindle elongation and the angle of the spindle in relation to the longitudinal axis of the cell.

Chapter 2

Materials and Methods

2.1 Yeast Techniques

2.1.1 Yeast strains

A full list of *S.pombe* strains used in this study is given in table 2.1.

2.1.2 Yeast media

All media were autoclaved at 120°C 15p.s.i. for 10 minutes.

Selective media – Edinburgh Minmal Media (EMM):
0.3% KH phthallate, 0.22% Na_2HPO_4, 0.5% NH_4Cl, 2% glucose, 20ml/l salts, 1ml/l vitamins, 0.1ml/l minerals (as detailed in Moreno *et al.*, 1991).
EMM agar was made by adding 2% Bacto Agar (Difco) to EMM liquid.
Glucose, EMM stocks and vitamins were added separately after autoclaving.
Additional nutritional supplements (adenine, histidine, leucine and uracil) were added to the media as required from sterile stocks of 10mg/ml to a final concentration of 100μg/ml

Rich media – Yeast Extract plus Supplements (YES):
0.5% Oxoid yeast extract, 2% glucose, 100mg/l adenine.
YES agar was made by adding 2% Bacto Agar (Difco) to YES liquid.
Glucose and adenine were added separately after autoclaving.

For the selective growth of antibiotic resistant strains, G418 (Invitrogen) or Hygromycin B (Sigma) was added at 100μg/ml to YES agar plates.
The actin depolymerisation agent Latrunculin A (Molecular Probes) was dissolved in dimethyl sulfoxide at a stock concentration of 1mg/ml, and used at concentrations indicated in individual experiments. Latrunculin A was added to

Table 2.1 Strains used in this study

Strain	Genotype	Source
JM100	*leu1-32 ura4-D18 h+*	Lab stocks
JM109	*leu1-32 ura4-D18 h-*	Lab stocks
JM2977	*mto1::hygR leu1-32 ura4-D18 h+*	This study
JM2978	*mto1::hygR leu1-32 ura4-D18 h-*	This study
JM2566	*lys1:nmt1-atb2-gfp leu1-32 ura4-D18 h+*	Lab stocks
JM3096	*mto1::hygR lys1:nmt1-atb2-gfp leu1-32 ura4-D18 h+*	This study
JM2887	*dam1::kanR lys1:nmt1-atb2-gfp leu1-32 ura4-D18 h?*	Lab stocks
JM2763	*ndc80-gfp:kanR cdc11-cfp:kanR leu1-32 ura4-D18 h-*	Lab stocks
JM2979	*mto1::hygR ndc80-gfp:kanR cdc11-cfp:kanR leu1-32 ura4-D18 h-*	This study
JM3237	*mal3::ura4 ndc80-gfp:kanR cdc11-cfp:kanR leu1-32 ura4-D18 h-*	Lab stocks
JM2576	*cdc7-gfp:ura4 leu1-32 ura4-D18 h-*	Lab stocks
JM2574	*sid1-gfp:ura4 leu1-32 ura4-D18 h-*	Lab stocks
JM2926	*mto1::kanR leu1-32 ura4-D18 h+*	K. Sawin
JM2955	*mto1::kanR cdc7-gfp:ura4 leu1-32 ura4-D18*	This study
JM2956	*mto1::kanR sid1-gfp:ura4 leu1-32 ura4-D18*	This study
JM2945	*lys1:nmt1-atb2-gfp cdc15-gfp:ura4 leu1-32 ura4-D18 h-*	Lab stocks
JM2835	*ndc80-cfp:kanR leu1-32 ura4-D18 h+*	Lab stocks
JM3045	*lys1:nmt1-atb2-gfp ndc80-cfp:kanR cdc15-gfp:ura4 leu1-32 ura4-D18 h+*	This study
JM2736	*cdc11-gfp:kanR leu1-32 ura4-D18 h+*	Lab stocks
JM3193	*mto1::hygR cdc11-gfp:kanR leu1-32 ura4-D18 h+*	This study
JM2761	*act1-188 ndc80-gfp:kanR leu1-32 ura4-D18 h-*	Lab stocks
JM3315	*act1-188 ndc80-gfp:kanR cdc11-cfp:kanR leu1-32 ura4-D18 h-*	This study
JM3387	*act1-188 ndc80-gfp:kanR cdc11-cfp:kanR leu1-32 leu1$^+$ ura4-D18 pJK148 h-*	This study
JM3388	*leu1:act1 act1-188 ndc80-gfp:kanR cdc11-cfp:kanR leu1-32 leu1$^+$ ura4-D18 pJK148 h-*	This study

JM3389	*leu1:act1(R183A,D184A) act1-188 ndc80-gfp:kanR cdc11-cfp:kanR leu1-32 leu1^{+} ura4-D18 pJK148 h-*	This study
JM3390	*leu1:act1(D157E) act1-188 ndc80-gfp:kanR cdc11-cfp:kanR leu1-32 leu1^{+} ura4-D18 pJK148 h-*	This study
JM3406	*leu1:act1 act1::hygR ndc80-gfp:kanR cdc11-cfp:kanR leu1-32 leu1^{+} ura4-D18 pJK148 h-*	This study
JM3407	*leu1:act1(R183A,D184A) act1::hygR ndc80-gfp:kanR cdc11-cfp:kanR leu1-32 leu1^{+} ura4-D18 pJK148 h-*	This study
JM3408	*leu1:act1(D157E) act1::hygR ndc80-gfp:kanR cdc11-cfp:kanR leu1-32 leu1^{+} ura4-D18 pJK148 h-*	This study
JM3206	*ase1-gfp:kanR leu1-32 ura4-D18 h-*	T. Toda
JM2608	*cdc11-cfp:kanR leu1-32 ura4-D18 h+*	Lab stocks
JM3350	*ase1-gfp:kanR cdc11-cfp:kanR leu1-32 ura4-D18 h-*	This study
JM3207	*ase1::hygR leu1-32 ura4-D18 h+*	This study
JM3208	*ase1::hygR leu1-32 ura4-D18 h-*	This study
JM3217	*ase1::hygR ndc80-gfp:kanR cdc11-cfp:kanR leu1-32 ura4-D18 h+*	This study
JM2894	*tea1::ura4 leu1-32 ura4-D18 h-*	Lab stocks
JM2893	*tip1::kanR leu1-32 ura4-D18 h-*	Lab stocks
JM2881	*dam1::kanR leu1-32 ura4-D18 h-*	Lab stocks
JM2844	*mal3::ura4 leu1-32 ura4-D18 h-*	Lab stocks
JM3093	*klp2::ura4 leu1-32 ura4-D18 h-*	Lab stocks
JM3137	*klp3::ura4 leu1-32 ura4-D18 h-*	Lab stocks
JM3007	*klp5::ura4 leu1-32 ura4-D18 h-*	Lab stocks
JM3089	*klp6::ura4 leu1-32 ura4-D18 h-*	Lab stocks
JM3355	*klp8::kanR leu1-32 ura4-D18 h-*	This study
JM3219	*klp9::kanR leu1-32 ura4-D18 h-*	This study
JM3318	*klp9-gfp:kanR leu1-32 ura4-D18 h+*	This study
JM2666	*ndc80-cfp:kanR leu1-32 ura4-D18 h-*	Lab stocks
JM3325	*klp9-gfp:kanR ndc80-cfp:kanR leu1-32 ura4-D18 h+*	This study
JM3236	*klp9::hygR leu1-32 ura4-D18 h+*	This study
JM3323	*klp9::hygR ndc80-gfp:kanR cdc11-cfp:kanR leu1-32 ura4-D18 h+*	This study

JM3357	*fin1-4gfp:kanR ura4-D18 h+*	I. Hagan
JM3368	*fin1-4gfp:kanR cdc11-cfp:kanR leu1-32 ura4-D18 h+*	This study
JM2610	*mid1-gfp:ura4 cdc11-cfp:kanR leu1-32 ura4-D18 h+*	Lab stocks

YES liquid for cell cycle experiments or to EMM plugs for live cell microscopy (see section 2.2.3.2).

2.1.3 Yeast growth conditions

Liquid yeast cultures were grown in supplemented EMM or YES media in a New Brunswick gyratory shaker at 200r.p.m. at 30°C unless otherwise stated. Cells on agar plates were incubated in a constant temperature incubator at 30°C.

2.1.4 Yeast storage conditions

Yeast strains were stored in 70% YES; 30% glycerol at 80°C.

2.1.5 Cell cycle synchronisation

Cell synchrony was achieved by lactose gradient size selection. A YES-lactose gradient (10-40% lactose) was manufactured in a 50ml centrifuge tube using a Fisherbrand gradient mixer. Cell cultures were grown to a density of $5x10^6$ cells/ml in YES. 50ml of this culture was chilled on ice for 10 minutes and then concentrated by centrifugation (2800r.p.m. for 1 minute in a Sorvall benchtop centrifuge). Cell pellets were resuspended in 1ml of chilled YES and carefully deposited on top of the YES-lactose gradient, which was then centrifuged at 1300r.p.m. for 7 minutes at 4°C. Using a pipette a 3ml sample was gently extracted from the top of a broad band of cells that collected at the centre of the gradient during centrifugation. These cells were flushed into 40ml of chilled YES before being harvested by centrifugation at 2800r.p.m. for 1 minute. Cells were resuspended in 2ml of fresh YES. Following release at 30°C in an Innova water bath shaker, cell samples were collected at regular intervals and processed as described in 2.2.2.

2.1.6 Yeast transformations by lithium acetate

Cells were grown to a density of $5x10^6$cells/ml. 100ml of cells was harvested by centrifugation (3200r.p.m. for 2 minutes in a benchtop centrifuge), washed twice

in distilled water and resuspended in 500μl of LiAc.TE (0.1M LiAc.1xTE (10mM Tris/HCl pH8.0 and 1mM EDTA)). To 100μl of LiAc.TE cell suspension was added 1—20μg of transforming DNA and 100μg of sterile sonicated single stranded salmon sperm carrier DNA in a volume of 10μl. 160μl of LiAc.TE.40% PEG_{3350} was added and the mix incubated at 30°C with agitation for 30 minutes. Cells were then heat shocked at 42°C for 15 minutes and harvested by centrifugation (13000r.p.m. for 10 seconds in a benchtop Heraeus Biofuge Pico microcentrifuge) before being resuspended in 200μl of TE. This cell solution was then spread onto the appropriate selective EMM plates or, in the case of selection by antibiotic resistance, cells were initially spread onto YES agar plates and after 24 hours incubation at 30°C, replica plated to YES agar plates containing G418 or Hygromycin B.

2.1.7 Isolation of yeast genomic DNA

A freshly growing yeast colony was resuspended in 200μl of STET buffer (2% Triton X-100, 1% SDS, 100mM NaCl, 100mM Tris pH8.0, 1mM EDTA) in a microtube. 200μl of phenol-chloroform-isoamyl alcohol (25:24:1) was added, and glass beads (Biospec Products Inc.) added to the level of the meniscus. The cells were lysed in a Hybaid ribolyser (3x speed 4 for 10 seconds, chilled on ice between pulses). The lysate/phenol mix was collected by piercing the bottom of the sample tube with a heated needle and collecting into a fresh tube by centrifugation (2000r.p.m. for 30 seconds). The aqueous layer was then separated by centrifugation 13000r.p.m. for 10 minutes) and transferred to a fresh tube. To this was added ammonium acetate to a final concentration of 0.3M and 2.5 volumes of 100% ethanol and the sample chilled on ice for 15 minutes. The DNA was pelleted by centrifugation (13000r.p.m. for 10 minutes) and washed with 500μl of 70% ethanol. The tube was re-centrifuged briefly and any remaining liquid aspirated before the DNA pellet was dried in a 37°C incubator for 15 minutes. The DNA pellet was resuspended in 50μl of water and 1μl used in a 50μl polymerase chain reaction (PCR) reaction.

2.1.8 Mating

Equal quantities of freshly growing cells of opposite mating types were mixed with a toothpick on an EMM agar plate containing all nutrients and incubated at 28°C for 3 days. The formation of asci was monitored microscopically.

2.1.8.1 Random spore analysis

A small amount of the mated cell mix was resuspended in 1ml distilled water containing 0.5% Glucoronidase (Sigma) and incubated overnight at room temperature on a rotary wheel to digest asci. Spore numbers were estimated using a Thoma haemocytometer (Assistent) and, after washing out the Glucoronidase with H_2O, approximately 500 spores were spread onto a YES agar plate and incubated at 30°C. After 3-4 days the colonies were replica plated to selective agar plates containing the appropriate nutritional supplements or antibiotics.

2.1.8.2 Tetrad dissection

Using a micromanipulator (Singer MSM), mature asci were placed in a line 3mm apart on a YES agar plate. The asci were left at 37°C for 3-4 hours to allow asci walls to break down. The 4 spores from each asci were then micromanipulated into a line 3mm apart and incubated at 30°C. After 3-4 days colonies were replica plated to selective agar plates containing the appropriate nutritional supplements or antibiotics.

2.2 Microscopy

2.2.1 (4'6-diamino-2-phenylindole) DAPI and calcofluor staining

Cells were fixed in 70% ethanol and stored at 4°C until required. Fixed cells in ethanol were pelleted by centrifugation (3000r.p.m. for 1 minute) and rehydrated in distilled water. 2μl of rehydrated cells were spread onto a microscope slide to form a monolayer of cells, and allowed to dry at room temperature. 1μl of DAPI plus calcofluor (1.5μg/ml DAPI (Sigma) and 50μg/ml

calcofluor fluorescent brightener (Sigma) in 1ml of Vectashield mounting medium (Vector Lab.)) was dotted onto the dried cells and sealed with a glass coverslip.

2.2.2 Fixation of cells expressing green fluorescent protein (GFP) and cyan fluorescent protein (CFP)

Cells in suspension were fixed by the addition of 0.1 volumes of 37% formaldehyde (Fisher Chemicals) for 10 minutes at their growth temperature, before being pelleted by centrifugation (3000r.p.m. for 1 minute) and washed 3 times in PBSA. 2μl of cell slurry was spread onto a microscope slide to form a monolayer of cells and dried at room temperature. 1μl of DAPI plus calcafluor was dotted onto the surface and covered with a glass coverslip, as above (section 2.2.1).

2.2.3 Image acquisition

Fluorescence microscopy was performed on Deltavision Spectris and RT systems containing a photometrics CH350L liquid cooled charge-coupled device camera and an Olympus IX70 inverted microscope with a 100x objective equipped with Deltavision data collection system (Applied Precision).

2.2.3.1 Fixed cells

Typically 18 images (0.2μm apart) were acquired and processed using the Softworx image processing suite (Applied Precision). Out of focus images were discarded prior to projecting the stack of images to one plane. Images were stored as 24 bit TIFF files and transferred to Photoshop (Adobe) to assemble figures. 3-dimensional cell reconstruction was performed using the Softworx application "volume viewer".

2.2.3.2 Live cells

Live analysis of cells was performed in an imaging chamber (CoverWell PCI-2.5; Grace Bio-Labs) filled with 1ml of 1% agarose in EMM medium with or

without 0.625μM or 1.25μM Latrunculin A and sealed with a 22 x 22mm glass coverslip. All time-lapse movies, unless otherwise indicated, were carried out at 30°C. Constant temperature conditions were maintained using a full enclosure incubation chamber (Solent Scientific Ltd.). Stacks of six Z-sections (0.6μm apart) were taken at each time point with exposure times of 1 second for both GFP and CFP with a 33% neutral density filter used to limit photobleaching. Images were taken every 30 seconds unless otherwise stated. Projected images were made for each time point followed by intensity adjustments and conversion to 24 bit TIFF files. Movie files were transferred to ImageReady (Adobe) for signal balancing throughout the movie and compression to QuickTime (Apple) format.

Apparent spindle length was corrected for Z-axis skewing in strains with fluorescently tagged spindle poles by counting the number of focal stacks that separate the poles (stacks are 0.6μm apart). This provides an estimate of Z-depth (d), whilst the projected image gives the flat spindle length (uncorrected length, l). Pythagoras's theorem was used to calculate spindle length (corrected spindle length $=\sqrt{(d^2 + l^2)}$). Measurement of spindle length and angle was performed using the SoftWorx image processing suite. Spindle elongation rate was calculated by dividing the distance that the spindle elongates in phase 3 by the time taken. Spindle orientation plots are illustrated as graphs, with 0° representing the longitudinal axis of the cell and with ± values used for the spindle angle so that movement past 0° can be shown. ± values are assigned to movies randomly so that a spread of plots either side of zero can be observed. The spreadsheet program Excel (Microsoft) was used throughout to record data extracted from time-lapse sequences and for the production of graphs.

2.3 Nucleic acid manipulation

2.3.1 Polymerase chain reaction (PCR)

PCR was carried out using an OmnE or Techne thermal cycler in accordance with the manufacturer's instructions. For amplification of DNA for cloning, gene disruptions and tagging, the Expand High Fidelity polymerase was used in accordance with the manufacturer's instructions. Diagnostic PCRs were carried

out using *Taq* polymerase (AB Technologies) according to the manufacturer's instructions. A typical 50μl PCR mix contained 1xPCR buffer (either Expand PCR buffer or *Taq* PCR buffer), 1.5mM $MgCl_2$, 200μM dNTPs, 3μM of each primer, 0.1-250ng template DNA, and the recommended units of enzyme. Oligonucleotides were manufactured by Genosys or Oswel (for a list of oligonucleotide primers used in this study see table 2.2) and were diluted to stock solutions of 1μg/μl.

2.3.2 Agarose gel electrophoresis

Agarose gel electrophoresis was carried out in 1% agarose (Invitrogen) gels in 1xTAE (40mM Tris base, 1mM EDTA and 20mM glacial acetic acid, pH8.3) with 1xTAE electrophoresis buffer. DNA was loaded with 1/6 volume DNA loading buffer (0.25% Bromophenol blue; 40% glycerol) and electrophoresed with a constant current of 60-100mA. DNA was stained by including ethidium bromide (Life Technologies) in the gel at a final concentration of 0.5μg/ml, and visualised on a UV transilluminator. The molecular size of DNA fragments was determined by comparison to DNA size markers (Invitrogen).

2.3.3 Recovery of DNA fragments from agarose gels

DNA was extracted from agarose gels using a "MinElute Gel Extraction Kit" (Qiagen, ref. 28604) according to the manufacturer's instructions.

2.3.4 Restriction endonuclease digestion and DNA modification

DNA was incubated with restriction endonucleases (New England BioLabs) and the appropriate buffers for 4 hours at 37°C. Calf intestinal phosphatase (Boehringer Mannheim) was used according to the manufacturer's instructions and removed after reaction by gel electrophoresis (section 2.3.2) and recovery of the fragment (2.3.3). Ligation of DNA fragments was carried out in a 10μl volume of 1x ligation buffer (50mM Tris/HCl pH7.5, 10mM $MgCl_2$, 10mM dithiothreitol (DTT), 1mM ATP and 25μg/ml bovine serum albumin (BSA)) and 0.4 unit of T4 DNA ligase (New England Biolabs). Ligations were incubated at room temperature for 4 hours.

Table 2.2 Oligonucleotide primers used in this study

Italics represent plasmid specific sequence, restriction sites are underlined and mutagenic bases are shown in bold.

Ref. No.	5'-3' Sequence	Function
1290	AGTTTTCATATCTTCCTTTATATTCTA TTAATTGAATTTCAAACATCGTTTTAT TGAGCTCATTTACATCAACCGGTTCA *CGGATCCCCGGGTTAATTAA*	*ase1* del.F
1291	CTTTTATGAATTATCTATATGCTGTAT TCATATGCAAAAATATGTATATTTAAA TTTGATCGATTAGGTAAATAAGAAGC *GAATTCGAGCTCGTTTAAAC*	*ase1* del.R
1292	TACTTTCGCAGGCCAAGCC	*ase1* 5'tester
1293	AGTCTTTTAATTATGACCTCAGT	*ase1* 3'tester
1056	ACATCTTCTTCTGGAGGCCG	*hygR* F
1057	CGGCCTCCAGAAGAAGATGT	*hygR* R
1355	TCAGCCATTAATTGTTCCCCATACGA TTTAATTGATATTCTATTGTTATTACCT GGTTAAGTCCGATATTTTAGCAATCA *CGGATCCCCGGGTTAATTAA*	*klp8* del.F
1356	TTTATATAATTGGTAACCTCTATTATT CAATCTAACAAGGAATCATGCCTTAA ACTCTCCATATCCATGTCTATATCAGA *GAATTCGAGCTCGTTTAAAC*	*klp8* del.R
1359	TCCGATTTTACTAACAATCCTAG	*klp8* 3' tester
1372	GGAAATCTAATTTTTAATCTTTCT	*klp8* 5'tester
177	GCTAGGATACAGTTCTCACATCACATCCG	*kanR* F
179	CGGATGTGATGTGAGAACTGTATCCTAGC	*kanR* R
1294	AGCAACTGTCTTCCAACACTTCCATCA TTCTTGTACACAAAGGATTGCTTTTAA GTCCCTTTAAACTCTGAAATTGACCA *CGGATCCCCGGGTTAATTAA*	*klp9* del.F
1295	TAAAACCATTAAGCCCCTCTCGACGCC CTCCGTTGACTTCTTTGTATAGTGGGAC AACTGATATCGATATTAATGAATTG *CGGATCCCCGGGTTAATTAA*	*klp9* tag.F
1296	CATGTGAAGGCAAGAGCTAAATATTAC TCAAATAAGAGTTATGAACACATTTTGC CATTCTTGGTAACTTTAATGATATA *GAATTCGAGCTCGTTTAAAC*	*klp9* del/tag.R

1297	CTATTTAACTAGATTGAACATTAC	*klp9* 5'tester
1298	CAAGAAGATCTTAAGGACTATC	*klp9* 3'tester
JP7	CAAAGATGATACATGCCGCAG	*mto1* del.w
JP8	*TTAATTAACCCGGGGATCCG* TAATCTGGATAGTTTGCGG	*mto1* del.x
JP9	*GTTTAAACGAGCTCGAATTC* AATTGATTAGAAAACGAAC	*mto1* del.y
JP10	CCGCAATTACAAGTCTACTAC	*mto1* del.z
JP11	GAGTACACGTTGTGCCTG	*mto1* 5'tester
JP12	CTAACACAAACATTAAACCTTC	*mto1* 3'tester
1342	GGGTGTATTGAAGGTACATAC	*leu1* 3' seq
1346	TACCAATTAAATCAGTACTGAAG	*RADA* 3'right
1347	CTCGCCGGT**GC**TG**C**CTTGACTGACTA	*RADA* 5'right
1348	TAGTCAGTCAAG**G**CA**GC**ACCGGCGAG	*RADA* 3'left
1349	AATAACGCGGAAATTATATTTCC	*RADA* 5'left
1351	GCTTCGTGTTGCTCCTGAG	*act1*.F internal
1352	GTAAGTAGCCTCATGAATACC	*act1*.R internal
1353	GACTCTGGTGA**G**GGTGTTACCCA	*D157E* 5'right
1354	TGGGTAACACC**C**TCACCAGAGTC	*D157E* 3'left
1365	CTAAGCTCCTCTTACTTTTTG	*act1*.5'upstrm
1366	AGCCAGTGGGATTTGTAGCTGAA ATATTTCTGTAACTTCAATATG	*act1*.3'dwnstrm
1369	TATATTCGATATCGTGAACTTTC	*act1* 5'forward
1370	CAGGAAAA<u>GAGCTC</u>CTTAATTTT TATGTTAATGATTATTC	*act1-Sac1 F*
1371	CAGG<u>ACGCGT</u>CGACCACTAATCA TAACCAATGTCTTAC	*act1-Sal1 R*
1374	CTCAGCCAGCCGTGTTATAACTTACCG TTTACCAACTACATTTTTTGTAACGAAC CAAAAAACCCTCAAAAGACAAGACC *GGATCCCCGGGTTAATTAAG*	*act1* del.F
1375	AAGATTGAAATTTATATATATCAGAA GAATCGATGTTATTCAAAAGTATGT AAAAAACGTTACAAAAAGTAAGAGGAGC *GAATTCGAGCTCGTTTAAAC*	*act1* del.R

2.3.5 DNA sequencing

DNA sequencing reactions were performed using the Big Dye DNA sequencing kit (Applied Biosystems) according to the manufacturer's instructions. DNA sequencing was carried out by the in-house sequencing facility at the National Institute for Medical Research. DNA sequence results were analysed using DNAStar.

2.4 Bacterial techniques

2.4.1 Bacterial strain

Escherichia coli strain DH5-α (suppE44 Δlac U169 (Φ80 lacZΔM15) hsdR17 endA1$^-$ thi-1 gyrA96 relA1) was used throughout.

2.4.2 Bacterial media

All media were autoclaved at 120°C 15p.s.i. for 10 minutes.
E.coli strains were grown in Luria-Bertani broth (LB):
1% Bacto-tryptone, 0.5% Bacto yeast extract, 1% NaCl, pH7.5.
LB Agar was made by adding 2% Bacto Agar (Difco) to LB liquid.
For the selection of all plasmids used in this study 100μg/ml ampicillin was added to LB media.

2.4.3 Bacterial growth conditions

Cells in liquid culture were incubated at 37°C in a New Brunswick gyratory shaker at 300r.p.m. Cells on agar plates were incubated at 37°C in a constant temperature incubator.

2.4.4 Bacterial storage conditions

Strains were grown to stationery phase in LB and stored at –80°C in 30% glycerol.

2.4.5 Bacterial transformation

2.4.5.1 Preparation of competent E.coli cells

A 200μl aliquot of an overnight culture of *E.coli* DH5-α was inoculated into 50ml of fresh LB medium and grown to an OD_{600} of 0.3-0.4 then cooled on ice and harvested (2500r.p.m. for 7 minutes at 4°C in a Sorvall benchtop centrifuge). Cells were washed twice in ice-cold 10ml $CaCl_2$ solution (60mM $CaCl_2$, 15% glycerol, 10mM PIPES; pH 7.0) before being resuspended in 2ml ice-cold $CaCl_2$ solution and either used immediately or stored at –80°C in 100μl aliquots.

2.4.5.2 Transformation of E.coli cells

A 100μl aliquot of competent *E.coli* DH5-α cells with 1-5μg of transforming DNA was incubated on ice for 10 minutes then heat-shocked at 42°C for 2 minutes. 1ml of LB was added and the cells incubated at 37°C for 1hr to allow cells to recover and express the *ampR* gene. An aliquot of cells was then plated onto selective LB agar plates containing 100μg/ml of ampicillin.

2.4.6 Isolation of plasmid DNA

Plasmid DNA was isolated from bacterial strains using a "Quantum Prep" plasmid mini-prep kit (Bio-Rad, ref. 732-6100) according to the manufacturer's instructions.

2.5 Strain construction

2.5.1 Deletion of genomic loci

Genes were deleted either by the one-step protocol described by Bahler *et al.* (1998b) or by a two-step process described by Krawchuk and Wahls (1999). Essentially, in both methods custom-made oligonucleotides are used to amplify a selective marker flanked by 5' and 3' non-coding sequence derived from the sequences immediately upstream and downstream of the open reading frame (ORF) of the target gene. The one-step method generates 80 base pairs of

flanking sequence whereas the two-step method generates 250 base pairs, thus improving the efficiency of gene replacement following transformation.

ase1::hygR

The single-step PCR-based insertion protocol was used to generate strains lacking Ase1. First, the HygR cassette was amplified from pFA6a-hphMX6 (Hentges *et al.*, 2005) using the oligos 1290 and 1291 (table 2.2). The 5' end of oligo 1290 contains 80 base pairs homologous to the 5' region immediately upstream of the *ase1* ORF followed by 20 nucleotides corresponding to the 5' region of the HygR cassette. Oligo 1291 contains 80 base pairs of homology to the complementary strand at the 3' region immediately downstream of the *ase1* ORF followed by 20 nucleotides corresponding to the 3' region of the HygR cassette. This amplified cassette was then transformed into the wild type strains JM100 and JM109 (table 2.1). Stable integrants were selected by first spreading the transformed cells onto YES agar plates and, following growth at 30°C for 24 hours, replica plating onto YES plus Hygromycin B plates. Integration of the cassette at the correct locus was confirmed by the generation of the correct size of PCR products using oligo 1292 (5' sequence upstream of integration site) with 1057 (reverse oligo internal to *hygR*), and oligo 1293 (3' sequence downstream of integration site) with 1056 (forward oligo internal to *hygR*) (table 2.2).

klp8::kanR

Deletion strategy as for *ase1::hygR* except that the kanR cassette was amplified from plasmid pFA6a-KanMX6 (Bahler *et al.*, 1998b) using the oligos 1355 and 1356 (table 2.2) which contain 5' and 3' regions of klp8 immediately flanking the ORF fused to sequences from the KanR cassette. The cassette was transformed into the wild type strain JM109 and integrants selected for by G418 resistance (as above for Hygromycin B resistance). Integration was confirmed by PCR using oligo 1372 with 179 and oligo 1359 with 177 (table 2.2).

klp9::hygR and klp9::KanR

Deletion strategy as for *ase::hygR* and *klp8::kanR* except using oligos 1294 with 1296 (table 2.2). Integrated deletions were checked using oligo 1297 with either 179 (*kanR*) or 1057 (*hygR*) and oligo 1298 with either 177 (*kanR*) or 1056 (*hygR*) (table 2.2).

mto1::hygR

Strains lacking Mto1 were generated using a two-step PCR-based insertion protocol (Krawchuk and Wahls, 1999). In the first stage, using genomic library as a template (Barbet *et al.*, 1992), primer pairs JP7 and JP8, and JP9 and JP10 (table 2.2) were used in 2 separate PCRs to amplify 250 base pair regions 5' and 3' of the *mto1* locus. The 5' ends of oligos JP8 and JP9 contain sequence complementary to the 5' and 3' region of the HygR cassette respectively. The products of the first stage were purified by gel extraction (section 2.3.3) and used in a second PCR with JP7 and JP10 to amplify the HygR cassette from pFA6a-hphMX6 (Hentges *et al.*, 2005) containing the 250 base pair *mto1* flanking sequences. This product was gel purified and transformed (section 2.1.6) into the wild type strains JM100 and JM109 (table 2.1). Stable integrants were selected for Hygromycin B resistance as above. Integration of the cassette at the correct locus was confirmed PCR using oligo JP11 with 1057 and oligo JP12 with 1056 (table 2.2).

2.5.2 C-terminal tagging of genomic loci

klp9-gfp:kanR

klp9 was endogenously tagged with GFP(S65T) using the single-step PCR-based approach. First, the GFP tag was amplified from plasmid pFA6a-GFP(S65T)-KanMX6 (Bahler *et al.*, 1998b) using oligos 1295 and 1296 (table 2.2). 1295 contains the final 80 base pairs of the gene with the exception of the stop codon to allow read through of the GFP protein. 1296 contains homology approximately 200bp 3' of the *klp9* locus. This amplified cassette was then gel purified and transformed into PR100 and colonies selected for growth on G418 as above. Integrants were confirmed by PCR with oligos 1298 and 177.

2.5.3 Latrunculin A-insensitive actin strain construction

(a) *act1::hygR leu1:act1*
(b) *act1::hygR leu1:act1-R183A,D184A*
(c) *act1::hygR leu1:act1-D157E*

The above strains were constructed stepwise as follows:

Construction of pJK148-act1$^+$

First, full-length *act1*$^+$ (~2620bp, open reading frame plus ~760bp upstream and ~730 downstream sequence) was amplified (Expand) using oligos 1370 and 1371, which incorporate *Sac1* and *Sal1* tails, respectively. The product was cloned into *Sac1-Sal1*-cut pJK148 (Keeney and Boeke, 1994) and transformed into bacteria (section 2.4.4). Bacterial colonies were selected for ampicillin resistance and the plasmid insert verified by sequencing with oligos 1347, 1349, 1351, 1352, 1354, 1365 and 1366.

Construction of pJK148-act1(R183A,D184A) and pJK148-act1(D157E)

The actin R183A,D184A (RADA) mutation was amplified from genomic DNA (JM100) using a 2-step mutagenic PCR process. In the first step, oligos 1346 and 1347 and oligos 1348 and 1349 were used to amplify the right (~1150bp) and left (~940bp) mutagenic arms of the product. The mutagenic arms were then used to prime each other in a secondary PCR which was further amplified with the 1346 and 1349 end oligos to generate a ~2070 full-length product. This was then cut with *SacII* and *BamHI* and the ~1300bp fragment gel purified before being used to replace the equivalent *SacII-BamHI* cassette in pJK148-act1$^+$. Exactly the same strategy was used to generate pJK148-act1(D157E) except that oligos 1347 and 1348 were replaced with oligos 1353 and 1354 and the left and right primary products were approximately 870bp and 1230bp respectively.

To verify the mutations in both pJK148-act1(R183A,D184A) and pJK148-act1(D157E), the *SacII-BamHI* inserts were completely sequenced using oligos 1351, 1352 and 1369.

Transformation of strain *act1-188^{ts}*

The *act1+* and *act1* mutant alleles were integrated at the *leu1* locus as follows: pJK148 plasmid control together with pJK148-act1^{+} and both mutant variants were cut to completion with *HindIII* and used to transform *S.pombe* strain JM1315 (*act1-188^{ts} ndc80-gfp:kanR cdc11-cfp:kanR leu1-32 ura4-D18* h-) to *leu1^{+}*. Transformants were selected on EMM medium lacking leucine and checked for stability. Strains were then grown at 33.5°C to verify that the wild type and both mutant alleles of *act1*, but not the control, were able to rescue the temperature-sensitivity of *act1-188^{ts}* (figure 2.1).

Removing the *act1-188^{ts}* allele

The *act1-188^{ts}* allele was then deleted and replaced by a hygromycin cassette using the method from Bahler and colleagues (1998b). The HygR sequences flanked by 5' and 3' act1 non-coding sequence cassette were amplified from pFA6a-hphMX6 (Hentges *et al.*, 2005) using the oligos 1374 and 1375. All three strains (JM3388, JM3389 and JM3390; table 2.1) were then transformed to HygR (section 2.1.6) and stable colonies tested for growth at 33.5°C. Temperature sensitive transformants were discarded as they were judged to have been converted at the *act1:leu1* locus rather than at the *act1-188^{ts}* locus. Finally, the position of the three *act1* alleles in each of the three strains (i.e. nested within the *leu1* locus) was confirmed by PCR using oligos 1365 and 1342.

2.6 Bioinformatics

2.6.1 BLAST searches

BLAST searches were performed using the NCBI (www.ncbi.nlm.gov) and the Sanger Centre (www.sanger.ac.uk) sequence databases.

2.6.2 Sequence alignment

Sequence alignments were performed using DNAStar megalign programme (cluster method).

act1-188 ndc80-gfp cdc11-cfp pJK148

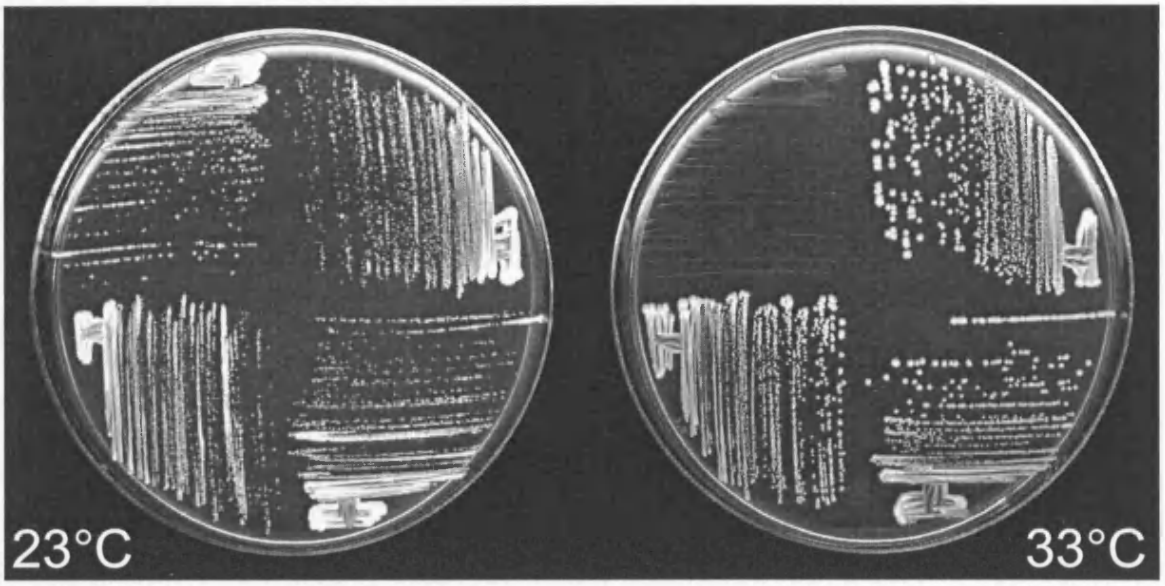

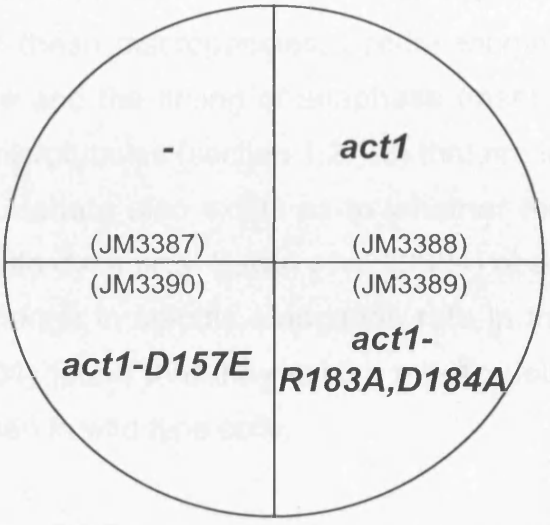

Figure 2.1 *act1*, *act1-R183A,D184A* and *act1-D157E* rescue *act1-188^{ts}* at restrictive temperature

Vector PJK148 either empty or containing *act1^{+}*, *act1-R183A,D184A* or *act1-D157E* was integrated at the *leu1* locus of JM3315 (*act1-188^{ts} ndc80-gfp cdc11-cfp*). The top panel shows the strains as annotated in the schematic below at both permissive (23°C) and restrictive (33°C) temperature for the *act1-188^{ts}* allele. Strain names are given in brackets.

Chapter 3

Relationship between spindle angle and the timing of anaphase onset in fission yeast

3.1 Introduction

It has been previously suggested that in *S.pombe*, mitotic spindle orientation is monitored by a checkpoint that delays anaphase onset if the spindle is mis-orientated by more than 30° from the longitudinal axis of the cell (spindle orientation checkpoint (SOC); section 1.3.2.2.2). Several groups have examined the relationship between spindle orientation and mitotic progression by the use of pharmacological agents, such as Lat A, or genetic mutants (Gachet *et al.*, 2001, 2004; Oliferenko and Balasubramabian, 2002; Rajagopalan *et al.*, 2004; Tournier *et al.*, 2004). These different approaches have led to some discrepancies in the literature (summarised in section 1.3.2.2.2). To resolve these discrepancies, I re-investigated the relationship between spindle angle and the timing of anaphase onset using *mto1D* cells, which lack the astral microtubules (section 1.2.1.3) that are implicated in spindle orientation. However, debate also exists as to whether the absence of Mto1 influences mitotic spindle dynamics. Sawin *et al.* (2004) observed no delay over anaphase onset or change in spindle elongation rate in these cells, whereas Venkatram *et al.* (2004) found that they exhibit mitotic delay and that spindle elongation is slower than in wild type cells.

Previous studies on the SOC have primarily been based on cell populations. For this reason, I decided to use a time-lapse assay to simultaneously monitor both length and angle of the spindle in individual cells (figure 3.1). This approach requires fluorescently-tagging either the spindle itself or components of the mitotic machinery from which length and angle of the spindle can be calculated. I decided to utilise both approaches in parallel. To visualise the spindle, I used a strain containing fluorescently-tagged tubulin expressed from a thiamine inducible promoter (*lys1:nmt1-atb2-gfp*). In parallel, I used *ndc80-gfp cdc11-cfp* cells in which Ndc80, a constitutive component of the kinetochore, is

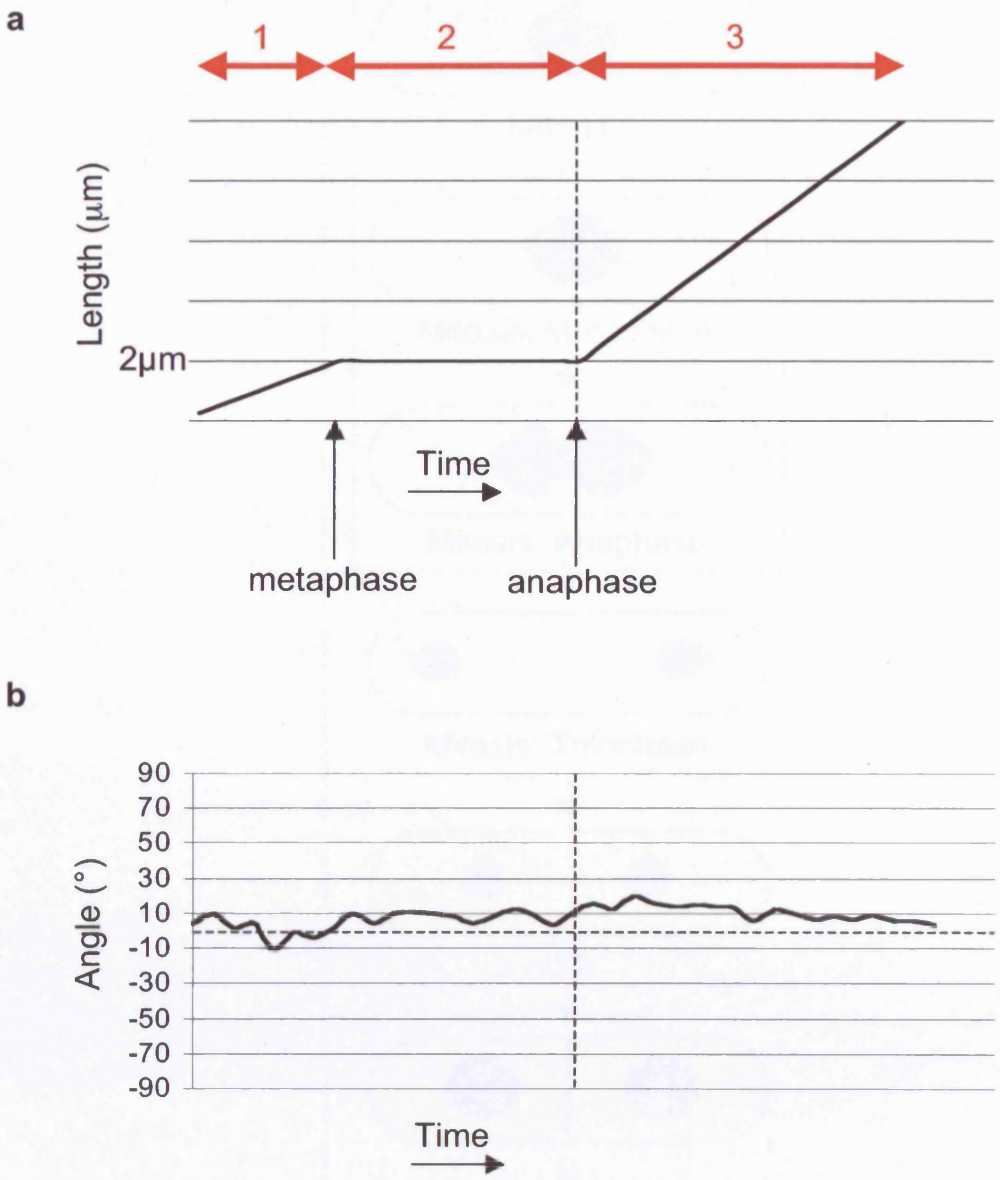

Figure 3.1 Profile of mitotic spindle dynamics

(**a**) Graph representing the elongation dynamics of the mitotic spindle over time. Spindle extension can be split into 3 distinct phases with a characteristic 2 micron plateau (Phase 2) separating 2 growth phases (Phases 1 and 3).
(**b**) Graph showing a typical plot of the angle of a wild type mitotic spindle over the same time. 0° represents the longitudinal axis of the cell.

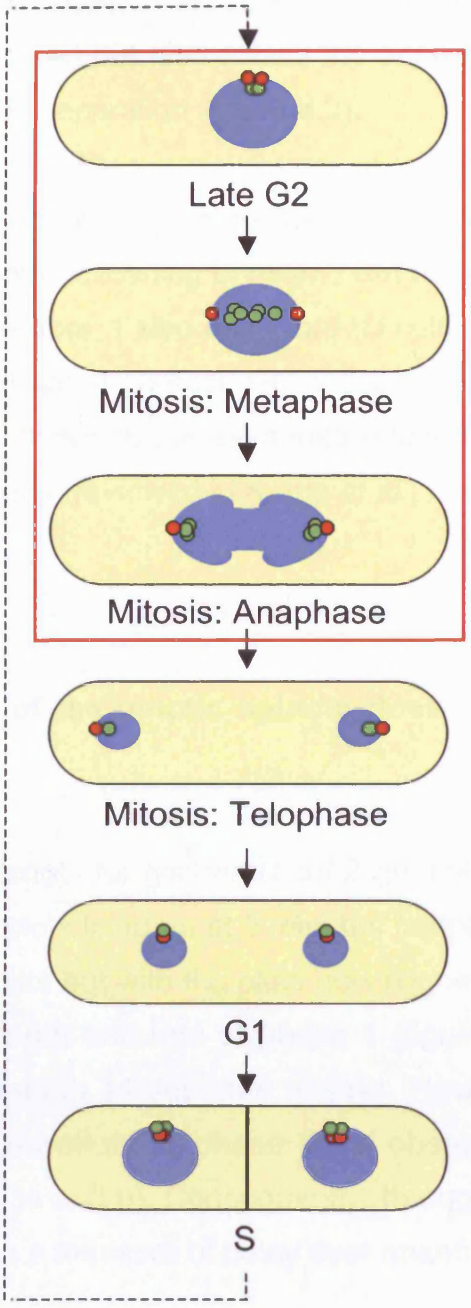

Figure 3.2 Positioning of spindle pole bodies and kinetochores throughout the cell cycle

A schematic representation of *ndc80-gfp cdc11-cfp* cells progressing through the various stages of the cell cycle, G1, S, G2 and Mitosis. Ndc80-GFP identifies kinetochores shown in green and Cdc11-CFP identifies spindle pole bodies (SPBs) in red. Nuclei are blue. The boxed section is the portion of the cell cycle under investigation in this study.

tagged with GFP, and Cdc11, a constitutive component of the SPB, is tagged with CFP (Tournier *et al.*, 2004). The latter strain not only allows spindle length and angle to be determined but also allows the accurate determination of the timing of sister chromatid separation (figure 3.2).

Astral microtubule disruption in *S.cerevisae*, *via* the addition of nocadazole, leads to a loss of asymmetric loading of mitotic exit network (MEN) components (section 1.3.2.2.1). Therefore, I also used *mto1D* cells to examine whether the proposed asymmetrical astral contact with the cortical-actin ring in *S.pombe* (Gachet *et al.*, 2004) influences the asymmetric loading of septation initiation network (SIN) components (reviewed in Krapp *et al.*, 2004) in fission yeast.

3.2 Results

3.2.1 Mis-orientation of the mitotic spindle does not delay the onset of anaphase

I have plotted spindle length for *lys1:nmt1-atb2-gfp* cells in two different ways. Figure 3.3a shows the plots lined up at 0 minutes (mitotic entry) whereas figure 3.3b shows the same data but with the plots now aligned at the end of phase 2. This shows that the length and rate of phase 1 (figure 3.3a) and of phase 3 (figure 3.3b) are invariant in 14 separate assays. However, significant cell-to-cell variation in the duration of phase 2 is observed even at constant temperature (figures 3.3a and b). Consequently, throughout this work I present the length of phase 2 as a measure of delay over anaphase onset.

To examine the effect of loss of Mto1 on spindle orientation and anaphase onset, I first utilised strains in which tubulin is fluorescently tagged (*lys1:nmt1-atb2-gfp*). In this assay, *mto1D* cells remain in phase 2 for 11 ± 2.5 minutes whilst the control is 9 ± 2.5 minutes (figures 3.4a-d). The length of phase 2 in cells lacking Mto1 is not significantly longer when compared to control cells. However, both strains have a significantly shorter phase 2 compared to cells lacking Dam1, which are known to undergo a SAC-mediated delay over anaphase onset (Sanchez-Perez *et al.*, 2005). The average length of phase 2 in *dam1D* cells is 24 ± 10.5 minutes (figure 3.4c and d). Using data from the same

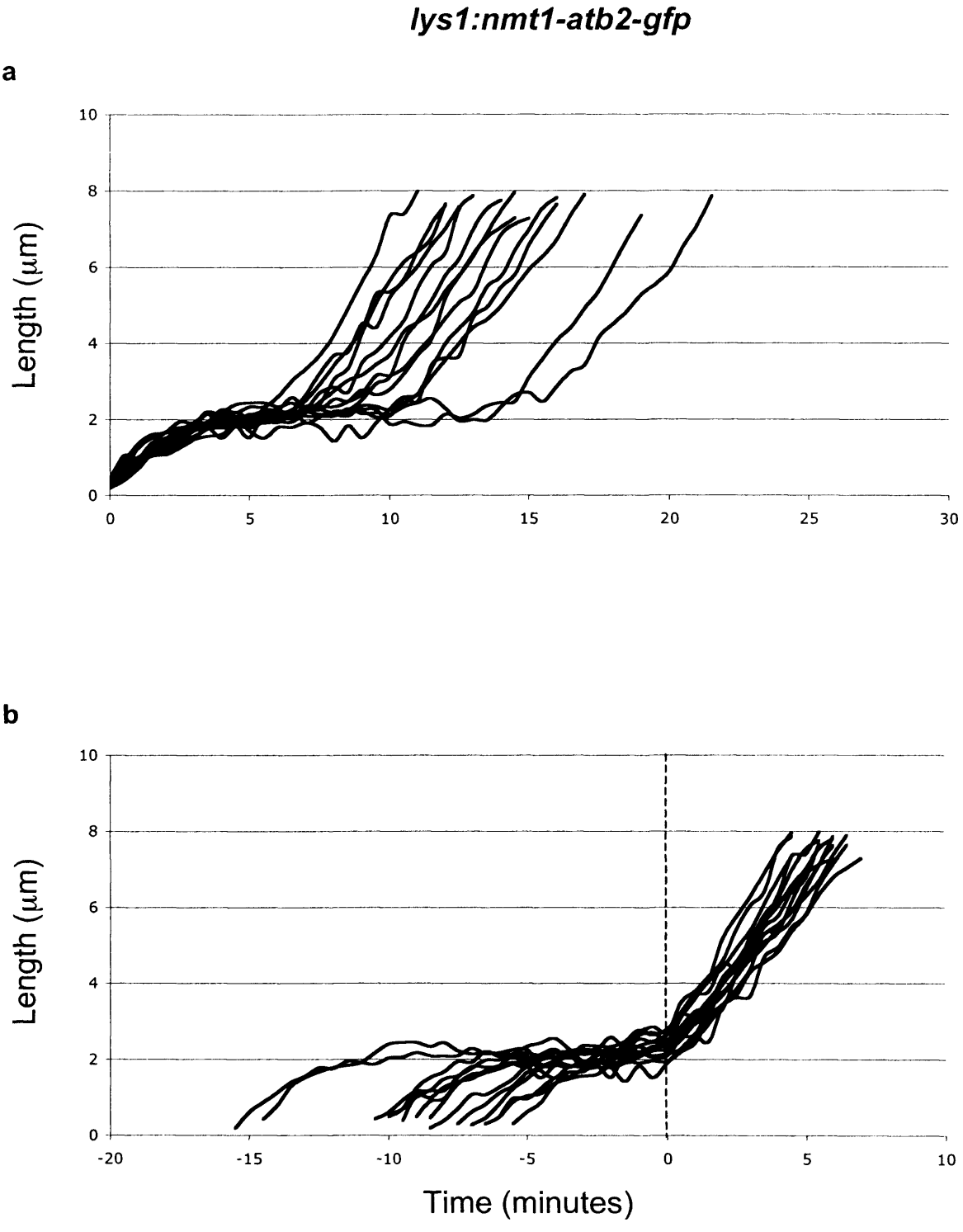

Figure 3.3 Phase 2 is variable whereas phases 1 and 3 are invariant

(**a**) Graph showing the spindle length of 14 *lys1:nmt1-atb2-gfp* cells aligned at mitotic onset.
(**b**) Graph showing the same data as (a) aligned at the end of phase 2.

cells, and shown in figure 3.5, cells lacking Mto1, however, have significantly mis-orientated spindles. *mto1D* cells exit phase 2 with an average spindle angle of 29 ± 5° compared to 18 ± 4° for the control strain and 15 ± 3° for *dam1D* cells (figure 3.5a-d). Strikingly, *mto1D* cells are severely mis-oriented when compared to the control strain but do not undergo any phase 2 delay.

As well as comparing spindle length and angle dynamics between different strains, I also analysed whether there is any correlation between these variables within each strain. In order to test for a correlation, Pearson's correlation co-efficient was calculated for all 3 strains for spindle angle versus length of phase 2. As with the inter-strain comparison it is apparent that whilst length of phase 2 varies significantly from cell to cell within each strain there is no correlation between this and spindle mis-orientation.

I next examined spindle orientation and anaphase onset in cells in which SPBs and kinetochores were fluorescently tagged (*ndc80-gfp cdc11-cfp* (*wild type*) and *mto1D ndc80-gfp cdc11-cfp* (*mto1D*)). Figure 3.6 is a series of time-lapse images showing these organelles in representative movies (movies 3.1 and 3.2) of single *wild type* (a) and *mto1D* (b) cells. Figure 3.6a shows that the *wild type* cell enters mitosis with the spindle parallel to the longitudinal axis of the cell. The end of anaphase A occurs at 660 seconds. Figure 3.6b shows an *mto1D* cell, which undergoes mitosis with the spindle almost perpendicular to the longitudinal axis of the cell. The end of anaphase A takes place at 630 seconds. Measurements of spindle length and angle were taken from 29 *wild type* cells and 20 *mto1D* cells and the results plotted in figures 3.7 and 3.8 respectively. When using these strains, graphs relating to spindle length are aligned precisely at the end of anaphase A, which is possible due to the presence of fluorescently labelled kinetochores. Figure 3.7 a, b and c show that *mto1D* cells have an average phase 2 of 12 ± 2.5 minutes that is statistically unchanged from the control, which have a phase 2 of 11 ± 3 minutes. By comparison, *mal3D ndc80-gfp cdc11-cfp* (*mal3D*) cells have a longer phase 2 (19 ± 8 minutes) than control cells (figure 3.7 a, b and d). Cells lacking Mal3 have previously been shown to have a delay over anaphase onset (Asakawa *et al.*, 2005). Despite this *mto1D* cells are significantly mis-orientated at the end of phase 2 (34 ± 4°) compared to *wild type* (17 ± 3°) or *mal3D* cells (16 ± 2°)

Figure 3.4 *lys1:nmt1-atb2-gfp* cells lacking Mto1 show no mitotic delay

Graphs representing multiple time-lapse movies of (**a**) *lys1:nmt1-atb2-gfp* (*atb2-gfp*) cells (n=14) (**b**) *mto1D lys1:nmt1-atb2-gfp* (*mto1D atb2-gfp*) cells (n=22), and (**c**) *dam1D lys1:nmt1-atb2-gfp* (*dam1D atb2-gfp*) cells (n=14) showing the length of the mitotic spindle through time. Plots are aligned at the end of phase 2 (dashed line).
(**d**) Histogram showing the average length of phase 2 in (a), (b) and (c) above. Error bars show standard error.

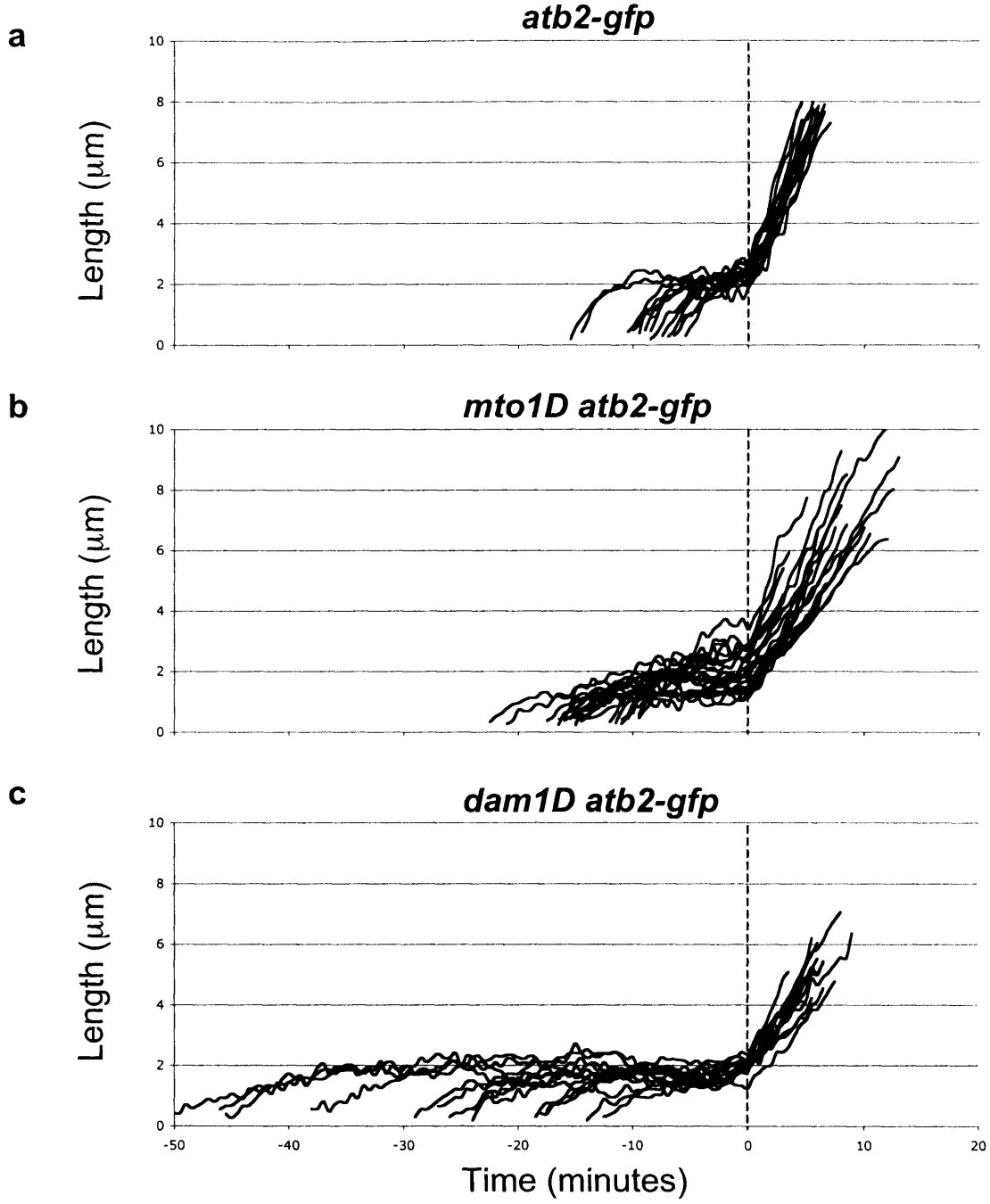
a
atb2-gfp
Length (μm)
b
mto1D atb2-gfp
Length (μm)
c
dam1D atb2-gfp
Length (μm)
Time (minutes)
d
Time (minutes)
atb2-gfp
mto1D atb2-gfp
dam1D atb2-gfp

Figure 3.5 *lys1:nmt1-atb2-gfp* cells lacking Mto1 show severe mis-orientation of the mitotic spindle

Graphs representing multiple time-lapse movies of (**a**) *lys1:nmt1-atb2-gfp* (*atb2-gfp*) cells (n=14) (**b**) *mto1D lys1:nmt1-atb2-gfp* (*mto1D atb2-gfp*) cells (n=22), and (**c**) *dam1D lys1:nmt1-atb2-gfp* (*dam1D atb2-gfp*) cells (n=14) showing the angle of the mitotic spindle relative to the longitudinal axis of the cell through time. Plots derived from the same data set as for figure 3.4.
(**d**) Histogram showing average angle of spindle at the end of phase 2 in (a), (b) and (c) above. Error bars show standard error of the mean (SEM).

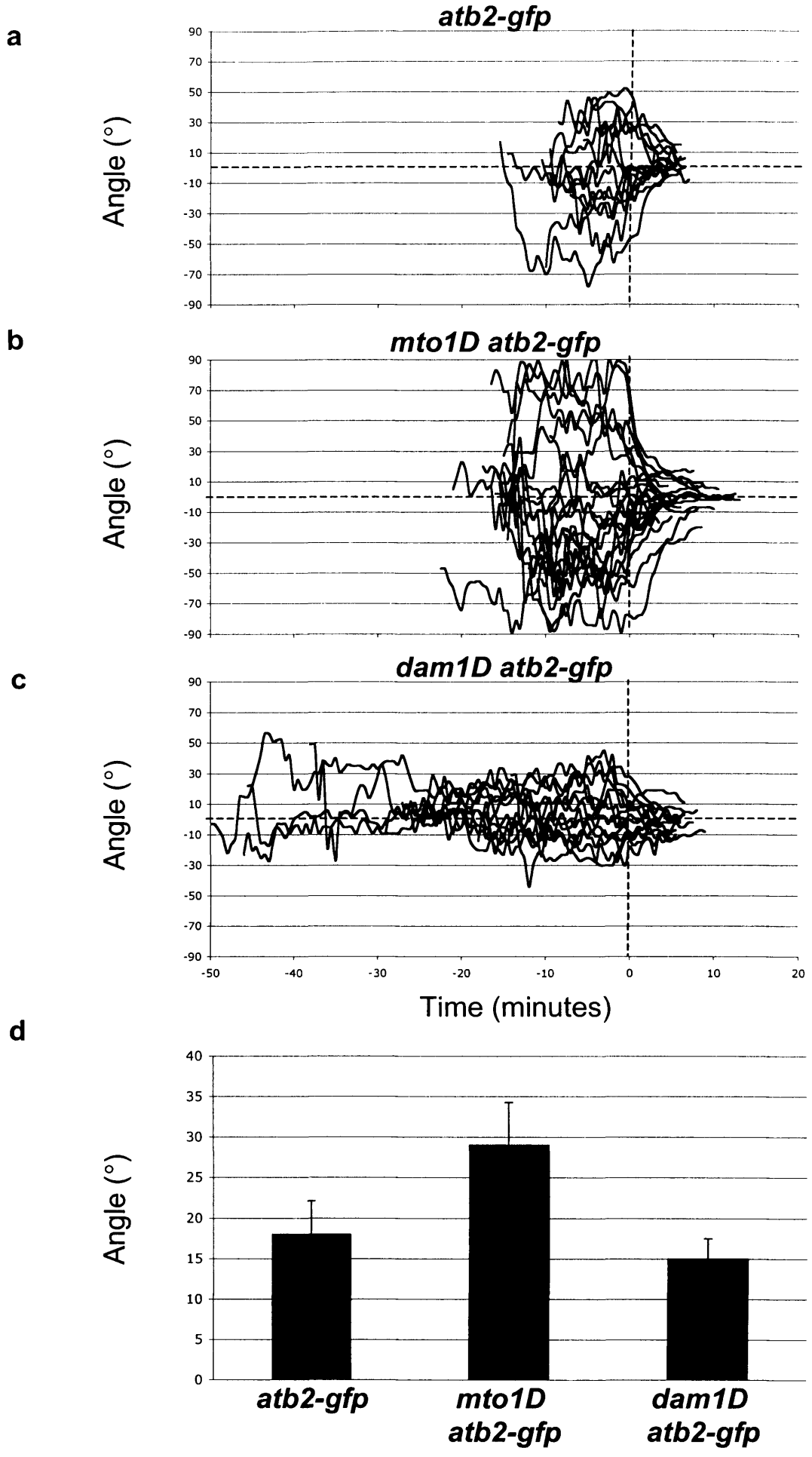
a
atb2-gfp
Angle (°)
b
mto1D atb2-gfp
Angle (°)
c
dam1D atb2-gfp
Angle (°)
Time (minutes)
d
Angle (°)
atb2-gfp
mto1D atb2-gfp
dam1D atb2-gfp

Figure 3.6 *mto1D ndc80-gfp cdc11-cfp* cells show severe mis-orientation, but no delay over anaphase onset

The upper series of frames (**a**) shows images from a time-lapse movie of a cell expressing Ndc80-GFP (marking the kinetochores, red) and Cdc11-CFP (marking the SPBs, green). Time is shown in seconds. Phase 1 occurs between 0-120 seconds, phase 2 between 150-630 seconds and phase 3 between 660-1110 seconds. The end of anaphase A (arrow) occurs at 660 seconds. The lower series (**b**) shows an *mto1D* cell in the same background. Phase 1 occurs between 0-150 seconds, phase 2 between 180-630 seconds and phase 3 between 660-1110 seconds. The end of anaphase A (arrow) occurs at 630 seconds.

a

ndc80-gfp cdc11-cfp

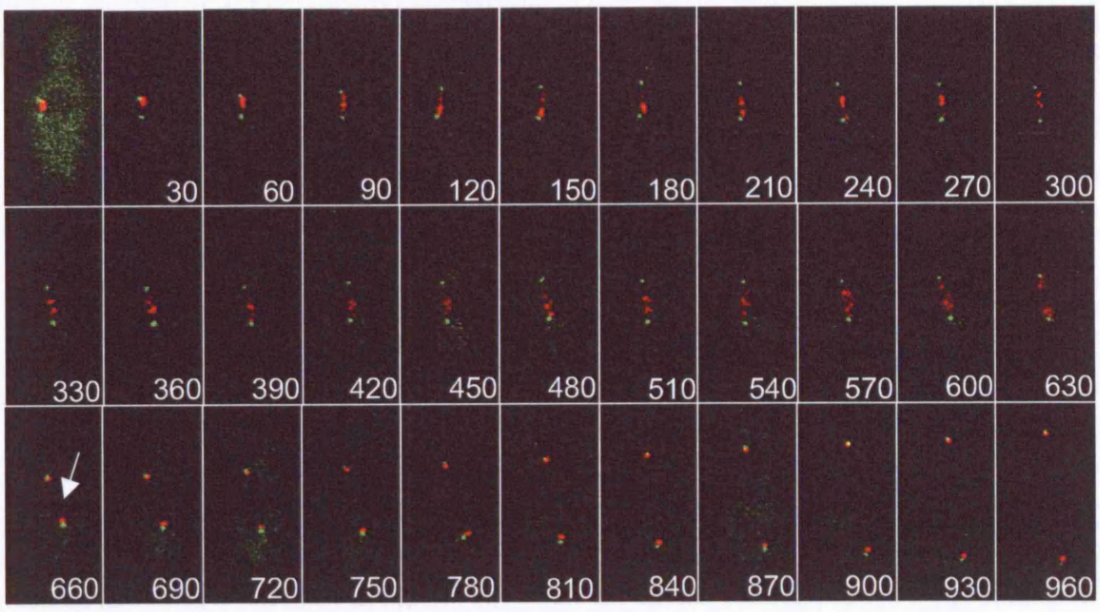

b

mto1D ndc80-gfp cdc11-cfp

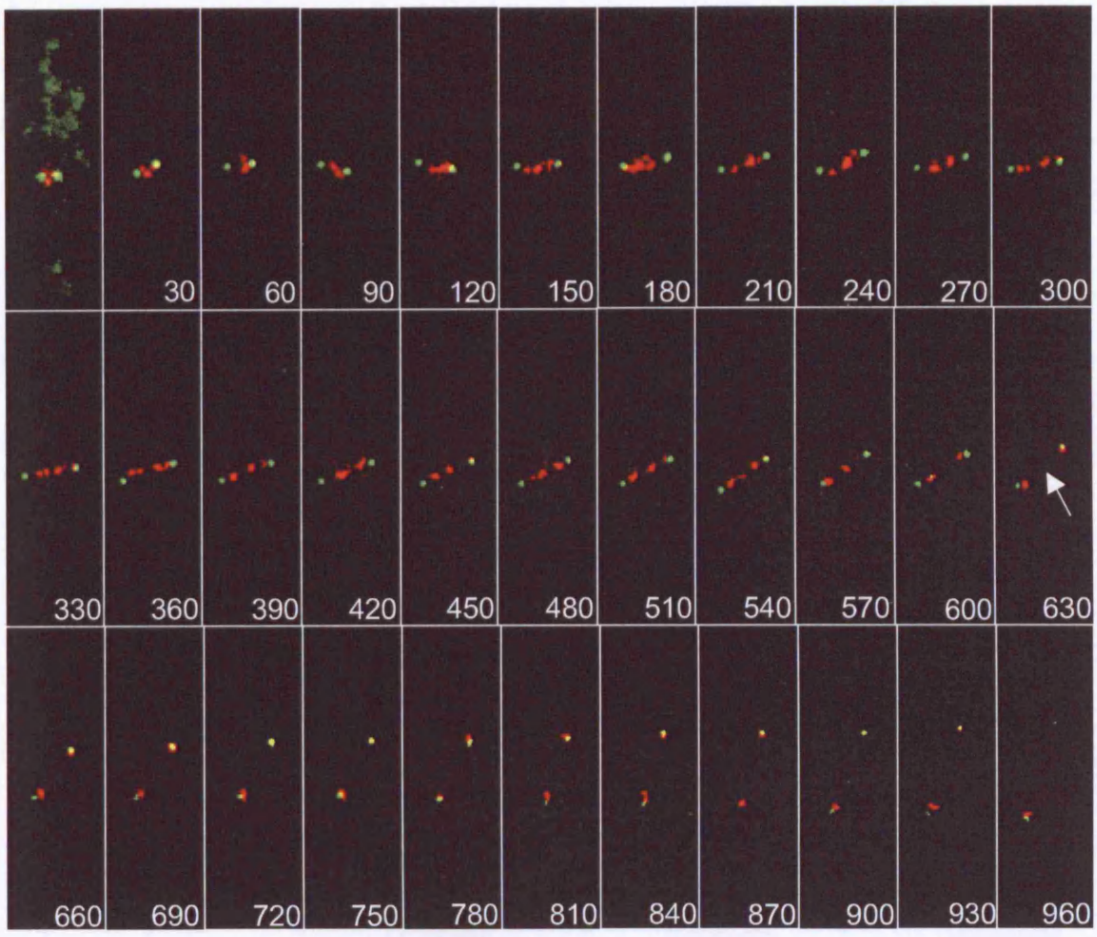

Figure 3.7 *ndc80-gfp cdc11-cfp* cells lacking Mto1 show no mitotic delay

Graphs representing multiple time-lapse movies of (**a**) *ndc80-gfp cdc11-cfp* (*wild type*) cells (n=29) (**b**) *mto1D ndc80-gfp cdc11-cfp* (*mto1D*) cells (n=20), and (**c**) *mal3D ndc80-gfp cdc11-cfp* (*mal3D*) cells (n=18) showing the length of the mitotic spindle through time. Plots are aligned at the end of anaphase A (dashed line).
(**d**) Histogram showing the average length of phase 2 in (a), (b) and (c) above. Error bars show standard error.

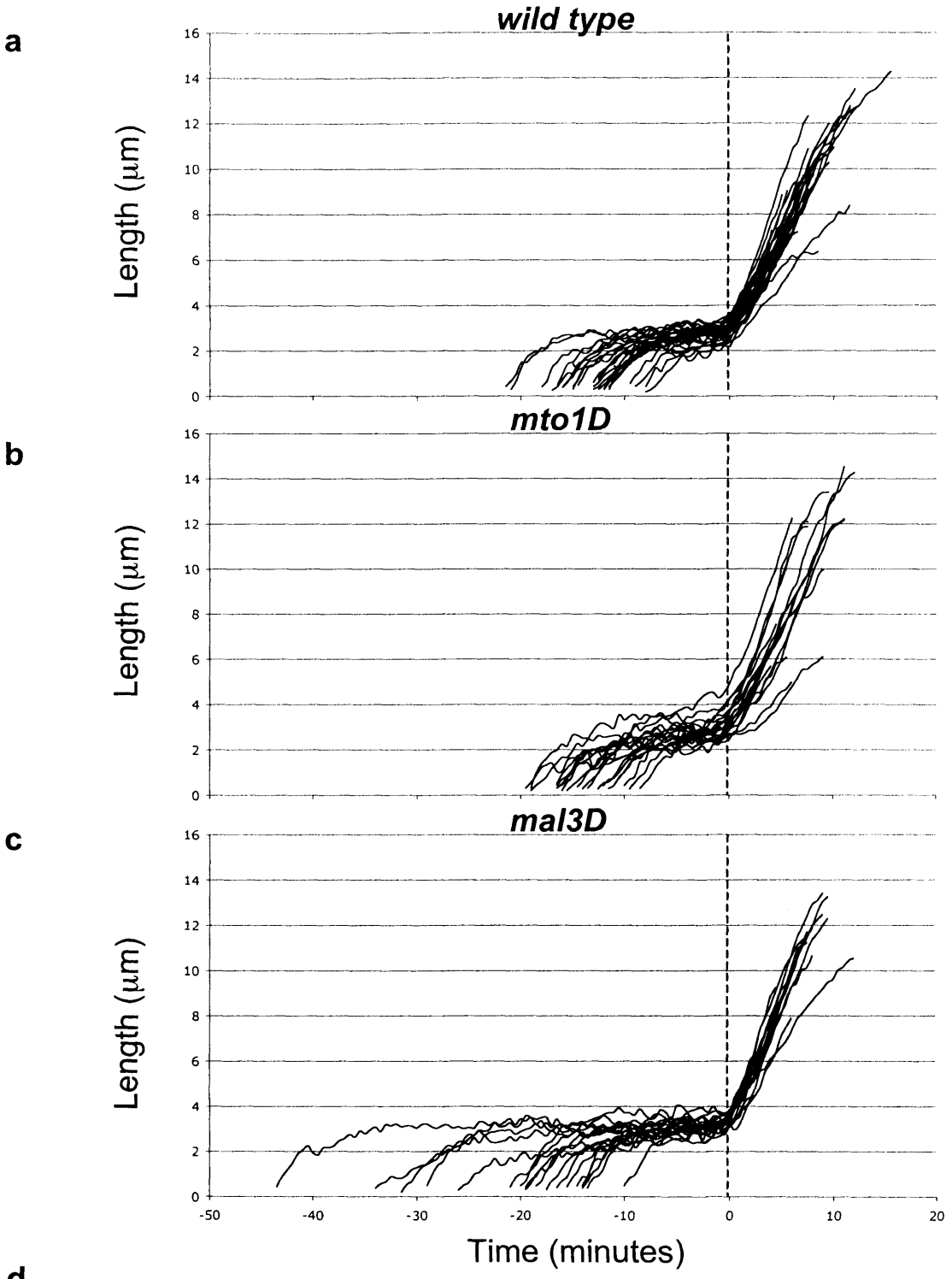
a
wild type
Length (μm)
b
mto1D
Length (μm)
c
mal3D
Length (μm)
Time (minutes)
d
Time (minutes)
wild type
mto1D
mal3D

Figure 3.8 *ndc80-gfp cdc11-cfp* cells lacking Mto1 show severe mis-orientation of the mitotic spindle

Graphs representing multiple time-lapse movies of (**a**) *ndc80-gfp cdc11-cfp* (*wild type*) cells (n=29) (**b**) *mto1D ndc80-gfp cdc11-cfp* (*mto1D*) cells (n=20), and (**c**) *mal3D ndc80-gfp cdc11-cfp* (*mal3D*) cells (n=18) showing the angle of the mitotic spindle relative to the longitudinal axis of the cell through time. Plots are derived from the same data set as for figure 3.7.
(**d**) Histogram showing average angle of the spindle at the end of phase 2 in (a), (b) and (c) above. Error bars show standard error of the mean (SEM).

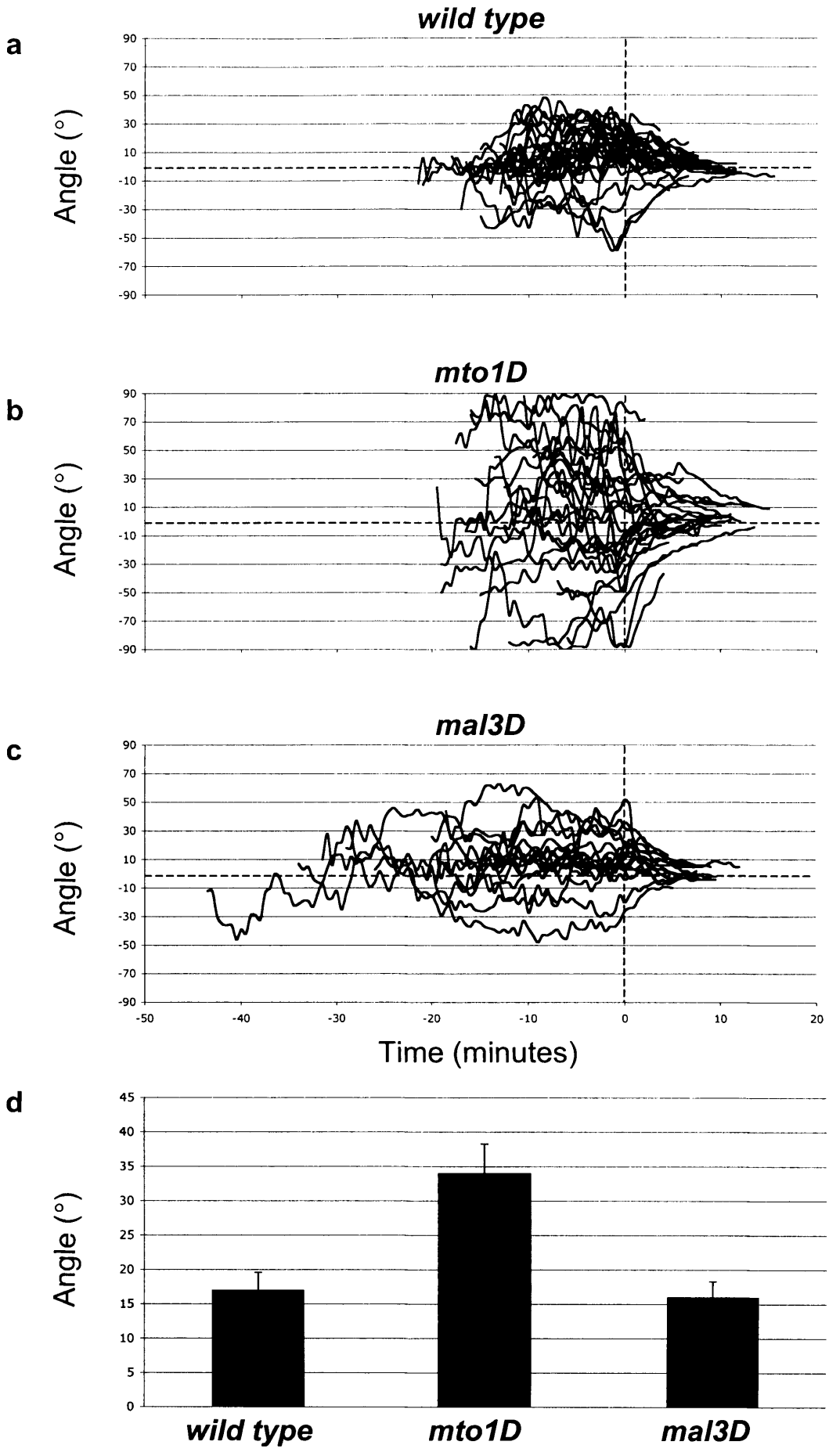
a
wild type
Angle (°)
90
70
50
30
10
-10
-30
-50
-70
-90
b
mto1D
Angle (°)
c
mal3D
Angle (°)
-50
-40
-30
-20
-10
0
10
20
Time (minutes)
d
Angle (°)
45
40
35
30
25
20
15
10
5
0
wild type
mto1D
mal3D

(figure 3.8a-d). I also analysed these data sets for any intra-strain correlation between spindle orientation and length of phase 2 by the application of Pearson's correlation co-efficient, which revealed no positive association.

The above experiments were carried out at 30°C. I decided to repeat my analysis at 26°C (figure 3.9), as Gachet *et al.* (2004) and Tournier *et al.* (2004 conducted their experiments at 25°C and 28°C respectively. Although there is an overall increased length of phase 2 at 26°C, there is no significant difference in the length of phase 2 between cells lacking Mto1 (18 ± 5.5 minutes) and the control (18.5 ± 4.5 minutes) (figures 3.9a and b). The level of mis-orientation at the end of phase 2 is also not affected by the change in temperature in either strain, with *mto1D* cells still significantly more mis-orientated (29 ± 8°) than the control cells (15 ± 3°) (figure 3.9c).

I conclude that there is no correlation between spindle angle and the timing of anaphase onset.

3.2.2 Astral microtubules do not effect the rate of spindle elongation

It has been suggested that astral microtubules play a role in elongating the mitotic spindle in phase 3 (section 1.2.1.3). I have analysed the rate of spindle elongation in both the astral-less *mto1D ndc80-gfp cdc11-cfp* strain and the equivalent *mto1*$^{+}$ control at both 30°C and 26°C (figure 3.10). Results show that in *mto1*$^{+}$ cells at 30°C the spindle elongates at 0.82 ± 0.19μm/minute compared to 0.84 ± 0.24μm/minute in cells lacking Mto1 at the same temperature (figure 3.10a). At 26°C the rates of spindle elongation for *mto1*$^{+}$ and *mto1D* are 0.66 ± 0.07μm/minute and 0.68 ± 0.22μm/minute, respectively (figure 3.10b). Therefore the absence of astral microtubules does not change the rate of spindle elongation at either temperature.

3.2.3 A proportion of cells lacking Mto1 have unclustered kinetochores

Careful analysis of *mto1D ndc80-gfp cdc11-cfp* cells revealed a novel phenotype. In control cells, the 6 kinetochores are held together at the nuclear envelope in close proximity to the SPBs, known as the Rabl configuration.

Figure 3.9 *mto1D* cells exhibit significant mis-orientation of the mitotic spindle but no difference in the timing of mitosis at 26°C

Graphs representing multiple time-lapse movies at 26°C of (**a**) *ndc80-gfp cdc11-cfp* (*wild type*) cells (n=10) and (**b**) *mto1D ndc80-gfp cdc11-cfp* (*mto1D*) cells (n= 9) showing the length of the mitotic spindle through time. Plots are aligned at the end of anaphase A (dashed line).
(**c**) Histogram showing the average angle of the mitotic spindle relative to the longitudinal axis of the cell at the end of phase 2 for the cells shown in (a) and (b). Error bars show standard error.

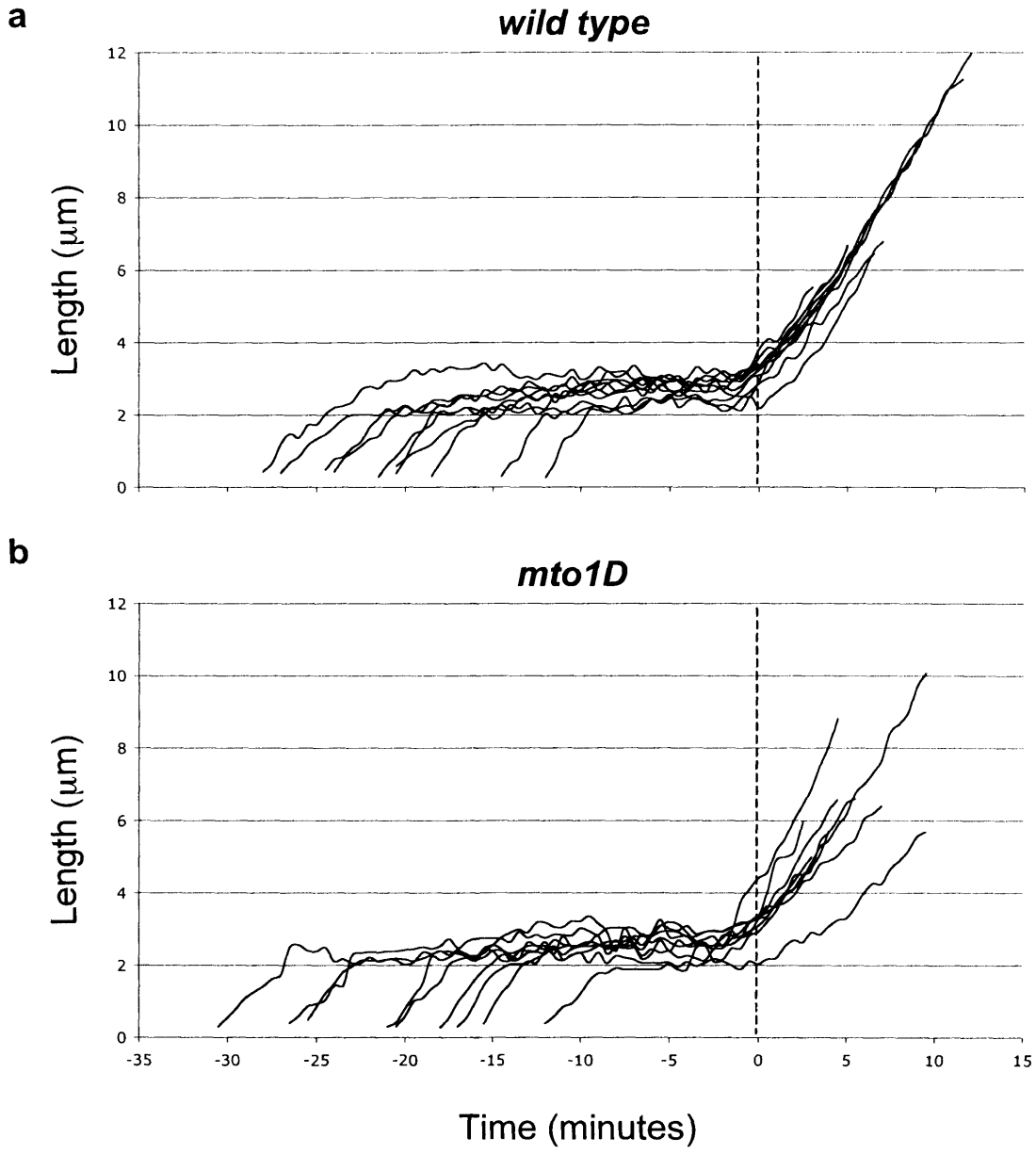
a
wild type
Length (μm)
0
2
4
6
8
10
12
b
mto1D
Length (μm)
0
2
4
6
8
10
12
-35
-30
-25
-20
-15
-10
-5
0
5
10
15
Time (minutes)

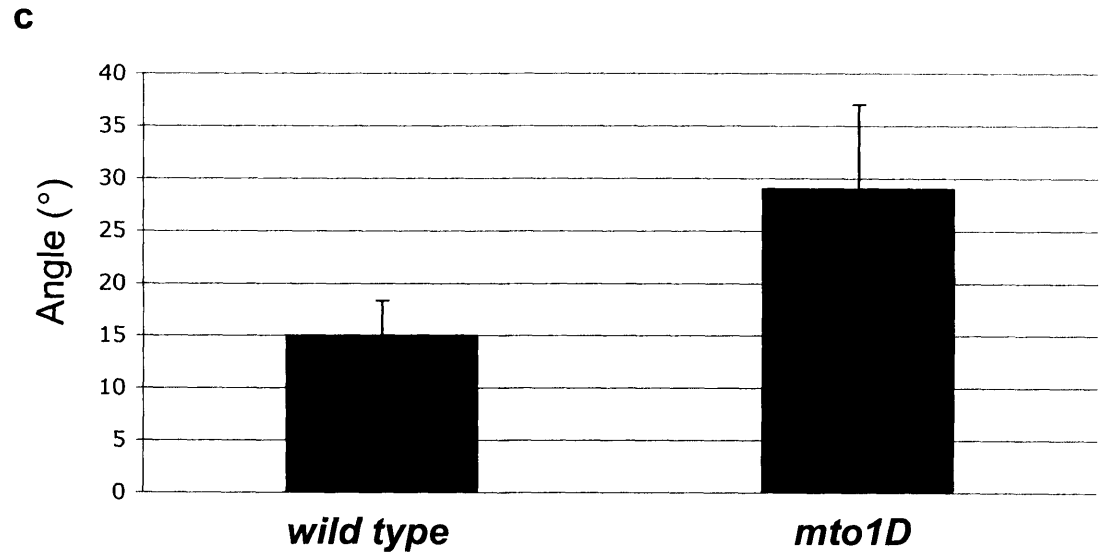
c
Angle (°)
0
5
10
15
20
25
30
35
40
wild type
mto1D

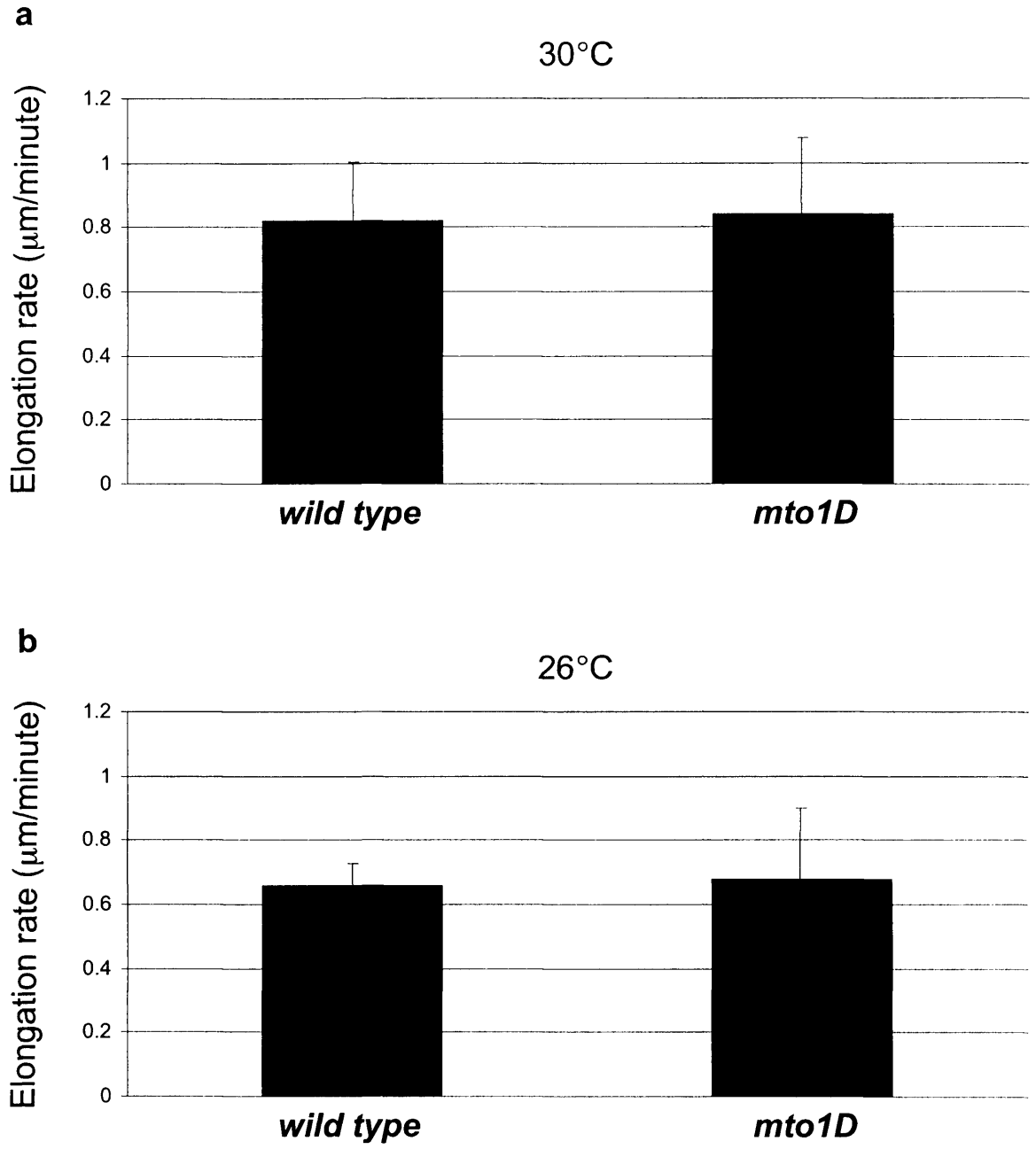

Figure 3.10 Spindle elongation rates remain unchanged in cells lacking Mto1

(**a**) Histogram showing the spindle elongation rate for *ndc80-gfp cdc11-cfp* (*wild type*) and *mto1D ndc80-gfp cdc11-cfp* (*mto1D*) cells at 30°C. Derived from data collected for figures 3.7a and 3.7b. Error bars show standard error.
(**b**) Histogram showing the spindle elongation rate for *ndc80-gfp cdc11-cfp* (*wild type*) and *mto1D ndc80-gfp cdc11-cfp* (*mto1D*) cells at 26°C. Derived from data collected for figures 3.9a and 3.9b. Error bars show standard error.

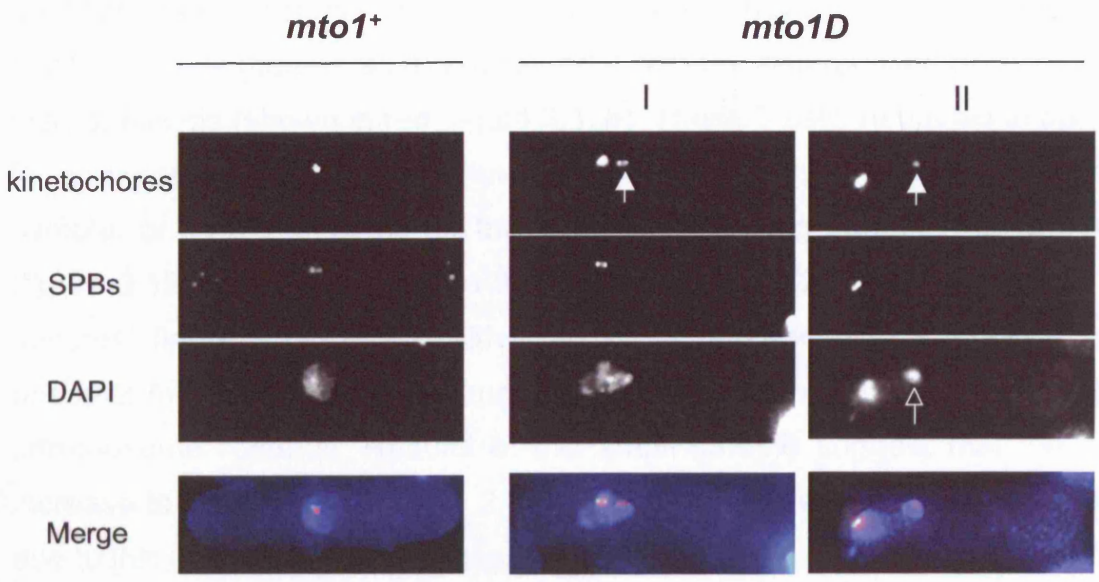

Figure 3.11 A small proportion of cells lacking Mto1 have unclustered kinetochores

Log phase *mto1*$^{+}$ and *mto1D* cells expressing Ndc80-GFP (marking the kinetochores, red) and Cdc11-CFP (marking the SPBs, green) were fixed and the DNA stained with DAPI (blue). Left panel shows *mto1*$^{+}$ cell and right panels are two examples of *mto1D* cells displaying the unclustered kinetochores phenotype. Arrows indicate unclustered kinetochores. The unclustered kinetochore is DAPI-associated (open-headed arrow).

However, a proportion of *mto1D ndc80-gfp cdc11-cfp* cells display a defect in Rabl formation where one pair of sister kinetochores are observed at another part of the nuclear envelope away from the SPBs (figure 3.11). This phenotype was observed in 9% of interphase cells (n=500) after formaldehyde fixation of log phase cells. By observing time-lapse images of live cells in mitosis, I found that unclustered kinetochores rapidly move back to one of the two spindle poles before the kinetochore pair is bi-oriented. Figure 3.12a and movie 3.3 show that transport of the unclustered kinetochore pair to the spindle pole takes 330 seconds over a distance of 1.32 microns. In 20 movies of *mto1D ndc80-gfp cdc11-cfp* cells (figures 3.7b) I observed 3 with unclustered kinetochores at the start of mitosis (shown in red, figure 3.12b). These 3 cells remained in phase 2 for an average of 14.5 ± 2.5 minutes compared to 12 ± 2.5 minutes for the total sample, or 11 ± 2 minutes for the 17 cells displaying normal Rabl formation (figure 3.12c). This is similar to the length of phase 2 in *mto1*$^{+}$ cells (11 ± 3 minutes, figure 3.7a). Cells with unclustered kinetochores spend longer in phase 2 than wild type cells, and this correlates with the time necessary for chromosome retrieval. Results of this small sample suggest that the slight increase in the length of phase 2 in the *mto1D* cell sample versus wild type is due to this unclustering phenomenon.

3.2.4 Asymmetry of SIN activation is independent of astral microtubule contact with the cell cortex

I next examined whether the presence or absence of astral microtubules influences the asymmetric loading of the septation initiation network (SIN) components. To test this, I examined the localisation of Cdc7-GFP and Sid1-GFP, which bind asymmetrically to one of the two SPBs in anaphase B. I found that localisation of Cdc7 and Sid1 remained unaltered in *mto1D* cells compared to *mto1*$^{+}$ (figure 3.13). This indicates that the reported asymmetry of astral contact with the AMIZ (Gachet *et al.*, 2004) is not responsible for the asymmetry of SIN component loading and is consistent with previous observations that the asymmetry of the SIN activation is microtubule independent (Sohrmann *et al.*, 1998).

Figure 3.12 *mto1D* cells with unclustered kinetochores have an extended phase 2

(**a**) Frames from a time-lapse movie of an *mto1*D cell expressing Ndc80-GFP (marking the kinetochores, red) Cdc11-CFP (marking the spindle pole bodies, green) in metaphase with an unclustered pair of kinetochores (arrow) that are transported to the spindle pole in 330 seconds.
(**b**) The graph represents multiple time-lapse movies of *mto1D ndc80-gfp cdc11-cfp* (*mto1D*) cells (n=20) showing spindle length through time. Data reproduced from figure 3.7b. 3 cells entered mitosis with unclustered kinetochores and these are shown in red.
(**c**) Histogram comparing the average length of phase 2 in *ndc80-gfp cdc11-cfp* cells (*wild type*;n=29) with the average length of *mto1D ndc80-gfp cdc11-cfp* (*mto1D*; n=20) cells (Black bars, data derived from figure 3.7c). *mto1D* sample is further split into (i) 17 cells with Rabl conformation (hatched), and (ii) 3 cells with unclustered kinetochores (red). Error bars show standard error.

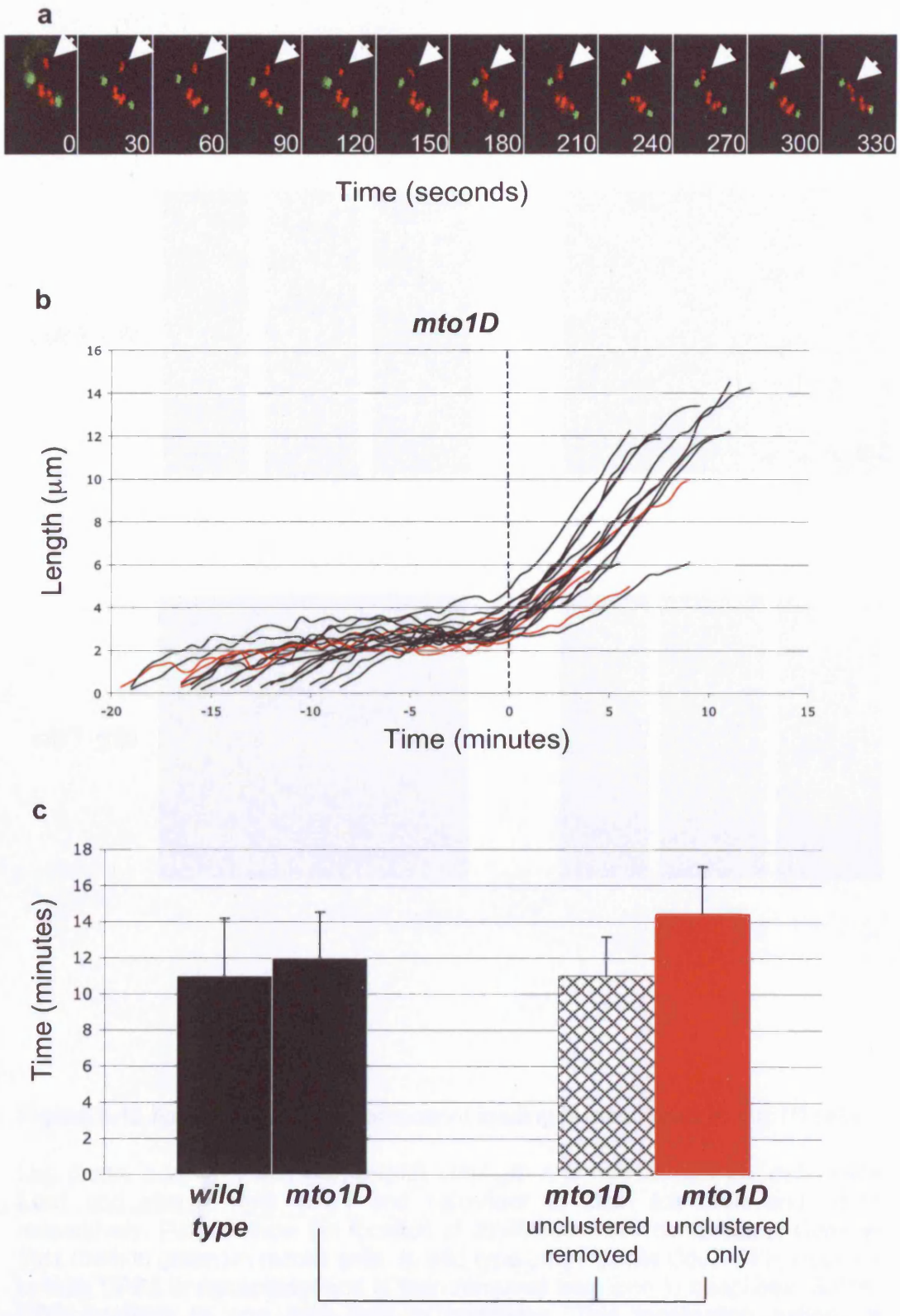
a
0
30
60
90
120
150
180
210
240
270
300
330
Time (seconds)
b
mto1D
Length (μm)
Time (minutes)
c
Time (minutes)
wild type
mto1D
mto1D unclustered removed
mto1D unclustered only

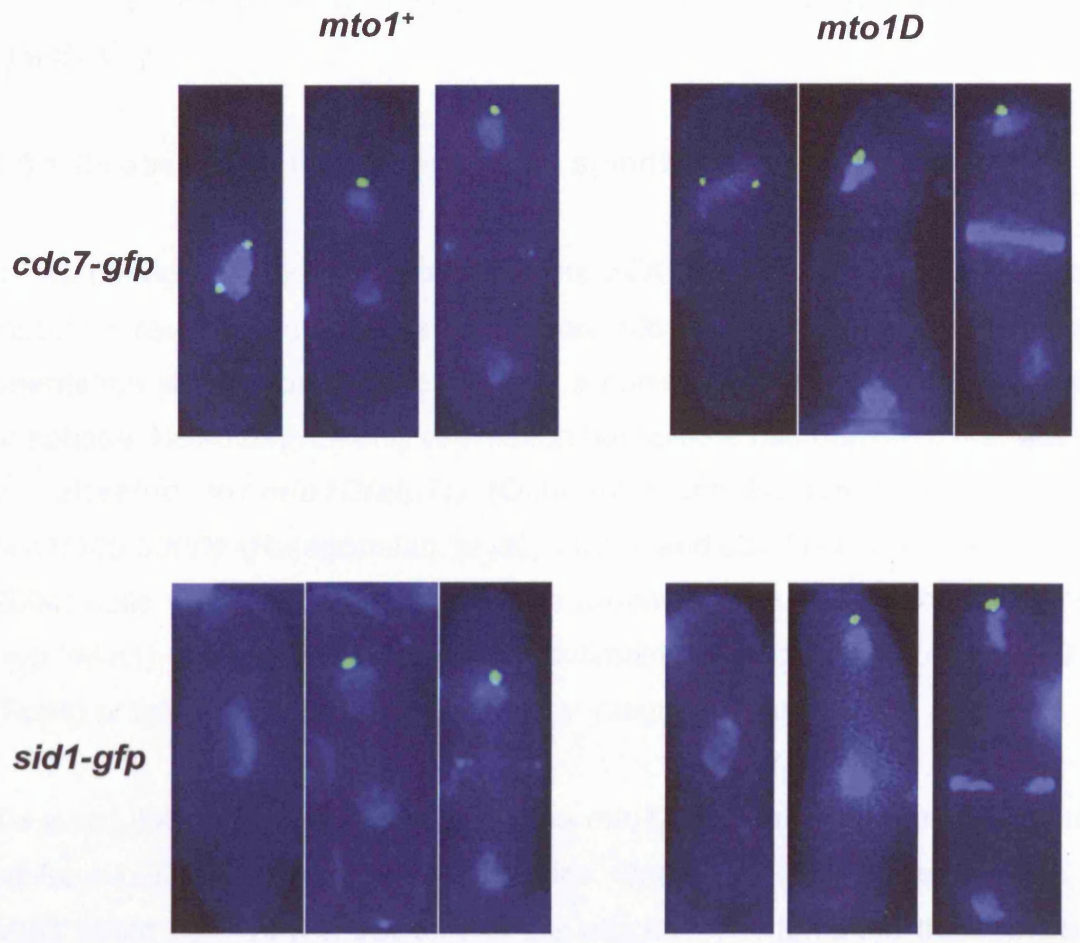

Figure 3.13 Asymmetry of SIN component loading is maintained in *mto1D* cells

Log phase *cdc7-gfp*, *sid1-gfp*, *mto1D cdc7-gfp* and *mto1D sid1-gfp* cells were fixed and stained with DAPI and calcofluor to stain for DNA and septa respectively. Panels show the location of asymmetric SIN components Cdc7 or Sid1 (both in green) in mitotic cells. In wild type (*mto1*$^{+}$) cells Cdc7-GFP localises to both SPBs in metaphase and is then removed from one in anaphase. Sid1p-GFP localises to one SPB only in anaphase. This localisation pattern is unchanged in *mto1D* cells.

3.3 Discussion

In this chapter I have revisited the concept of a SOC in fission yeast. Results with *mto1D* cells show that mis-orientation of the mitotic spindle *per se* does not lead to a significant delay in anaphase onset. This argues against the existence of a SOC.

3.3.1 Re-assessing the evidence for a spindle orientation checkpoint

It has previously been reported that the SOC can be activated with various mutant strains that cause astral microtubule defects. In each case, a mis-orientation was reported together with a corresponding delay in the onset of anaphase. However, not only orientation but spindle microtubule dynamics may be affected in *mia1D/alp7D* (Oliferenko and Balasubramanian, 2002), *pcp1(400-900D)* (Rajagopalan *et al.*, 2004) and *cdc11-123* (Tournier *et al.*, 2004) cells either because these gene products bind to spindle microtubules (Alp7/Mia1), are required for proper attachment of spindle microtubules to SPBs (Pcp1) or interfere with spindle pole body integrity (Cdc11).

To avoid these problems I chose to use *mto1D* cells to cause mis-orientation, whilst avoiding altering spindle dynamics. One caveat to this approach is that Mto1 could be involved not only in the process of orientating the spindle but also in sensing the mis-orientation or activating the checkpoint response. In this case, *mto1D* cells would be unable to have a SOC delay imposed on them. This is an important consideration that I address in chapter 5, where I present data that this is not the case.

Therefore, the evidence presented in this chapter shows that there is no correlation between spindle angle and timing of anaphase onset in single cells, indicating that spindle angle and anaphase onset are not functionally linked. Whilst this thesis was in preparation, Vogel *et al.* (2007) published a paper that agrees with several of the principal findings in this chapter. The authors present data to illustrate that there is no correlation within a strain between spindle angle and anaphase onset. However, since these authors use *mia1D* cells, which have been previously been shown to be delayed in anaphase onset due

to inherent activation of the SAC mediated delay (Sato *et al.*, 2003), they were unable to formally conclude that spindle mis-orientation is unlinked to the timing of anaphase onset.

3.3.2 Mitotic spindle dynamics in the absence of Mto1

Other conflicting evidence in the literature pertains to whether or not *mto1D* cells are delayed in anaphase onset. Sawin *et al.* (2004) observe no delay whereas Venkatram *et al.* (2004) record an elongated phase 2 for *mto1D* cells versus wild type. In addition there is confusion as to whether the presence of astral microtubules influences spindle elongation rate during phase 3. Venkatram *et al.* (2004) find that in cells lacking Mto1, spindles elongate at approximately 30% the rate of wild type. However, Sawin *et al.* (2004) report no change in elongation rate between *mto1*$^{+}$ and *mto1D* cells. These differences could be explained by their use of differing Atb2-GFP constructs. From my own work, I have observed that there is a high level of cell-to-cell variation in tubulin-GFP levels, which may influence the timing of mitosis. Also, *mto1D* could be more sensitive to changes in tubulin levels and it is this sensitivity that is being revealed by Venkatram *et al.* (2004) rather than a true reflection of unperturbed spindle dynamics in the strain.

I find that *mto1D* strains are not delayed in anaphase onset in either the *lys1:nmt1-atb2-gfp* or *ndc80-gfp cdc11-cfp* backgrounds in agreement with Sawin *et al.* (2004). Similarly, in agreement with the same authors, I observe no effect on the rate of spindle elongation. Further, Tolic-Norrelykke *et al.* (2004) conclude, from laser ablation studies, that astral microtubules push the spindle away from the cortex but do not contribute to the rate of spindle elongation. To avoid the potential problems, discussed above, of visualising the spindle using over-expressed tubulin (which is also structurally altered via the addition of a GFP tag), I present data primarily from *ndc80-gfp cdc11-cfp* strains throughout the remainder of this thesis. This strain offers additional benefits including (i) the ability to accurately determine the end of anaphase A and (ii) a means for correcting for spindle angle in the Z-axis (compare the spread of data points around 0 minutes for spindle length in both *mto1D lys1:nmt1-atb2-gfp* and

mto1D ndc80-gfp cdc11-cfp to see the effect of this correction (figures 3.4b and 3.7b).

3.3.3 Unclustering of kinetochores in cells lacking Mto1

I demonstrate that a percentage of kinetochores are unclustered from the SPBs during interphase. This phenotype raises several interesting questions.

How does the loss of Mto1 cause centromere unclustering?

One possibility is that a small proportion of Mto1 is present on the inner face of the SPB and is involved in spindle nucleation. In the absence of Mto1, tethering of kinetochores to the SPBs may not be as efficient. Alternatively, unclustered kinetochores may bind to the inner side of the nuclear envelope underlying inactive interphase microtubule organising centres (iMTOCs). It is known that *mto1D* cells, have only one interphase microtubule bundle and this is either not attached or only loosely attached to either the SPB or the nuclear envelope (Zimmerman and Chang, 2005). It is possible that the lack of attachment of interphase microtubules to the cytoplasmic face of iMTOCs could lead to a conformational change on the nuclear face, which permits association of kinetochores. Regardless of the reasons, unclustering occurs only in a proportion of cells.

Why does centromere unclustering occur in only a proportion of cells?

Intriguingly, *mto1D* cells with a nucleus positioned at the cell tip have a significantly higher frequency of unclustered kinetochores than *mto1D* cells with the nucleus positioned in the middle of the cell (Alejandro Franco-Sanchez, unpublished data). Therefore, the answer to this question could lie in cell-to-cell variation of distribution of interphase microtubules in cells lacking Mto1. The misplaced nuclei in *mto1D* cells are those that are not being correctly positioned by their remaining interphase microtubule. It follows that these are the nuclei that are less likely to have an interphase microtubule attached to the outer face of their SPBs, meaning that they are more likely to undergo the events leading

to unclustering as speculated above. However, recovery of the unclustered kinetochores seems to be highly efficient.

How are unclustered kinetochores recovered?

The unclustering phenotype occurs in 9% of *mto1D* interphase cells. However, cells lacking Mto1 only have a mis-segregation event in 0.08% of cells (Sawin *et al.*, 2004). The process of capture and retrieval of the unclustered kinetochores must therefore be highly efficient. In *S.cerevisae*, Tanaka and colleagues (Tanaka *et al.*, 2005) have developed a system to monitor the retrieval of chromosomes by spindle microtubules. In these cells, a lost chromosome is retrieved by the Kar3 minus end-directed kinesin motor on the lateral face of a stabilised microtubule. By contrast unclustered kinetochores in *mto1D* cells are generated without imposing a protracted cell cycle delay or centromere inactivation and activation. Furthermore, initial results suggest that the fission yeast Kar3 homologues, Klp1 (Pkl1) and Klp2, are not required for unclustered kinetochore retrieval. Instead, the DASH complex is absolutely required (Franco *et al.*, 2007).

3.3.4 Astral microtubules do not impose the asymmetry of SIN activation

Activation of cytokinesis involves the asymmetrical distribution of some components of the MEN (budding yeast) or SIN (fission yeast) to the SPBs (reviewed in, Simanis 2003). Pereira *et al.* (2001) demonstrated that when astral microtubules are disrupted, key MEN components fail to localise asymmetrically and are present on both SPBs. In contrast, I have shown that a lack of astral microtubules does not prevent asymmetric loading of SIN components in fission yeast, consistent with (Sohrmann *et al.*, 1998). A detailed study of the timing of cytokinesis may reveal a minor role for astral microtubules in the timing of SIN asymmetry, but is outside the scope of this study.

3.4 Conclusions

- There is no relationship between the angle of the mitotic spindle and the onset of anaphase, and therefore no spindle orientation checkpoint.
- The rate of spindle elongation in phase 3 is not controlled by astral microtubules.
- Mto1 is required for efficient Rabl configuration of kinetochores in fission yeast.
- Asymmetry of SIN activation is not dependent on astral microtubules.

Chapter 4

Mechanism controlling mitotic spindle orientation in fission yeast

4.1 Introduction

It has previously been proposed that spindle orientation occurs during phase 2 and is mediated by interaction of astral microtubules with a region of the medial cell cortex termed the astral microtubule interaction zone (AMIZ) (Gachet *et al.*, 2004; section 1.2.1.3). Additionally, Gachet *et al.* (2004) found that only one of the two astral microtubules interacts with the cytokinetic actomyosin ring (CAR) and suggested that this contact may initiate anaphase onset. Mis-orientation of spindles was also observed in *mia1D/alp14D* mutants, which have defective astral microtubules (Oliferenko and Balasubramanian, 2002; section 1.3.2.2.2). These authors concluded that metaphase spindle alignment might be imposed by a tension-sensing checkpoint. However, subsequent analysis showed that Mia1/Alp14 also binds the mitotic spindle and that loss of Mia1/Alp14 disrupts mitotic spindle integrity causing activation of the spindle assembly checkpoint (SAC) (Sato *et al.*, 2003). Similarly, defects in spindle orientation and a delay in anaphase onset were observed in *cdc11-123* cells and *pcp1(600-900D)* cells (Gachet *et al.*, 2004; Rajagopalan *et al.*, 2004). However, it was not possible to determine whether the delay in anaphase onset was due to defective astral or spindle microtubule function. During the course of this thesis, however, Zimmerman and colleagues (2004) demonstrated that cytoplasmic astral microtubules are in fact only nucleated during phase 3, although the precise timing of anaphase onset was not determined. Instead, these authors proposed that intra-nuclear astral (INA) microtubules orientate the spindle during phase 2. Others suggest that both classes of astral are present simultaneously prior to anaphase onset (Gachet *et al.*, 2006). In this chapter I re-examine the mechanism of spindle orientation in *S.pombe*.

4.2 Results

4.2.1 Spindle orientation during prometaphase and metaphase

To test whether the spindle is rotated towards the longitudinal axis of the cell by the action of astral microtubules during phase 2 (Gachet *et al.*, 2004) I used the detailed measurements collected previously (section 3.2.1) to calculate the average angle of the mitotic spindle at the start and end of phase 2 in *lys1:nmt1-atb2-gfp* cells (*mto1*$^{+}$; figure 4.1a). I found that there is no directed correction towards the longitudinal axis of the cell as these cells have an average spindle angle of 15 ± 4° at the onset of phase 2 and 18 ± 4° at the end. The same is true for *mto1D lys1:nmt1-atb2-gfp* cells, which enter phase 2 with spindles at an angle of 34° ± 5° and exit at 29 ± 5°. Likewise, *dam1D lys1:nmt1-atb2-gfp* cells show no corrective movement from the beginning to the end of phase 2, despite an extended SAC-mediated delay (14 ± 4° to 15 ± 3°). To further support this data I analysed the average spindle angle at the start and at end of phase 2 in *ndc80-gfp cdc11-cfp* cells (figure 4.1b). These cells start phase 2 with a mean spindle angle of 15 ± 3° and end at 17 ± 3°. Similar measurements revealed that *mto1D ndc80-gfp cdc11-cfp* cells exhibit no significant corrective spindle orientation from 37 ± 7° at the start to 34 ± 4° at the end. Lastly, *mal3D ndc80-gfp cdc11-cfp* cells, originally analysed as a positive control for phase 2 delay, average a spindle angle of 16 ± 3° at the start of phase 2 and 16 ± 2° at the end. Similar data were obtained from cells undergoing mitosis at the lower temperature of 26°C (figure 4.1c). The start/end averages in *ndc80-gfp cdc11-cfp* cells were 11 ± 3° and 15 ± 3° respectively, while those of *mto1D ndc80-gp cdc11-cfp* cells were 31° ± 7° and 29° ± 8° respectively. Therefore, there is no corrective spindle orientation between the beginning and the end of phase 2 in any of the strains analysed. Notably, however, in all strains I observed substantial oscillations in the angle of the spindle both towards and away from the longitudinal axis of the cell during prometaphase and metaphase (figures 3.5 and 3.8). These oscillations may or may not be due to interaction of intra-nuclear spindle microtubules with the inner face of the nuclear envelope. Notwithstanding, the average angle of the spindle remains unchanged during prometaphase and metaphase. This is clearly shown in figure 4.2 where the average spindle angle of *ndc80-gfp*

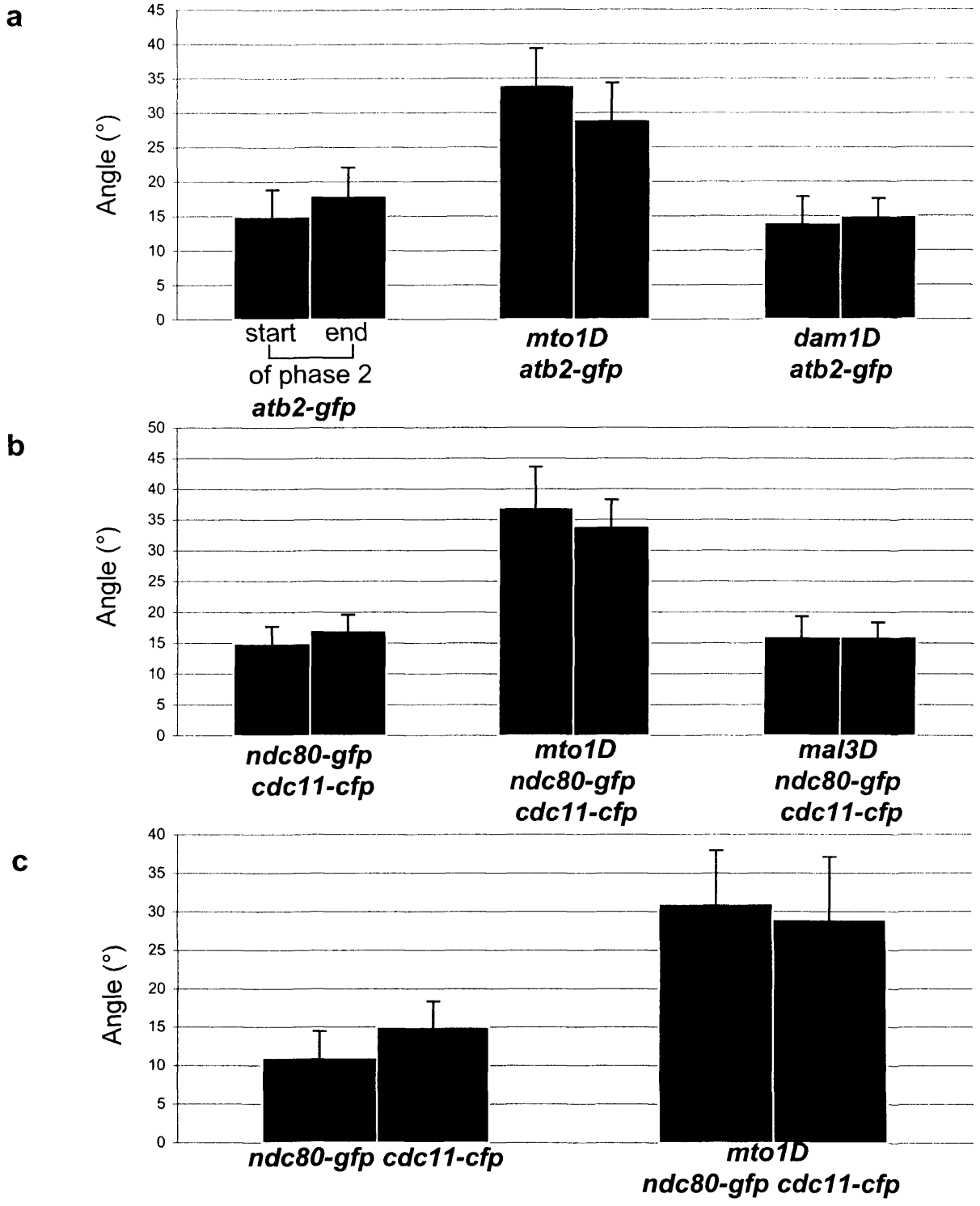

Figure 4.1 There is no corrective orientation of the mitotic spindle during phase 2

Histograms showing the average angle of the mitotic spindle relative to the longitudinal axis of the cell at the start and end of phase 2 for the following: (**a**) *lys1:nmt-atb2-gfp* (*atb2-gfp*), *mto1D lys1:nmt1-atb2-gfp* (*mto1D atb2-gfp*) and *dam1D lys1:nmt1-atb2-gfp* (*dam1D atb2-gfp*) cells. Data extracted from figures 3.5a-c; (**b**) *ndc80-gfp cdc11-cfp*, *mto1D ndc80-gfp cdc11-cfp* and *mal3D ndc80-gfp cdc11-cfp* cells. Data extracted from figures 3.8a-c; (**c**) *ndc80-gfp cdc11-cfp* and *mto1D ndc80-gfp cdc11-cfp* cells at 26°C. Data extracted from figures 3.9a and b. In each case error bars show standard error of the mean (SEM).

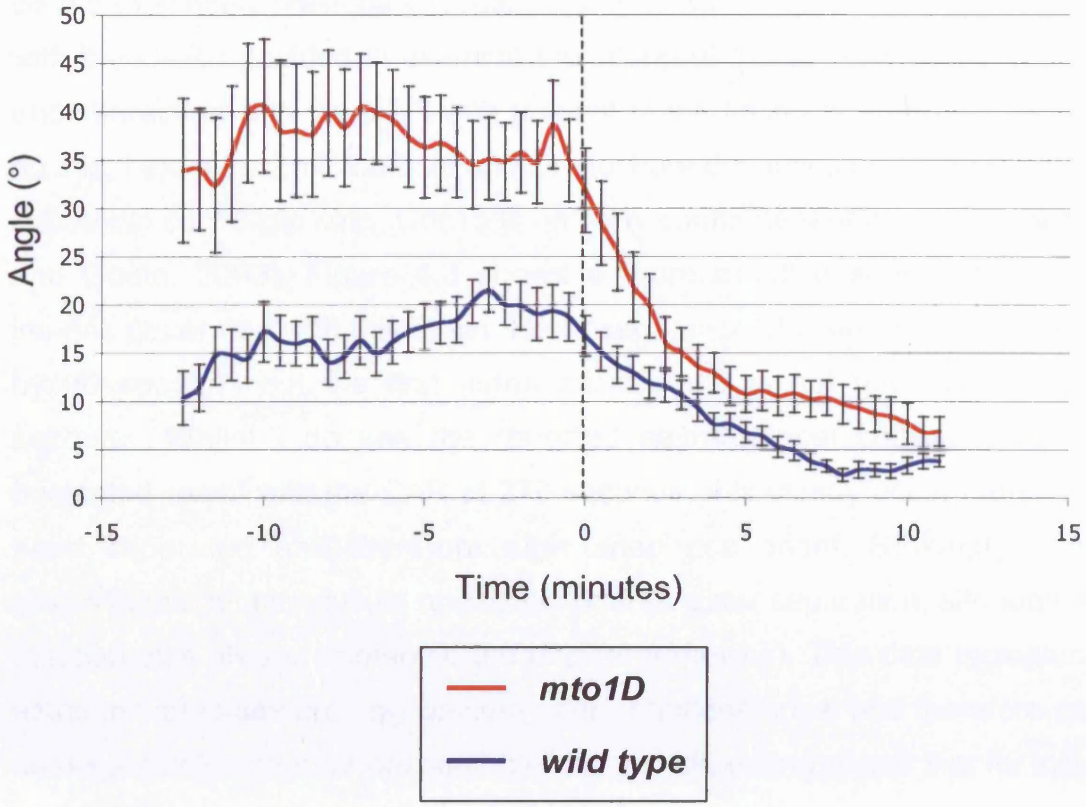

Figure 4.2 The average spindle angle of both *mto1D* and control cells remains constant prior to anaphase

Graph shows the average spindle angle relative to the longitudinal axis of the cell for *ndc80-gfp cdc11-cfp* (*wild type*; blue) and *mto1D ndc80-gfp cdc11-cfp* (*mto1D*; red) cells over time. Data extracted from figures 3.7a and b. Plots are aligned at the end of anaphase A (dashed line). Error bars show standard error of the mean (SEM).

cdc11-cfp cells with and without Mto1 is compared at multiple time points. Therefore, I conclude that intranuclear spindle microtubules are unable to direct orientation of the spindle towards the longitudinal axis of the cell.

4.2.2 Astral microtubules control spindle alignment during anaphase B

In the previous section I showed that there is no corrective angle adjustment during phase 2, in strains either with or without astral microtubules. Given the claims described previously (section 1.2.1.3) with respect to astral interaction with the CAR I decided to examine the timing of astral microtubule nucleation and interaction with the CAR with respect to the timing of anaphase onset. To do this, I examined microtubule and kinetochore dynamics in *lys1:nmt1-atb2-gfp ndc80-cfp cdc15-gfp* cells. Cdc15 is an early component of the CAR (Carnahan and Gould, 2003). Figure 4.3 shows a representative series of time-lapse images generated with this strain. Here, separation of sister chromatids occurs by 90 seconds but the first astral microtubule is not nucleated until 180 seconds. Whilst I do see the reported asymmetrical contact of the first nucleated astral with the CAR at 270 seconds, this clearly occurs after sisters have separated and therefore after anaphase onset. Strikingly, I never observed astral microtubule nucleation prior to sister separation, although astral microtubules always contacted the ring (n=9 movies). This data indicates that astral microtubules are only present after anaphase onset and therefore cannot be responsible either for orientation of the spindle during phase 2 or for initiating anaphase.

After the onset of anaphase A, spindles elongate at the same rate in wild type cells and in cells lacking Mto1 (section 3.2.2), confirming previous observations that astral microtubules do not contribute to the rate of anaphase B (Sawin *et al.*, 2004; Tolic-Norrelykke et al., 2004). Secondly, both spindle poles are never observed on the same side of the division plane in cells lacking Mto1, indicating that astral microtubules are not normally required for the maintenance of cell ploidy. Thirdly, the average spindle angle is reduced after anaphase A in both wild type cells and cells lacking Mto1 (figure 4.2), indicating that cell shape is more important for determining spindle orientation than the presence of astral microtubules. Despite this, spindles remain more mis-oriented during anaphase

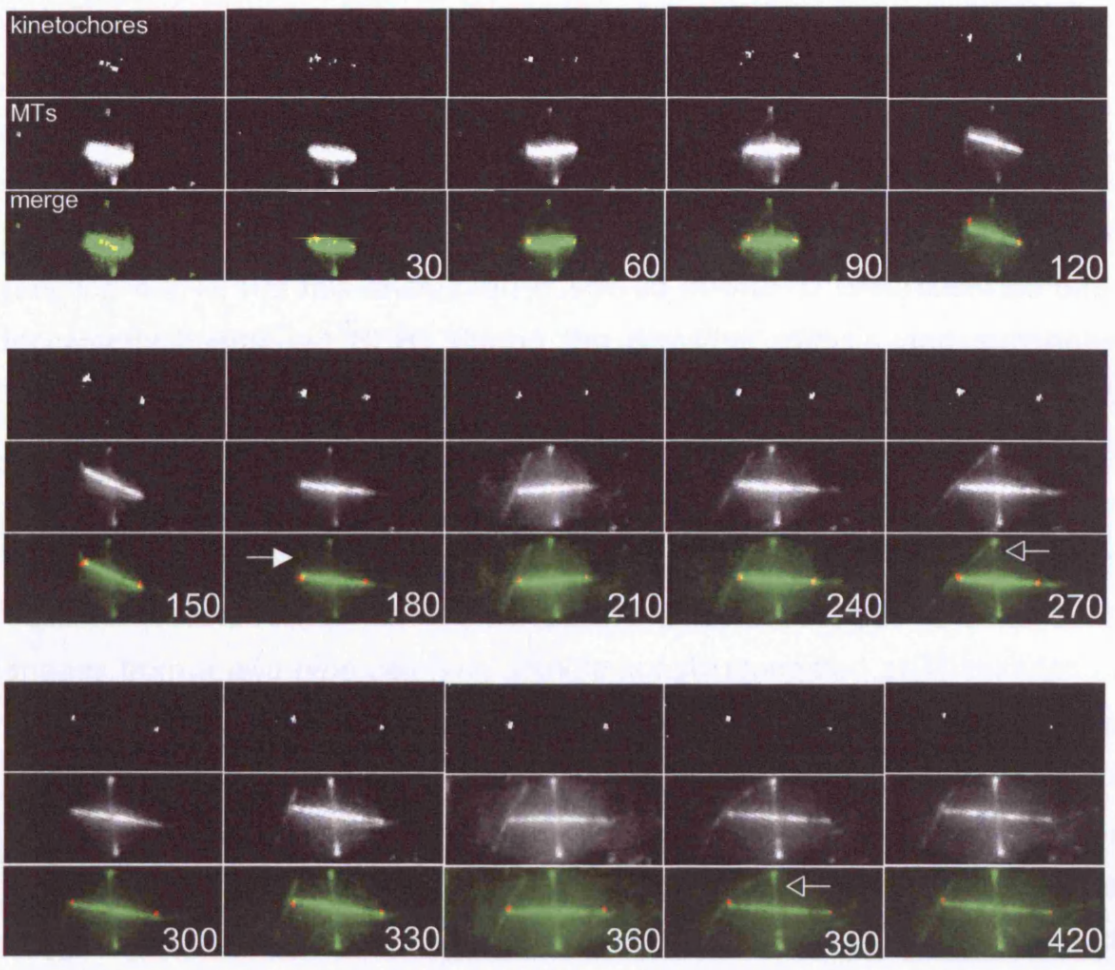

Figure 4.3 Microtubule contact with the ring occurs after sisters have separated

A time-lapse movie series showing a *lys1:nmt1-atb2-gfp* (microtubules, green) cell expressing Ndc80-CFP (kinetochores, red) and Cdc15-GFP (cortical actin ring, green). Time is in seconds. Sister chromatids separate at 60 seconds and the first nucleation of astrals occurs at 180 seconds (arrow). Astral microtubules contact the ring multiple times (open-headed arrows).

B in *mto1D ndc80-gfp cdc11-cfp* cells than in control cells, indicating that astral microtubules play a minor role in ensuring optimal spindle alignment, presumably by pushing spindle poles away from the cell cortex (Gachet et al., 2004; Tolic-Norrelykke et al., 2004). The precise mechanism underlying this effect is not fully understood.

4.2.3 Role of astral microtubules and the post-anaphase array in determining SPB position

As there is no corrective orientation of the mitotic spindle during phase 2 (section 4.2.1), the mis-orientation observed in *mto1D* cells could be due to incorrectly positioned SPBs during the previous mitosis and subsequent interphase. I used *cdc11-gfp* (*wild type*) and *mto1D cdc11-gfp* (*mto1D*) cells, where SPBs are fluorescently tagged, to further investigate the role of astral microtubules and the post-anaphase array (PAA) in controlling SPB position after the completion of spindle elongation. *mto1D* cells were used since they have neither astrals nor a PAA. Figure 4.4a shows a series of time-lapse images from a *wild type* cell. The spindle is fully elongated at 10 minutes and the SPBs then move rapidly away from the cell tips and by 13 minutes are towards the middle of what will be the daughter cells. However in the *mto1D* cell, after the spindle reaches its maximum elongation at 14 minutes, the SPBs remain at the cell tips for an additional 19 minutes (figure 4.4b). This data suggests that the repositioning of the SPB away from the cell tip is driven by the interaction of astral microtubules with the cell tip and/or microtubules from the PAA.

To further examine the mechanism of SPB re-positioning following mitosis *ndc80-gfp cdc11-cfp* (*wild type*) and *mto1D ndc80-gfp cdc11-cfp* (*mto1D*) cells were synchronised via lactose gradient centrifugation (materials and methods, 2.1.5). Cells were then fixed at 100 minutes post-synchronisation and stained with DAPI and calcofluor to allow visualisation of the DNA and septa respectively. Figure 4.5a shows that in 4 representative *wild type* cells, the nuclei are re-positioned in the middle of the daughter cells after septation. In addition, if the nucleus is imagined as a globe, SPBs are located on the nuclear equator perpendicular to the longitudinal axis of the cell. By contrast, in *mto1D*

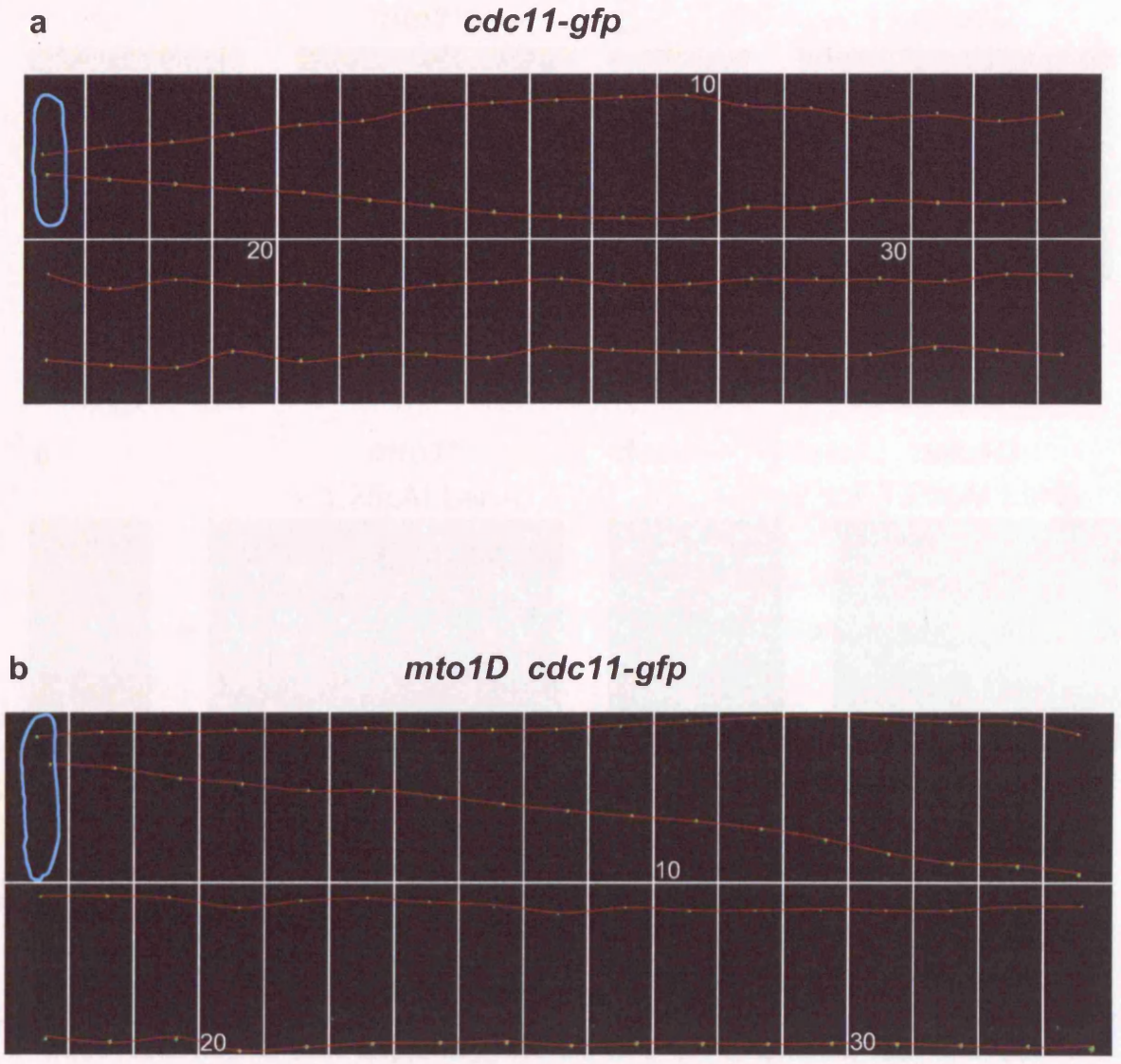

Figure 4.4 SPB repositioning post-mitosis is deficient in cells lacking Mto1

The upper series of time-lapse images (**a**) shows a cell expressing Cdc11-GFP (spindle pole bodies, green) undergoing phase 3 spindle elongation (0-10 minutes) followed by spindle pole body re-positioning. The lower series (**b**) shows an *mto1D* cell in the same background. Here phase 3 elongation finishes at 14 minutes. However, there is no repositioning of the poles.

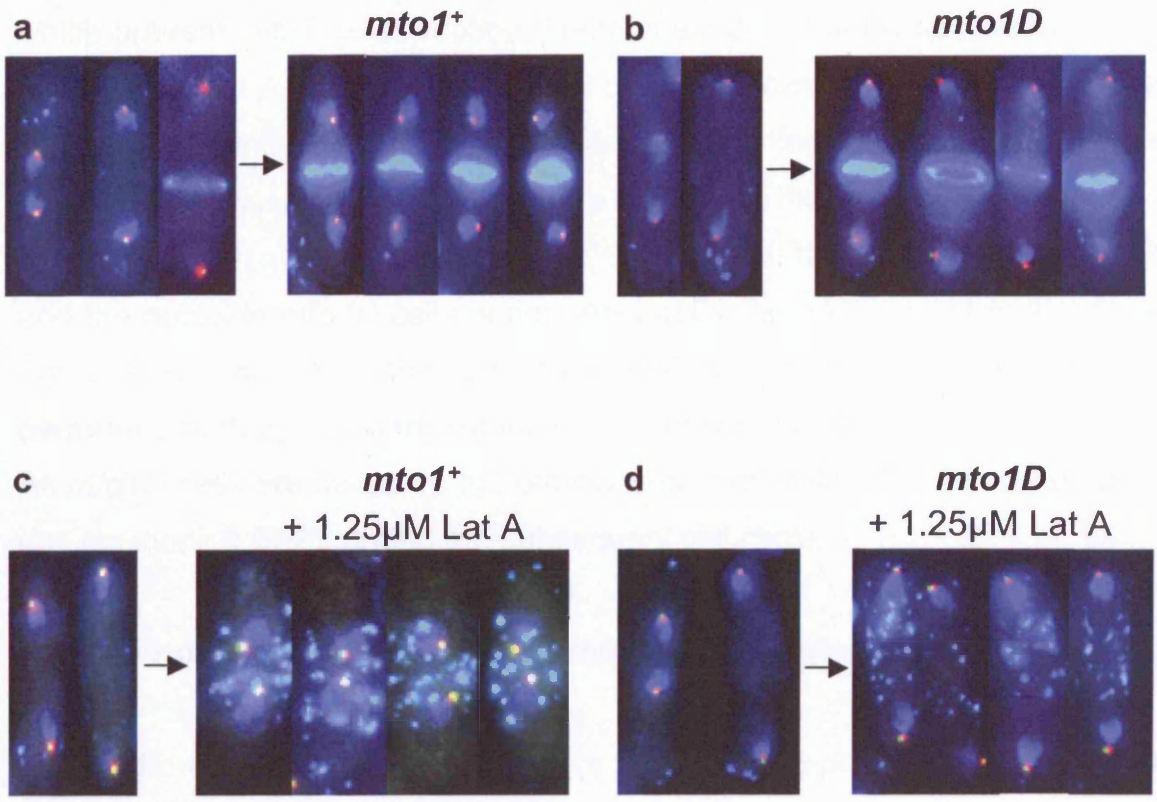

Figure 4.5 SPB repositioning post-mitosis is dependent on astrals and the PAA

mto1^{+} and *mto1D* cells expressing Ndc80-GFP (kinetochores, red) and Cdc11-CFP (spindle pole bodies, green) were synchronised by lactose gradient centrifugation. Each culture was then split in half and released into liquid media in the presence and absence of 1.25μM Lat A. Cells were fixed at 100 minutes after release at 30°C and stained with DAPI and calcofluor to visualise DNA (blue) and septa (light blue).

(**a**) Images of *ndc80-gfp cdc11-cfp* (*wild type*) cells in the absence of Lat A. The images on the left of the arrow are cells fixed earlier during mitotic progression. The 4 cells to the right of the arrow were fixed at 100 minutes after lactose synchronisation.

(**b**) Images of *mto1D ndc80-gfp cdc11-cfp* (*mto1D*) cells in the same format as (a).

(**c**) Images of *ndc80-gfp cdc11-cfp* (*wild type*) cells in the presence of 1.25μM Lat A in the same format as (a).

(**d**) Images of *mto1D ndc80-gfp cdc11-cfp* (*mto1D*) cells in the presence of 1.25μM Lat A in the same format as (a).

cells, the nuclei remain at the cell tips with the SPBs facing away from the cell middle (figure 4.5b). To separate the role of the PAA in nuclear and SPB positioning, this experiment was repeated in the presence of 1.25μM Lat A, which prevents eMTOC formation (Heitz *et al.*, 2001) but retains astrals. In the presence of Lat A, the nuclei of control cells are located close to the cell middle with SPBs facing each other (figure 4.5c). Calcoflour staining is shown as a dispersed granular pattern around the middle of the cell as a septum is not deposited when actin is depolymerised. By contrast, the positioning of the SPBs and the nuclei in *mto1D* cells is not affected by the addition of Lat A (compare figure 4.5b and d). I conclude that SPB and nuclear re-positioning are performed both by astral microtubules and microtubules derived from the PAA. As *mto1D* cells are defective in both classes of microtubules this contributes to mis-positioning SPBs during the subsequent cell cycle.

4.2.4 Interphase SPB position determines initial spindle angle in mitosis

I have shown that nuclei and SPBs are incorrectly re-positioned in *mto1D* cells and in cells lacking a PAA following mitosis. Interphase microtubules are known to be involved in nuclear positioning (section 1.2.1.1), but may also have a role in SPB positioning prior to mitosis. This, together with the absence of astral and PAA microtubules, may explain the severe mis-orientation seen in *mto1D* cells, which are also deficient for interphase microtubules (section 1.2.1.5). To examine this possibility I analysed 3D position of the SPBs (materials and methods, 2.2.3.1) in *cdc11-gfp* and *mto1D cdc11-gfp* interphase cells. In this way I could effect a virtual rotation of the whole cell through 90° so that the longitudinal axis of the cell, which was aligned along the x-axis, could be realigned along the z-axis. In effect this enables a cross section of the cell to be visualised allowing the precise location of the SPBs to be analysed in 3D. Figure 4.6a shows this analysis performed on a *cdc11-GFP* cell stained with DAPI together with a diagram of the poles and nucleus. In this case the replicated SPBs are positioned on the nuclear equator that lies perpendicular to the longitudinal axis of the cell. Spindle nucleation when the SPBs are positioned in this manner would result in an orientated mitotic spindle. However, in the *mto1D cdc11-cfp* cell, shown in figure 4.6b, the SPBs are located away from this nuclear equator. This configuration would result in a mis-orientated

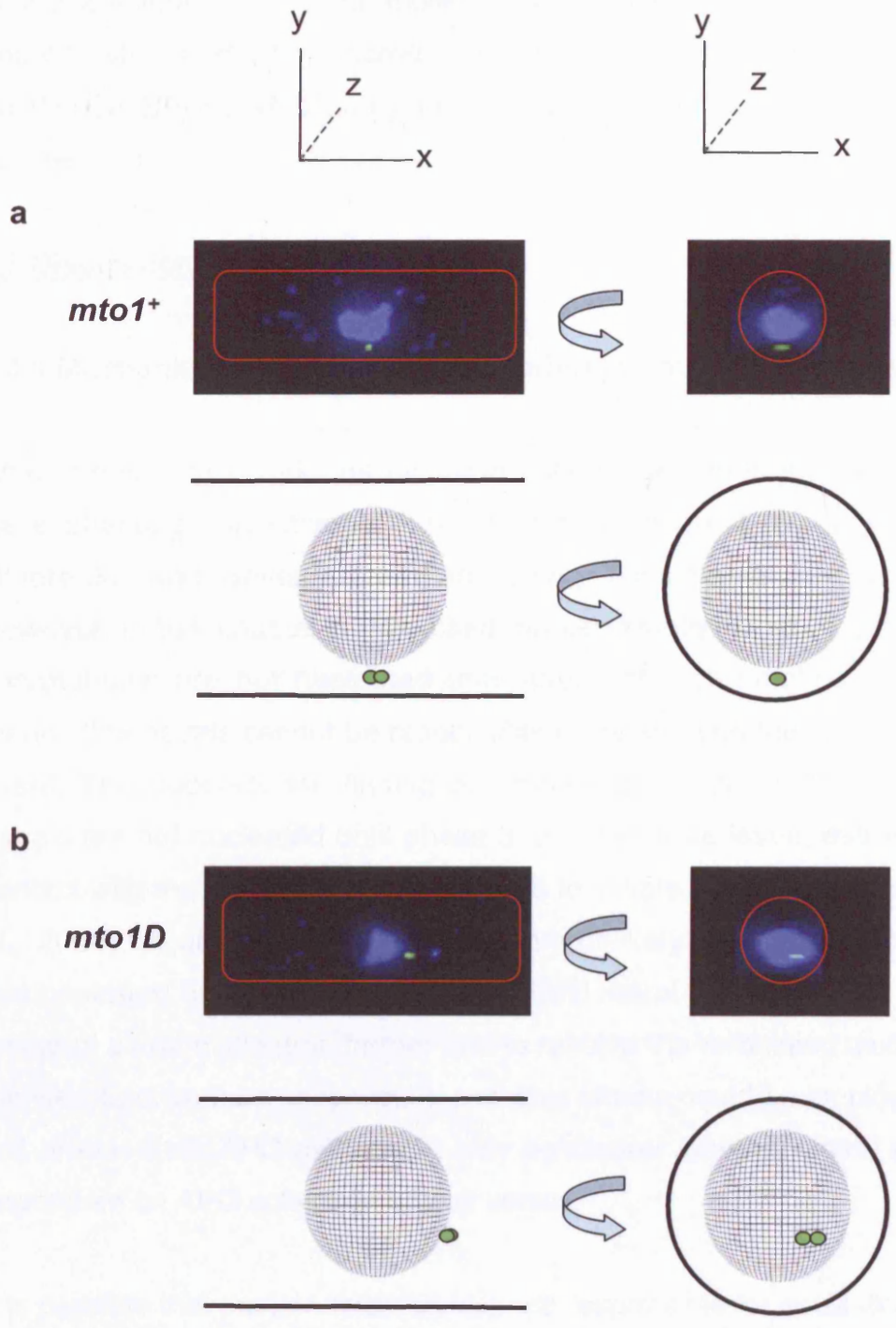

Figure 4.6 Cells lacking Mto1 have mis-positioned SPBs in interphase

mto1^{+} and *mto1D* cells expressing Cdc11-GFP (spindle pole bodies, green) were fixed and stained with DAPI to visualise DNA. The left column shows cells with the longitudinal axis aligned along the x-axis. The right column shows the same cells rotated through 90° so that the longitudinal axis is now aligned along the z-axis. (**a**) Shows a *cdc11-gfp* cell image manipulated in this way with a diagrammatic representation of the cell, nucleus and spindle poles below. (**b**) Shows an *mto1D cdc11-gfp* cell image presented in the same way.

phase 2 spindle. This data implies that the lack of interphase microtubules, and/or astral and PAA microtubules, in cells lacking Mto1 results in mis-positioned SPBs, which may consequently result in mis-orientated mitotic spindles.

4.3 Discussion

4.3.1 Mechanism controlling spindle orientation: previous hypotheses

When I began this work, the available data suggested that astral microtubules were effecting corrective orientation during phase 2 (Gachet *et al.*, 2004; Oliferenko and Balasubramanian, 2004; Tolic-Norrelykke *et al.*, 2004). However, in this chapter I have used marked kinetochores to show that astral microtubules are not nucleated until after sister chromatids separate. This means that astrals cannot be responsible for orientating the spindle prior to this event. This supports the finding of Zimmerman *et al.* (2004) who show that astrals are not nucleated until phase 3. In a separate issue, astral microtubule contact with the CAR has been proposed to initiate anaphase onset (Gachet *et al.*, 2004). Again, this now seems highly unlikely due to the relative timing, demonstrated here, of sister separation and astral nucleation. To examine the timing of astral nucleation further and to resolve the remaining discrepancies in the literature, various temperature sensitive strains could be employed. With the cell arrested *via* APC mutants, it may be clearer whether astral nucleation is dependent on APC activation or vice versa.

It is possible that the INA microtubules are responsible for oscillations in spindle angle during prometaphase and metaphase. Zimmerman *et al.* (2004) proposed that INAs are used for spindle orientation during phase 2. However, I have never observed a significant corrective orientation during phase 2, including in cells lacking Dam1, which have a significant delay in anaphase onset. However, it is possible that since *dam1D* cells lack a functional DASH complex, which binds to the tips of INA microtubules (Sanchez-Perez *et al.*, 2005), INA microtubule function could be impaired. Zimmerman *et al.* (2004) present movies showing that the last INA microtubule appears to interact with the ring before anaphase onset. For this to occur, INA microtubules would have to

penetrate the nuclear envelope at the end of phase 2, which seems unlikely. To address this question more carefully spindle microtubule dynamics could be monitored in *orb* mutants in conjunction with a nuclear envelope marker. Since *orb* mutants have a round phenotype the nuclear envelope is further from the cell cortex (Verde *et al.*, 1995). This would help to determine whether INA microtubules genuinely penetrate the nuclear envelope. More recently, it has been shown that INAs are instead required for the retrieval of unclustered kinetochores. (Alejandro Franco-Sanchez, unpublished data).

4.3.2 Mechanism controlling spindle orientation: a new model

In this section I describe a model for the orientation of the mitotic spindle. Figure 4.7a is a pictorial representation of the cell cycle in a wild type cell showing microtubules and both nuclear and SPB position throughout. The uppermost cell (i) is in interphase with the nucleus being maintained in the middle of the cell by the interphase array of microtubules (Tran *et al.*, 2001). The position of the SPBs is the determining factor for mitotic spindle orientation. I propose that the replicated SPBs prior to mitosis are on the nuclear equator that lies perpendicular to the longitudinal axis of the cell in a wild type situation. As the cell enters mitosis the duplicated SPBs migrate to either side of the nucleus, shown in cell (ii) in figure 4.7a, where the cell is in phase 2 of mitosis and INA and spindle microtubules are present. This is the stage of the cell cycle when it was previously thought that directed spindle orientation took place (Gachet *et al.*, 2004; Oliferenko and Balasubramanian, 2004; Tolic-Norrelykke *et al.*, 2004). However, according to my data there is no corrective orientation of the spindle during phase 2. In fact, this is the only point in the cell cycle when the poles are not being actively positioned. After anaphase onset astral microtubules are nucleated to correct and maintain the angle of the elongating mitotic spindle during phase 3 (iii, iv). It has previously been shown that repositioning of the nucleus occurs by a mechanism in which SPBs direct nuclear migration from the tips to the middle of cells (Hagan and Yanagida, 1997). I propose that after interaction with the cell tips astral microtubules push the nucleus towards the middle of the cell, and in doing so, reposition the nucleus and the SPB (v). Interaction with the cortical cell tip could cause a change in astral microtubule behaviour. Alternatively, disassembly of the mitotic

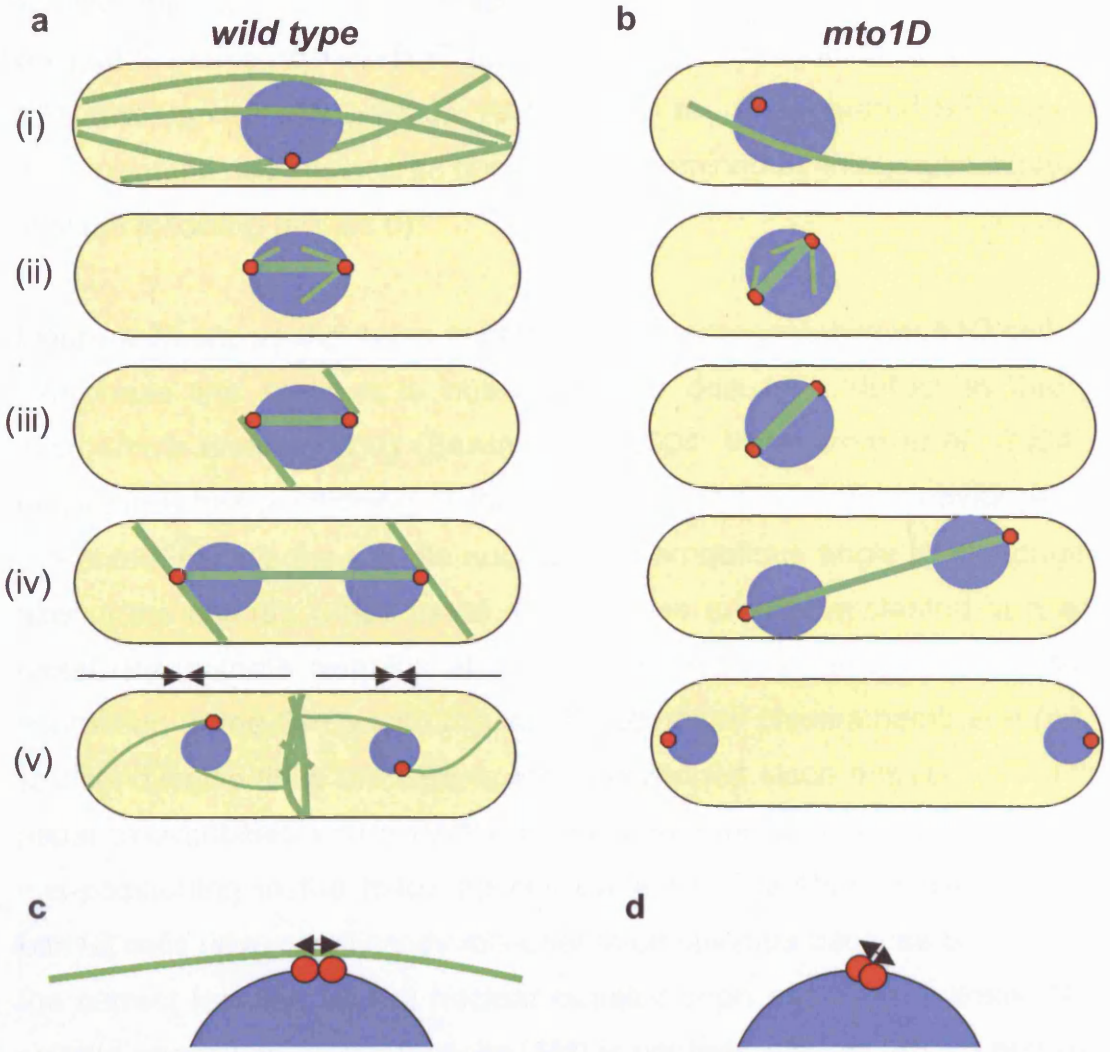

Figure 4.7 A model for orientation of the mitotic spindle being dependent on initial spindle pole body position and orientation

A schematic representation of the cell cycle in fission yeast showing microtubules (green), spindle pole bodies (SPBs) (red) and nuclei (blue). In *wild type* cells (**a**) the positioning of the SPBs is determined first by interphase microtubules (**i**) and then following anaphase (**iii**, **iv**) by astral microtubules and lastly the post-anaphase array of microtubules (**v**). In *mto1D* cells (**b**), cells are deficient in cytoplasmic microtubules resulting in mis-positioning of the SPBs in interphase (**i**). After anaphase, orientation of the spindle is achieved by interaction of the poles with the cell cortex as the spindle elongates (**iv**). Post-mitosis SPBs are not correctly re-positioned (**v**).
(**c**) Diagrammatic representation of SPB orientation in a *wild type* cell, where alignment of the "old" and "new" SPB is mediated by an interphase microtubule which is itself parallel to the longitudinal axis of the cell.
(**d**) Diagrammatic representation of SPB orientation in an *mto1D* cell. As cells lacking Mto1 are deficient in interphase microtubules, the SPBs in this case are not aligned with the longitudinal axis of the cell.

spindle may be necessary for spindle pole and nuclear re-positioning. During G1 and S phase, the eMTOC nucleates PAA microtubules, which capture the SPB and maintain its position. At this point the unseparated SPB lies on the equator of the nucleus and its position is maintained by interphase microtubules until the following mitosis (i).

Figure 4.7b shows the same schematic in a representative *mto1D* cell. During interphase the nucleus is mis-positioned due to a defect in interphase microtubule nucleation (i) (Sawin *et al.*, 2004; Venkatram *et al.*, 2004). This results in a mis-positioning of the SPBs around the nuclear envelope. As the cell enters mitosis the spindle nucleates at an oblique angle to the longitudinal axis of the cell (ii). Since astral microtubules are not nucleated at anaphase onset, the spindle remains at an oblique angle (iii) and is only moved by interaction of the SPBs with the inner face of the plasmamembrane (iv). After spindle disassembly, the SPB is not repositioned since *mto1D* cells lack both astral microtubules and a PAA (v). This contributes to both nuclear and SPB mis-positioning in the following cell cycle (i). Therefore, I hypothesise that *mto1D* cells have significantly mis-orientated spindles because SPBs are not in the correct location on the nuclear equator upon entry into mitosis. Notably, spindle orientation of *mto1D* cells (34°) is not truly random (45°). I propose this is due to the one remaining interphase microtubule, which may partially position the SPBs and nucleus prior to mitosis onset.

In order to test this model it would be necessary to carry out a series of microtubule re-growth experiments after centrifugation at low temperatures to cause microtubule depolymerisation and mis-positioning of SPBs. Cells could then be warmed to allow interphase microtubule to nucleate and SPB and nuclear position observed. In this way it should be possible to determine if the SPB positioning and nuclear positioning are inter-related events. This experiment could also be performed in *mto1D* cells to determine whether the one remaining interphase MT can partially correct the position of the nucleus and the SPBs. Similarly, the role of eMTOC formation in SPB and nuclear positioning needs to be examined in greater detail, perhaps by utilising a temperature sensitive allele of *sid2*, a SIN component (Sparks *et al.*, 1999). SIN mutants fail to undergo cytokinesis and form multi-nucleate cells with pairs of

nuclei close together and SPBs facing (Hagan and Yanagida, 1997). This phenotype is similar to that generated when Lat A is used to prevent PAA formation except that cells arrest after one nuclear division.

Whilst the position of the SPBs is of great importance in orientating the mitotic spindle, it also follows that the actual orientation of the "old" and "new" SPBs relative to the longitudinal axis is equally as important. Figure 4.7c illustrates my hypothesis that in a normal cell the "old" and "new" SPBs sit on an interphase microtubule that is parallel to the longitudinal axis of the cell. This ensures the correct orientation of the SPBs prior to mitosis. In an *mto1D* cell, which is deficient in interphase microtubules, this contact could be lost resulting in a mis-orientation of the spindle in the ensuing mitosis (figure 4.7d). To test this hypothesis, the orientation of the "old" and "new" SPBs could be examined in *sfi1-gfp cdc11-cfp* cells. Sfi1 localises to the half-bridge structure formed between replicated SPBs (Kilmartin, 2003) whilst Cdc11 binds to the outer plaque. A comparison between *mto1D* and control cells would provide extra information as to the role of interphase microtubules in orientating the SPBs. In conclusion, I propose that cytoplasmic microtubules both position the SPBs to determine the orientation of the mitotic spindle and determine nuclear position. Importantly, since the position of the nucleus dictates the location of cell division, I propose that perpendicular alignment of the spindle and axis of cell division is determined by a common cytoplasmic microtubule program.

[Note: Whilst this thesis was in preparation Vogel et al. (2007) published a paper that supports many of the conclusions I have drawn. The authors state that interphase microtubules are indeed responsible for initial spindle position. They provide a model that is strikingly similar to mine, generated by comparing cells with damaged or absent interphase microtubules relative to control cells. They also conclude, in agreement with this work, that astral and INA microtubules do not effect a corrective orientation during phase 2.]

4.3.3. Cell shape and a more important role for astral microtubules?

The mitotic spindle elongates down the longitudinal cell axis in anaphase B. It is conceivable that astral microtubules maintain and/or correct spindle position

during this period. Figure 4.2 compares the mean spindle orientation over time of *mto1D* cells with that of control cells. After anaphase A it is apparent that both strains orientate rapidly towards 0°. Therefore, despite a lack of astrals in phase 3, the spindle is re-orientated in *mto1D* cells due to interaction of the SPBs with the cell cortex. However, I find that spindle poles always migrate to either side of the division plane in *mto1D* cells, suggesting that neither astral microtubules nor moreover, mitotic spindle orientation is normally required for the maintenance of cell ploidy. However, in spherical cells the requirement for astral microtubules may be different. This could be investigated by the use of an *orb* mutant (Verde *et al.*, 1995). In a spherical cell, the lack of a SOC could prove disastrous for an astral-less *S.pombe* strain. In addition, spindle mis-orientation can cause chromosome mis-segregation when the rate of spindle elongation is decreased (Vogel *et al.*, 2007). In this situation, interaction of astral microtubules with the CAR may be necessary to ensure spindle poles migrate to either side of the division ring. Such a hypothesis merits further investigation.

4.4 Conclusions

- There is no corrective orientation of the mitotic spindle in phase 2 either by INAs or by cytoplasmic astrals.
- Cytoplasmic astrals are only nucleated after sisters separate and therefore cannot play a role in either the initiation of anaphase or in the regulation of orientation prior to anaphase.
- Phase 2 spindle orientation is determined by the position and orientation of the SPBs prior to mitosis, which is determined by astral, PAA and interphase microtubules.

Chapter 5

Actin is required for pre-anaphase mitotic spindle stability

5.1 Introduction

In chapter 3 I showed that spindle mis-orientation does not cause an anaphase delay in fission yeast. This is in conflict with the previous reports that the actin depolymerising agent Latrunculin A (Lat A) causes a spindle orientation dependent delay in the onset of anaphase by disrupting astral microtubule interaction with medial cortical actin cytoskeleton (Gachet *et al.*, 2001, 2004; Rajagopalan *et al.*, 2004; Tournier *et al.*, 2004). Therefore, I decided to re-evaluate the effect of Lat A on mitotic progression in fission yeast.

5.2 Results

5.2.1 Lat A delays anaphase onset and causes pre-anaphase spindle collapse

First, the effect of different concentrations of Lat A was examined in movies of single *ndc80-gfp cdc11-cfp* cells to simultaneously monitor spindle length, spindle angle and the timing of anaphase onset. The average duration of phase 2 in untreated cells was 11 ± 3 minutes compared to 14.5 ± 5.5 minutes in the presence of 0.625μM Lat A and 19 ± 9 minutes in the presence of 1.25μM Lat A (figure 5.1a-d). These data confirm previous results in population studies that Lat A delays the onset of anaphase. However, closer examination reveals that Lat A causes a mitotic delay in only a subset of cells (figure 5.2b). In 61% of cells (n=17/28) (figures 5.2b, c and f) the length of phase 2 is 11 ± 2 minutes in the presence of 1.25μM Lat A, which is indistinguishable from that in the absence of drug (11 ± 3 minutes; figure 5.2a and e). In the other 39% of cells (n=11/28), addition of 1.25μM Lat A causes a protracted extension of phase 2 (27.5 ± 4.5 minutes) with subsequent pre-anaphase spindle collapse (figures

Figure 5.1 Latrunculin A treatment causes a concentration dependent pre-anaphase delay

Graphs representing multiple time-lapse movies of (**a**) *ndc80-gfp cdc11-cfp* (*wild type*) cells (n=29) (reproduced from 3.7a), (**b**) *ndc80-gfp cdc11-cfp* cells + 0.625μM Lat A (n=12) and (**c**) *ndc80-gfp cdc11-cfp* cells + 1.25μM Lat A (n=28) showing the length of the mitotic spindle through time. Plots are aligned at the end of anaphase A (dashed line).
(**d**) Histogram showing the average length of phase 2 in (a-c) above. Error bars show standard error.

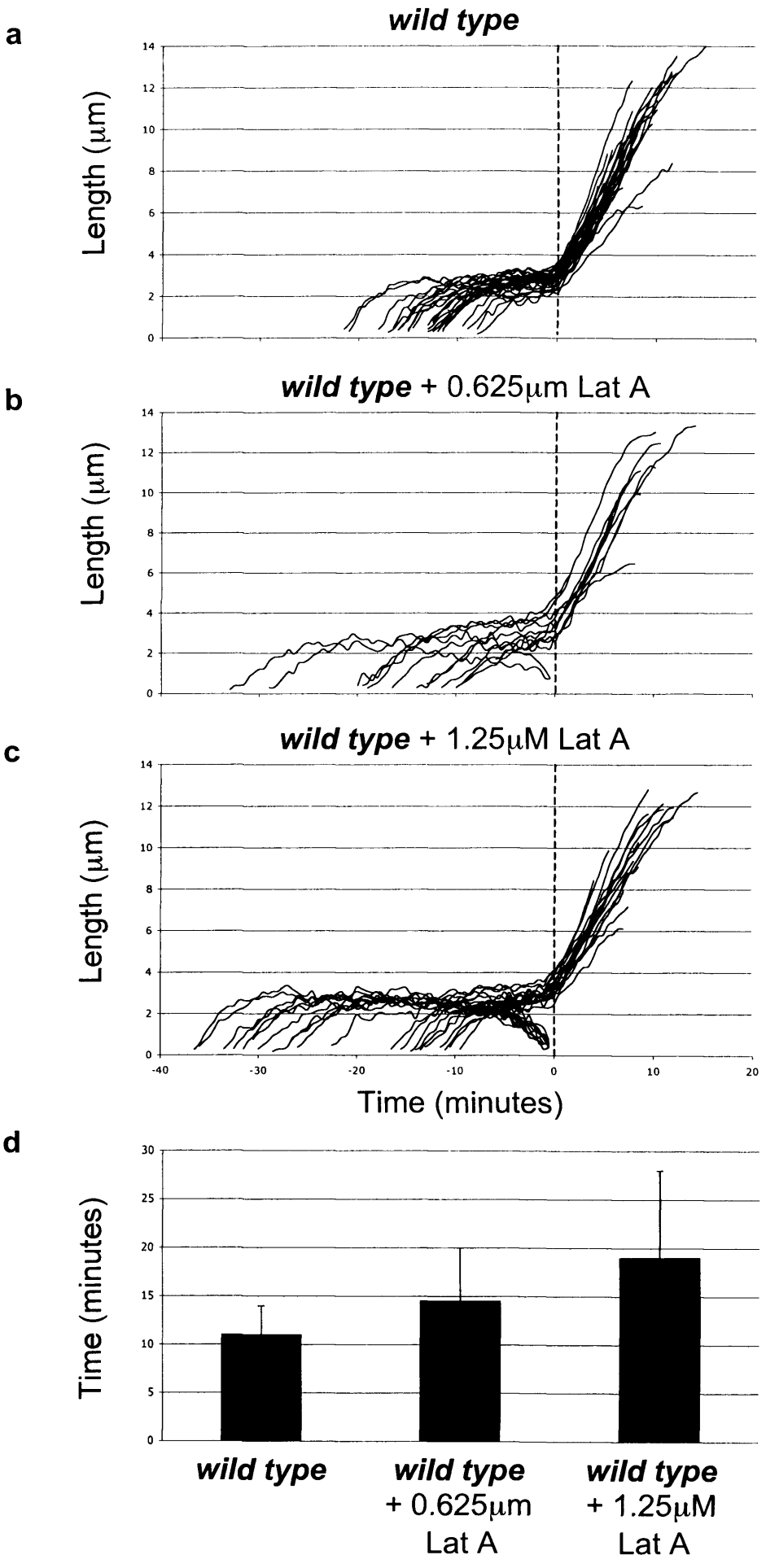
a
wild type
Length (μm)
b
wild type + 0.625μm Lat A
Length (μm)
c
wild type + 1.25μM Lat A
Length (μm)
Time (minutes)
d
Time (minutes)
wild type
wild type + 0.625μm Lat A
wild type + 1.25μM Lat A

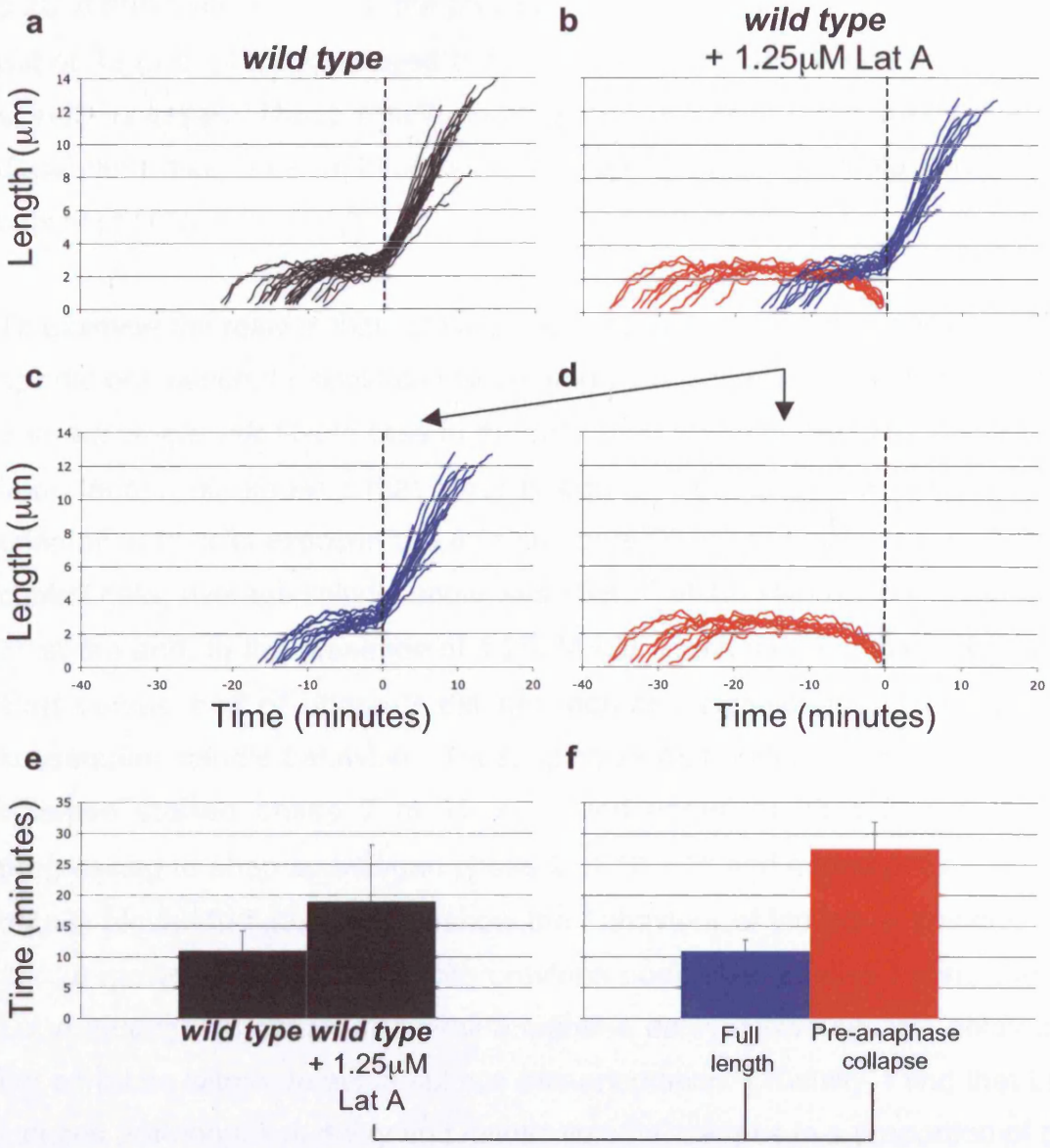

Figure 5.2 Latrunculin A treatment results in a proportion of cells that undergo an extended phase 2 and a subsequent pre-anaphase spindle collapse

(**a**) Multiple time-lapse movies of *ndc80-gfp cdc11-cfp* (*wild type*) cells (n=29) showing the length of the mitotic spindle through time. Reproduced from figure 5.1a.
(**b**) Multiple time-lapse movies of *ndc80-gfp cdc11-cfp* (*wild type*) cells + 1.25μM Lat A (n=28) showing the length of the mitotic spindle through time. Spindles that undergo anaphase are shown in blue (extracted and shown in (**c**)). Spindles that undergo a pre-anaphase collapse are shown in red (extracted and shown in (**d**)). Plots in (a), (b), (c) and (d) are aligned at the end of anaphase A.
(**e**) Histogram showing the average length of phase 2 in (a) and (b) above. Error bars show standard error.
(**f**) Histogram showing the average length of phase 2 in (c) and (d) above. Error bars show standard error.

5.2b, d and f; movie 5.1). In the presence of 0.625μM Lat A (figure 5.1b) only 2 out of 12 cells (17%) displayed a delay in anaphase onset and pre-anaphase spindle collapse. These results indicate that Lat A induces a concentration dependent delay in anaphase onset and pre-anaphase spindle collapse in a subset of cells.

To examine the relationship between the anaphase delay imposed by Lat A and spindle orientation, I calculated spindle angle at both the start and end of phase 2 in *ndc80-gfp cdc11-cfp* cells in the presence and absence of 1.25μM Lat A. Importantly, this showed that there is only a slight increase in spindle mis-orientation in cells exposed to Lat A compared to control cells (figure 5.3a). In control cells, average spindle angle was 15 ± 3° at the start of phase 2 and 17 ± 3° at the end. In the presence of 1.25μM Lat A, average spindle angle at the start versus end of phase 2 did not increase significantly, irrespective of subsequent spindle behaviour. Thus, spindles that underwent a pre-anaphase collapse started phase 2 at 19 ± 3° and ended at 23 ± 3° whilst those progressing to anaphase began phase 2 at 18 ± 3° and ended at 22 ± 4°. This data is plotted in figure 5.3b to show the behaviour of individual spindles from the 28 movies. In agreement with previous population studies I conclude that Lat A induces an apparent overall anaphase delay. However, this delay does not correlate with a defect in spindle mis-orientation. Crucially, I find that Lat A induces pre-anaphase delay and mitotic spindle collapse in a proportion of cells and suggest that it is this effect, rather than an effect on spindle orientation, that gives rise to the Lat A-dependent anaphase delay observed previously.

Additionally, in contrast to Gachet *et al.*, (2004), I found that the rate of spindle elongation in *ndc80-gfp cdc11-cfp* cells (0.82 ± 0.19μm/minute) is not significantly altered by the presence of 1.25μM Lat A (0.79 ± 0.16μm/minute). This is in agreement with my previous conclusions, and those of others, that astral microtubules do not contribute to the rate of spindle elongation (section 3.2.2).

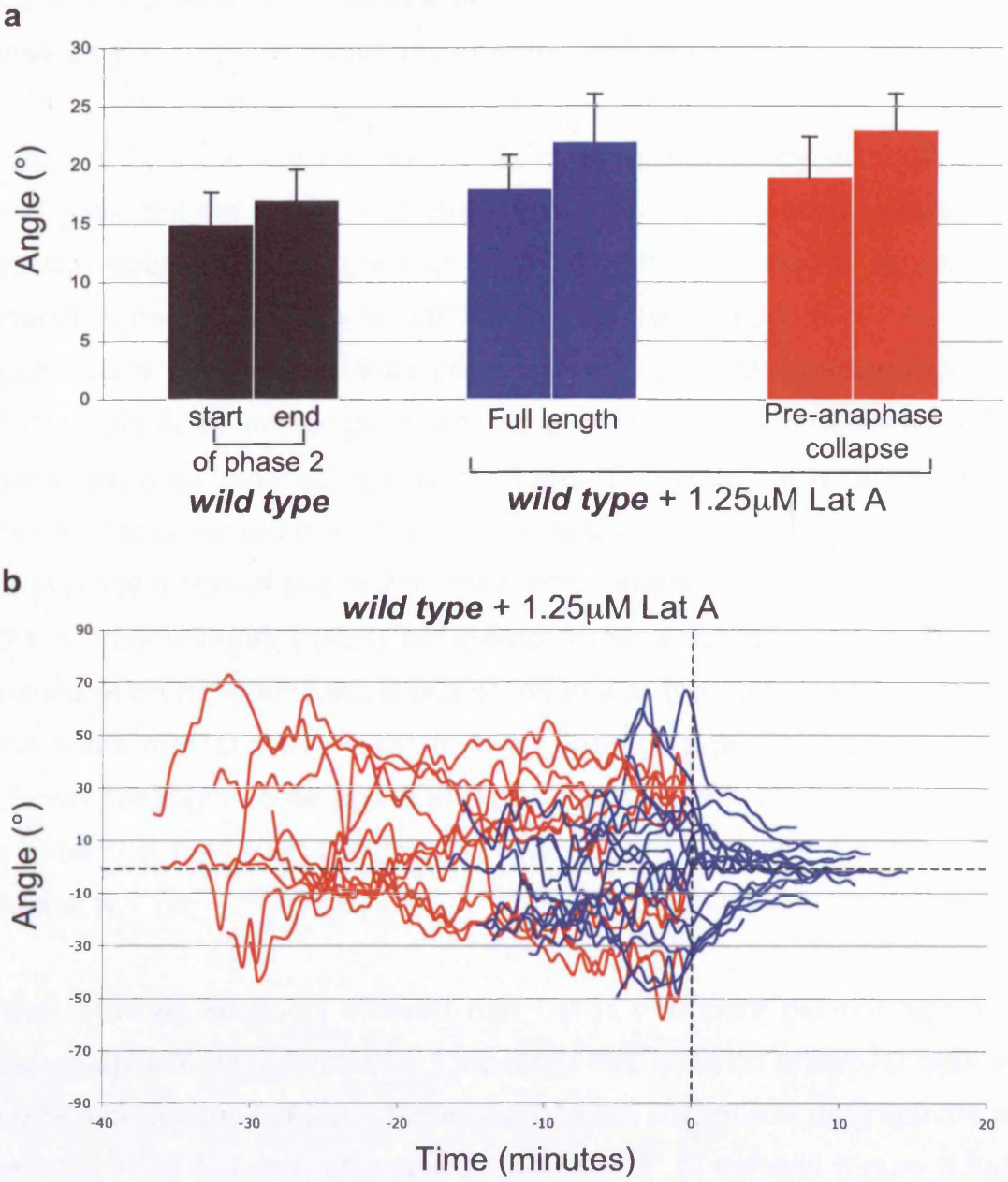

Figure 5.3 Spindle mis-orientation is not significantly elevated by Latrunculin A treatment

(**a**) Histogram showing average angle of the mitotic spindle relative to the longitudinal axis of the cell at the start and end of phase 2. *ndc80-gfp cdc11-cfp* (*wild type*) is shown in black, reproduced from figure 4.2b. *ndc80-gfp cdc11-cfp* (*wild type*) + 1.25μM Lat A is shown in blue and red respectively for those spindles which do not collapse and those that do. Error bars show standard error of the mean (SEM).
(**b**) Multiple time-lapse movies of *ndc80-gfp cdc11-cfp* (*wild type*) cells + 1.25μM Lat A (n=28) showing the angle of the spindle relative to the longitudinal axis of the cell through time. Spindles that undergo anaphase are shown in blue and those that undergo a pre-anaphase collapse in red. Plots are aligned at the end of anaphase A (dashed line).

5.2.2 In the presence of Lat A a proportion of cells lacking Mto1 undergo phase 2 delay and pre-anaphase spindle collapse

In chapter 3, I showed that mitotic spindles are severely mis-orientated in *mto1D* cells but the timing of anaphase onset is not delayed. One possibility is that Mto1 could either be a sensor of spindle mis-orientation or be required to transmit a mis-orientation signal to the cell cycle machinery. To test this hypothesis, I monitored mitotic progression in *mto1D ndc80-gfp cdc11-cfp* (*mto1D*) cells in the presence or absence of 1.25μM Lat A to determine whether a delay could be imposed. Exposure of *mto1D* cells to Lat A causes a similar effect to that observed in wild type cells (section 5.2.1 and figure 5.4a and c). The average length of phase 2 in *mto1D* cells in the presence of 1.25μM Lat A is 21 ± 11.5 minutes (n=28) compared to 12 ± 2.5 minutes (n=20) in the absence of drug (figure 5.4b, d and e). As in wild type cells, in the presence of Lat A some *mto1D* cells (n=13/28; 46%) undergo a protracted phase 2 (30 ± 10.5 minutes; figure 5.4d and f) and pre-anaphase spindle collapse, whereas the remaining (n=15/28; 54%) cells have a phase 2 of 13 ± 4 minutes (figure 5.4d and f).

In the previous section I showed that Lat A treatment did not significantly increase spindle mis-orientation. I repeated this analysis in *mto1D* cells in the presence or absence of Lat A (figure 5.5). In the absence of drug spindle angle was 37 ± 7° at the start of phase 2 and 34 ± 4° at the end (figure 5.5a). By contrast, in the presence of Lat A spindle angle was 33 ± 7° and 32 ± 7° respectively for spindles that progressed through anaphase, whilst those that collapsed prior to anaphase measured 34 ± 6° and 36 ± 8° (figure 5.5a). This data is plotted to show the angle of individual spindles over time in figure 5.5b, which clearly shows that there is no difference between *mto1D* cells irrespective of pre-anaphase collapse during mitosis.

Additionally, the rate of spindle elongation in *mto1D* cells in the absence of drug (0.84 ± 0.28μm/minute) is not significantly different from the rate of spindle elongation in *mto1D* in the presence of 1.25μM Lat A (0.76 ± 0.28μm/minute).

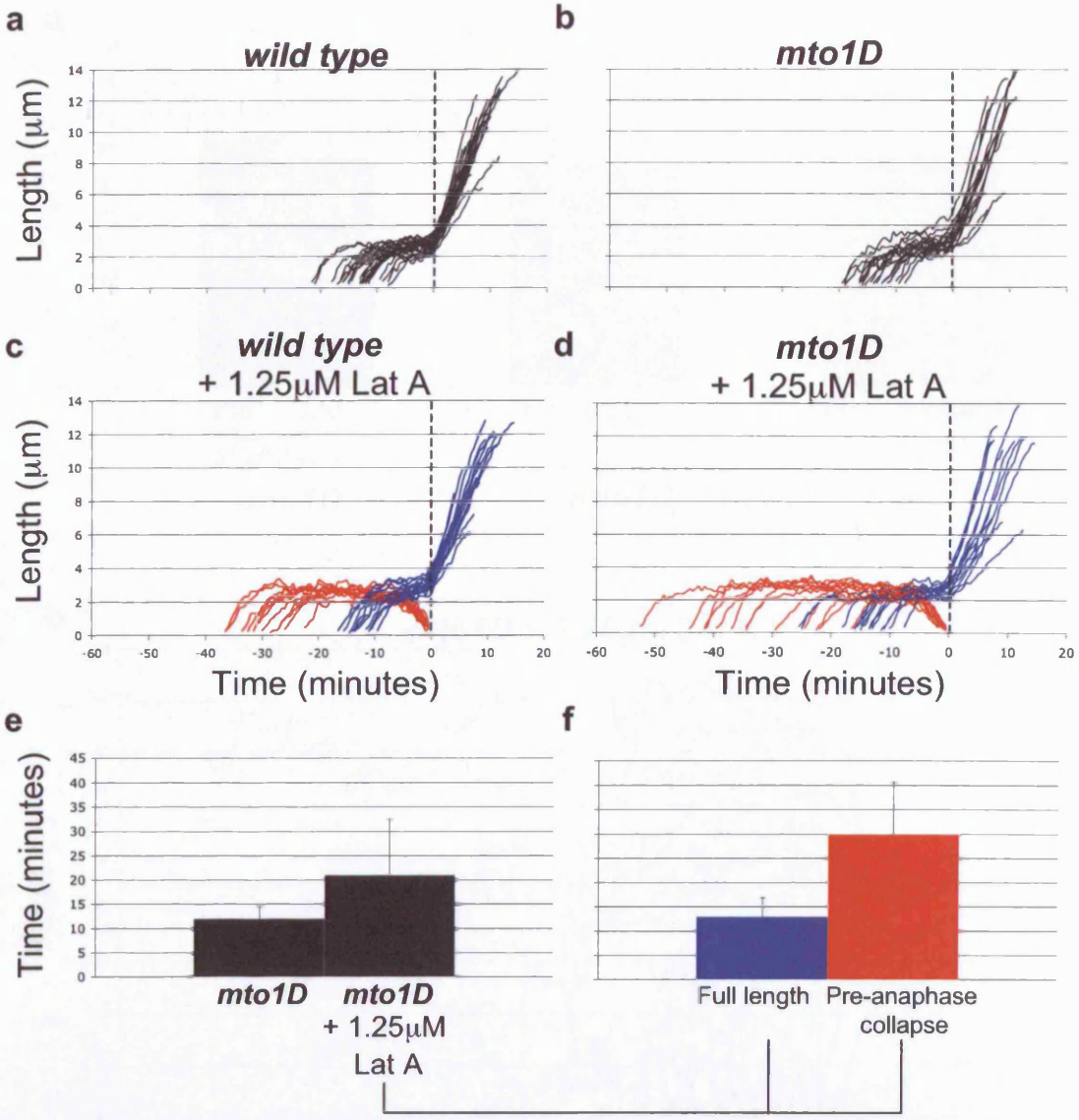

Figure 5.4 Latrunculin A treatment results in a proportion of *mto1D* cells with an extended phase 2 and a subsequent pre-anaphase spindle collapse

Multiple time-lapse movies showing the length of the mitotic spindle through time for: (**a**) *ndc80-gfp cdc11-cfp* (*wild type*) cells (n=29), reproduced from figure 5.1a.; (**b**) *mto1D ndc80-gfp cdc11-cfp* (*mto1D*) cells (n=20), reproduced from figure 3.7b.; (**c**) *ndc80-gfp cdc11-cfp* cells (*wild type*) cells + 1.25μM Lat A (n=28). Spindles that undergo anaphase are shown in blue and those that undergo pre-anaphase collapse in red.; (**d**) *mto1D ndc80-gfp cdc11-cfp* (*mto1D*) cells + 1.25μM Lat A (n=28). Spindles that undergo anaphase are shown in blue and those that undergo pre-anaphase collapse in red. Plots in (a), (b), (c) and (d) are aligned at the end of anaphase A (dashed line).
(**e**) Histogram showing the average length of phase 2 in (b) and (d) above. Error bars show standard error.
(**f**) Histogram showing the average length of phase 2 in (d) above. Spindles that undergo anaphase are shown in blue and those that undergo pre-anaphase collapse in red. Error bars show standard error.

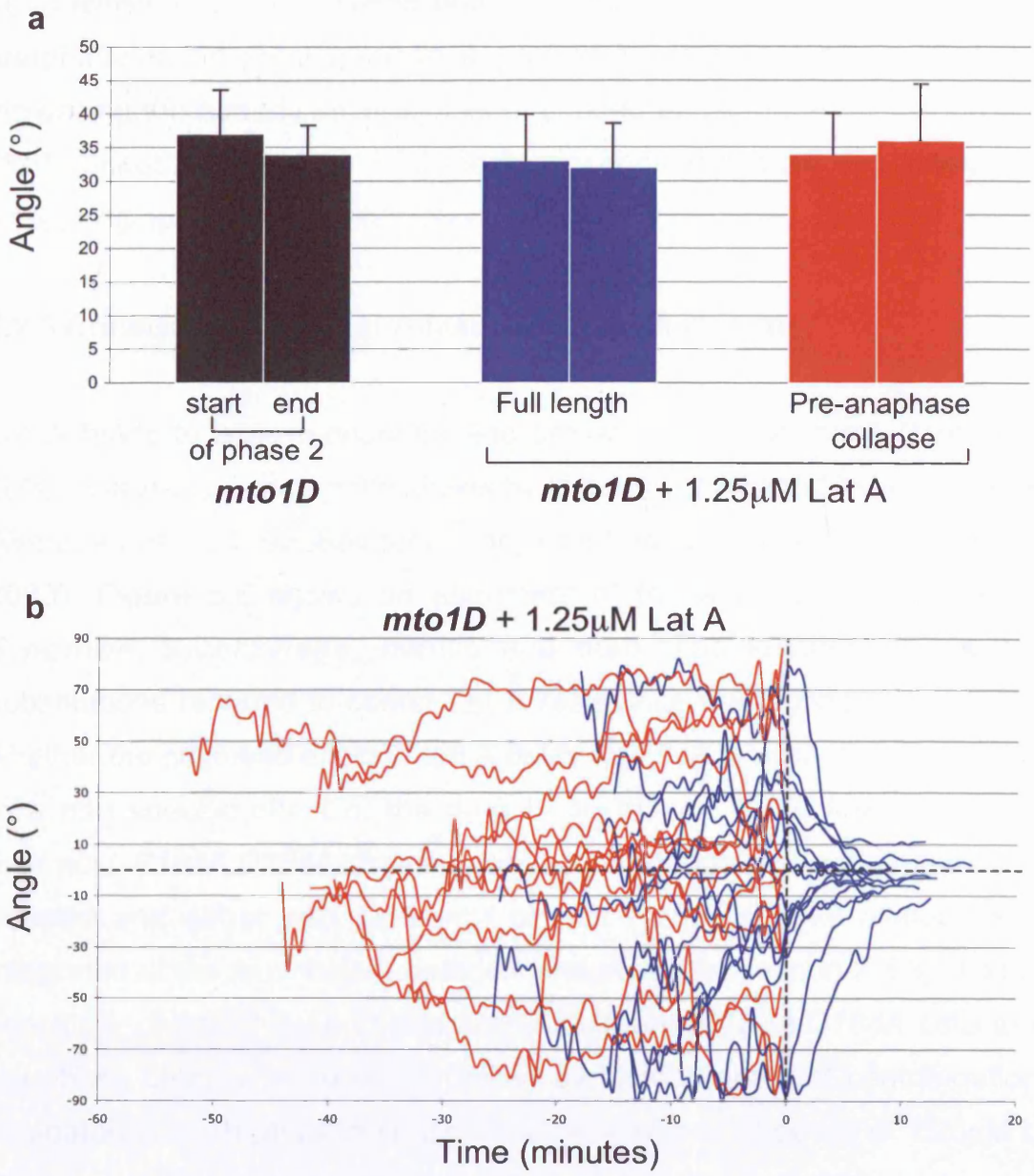

Figure 5.5 Latrunculin A treatment does not increase spindle mis-orientation in cells lacking Mto1

(**a**) Histogram showing the average angle of the mitotic spindle relative to the longitudinal axis of the cell at the start and end of phase 2. *mto1D ndc80-gfp cdc11-cfp* (*mto1D*) shown in black, reproduced from figure 4.2b. *mto1D ndc80-gfp cdc11-cfp* (*mto1D*) + 1.25μM Lat A shown in blue and red respectively for those spindles which do not collapse and those that do. Error bars show standard error of the mean (SEM).
(**b**) Graphs representing multiple time-lapse movies of *mto1D ndc80-gfp cdc11-cfp* (*mto1D*) cells + 1.25μM Lat A (n=28) showing the angle of the spindle relative to the longitudinal axis of the cell through time. Spindles that undergo anaphase are shown in blue and those that undergo a pre-anaphase collapse in red. Plots are aligned at the end of anaphase A (dashed line).

In conclusion, Lat A imposes both a phase 2 delay and a subsequent pre-anaphase spindle collapse on a proportion of cells lacking Mto1 without increasing the already severely mis-orientated angle of the spindle. Therefore, Mto1 cannot be part of the SOC machinery and Lat A is causing a delay without increasing spindle mis-orientation.

5.2.3 Construction of a Lat A-insensitive actin mutant

Lat A binds to actin monomers and prevents polymerisation (Morton *et al.*, 2000). Lat A-insensitive actin alleles have been constructed in both *S.cerevisae* (Wertman *et al.*, 1992; Belmont *et al.*, 1999) and human cell lines (Fujita *et al.*, 2003). Figure 5.6 shows an alignment of the actin protein sequences of *S.pombe*, *S.cerevisae*, mouse and man. The location of the residue substitutions required to confer Lat A resistance are highlighted. To examine whether the observed effect of Lat A delay was due to actin depolymerisation or to a non specific effect of the drug I constructed *act1D leu:act1* and *act1D leu1:act1-R183A,D184A* strains in which the endogenous actin gene had been deleted and either wild type *act1* or *act1-R183A,D184A* alleles had been integrated at the *leu1* locus (materials and methods, section 2.5.3). To test the sensitivity of *act1D leu:act1* and *act1D leu1:act1-R183A,D184A* cells to Lat A log phase cultures were synchronised by lactose gradient centrifugation and incubated in fresh medium either in the presence or absence of 1.25μM Lat A. Cells were fixed in formaldehyde at time 0 and every 20 minutes for 140 minutes thereafter, and stained with DAPI and calcofluor to observe nuclei and septa respectively (n=200 cells for each time point). In *act1D leu:act1* (control) cells, in the absence of Lat A, the peak of binucleate cells occurred at 60 minutes and the peak of septation at 70 minutes (figures 5.7a and 5.7c). In the presence of Lat A, the peak of bi-nucleate cells was delayed relative to the control and cytokinesis was completely blocked (figures 5.7a and 5.7c). Synchronised untreated *act1D leu1:act1-R183A,D184A* cells also underwent sister chromatid separation and septum formation. However in this case, addition of 1.25μM Lat A had no effect on the timing or appearance of bi-nucleates or the formation of septa (figures 5.7c and 5.7d). This data indicates that the *act1D leu1:act1-R183A,D184A* allele is insensitive to Lat A in fission yeast. I also constructed a second strain *act1D leu1:act1-D157E* based on the

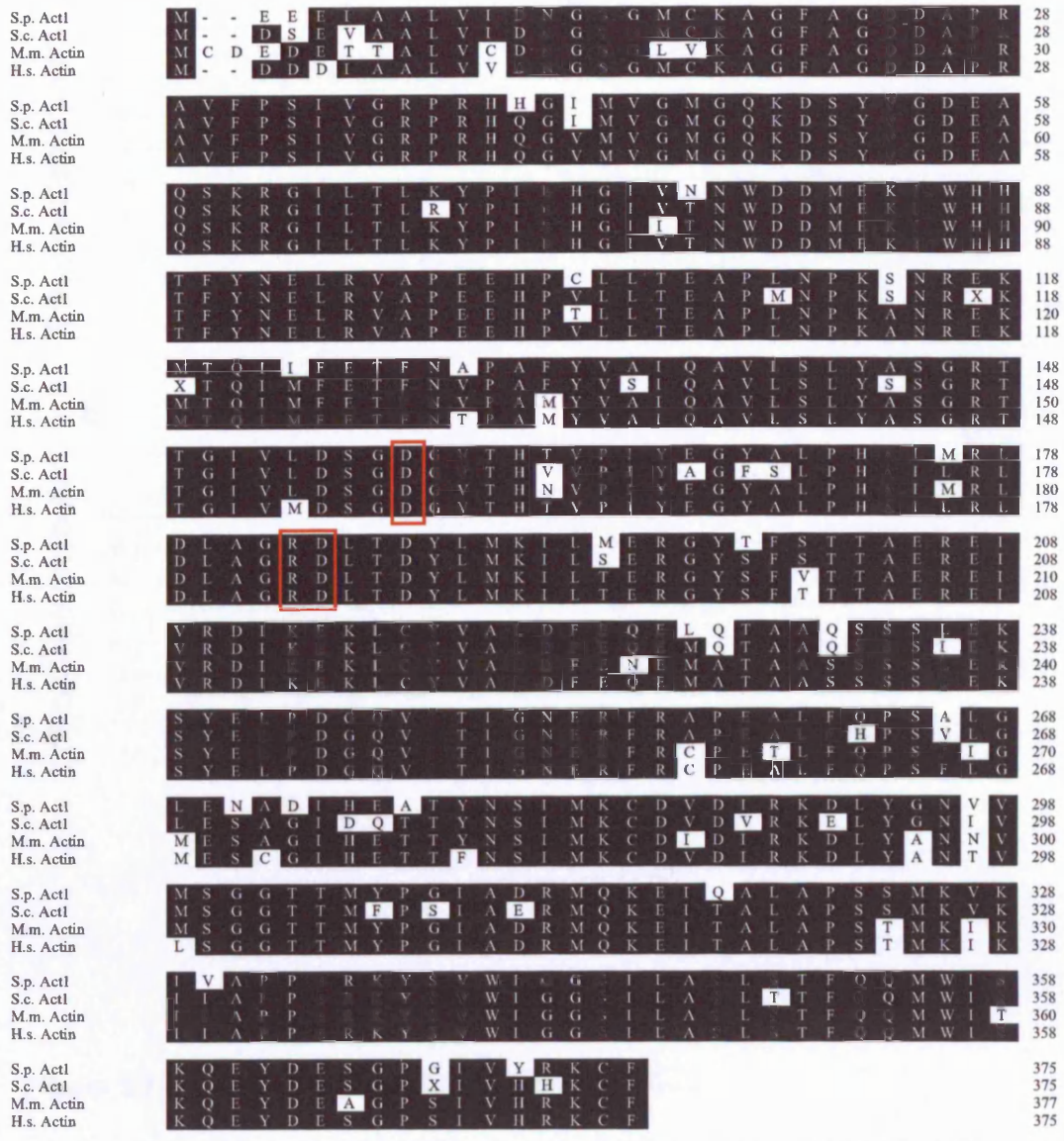

Figure 5.6 Actin sequence alignments between *S.pombe* (S.p.), *S.cerevisae* (S.c.), mouse (M.m.) and man (H.s.)

Black boxes indicate regions of homology. Red boxes indicate residues mutated to confer Latrunculin resistance on actin, namely D157 and R183,D184.

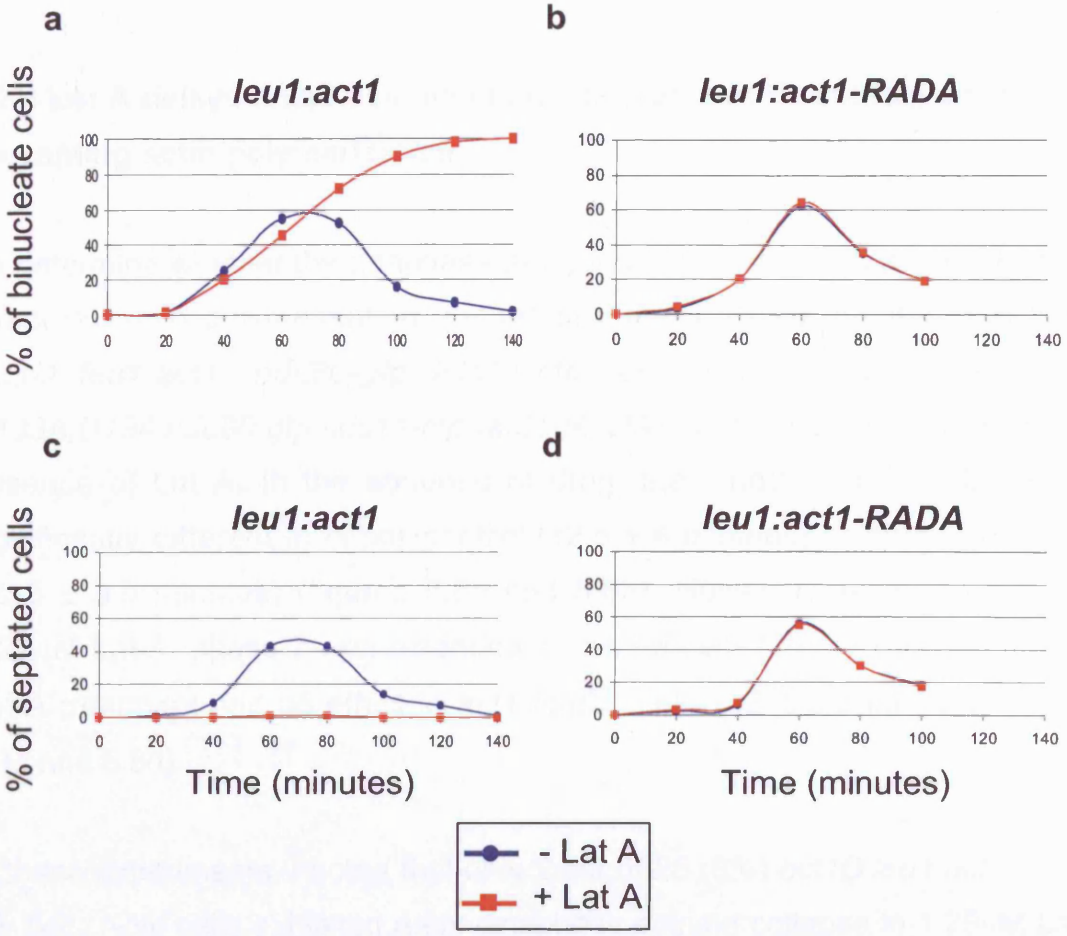

Figure 5.7 *act1-R183A,D184A* is resistant to Lat A

Log phase *act1D leu1:act1* (control) and *act1D leu1:act1-R183A,D184A* cells were synchronised by lactose gradient centrifugation and grown in the presence and absence of 1.25μM Lat A. Samples were taken and fixed at time 0 and every 20 minutes thereafter and stained with DAPI and calcofluor to visualise DNA and septa respectively.
(**a**) Graph showing the percentage of binucleate *act1D leu1:act1* (*leu1:act1*) cells over time in the presence (red) and absence (blue) of Lat A.
(**b**) As (a) for *act1D leu1:act1-R183A,D184A* (*leu1:act1-RADA*) cells.
(**c**) Graph showing the percentage of septated *act1D leu1:act1* (*leu1:act1*) cells over time in the presence (red) and absence (blue) of Lat A.
(**d**) As (c) for *act1D leu1:act1-R183A,D184A* (*leu1:act1-RADA*) cells.

identification of Lat A-insensitive actin alleles in budding yeast and this was also found to confer Lat A resistance in fission yeast (data not shown). However, I chose to use the *act1D leu1:act1-R183A,D184A* strain for the remainder of this work.

5.2.4 Lat A delays anaphase onset and causes mitotic spindle collapse by preventing actin polymerisation

To determine whether the anaphase delay induced by Lat A is due to its known effect on actin polymerisation, mitotic progression was monitored in single *act1D leu1:act1 ndc80-gfp cdc11-cfp* (*control*) and *act1D leu1:act1-R183A,D184 ndc80-gfp cdc11-cfp* (*act1-RADA*) cells either in the presence or absence of Lat A. In the absence of drug, the length of phase 2 was not significantly different in either *control* (12.5 ± 4 minutes) or *act1-RADA* cells (12.5 ± 3.5 minutes) (figures 5.8a and 5.8b). However, in the presence of 1.25μM Lat A, phase 2 was extended in *control* cells (20.5 ± 8 minutes) while Lat A treatment had no effect in *act1-RADA* cells (13 ± 3.5 minutes) (figures 5.8c and 5.8d).

In these experiments, I noted that only 2 out of 26 (8%) *act1D leu1:act1 ndc80-gfp cdc11-cfp* cells exhibited a pre-anaphase spindle collapse in 1.25μM Lat A (figure 5.8c), lower than that observed in *act1*$^{+}$ *ndc80-gfp cdc11-cfp* cells at the same dose (39%; figure 5.2b). I reasoned that actin may be expressed at a higher level from the *leu1* locus than at its normal chromosomal location which may lead to partial insensitivity to Lat A. For this reason, the experiments above were repeated in the presence of 2.5μM Lat A. At this concentration, pre-anaphase spindle collapse occurred in 8 out of 28 (30%) *act1D leu1:act1 ndc80-gfp cdc11-cfp* cells, whilst there was no discernible effect on the length of phase 2 in *act1D leu1:act1-R183A,D184 ndc80-gfp cdc11-cfp* cells (13 ± 4.5 minutes) and did not induce mitotic spindle collapse (figures 5.8e and 5.8f). The data, summarised in figure 5.9, strongly indicate that the effect of Lat A in inducing an anaphase delay and mitotic spindle collapse in fission yeast is due to its documented role in preventing actin polymerisation.

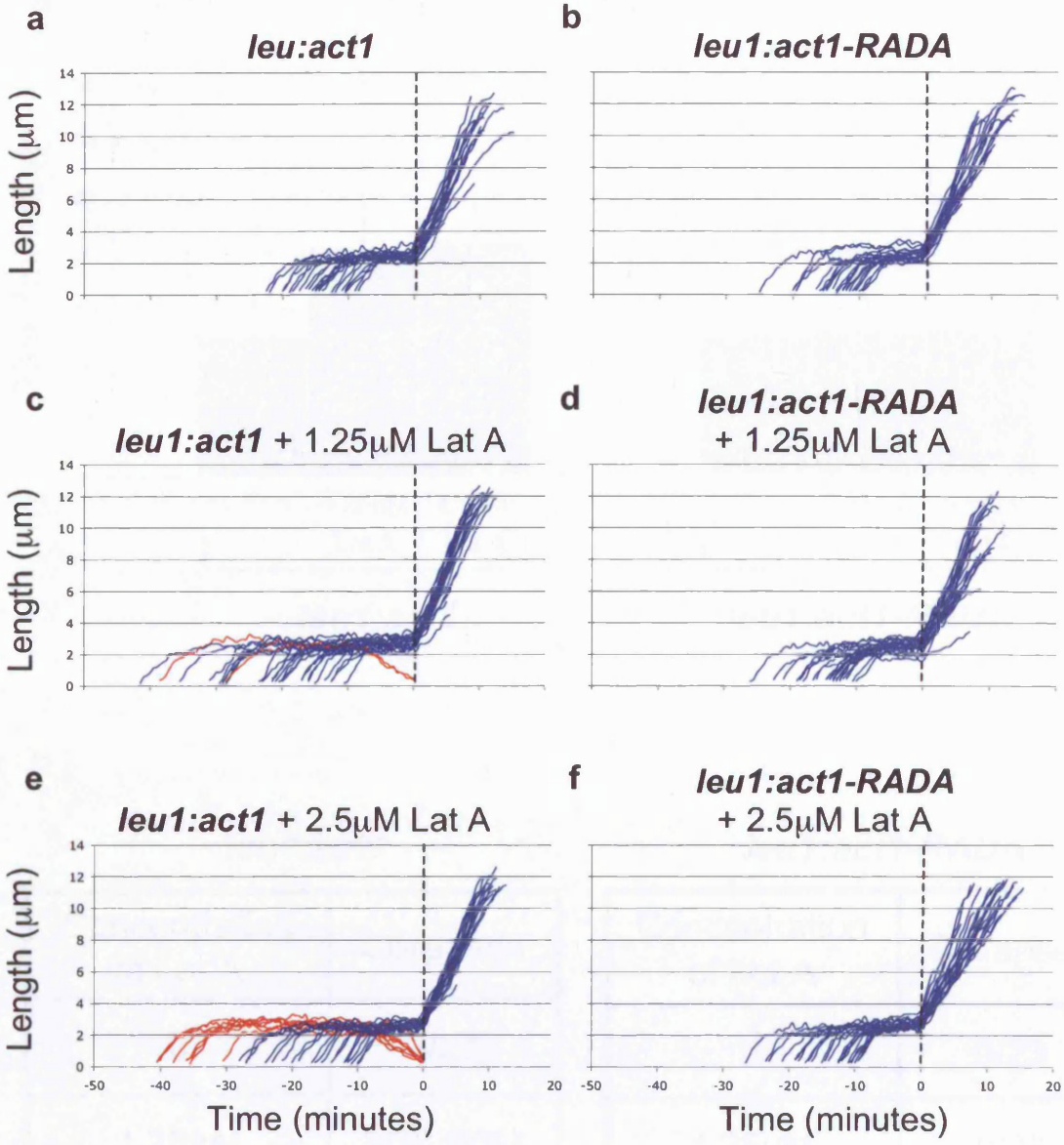

Figure 5.8 *act1-R183A,D184A* cells do not undergo a pre-anaphase delay or collapse in the presence of Lat A

Graphs representing multiple time-lapse movies showing the length of the mitotic spindle through time for: *act1D leu1:act1 ndc80-gfp cdc11-cfp* (*leu1:act1*) cells in the absence of Lat A (n=23) (**a**), in the presence of 1.25μM Lat A (n=26) (**c**) and 2.5μM Lat A (n=27) (**e**); *act1D leu1:act1-R183A,D184A ndc80-gfp cdc11-cfp* (*leu1:act1-RADA*) cells in the absence of Lat A (n=23) (**b**), in the presence of 1.25μM Lat A (n=26) (**d**) and 2.5μM Lat A (n=25) (**f**). Spindles that undergo anaphase are shown in blue and those that undergo a pre-anaphase collapse in red. Plots are aligned at the end of anaphase A.

a

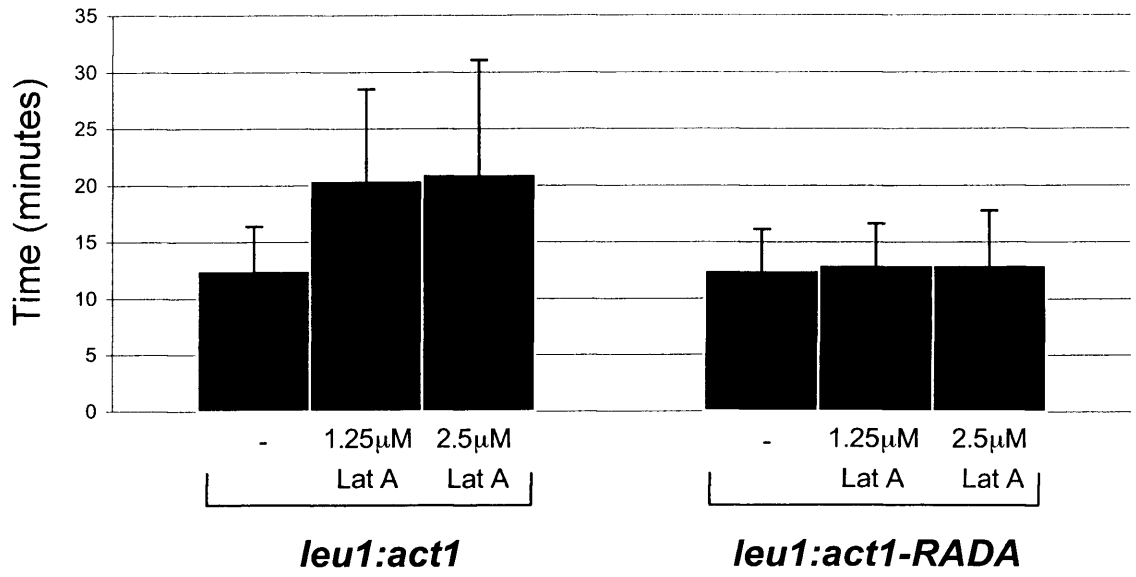

b

leu1:act1

Concentration of Lat A	Collapses
0	0/23
1.25μM	2/26 (8%)
2.5μM	8/27 (30%)

leu1:act1-RADA

Concentration of Lat A	Collapses
0	0/23
1.25μM	0/26
2.5μM	0/25

Figure 5.9 Latrunculin A has no effect on the length of phase 2 or spindle stability in an *act1-R183A,D184A* mutant

(**a**) Histogram showing the average length of phase 2 for *act1D leu1:act1 ndc80-gfp cdc11-cfp* (*leu1:act1*) and *act1D leu1:act1-R183A,D184A ndc80-gfp cdc11-cfp* (*leu1:act1-RADA*) cells in the presence and absence of 1.25 and 2.5μM Lat A. Data extracted from figure 5.8 a-f. Error bars show standard error.
(**b**) Number and percentage of pre-anaphase spindle collapses observed in the same data set.

5.3 Discussion

5.3.1 The target of Lat A: previous assumptions

It was previously reported that in fission yeast, the addition of Lat A caused a delay in the onset of anaphase by causing spindle mis-orientation. This phenomenon was termed a spindle orientation checkpoint (SOC) (section 1.3.2.2.2). In this chapter, I confirm that Lat A does indeed induce a mitotic delay but demonstrate that this is not due to an effect on spindle orientation. Since there is also no relationship between spindle angle and the timing of anaphase onset (section 3.2.1), I conclude that fission yeast does not possess a spindle orientation checkpoint. Therefore, the previous conclusion that Lat A imposes a mitotic delay by preventing astral microtubule interaction with the cell cortex must be erroneous. In addition, it was found in a previous study that the elongation rate in phase 3 was slowed by the presence of Lat A (Gachet *et al.*, 2004). However, I have found no such effect in either wild type cells or cells lacking Mto1. This is consistent with my previous findings that the absence of astrals does not affect elongation rate (section 3.2.2). Additionally, I have found that a significant effect of Lat A, not previously observed, is that it causes a collapse of pre-anaphase spindles in a proportion of cells.

5.3.2 Why is pre-anaphase collapse only seen in a proportion of cells?

An important question raised by the novel observation described in these studies is why Lat A treatment causes an anaphase delay and spindle collapse is only a proportion of cells? One answer might be that I was using a sub-optimal concentration of drug. However, this is difficult to test because complete de-polymerisation of the actin cytoskeleton by high Lat A concentrations prevents mitotic entry as cells are not able to grow to a critical size to allow mitotic onset (Rupes *et al.*, 2001). Notably however, complete depolymerisation of the actin cytoskeleton in *cdc25-22* cells, which do not need to satisfy a size threshold as they are already large, delays but does not prevent the onset of anaphase. This argues that resistance to Lat A is an inherent property of at least a proportion of the cell population. Another possibility is that the number of spindle collapses observed correlates with the length of exposure of the cells to

Lat A. However I find there is no such correlation. Indeed the spindles of cells in the same visual field, which have therefore been exposed to Lat A for the same amount of time, experience different fates, namely some collapse and some do not. Similarly, photo-toxicity due to an extended period of light exposure is not responsible for the collapses, since the same conditions were used to image *mal3D* cells, which have a delayed phase 2 but do not undergo spindle collapse. At present it is unclear whether the pre-anaphase collapse phenomenon is reversible. However, in synchronisation experiments, all cells eventually become bi-nucleate which argues that mitotic spindle collapse is not irreversible. Further efforts, however, could be made to visualise spindle reformation following spindle collapse in single cells.

5.3.3 What is the real target of Lat A?

By use of a single cell based approach, I have found that Lat A causes mitotic spindles to collapse prior to anaphase onset in a proportion of cells. This phenotype would not have been apparent in population studies. Additionally, the collapses may have been prevented when mitotic progression was monitored in *nmt1-gfp-atb2* cells, in which tubulin is overexpressed. This possibility is explored in more detail in chapter 6. Regardless, my data suggest that Lat A delays the onset of anaphase by disrupting mitotic spindle stability rather than by causing spindle mis-orientation. Furthermore, I demonstrate that the effect of Lat A is due to its effect on actin polymerisation rather than to a non-specific effect of the drug. One possibility is that Lat A influences the stability of the spindle midzone. Interestingly, Lat A induces a delay in activation of the anaphase promoting complex (APC) through a mechanism that requires a subset of spindle assembly checkpoint proteins, including Mad3, Bub1, Bub3 and Mph1, but not Mad1 or Mad2 (Tournier *et al.*, 2004; section 1.3.2.2.2). It is possible that the stability of the spindle midzone is monitored by a checkpoint which is activated in the presence of Lat A. This possibility is explored further in chapter 6.

The question remains with respect to the role of actin in mitotic spindle stability. There are at least three possibilities:

Firstly, actin could be maintaining spindle stability by affecting the transcription of other players. Actin is a component of the NuA4, Ino80 and Swr chromatin remodelling complexes (reviewed in Blessing *et al.*, 2004) and there is evidence to suggest that these can affect sister chromatid cohesion (reviewed in Riedel *et al.*, 2004). Furthermore, actin is a component of the pre-initiation complex for RNA ploymerases I, II and III and also acts at a step immediately following transcript initiation (reviewed in Pederson and Aebi, 2005). However, it is unknown whether actin in these roles is monomeric, oligomeric or filamentous. The possibility that Lat A treatment is revealing a role for actin in transcription regulation seems unlikely, since Lat A only seems to effect pole-to-pole microtubules rather than k-fibres (the spindle assembly checkpoint is not activated). However, this possibility cannot be discounted although it would require microarray experiments in the presence and absence of Lat A to verify.

Secondly, actin depolymerisation could cause a redistribution of interphase microtubule "plus" end proteins to the nucleus. This would be the case if actin were required to tether proteins such as Tea1-4 and Tip1 in the cytoplasm to prevent them from entering the nucleus and binding the tips of spindle microtubules. Again, however, if this were the case one might expect Lat A to affect both pole-to-pole microtubules and interaction with the kinetochores resulting in a full SAC activation. This hypothesis could be easily tested by analysing kinetochore and SPB dynamics in Tea1-complex delete cells.

Thirdly, there could be an actin-based spindle matrix in fission yeast. There is some evidence for such a structure in crane fly spermatocytes (Fabian and Forer, 2005). Actin is also required for chromosome congression in very large oocytes (Lenart *et al.*, 2005). In addition, mDia3 (formin) is found at the plus end of spindle microtubules and is required for microtubule-kinetochore interactions (Yasuda *et al.*, 2004). In bacteria, the actin homologue MreB is utilised in the division of the genetic material (reviewed in Thanbichler and Shapiro, 2006). Spindle matrix proteins, not related to actin, have been discovered in *Drosophila* (Skeletor, Chromator and Megator: Walker *et al.*, 2000; Rath *et al.*, 2004; Qi *et al.*, 2004) and in budding yeast (Fin1: van Hemert *et al.*, 2003; Woodbury and Morgan, 2007). The genetics of Fin1 in *S.cerevisae* are particularly intriguing since it is required for viability in the absence of Ase1

(which will be discussed in the following chapter). At present, a spindle matrix factor has not been found in fission yeast. Actin as a spindle-matrix factor in *S.pombe* is an attractive possibility but is difficult to directly test. Phalloidin staining of a filament at the mitotic spindle may be masked by actin at the division ring. Also some evidence suggests that the form of actin in the nucleus cannot bind phalloidin (Schoenenberger *et al.*, 2005). Monoclonal antibodies (2G2 and 1C7) to conformation-specific forms of actin that specifically recognise nuclear actin structures have been produced but these have not yet been tested in fission yeast (Gonsior *et al.*, 1999; Schoenenberger *et al.*, 2005). The epitopes to which these antibodies were raised are conserved between *S.pombe* and mammalian actin, and so have a good chance of being effective in fission yeast.

Whilst it is clear from my data that actin plays an important role in maintaining the stability of the pre-anaphase mitotic spindle in fission yeast, the mode of action remains unclear at this time.

5.4 Conclusions

- Lat A delays the onset of anaphase and causes pre-anaphase spindle collapse
- Lat A does not cause anaphase delay by causing spindle mis-orientation.
- The effect of Lat A is due to its effect on actin polymerisation.
- Actin is required for pre-anaphase spindle stability in fission yeast

Chapter 6

Ase1 controls pre-anaphase spindle stability and the timing of anaphase onset

6.1 Introduction

In the last chapter, I presented data showing that actin controls pre-anaphase spindle stability in fission yeast. Bipolar spindle assembly and maintenance of spindle length and stability requires a number of kinesins and microtubule binding proteins. These include members of the ASE1/PRC1/MAP65 family, which bind, stabilise and bundle anti-parallel microtubules (Pellman *et al.*, 1995; Mollinari *et al.*, 2002; Schuyler *et al.*, 2003; Loiodice *et al.*, 2005; Yamashita *et al.*, 2005; Sasabe and Machida, 2006; Carazo-Salas and Nurse, 2007). Fission yeast cells lacking Ase1 are viable but undergo mitotic spindle collapse during anaphase B (Loiodice *et al.*, 2005; Yamashita *et al.*, 2005). In addition, Yamashita *et al.* (2005) show that *ase1D* cells are profoundly defective in the maintenance of an artificial minichromosome. Surprisingly, however, analysis of spindle dynamics in *ase1D nmt1-gfp-atb2* did not reveal a role for Ase1 before anaphase onset in some studies (Yamashita *et al.*, 2005), whereas it did in others (Loiodice *et al.*, 2005). This discrepancy could result from the use of different *atb2-gfp* constructs, which may affect the stability of the spindle. In this chapter I have re-investigated kinetochore and spindle pole dynamics in *ase1D* cells.

6.2 Results

6.2.1 Ase1 localises to the spindle midzone prior to anaphase onset

To visualise Ase1, a strain with the protein tagged with GFP at the C-terminus in a background containing Cdc11-CFP to visualise SPBs was used. Figure 6.1a shows log phase *ase1gfp cdc11-cfp* cells fixed with formaldehyde and stained with DAPI and calcofluor to visualise DNA and septa. As previously reported by Loiodice *et al.* (2005) and Yamashita *et al.* (2005), Ase1 localises to

overlapping anti-parallel microtubules during interphase. Importantly, Ase1 is present at the spindle midzone in mitotic cells. This is clearly shown in figure 6.1b and movie 6.1, which are a time-lapse series of images of an *ase1-gfp cdc11-cfp* cell during mitosis. Ase1 is present at the spindle midzone in phase 1 (0 to 3 minutes) and throughout phase 2 (3 to 18 minutes) and during spindle elongation in phase 3 (18 to 36 minutes). In addition, Ase1 binds to SPBs at 27 minutes, during anaphase B, when astral microtubules become bundled in an anti-parallel manner on the outer face of the SPB.

6.2.2 Cells lacking Ase1 are delayed in anaphase onset and undergo frequent pre-anaphase spindle collapse

To investigate the effect of loss of Ase1 on mitotic progression, individual *ase1D ndc80-gfp cdc11-cfp* cells were imaged throughout mitosis. Figure 6.2c shows that the average length of phase 2 in *ase1D ndc80-gfp cdc11-cfp* cells (22 ± 7 minutes) is extended compared to control cells (11 ± 3 minutes) at the same temperature. Further analysis reveals three mitotic phenotypes in cells lacking Ase1 (figure 6.2b). Firstly, in 9 cells from a sample of 20 (45%) I observed the phase 3 collapse previously reported by (Loiodice *et al.*, 2005; Yamashita *et al.*, 2005) (figure 6.2b). Secondly, pre-anaphase collapses, similar to those induced by Lat A (section 5.2.1), were seen in 7 out of 20 *ase1D* cells (35%) (figure 6.2b). Finally, a new class of spindle fate is revealed in the absence of Ase1, in which anaphase A takes place, meaning sister chromatids separate, but anaphase B does not occur; this phenotype was observed in 4 out of 20 cells (20%) (figure 6.2b). There is also a correlation between the 3 classes of spindle fate and the duration of phase 2 (figure 6.2d), the duration of which is as follows: in cells that undergo spindle collapse in phase 3 it averages 16.5 ± 3 minutes; in cells that undergo anaphase A but not anaphase B it is 21.5 ± 5 minutes; whilst in those that undergo pre-anaphase spindle collapse it is 29.5 ± 4.5 minutes. The reason for this is presently unknown but suggests that other factors apart from Ase1 influence the stability of the spindle midzone and the contribution of these other factors to spindle stability varies from cell to cell.

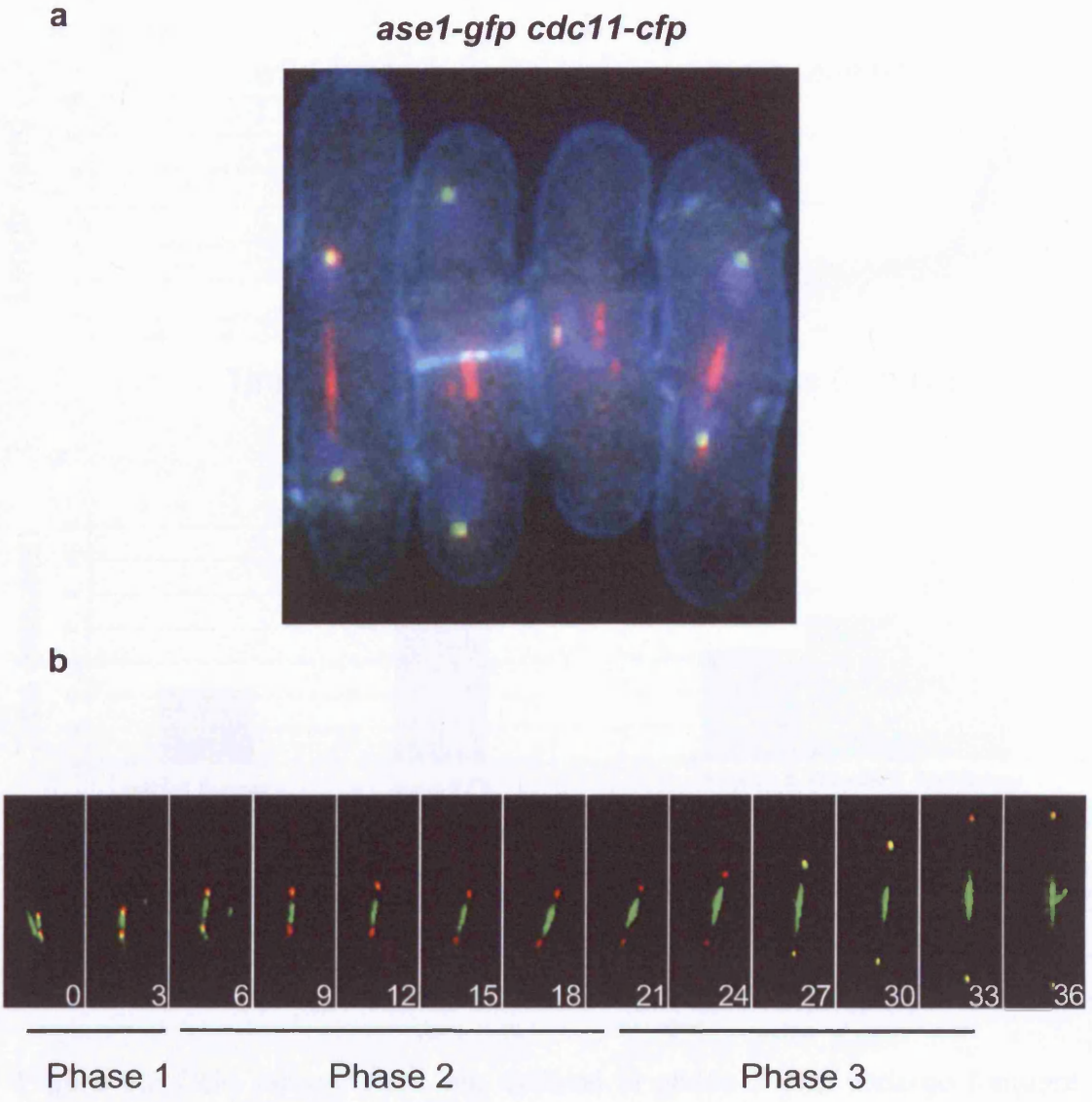

Figure 6.1 Ase1 localisation

(**a**) An image of fixed log phase cells expressing Ase1-GFP (red) and Cdc11-CFP (spindle pole bodies, green) and stained with DAPI and calcofluor to visualise DNA (blue) and septa (light blue) respectively. The third cell from the left is in interphase. The remaining three cells are in mitosis.
(**b**) Images from a time-lapse movie of a cell expressing Ase1-GFP (green) and Cdc11-CFP (spindle pole bodies, red) taken every 3 minutes. Phase 1 is 0-3 minutes, phase 2 is 3-21 minutes and phase 3 is 21-36 minutes.

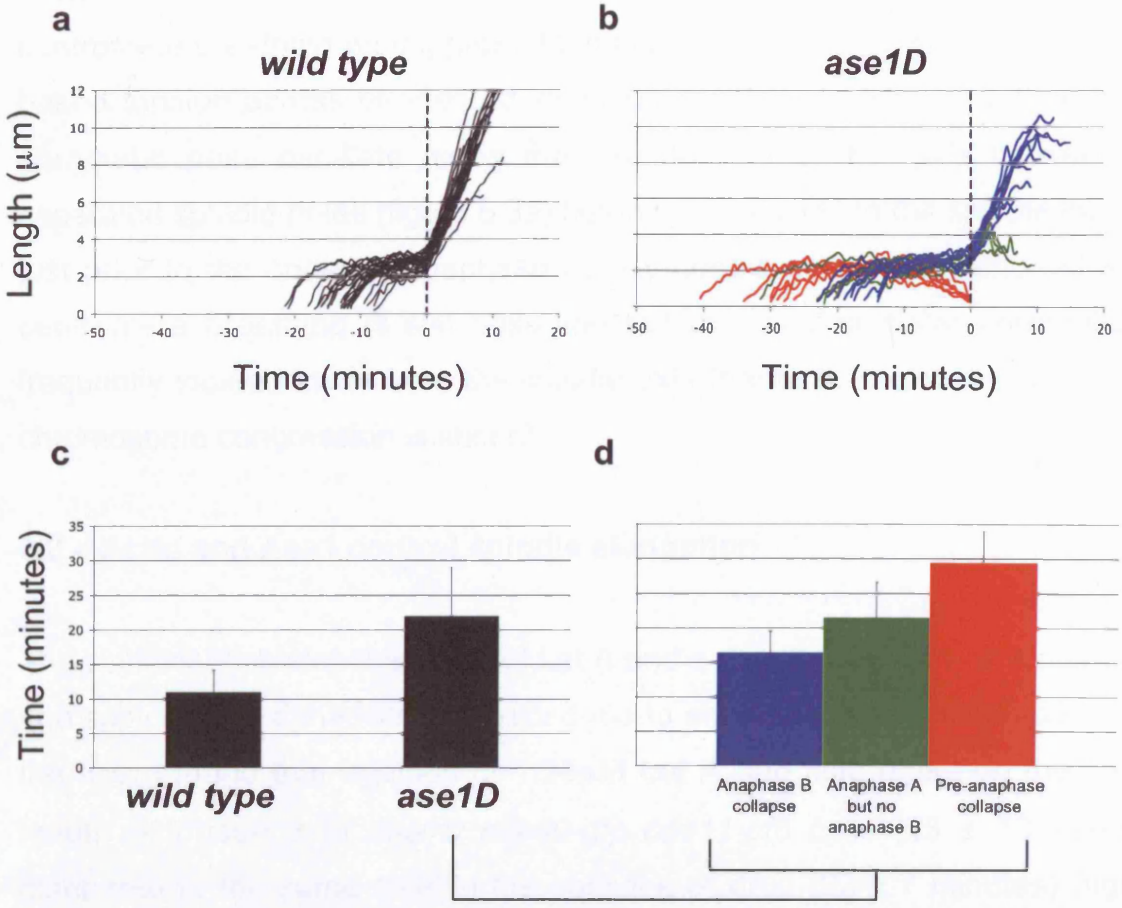

Figure 6.2 Cells lacking Ase1 are delayed in phase 2 and undergo frequent spindle collapse both before and after anaphase onset

(**a**) Graph representing multiple time-lapse movies showing the length of the mitotic spindle through time of *ndc80-gfp cdc11-cfp* (*wild type*) cells (n=29) (Reproduced from figure 3.7a).
(**b**) Multiple time-lapse movies showing the length of the mitotic spindle through time of *ase1D ndc80-gfp cdc11-cfp* (*ase1D*) cells (n=20). Spindles that collapse in anaphase B are shown in blue, those that undergo anaphase A but not B in green and those that undergo a pre-anaphase collapse in red. Plots for (a) and (b) are aligned at the end of anaphase A (dashed line).
(**c**) Histogram showing the average length of phase 2 in (a) and (b) above. Error bars show standard error.
(**d**) Histogram showing the average length of phase 2 in the sub-populations of (b) above. Error bars show standard error.

6.2.3 Abnormal kinetochore behaviour in the absence of Ase1

I noted that *ase1D ndc80-gfp cdc11-cfp* cells display abnormal kinetochore behaviour. In control cells (*ndc80-gfp cdc11-cfp*), kinetochores undergo centromere breathing during prometaphase and metaphase due to microtubule based tension across bi-oriented sister chromatids. At the same time, sister chromatid pairs oscillate along the line defined by the axis between the separated spindle poles (figure 6.3a) before congressing to the spindle midzone just prior to the onset of anaphase A. By contrast, in the absence of Ase1, centromere breathing is still observed but one pair of sister chromatids is frequently located away from the spindle axis (figure 6.3b and movie 6.2) and chromosome congression is absent.

6.2.4 Actin and Ase1 control spindle elongation

The similarity between the effect of Lat A and a deletion of Ase1 on kinetochore and spindle pole dynamics persuaded me to examine the relationship between the two. I found that addition of 1.25μM Lat A had little effect on the overall length of phase 2 in *ase1D ndc80-gfp cdc11-cfp* cells (23 ± 10 minutes) compared to the same cells in the absence of drug (22 ± 7 minutes) (figures 6.4b, d and e). However, the spindles of *ase1D ndc80-gfp cdc11-cfp* cells collapsed before the onset of anaphase A slightly more frequently in the presence of Lat A (9/20 movies; 45%) than in the absence of drug (7/20 movies; 35%) (figures 6.4b and 6.4d). However, the major effect of Lat A in *ase1D ndc80-gfp cdc11-cfp* cells was seen in phase 3 (figure 6.5c). Whereas all *ase1*$^{+}$ *ndc80-gfp cdc11-cfp* cells attained a spindle length of more than 4μm (29/29; 100%) this was reduced in the presence of Lat A (17/28; 61%). Similarly, fewer *ase1D ndc80-gfp cdc11-cfp* cells reached a spindle length of more than 4μm in the presence of Lat A (4/20; 20%) than in its absence (9/20; 45%). This is important since I calculated that a spindle length of 4μm is the minimum necessary to produce bi-nucleate cells. Together these data indicate Latrunculin A substantially inhibits spindle elongation in the absence of Ase1.

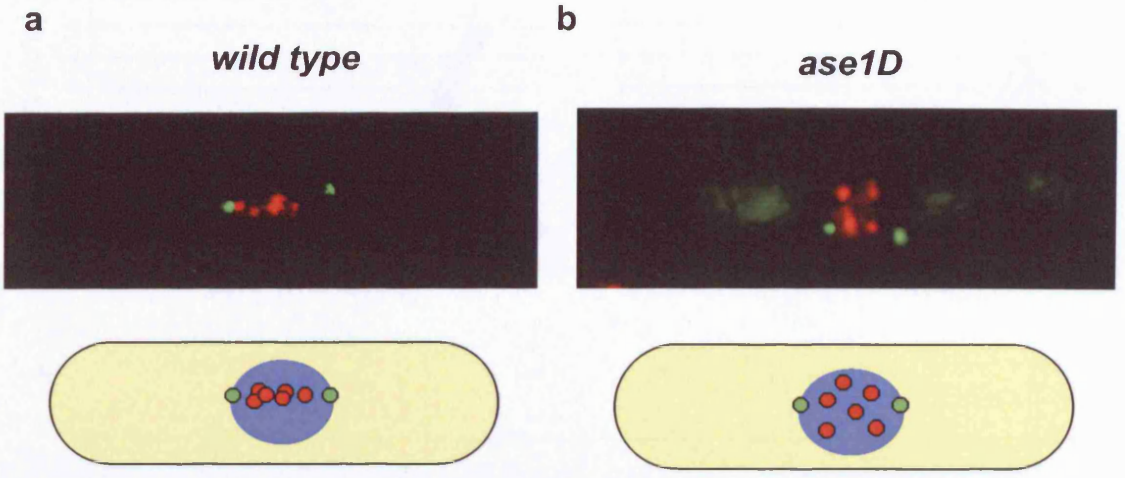

Figure 6.3 Kinetochore dynamics are perturbed in cells lacking Ase1

(**a**) Image from a time-lapse movie of an *ndc80-gfp cdc11-cfp* cell (*wild type*). Ndc80-GFP marks kinetochores (red) and Cdc11-CFP marks spindle pole bodies (green). Below is a diagrammatic representation superimposed on the presumed nuclear localisation (blue).
(**b**) As (a) for an *ase1D ndc80-gfp cdc11-cfp* (*ase1D*) cell.

Figure 6.4 Latrunculin treatment does not extend the length of phase 2 in cells lacking Ase1

Graphs representing multiple time-lapse movies showing the length of the mitotic spindle through time for: *ndc80-gfp cdc11-cfp* (*wild type*) cells in the absence (n=29, **a**) or presence (n= 28, **c**) of 1.25μM Lat A compared to *ase1D ndc80-gfp cdc11-cfp* (*ase1D*) cells in the absence (n=20, **b**) or presence (n=20, **d**) of 1.25μM Lat A. Plot colours in (b), (c) and (d) represent spindles that initiate anaphase B (blue), anaphase A but not B (green) and pre-anaphase collapse (red). All plots are aligned at the end of anaphase A (dashed line). (a), (b) and (c) are reproduced from figures 6.2a, 6.2b and 5.2b respectively.
(**e**) Histogram showing the average length of phase 2 (a-d) above. Error bars show standard error.

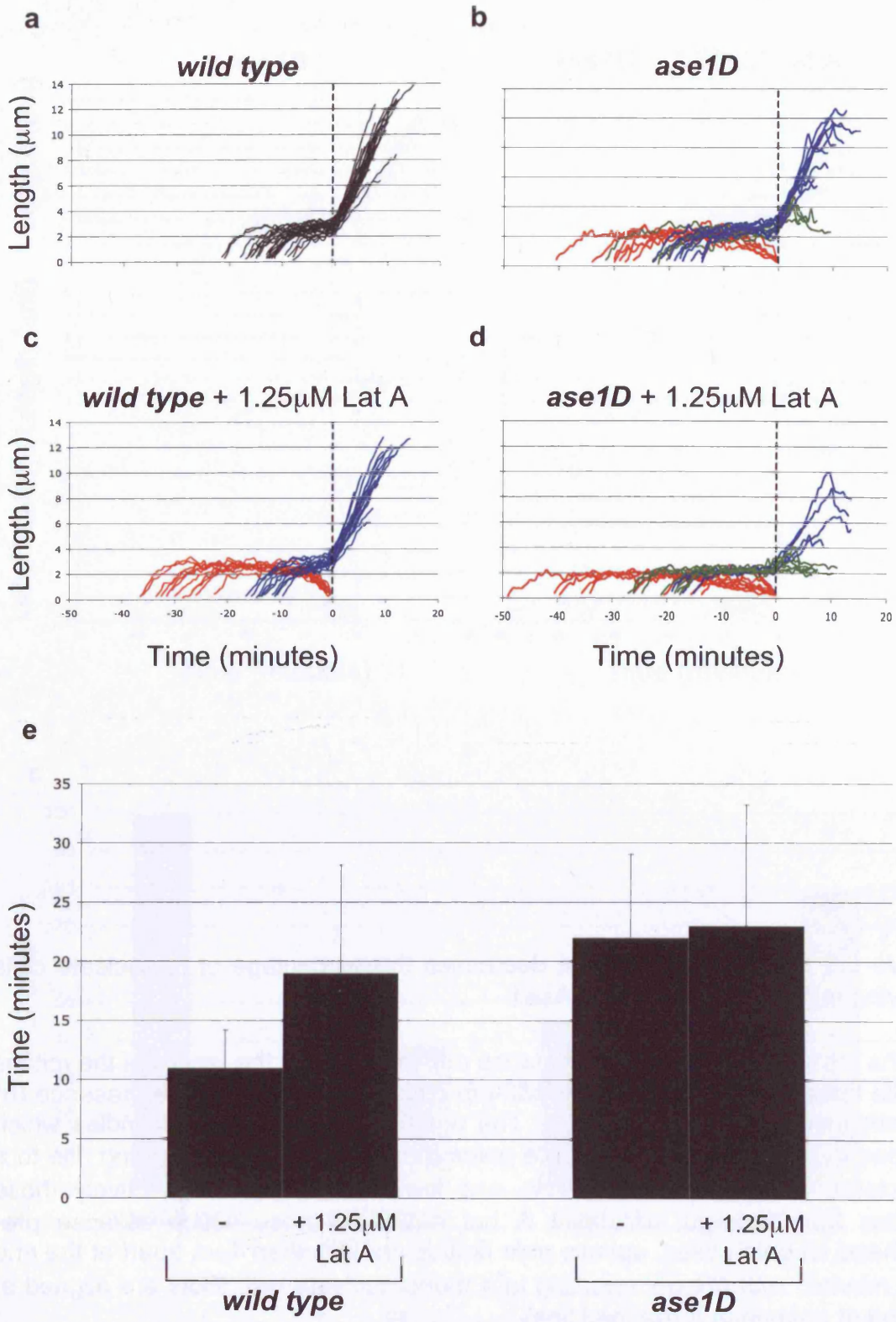
a
wild type
b
ase1D
Length (μm)
c
wild type + 1.25μM Lat A
d
ase1D + 1.25μM Lat A
Time (minutes)
e
Time (minutes)
- + 1.25μM Lat A
wild type
ase1D

Figure 6.5 Latrunculin treatment decreases the percentage of bi-nucleate cells following mitosis in cells lacking Ase1

Graphs representing multiple time-lapse movies showing the length of the mitotic spindle through time for *ase1D ndc80-gfp cdc11-cfp* (*ase1D*) in the presence (**b**) and absence (**a**) of 1.25μM Lat A. The upper row shows those spindles which collapse in anaphase B with spindle poles more than 4μm apart, giving rise to a bi-nucleate cell (blue). The middle and lower rows show respectively those spindles that undergo anaphase A but not B or those which collapse pre-anaphase. In both cases, spindle pole bodies are less than 4μm apart at the end of all movies, with mitosis resulting in a mono-nucleate cell. Plots are aligned at the end of anaphase A (dashed line).
(**c**) Histogram representing the percentage of bi-nucleate (blue) and mono-nucleate (red) cells following mitosis in figures 6.4a, c and 6.5 a, b. *wild type*, n=29 cells; *wild type* + Lat A, n=28; *ase1D*, n=20 cells; *ase1D* + Lat A, n=20.

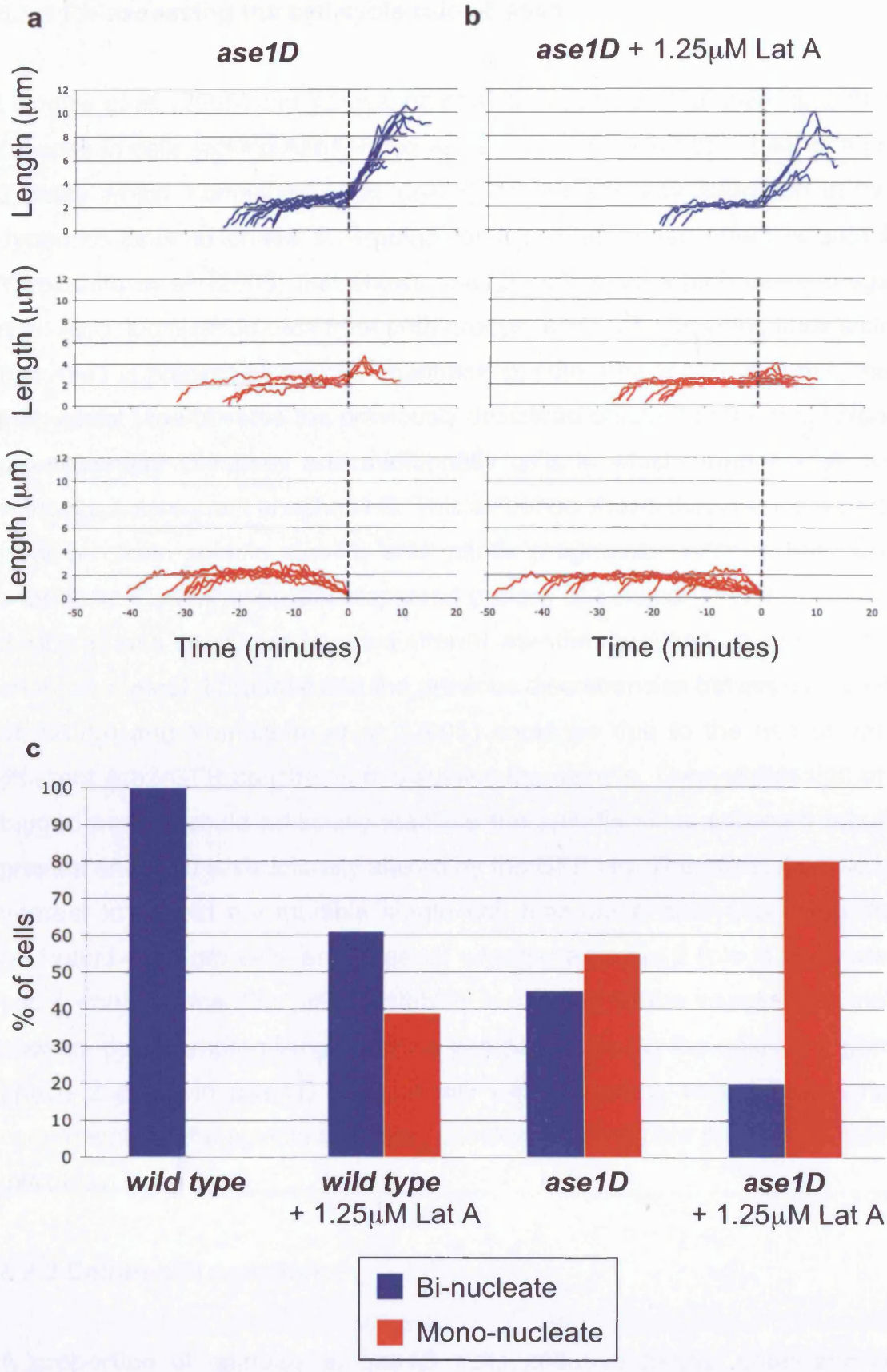
a
b
ase1D
ase1D + 1.25μM Lat A
Length (μm)
Length (μm)
Length (μm)
Time (minutes)
Time (minutes)
c
% of cells
wild type
wild type + 1.25μM Lat A
ase1D
ase1D + 1.25μM Lat A
Bi-nucleate
Mono-nucleate

6.3 Discussion

6.3.1 Re-assessing the cell cycle role of Ase1

Loiodice *et al.* (2005) and Yamashita *et al.* (2005) agree that there is a phase 3 collapse in cells lacking Ase1. However, Loiodice *et al.* (2005) observe a phase 2 delay whilst Yamashita *et al.* (2005) do not see any alteration in mitotic dynamics prior to phase 3. Arguing for a pre-anaphase effect is data from Yamashita *et al.* (2005) that shows *ase1D* cells have a high mis-segregation rate. Also, localisation data from both groups, and also this work, shows clearly that Ase1 is present on the pre-anaphase spindle. I have shown in this chapter that, whilst I too observe the previously described phase 3 collapses, I also see pre-anaphase collapses and additionally cells in which anaphase A occurs without a subsequent anaphase B. This evidence shows that Ase1 does indeed have a role in spindle stability and mitotic progression prior to the onset of anaphase. Furthermore, the dispersed pattern of kinetochores in *ase1D* cells during phase 2, which implies altered spindle bundling, confirms a pre-anaphase effect. I propose that the previous discrepancies between Loiodice *et al.* (2005) and Yamashita *et al.* (2005) could be due to the use of various different Atb2-GFP constructs to visualise the spindle. Over-expression of this tagged protein could artificially stabilise the spindle since (a) more tubulin is present and (b) it is structurally altered by the GFP tag. Therefore, it would be of interest to repeat my multiple single cell time-lapse analyses using *ase1D lys1:nmt1-atb2-gfp* cells and observe whether a phase 2 role is implicated. If not, it would appear that spindle stability is affected by the visualisation method chosen, thus compromising accurate interpretations. In the case of a genuine phase 2 delay in *ase1D* cells, it will be interesting to examine whether components of the spindle assembly checkpoint (SAC) are required to maintain this delay.

6.3.2 Cell-to-cell variation

A proportion of spindles in *ase1D* cells collapse before anaphase onset whereas others collapse after anaphase onset. The reason for this cell-to-cell variation is unknown. Notably, pre-anaphase spindle collapse is also seen in

ase1^{+} cells in the presence of Lat A. These phenotypes are not due to photo-toxicity since cells in the same field undergo different fates despite exposure to the same amount of light (movie 6.3), arguing that this variability is an inherent property of the cell population. An intriguing possibility is that spindle fate in *ase1D* cells reveals a lineage dependent cell-to-cell variation in the number of pole-to-pole microtubules. Alternatively, the composition of the spindle midzone or concentration of different spindle stabilising factors may vary between cells. Another possibility is that when Lat A is used, its concentration is not maximal. It would be interesting to examine the effect of complete disruption of the actin cytoskeleton on spindle stability. However, this is not possible in wild type cells since actin is required for cell growth and the attainment of a critical cell size necessary for the initiation of mitosis (Rupes *et al.*, 2001). This problem, however, could be circumvented in *cdc25-22* cells arrested at the restrictive temperature. These cells exceed the size control needed for mitotic entry and synchronously enter mitosis on release to the permissive temperature even when the actin cytoskeleton is completely destroyed (Rajagopalan *et al.*, 2004). The effect of complete disruption of the actin cytoskeleton in the absence of Ase1 could then be assessed.

6.4 Conclusions

- Loss of Ase1 causes altered kinetochore behaviour and pre-anaphase spindle collapse.
- Cells lacking Ase1 have a delay over anaphase onset.
- Ase1 and actin control spindle stability and spindle elongation

Chapter 7

Klp9 kinesin is a novel regulator of mitotic spindle stability

7.1 Introduction

In the previous chapter, I showed that loss of Ase1 or addition of Lat A induces pre-anaphase spindle collapse and a delay in anaphase onset. More importantly, I found that addition of Lat A exacerbated the phenotype observed in cells lacking Ase1, so that only a few cells underwent anaphase B. I reasoned that Lat A might inhibit a pathway that is essential in the absence of Ase1. For this reason, I looked for genetic mutants that were inviable in the absence of Ase1 in the hope that these may lie on an actin-dependent pathway controlling pre-anaphase spindle stability. As a prelude to performing a full synthetic lethality screen with *ase1D* cells, I tested whether loss-of-function mutants in known or putative microtubule binding proteins displayed such a genetic interaction with Ase1. In this chapter I describe the identification of two such proteins, the Mal3 (EB1) "plus" end microtubule binding protein and Klp9, a previously undescribed member of the kinesin-6 family. Members of the kinesin-6 family include the MKLP1/PAV/CHO1 kinesin, a component of the centralspindlin complex, which binds the spindle midzone and triggers cytokinesis in higher eukaryotes (Sellitto and Kuriyama, 1988; Nislow *et al.*, 1992; Adams *et al.*, 1998; Minestrini *et al.*, 2003; Mishima *et al.*, 2004; Neef *et al.*, 2006).

7.2 Results

7.2.1 Mal3 is essential for viability in the absence of Ase1

Mal3 is a member of the EB1 plus-end microtubule binding family of proteins and associates only with polymerising but not depolymerising microtubules. Recent experiments have shown that Mal3 binds and stabilises the microtubule lattice seam in *S.pombe* (Sandblad *et al.*, 2006). Fission yeast cells lacking

Mal3 exhibit altered cell polarity, due to its role in maintaining the localisation of the Tea1 complex at the plus-end of interphase microtubules (section 1.2.1.1). In addition, cells lacking Mal3 display a high incidence of chromosome loss during mitosis, indicating a mitotic function (Beinhauer *et al.*, 1997). Random spore analysis revealed that cells lacking both Mal3 and Ase1 are inviable (figure 7.1a), a synthetic lethality that was confirmed by tetrad analysis (figure 7.1b), from which no haploid *ase1D mal3D* cells could be isolated (materials and methods, 2.1.8). This is unlikely to be due to the function of Mal3 at the "plus" end of interphase microtubules, since loss of Ase1 is not lethal in cells lacking Mto1, which are deficient in interphase microtubules, or components of the Tea1 complex including Tea1, Tea2, and Tip1 (figure 7.1). Moreover, I find that *ase1D dam1D* cells are viable suggesting that loss of Mal3 is particularly damaging to the stability of pole-to-pole microtubules rather than kinetochore bound microtubules. The DASH complex exclusively binds to the "plus" ends of kinetochore associated microtubules but is not observed at the spindle midzone (Sanchez-Perez *et al.*, 2005). Time lapse analysis of *mal3D ndc80-gfp cdc11-cfp* cells in the presence of 1.25μM Lat A reveals that collapses also occur in this background (preliminary data, not shown). Genetic interactions between *ase1D* and deletion mutants in other microtubule binding proteins such as Peg1 (CLASP homologue: Grallert et al., 2006;), Alp7 (TACC homologue: Sato *et al.*, 2004), Alp14 and Dis1 (XMAP215/TOG homologues: Garcia *et al.*, 2001) were not explored.

7.2.2 Klp9 is essential for viability in the absence of Ase1

The fission yeast genome contains nine kinesins. Pkl1 and Klp2 are members of the minus-end directed kinesin-14 family (Troxell *et al.*, 2001). Klp3 is a member of the kinesin-1 family and is associated with organelle function (Brazer *et al.*, 2000). Klp4 (Tea2) is required for maintenance of interphase cell polarity and, in particular, for delivering Tea1 at the plus end of interphase microtubules to the cell tips (Browning *et al.*, 2000). Klp5 and Klp6 form a heterodimer that is required for accurate chromosome segregation (Garcia *et al.*, 2002; West *et al.*, 2002). I found that loss of Ase1 was not lethal in deletions of any of these kinesins (figure 7.2a). Cut7 is essential for bipolar spindle formation (Hagan and Yanagida, 1992) but genetic interactions between

a

Strain	Viability
ase1D	+
ase1D mto1D	+
ase1D tea1D	+
ase1D tea2D	+
ase1D tip1D	+
ase1D dam1D	+
ase1D mal3D	-

b

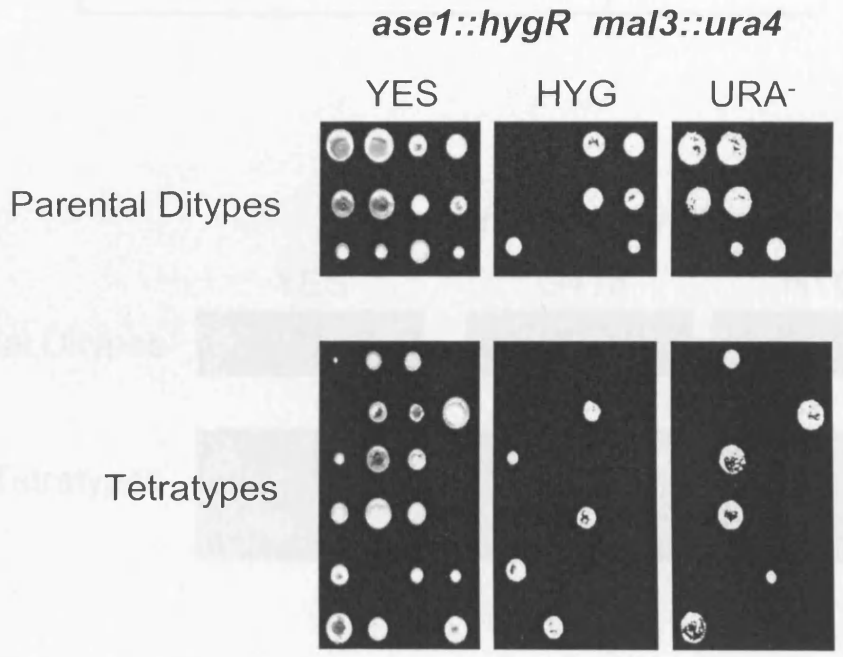

Figure 7.1 Mal3 is required for viability in cells lacking Ase1

(**a**) Viability of *ase1::hygR* cells and double mutants of *ase1::hygR* combined with deletions in a variety of microtubule associated genes, as assessed by random spore analysis. (+ viable; - inviable).
(**b**) Colonies resulting from the tetrad analysis of *ase1::hygR mal3::ura4* heterozygous diploid spores, shown on both rich (YES) and selective (HYG, URA^-) media. No *ase1::hygR mal3::ura4* haploids were recovered (n=40 asci dissected).

a

Strain	Viability
ase1D klp2D	+
ase1D klp3D	+
***ase1D klp4D* (*ase1D tea2D*)**	+
ase1D klp5D	+
ase1D klp6D	+
ase1D klp8D	+
ase1D klp9D	-

b

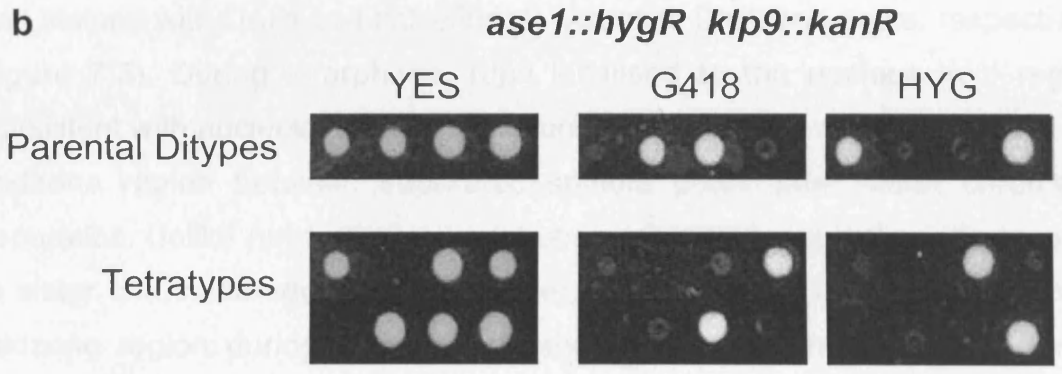

Figure 7.2 Klp9 is required for viability in cells lacking Ase1

(**a**) Viability of double mutants of *ase1::hygR* combined with deletions in a variety of kinesin genes, as assessed by random spore analysis. (+ viable; - inviable).
(**b**) Colonies resulting from the tetrad analysis of *ase1::hygR klp9::kanR* heterozygous diploid spores, shown on both rich (YES) and selective (G418, HYG) media. No *ase1::hygR klp9::kanR* haploids were recovered (n=40 asci dissected).

temperature sensitive *cut7* mutants and *ase1D* cells were not explored. In addition the fission yeast genome contains two other kinesins, Klp8 (SPAC144.14) and Klp9 (SPBC2D10.21c). Klp8 is a member of the kinesin-3 family, whose members are primarily involved in organelle transport (Miki *et al.*, 2005). Klp9 is a member of the kinesin-6 family, which contains MKLP1/PAV/CHO1 (section 7.1). Klp9 contains a motor domain at its N-teminus and three consensus sites for cyclin dependent kinase (Cdk) in its C-terminus.

Gene deletions for both *klp8* and *klp9* were constructed (section 2.5.1) revealing that neither is essential for viability. Moreover, no genetic interactions between Ase1 and Klp8 were observed. However, random spore analysis revealed that *ase1D klp9D* cells were inviable (figure 7.2a) and this was confirmed by tetrad analysis (figure 7.2b).

7.2.3 Klp9 localises to the spindle midzone

To determine the localisation of Klp9 during the cell cycle, it was tagged at its C-terminus with GFP (section 2.5.2) in *ndc80-cfp* cells, to allow visualisation of kinetochores. Log phase *klp9-gfp ndc80-cfp* cells were fixed in formaldehyde and stained with DAPI and calcofluor to visualise DNA and septa, respectively (figure 7.3). During interphase, Klp9 localised to the nucleus in a region consistent with nucleolar localisation. During mitosis, Klp9 could be seen in the midzone region between separated spindle poles after sister chromatid separation. Unlike Ase1, Klp9 was not observable at the spindle midzone prior to sister chromatid separation. However, it appeared strongly at the spindle midzone region during anaphase B and returned to the nucleolus during cytokinesis (movie 7.1). A more careful analysis will be required to precisely determine the timing of Klp9 association to the spindle midzone.

7.2.4 Effect of loss of Klp9 on mitotic progression

To analyse the effect of loss of Klp9 on mitotic progression, I monitored SPB and kinetochore position in *klp9D ndc80-gfp cdc11-cfp* cells. Surprisingly, I find that the average time spent in phase 2 in these cells is longer (19 ± 7 minutes) than in *klp9*$^{+}$ cells (11 ± 3 minutes) at the same temperature (figures 7.4a-c).

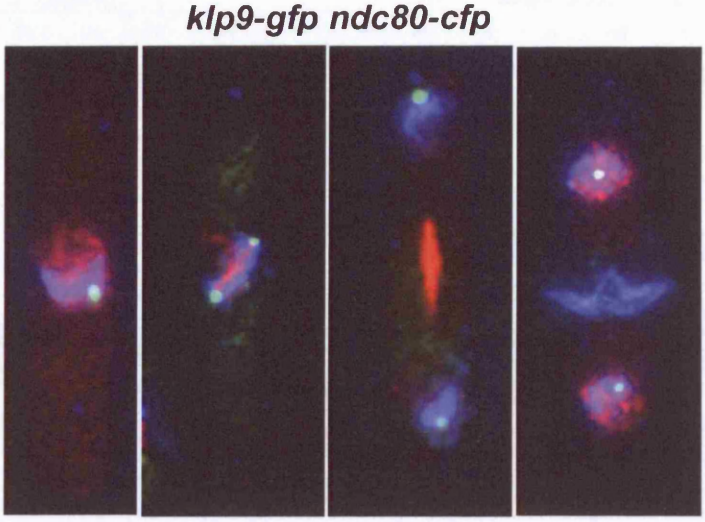

Figure 7.3 Klp9 localisation

Images of fixed log phase cells expressing Klp9-GFP (red) and Ndc80-CFP (kinetochores, green), stained with DAPI and calcofluor to visualise DNA and septa respectively (blue).

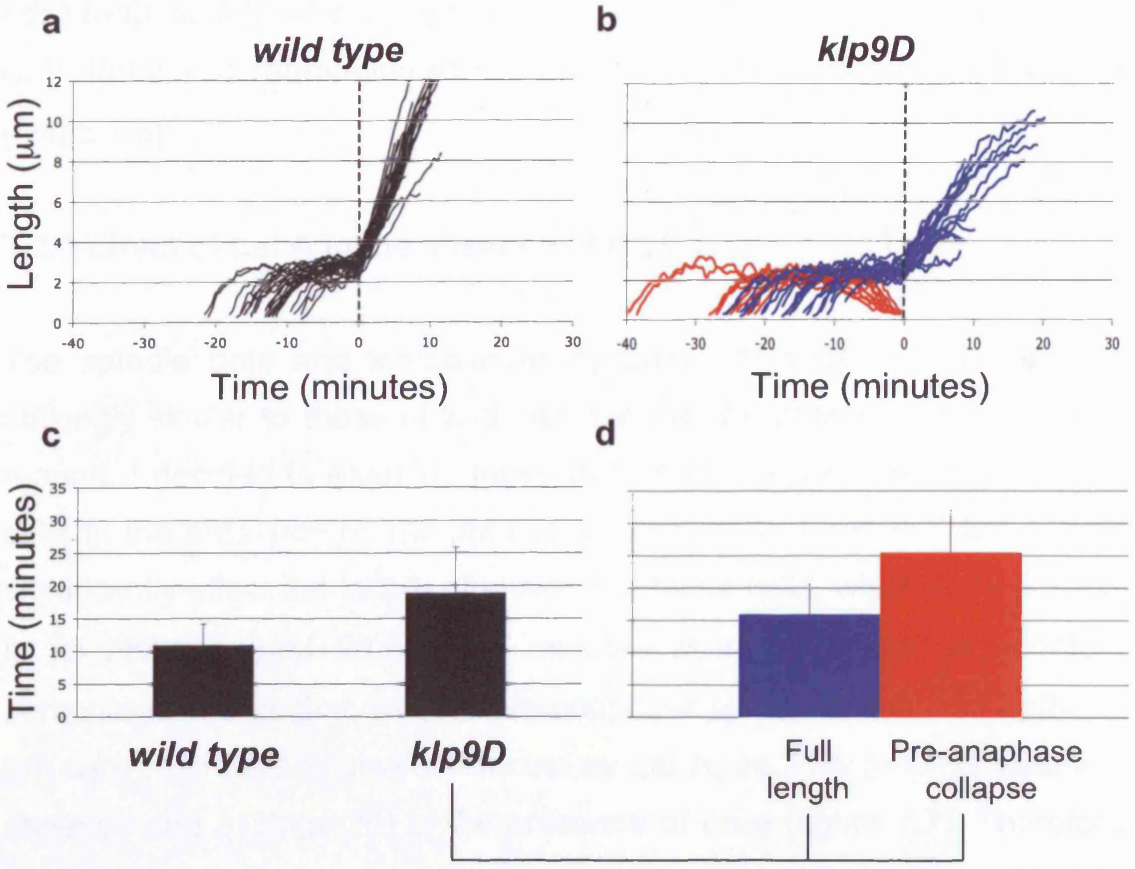

Figure 7.4 Cells lacking Klp9 are delayed in phase 2 and undergo frequent pre-anaphase spindle collapse

(**a**) Graph representing multiple time-lapse movies showing the length of the mitotic spindle through time of *ndc80-gfp cdc11-cfp* (*wild type*; n=29) cells. (Reproduced from figure 3.7a).
(**b**) Multiple time-lapse movies showing the length of the mitotic spindle through time of *klp9D ndc80-gfp cdc11-cfp* (*klp9D*; n=32) cells. Spindles that undergo anaphase B are shown in blue and those that collapse pre-anaphase in red. Plots for (a) and (b) are aligned at the end of anaphase A (dashed line).
(**c**) Histogram showing the average length of phase 2 in (a) and (b) above. Error bars show standard error.
(**d**) Histogram showing the average length of phase 2 of the two sub-classes of spindles depicted in (b) above. Error bars show standard error.

Moreover, a proportion of *klp9D ndc80-gfp cdc11-cfp* cells undergo pre-anaphase spindle collapse (31%, n=32). Closer analysis revealed that those cells that do not undergo spindle collapse stay in phase 2 for an average of 16 ± 4.5 minutes compared to 25.5 ± 6.5 minutes in those that do collapse (figures 7.4b and d). I also noted that the rate of spindle elongation in *klp9D ndc80-gfp cdc11-cfp* cells (0.44 ± 0.15μm/minute) is significantly slower than either *klp9*$^{+}$ cells (0.82 ± 0.19μm/minute) or cells lacking Mto1 (0.84 ± 0.24μm/minute) (figure 7.5).

7.2.5 Effect of Lat A in the absence of Klp9

The spindle pole and kinetochore dynamics of cells lacking Klp9 appear strikingly similar to those of wild type cells in the presence of Lat A. For this reason, I decided to examine these dynamics in *klp9D ndc80-gfp cdc11-cfp* cells in the presence of 1.25μM Lat A (figure 7.6). I find that Lat A does not significantly effect the length of phase 2 in these cells, which is 19 ± 7 minutes in its absence and 20.5 ± 6.5 minutes in its presence. In addition, the percentage of cells that undergo pre-anaphase spindle collapse in *klp9D ndc80-gfp cdc11-cfp* cells is also unaffected by Lat A, as 31% (n=31) collapse in the absence and 31% (n=26) in the presence of drug (figure 7.7). Therefore, the mitotic defect in cells lacking Klp9 is not exacerbated by addition of Lat A. This may indicate that Klp9 and actin lie on the same pathway controlling pre-anaphase spindle midzone stability. However, I note that loss of Klp9 reduces the rate of anaphase B whilst addition of Lat A does not, indicating that Klp9 has additional functions during anaphase B which are not shared by actin (figure 7.5).

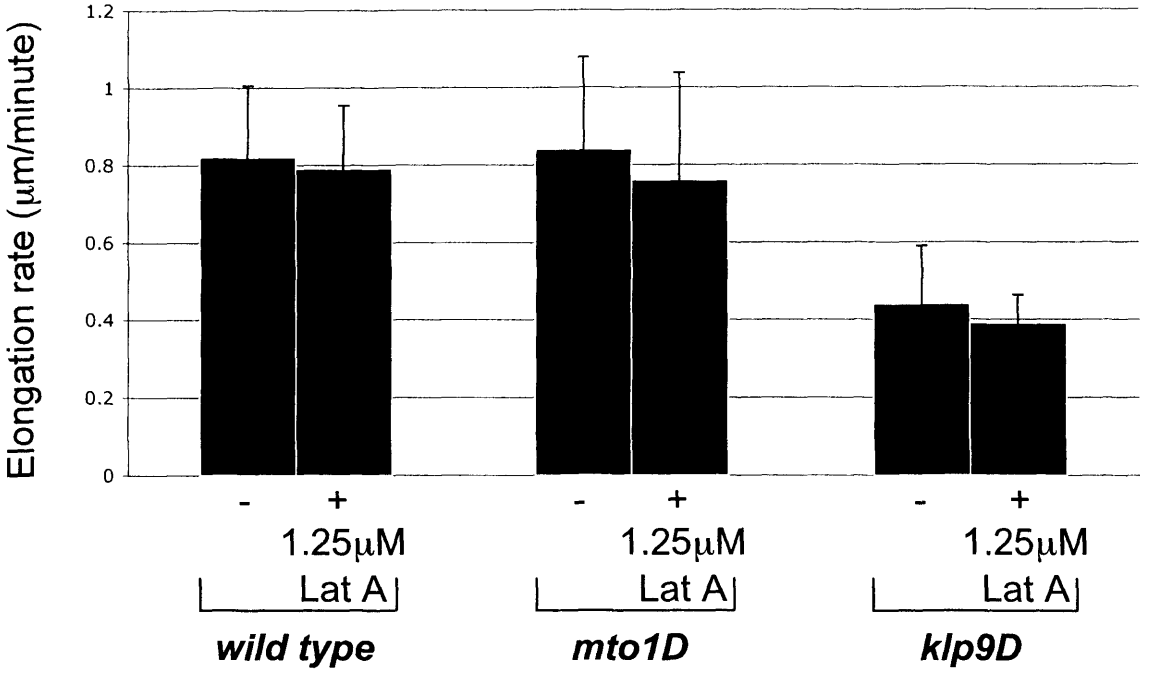

Figure 7.5 Spindle elongation rate in anaphase B is reduced in cells lacking Klp9

Histogram showing the average spindle elongation rate in *ndc80-gfp cdc11-cfp* (*wild type*), *mto1D ndc80-gfp cdc11-cfp* (*mto1D*) and *klp9D ndc80-gfp cdc11-cfp* (*klp9D*) cells in the presence and absence of 1.25µM Lat A. Compiled from data previously presented in figures 3.10a, 5.2b, 5.4d, 7.4b and 7.6d. Error bars show standard error.

Figure 7.6 Latrunculin treatment does not extend phase 2 in cells lacking Klp9

Graphs representing multiple time-lapse movies showing the length of the mitotic spindle through time for: *ndc80-gfp cdc11-cfp* (*wild type*) cells in the absence (n=29, **a**) or presence (n=28, **c**) of 1.25μM Lat A compared to *klp9D ndc80-gfp cdc11-cfp* (*klp9D*) cells in the absence (n=32, **b**) or presence (n=26, **d**) of 1.25μM Lat A. Plot colours in (b), (c) and (d) represent spindles that undergo anaphase (blue) and pre-anaphase collapse (red). All plots are aligned at the end of anaphase A (dashed line). (a), (b) and (c) are reproduced from figures 7.4a, 7.4b and 5.2b respectively.
(**e**) Histogram showing the average length of phase 2 in (a-d) above. Error bars show standard error.

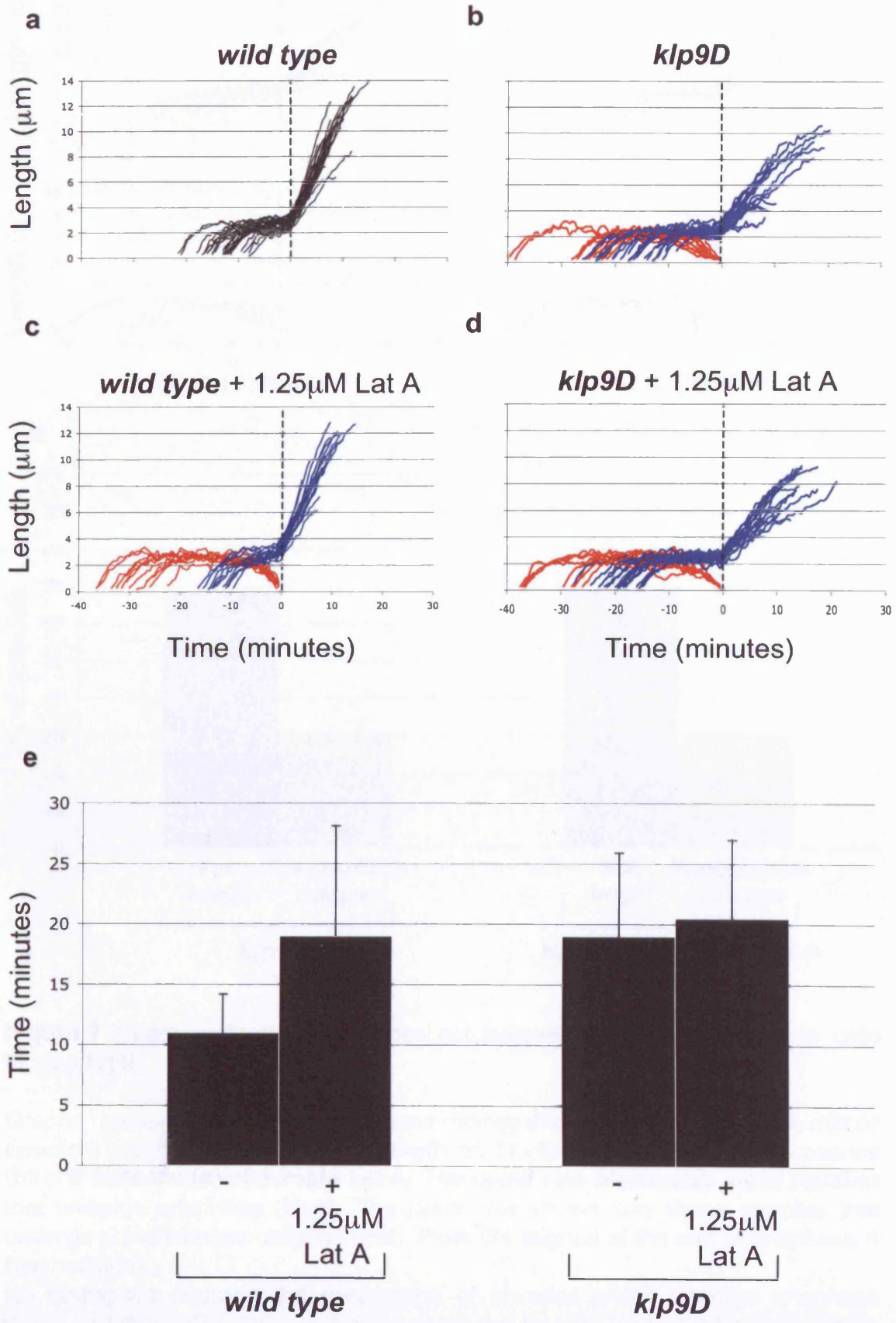
a
wild type
b
klp9D
Length (μm)
c
wild type + 1.25μM Lat A
d
klp9D + 1.25μM Lat A
Length (μm)
Time (minutes)
Time (minutes)
e
Time (minutes)
-
+
1.25μM
Lat A
wild type
-
+
1.25μM
Lat A
klp9D

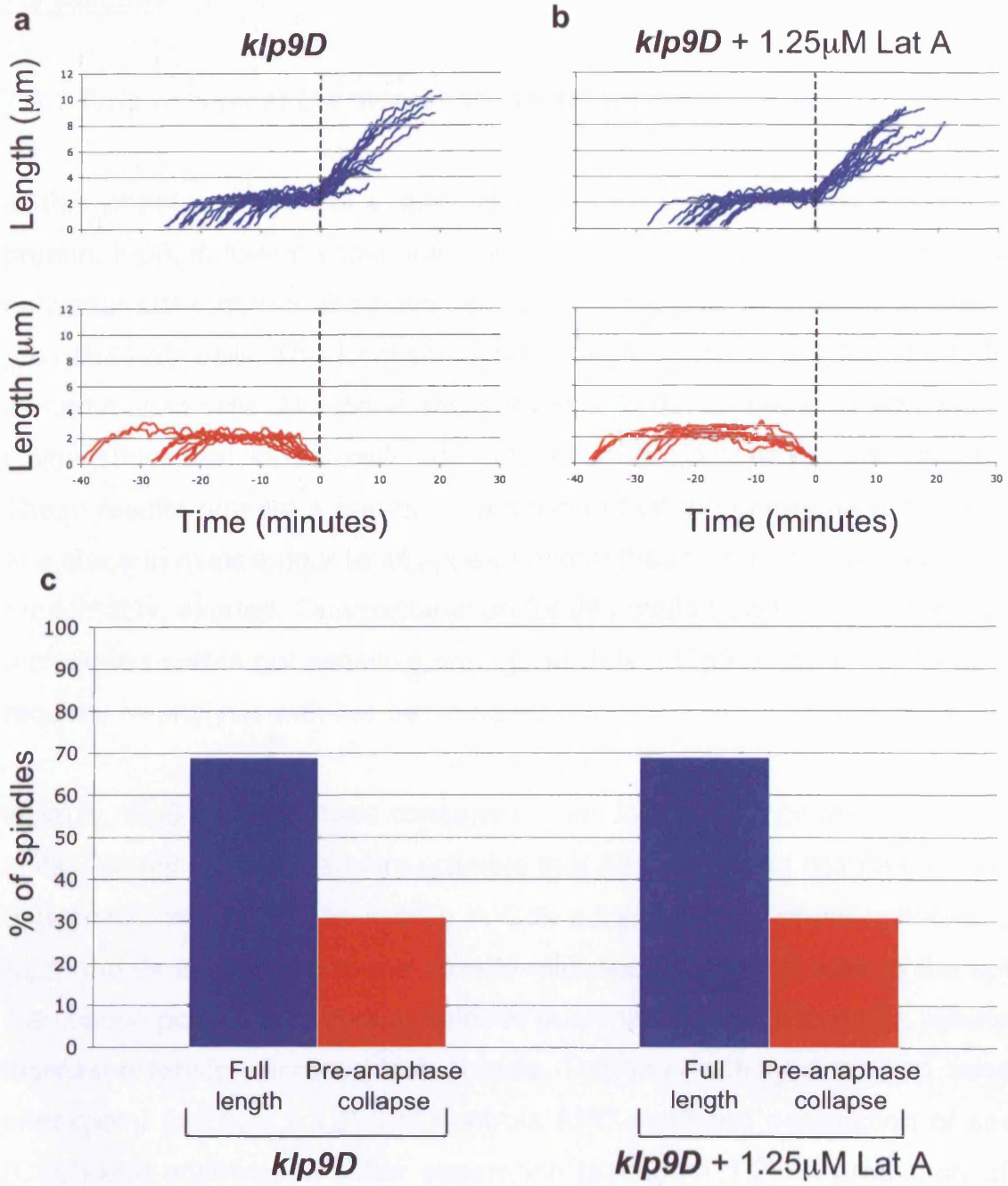

Figure 7.7 Latrunculin treatment does not increase collapse frequency in cells lacking Klp9

Graphs representing multiple time-lapse movies showing the length of the mitotic spindle through time for *klp9D ndc80-gfp cdc11-cfp* (*klp9D*) cells in the presence (**b**) and absence (**a**) of 1.25μM Lat A. The upper row shows only those spindles that undergo anaphase (blue). The lower row shows only those spindles that undergo pre-anaphase collapse (red). Plots are aligned at the end of anaphase A (dashed line).

(**c**) Histogram showing the percentage of spindles which undergo anaphase (blue) and those that collapse before anaphase (red) in (a) and (b) above. *klp9D*, n=32 cells; *klp9D* + Lat A, n=26 cells.

7.3 Discussion

7.3.1 Role of Klp9 at the metaphase to anaphase transition

In this chapter, I present a preliminary analysis of the novel kinesin motor protein, Klp9, in fission yeast. Intriguingly, Klp9 localises to the spindle midzone only after sister chromatids have separated, as judged by imaging of fixed *klp9-gfp ndc80-cfp* cells. This localisation is strikingly similar to that found for MKLP1 in mammalian cells (Matuliene and Kuriyama, 2002; Zhu *et al.*, 2005). However, I also show that *klp9D* cells are delayed in prometaphase and metaphase. These results present a paradox, suggesting that the gene product is required at a stage in mitosis prior to its appearance at the midzone where its function is, presumably, exerted. One explanation for this could be simply that the imaging technique used is not sensitive enough to detect Klp9 at the earlier stage and requires re-analysis with live cell imaging.

Notably, Klp9 contains three consensus sites for cyclin dependent kinase (Cdk) in its C-terminus. It is therefore possible that APC-mediated destruction of cyclin B (Cdc13), which causes a drop in Cdk activity, allows dephosphorylation of Klp9 and its association to the spindle midzone. Binding of Klp9 to the spindle may cause pole-to-pole microtubules to push away from each other, resulting in increased tension across kinetochores. This may satisfy a tension sensitive checkpoint (section 1.3.2) that controls APC-mediated destruction of securin (Cut2) and consequent sister separation (section 1.1.2). A prediction of this model is that destruction of Cdc13 would not be effected by loss of Klp9 but destruction of Cut2 would be. This is an interesting possibility since cyclin B and securin destruction are generally thought to occur co-incidentally. In budding yeast the Cdc14 phosphatase is critical for microtubule stabilisation following anaphase onset (Higuchi and Uhlmann, 2005), though its relevant targets in this process are unknown. One possibility that merits further investigation is that Clp1, the *S.pombe* Cdc14 homologue (Trautmann *et al.*, 2001), dephosphorylates Klp9 to induce a change in microtubule dynamics required for timely onset of anaphase. Notably, however, budding yeast does not contain a member of the kinesin-6 family.

7.3.2 Does fission yeast possess genetically separable attachment and tension checkpoints?

The anaphase delay induced by Lat A requires the Mad3, Bub1, Bub3 and Mph1, but not Mad1 or Mad 2 spindle assembly checkpoint (SAC) proteins (Tournier *et al.*, 2004). This subset of SAC components was previously thought to delay anaphase in response to inappropriate spindle orientation. However, as I showed in chapter 3, spindle orientation has no effect on the timing of anaphase onset. A more likely explanation is therefore that Lat A induces an anaphase delay *via* these proteins by disrupting spindle stability. Notably, the anaphase delay in cells lacking Mal3 also requires the exact same subset of SAC proteins (Asakawa *et al.*, 2005). Since *ase1D mal3D* cells are inviable, loss of Mal3 may effect the stability of pole-to-pole microtubules more profoundly than microtubule-kinetochore interaction and, by inference, the anaphase delay in *mal3D* cells may reflect this defect. Likewise Klp9 binds selectively to the spindle midzone and loss of Klp9 is lethal in the absence of Ase1. This suggests that the anaphase delay in *klp9D* cells is primarily due to a defect in pole-to-pole microtubules rather than a defect in microtubule interaction with kinetochores. It would be of great interest to examine whether the anaphase delay in cells lacking Ase1 or Klp9 is due to a delay in activation of the APC and, if so, which SAC proteins are required to impose this delay. It remains possible that a subset of SAC components monitors either the integrity of the pre-anaphase spindle midzone or spindle tension across kinetochores as a consequence of a defect in bipolar spindle stability but, importantly, is distinct from the checkpoint that monitors occupancy of kinetochores by spindle microtubules.

7.3.3 Role of Klp9 during anaphase B

I find that the rate of anaphase B in cells lacking Klp9, a putative motor-protein, is approximately half of that in control cells. This suggests that Klp9 kinesin pushes antiparallel microtubules apart and in doing so, pushes spindle poles away from each other. Other plus-end-directed kinesin motors which bind the spindle midzone, such as Cut7, may operate in a similar manner. The role of other kinesin motors, such as Klp5 and Klp6, at the spindle midzone is less

clear. Electron micrographs of mitotic spindles by Ding and colleagues (1993) have revealed that pole-to-pole microtubules are bound in a loosely packed hexagonal arrangement at the spindle midzone before anaphase onset and in a tight square-packed arrangement during anaphase B. One possibility is that Klp9 and/or Ase1 could be necessary for the structural rearrangement of pole-to-pole microtubules at the metaphase to anaphase transition. Electron microscopy studies of spindle microtubules in *klp9D* and *ase1D* cells would be of significant interest in this respect.

7.3.4 Do Klp9 and actin lie on the same pathway controlling pre-anaphase spindle stability?

The frequency of pre-anaphase spindle collapse in *klp9D* cells is unchanged by addition of Lat A and the same proportion of cells undergoes anaphase B. One possibility is that Lat A prevents Klp9 from binding the spindle midzone. I believe that this is unlikely since Lat A alone does not effect the rate of anaphase B. However, there remains the possibility that Klp9 has a distinct pre-anaphase role that may be affected by Lat A treatment. The identity of proteins that interact with Klp9 is likely to shed more light on the relationship between actin and Klp9.

7.4 Conclusions

- Mal3 and Klp9 are required for viability in the absence of Ase1.
- Klp9 localises to the spindle midzone and controls the timing of anaphase onset and pre-anaphase spindle stability.
- Pre-anaphase kinetochore behaviour in cells lacking Klp9 is unaffected by the addition of Lat A.
- Klp9 controls the rate of spindle elongation in anaphase B.

Chapter 8

General Discussion

8.1 Summary

Since the first description of a spindle orientation checkpoint (SOC) in fission yeast by Gachet *et al.* (2001), there have been several reports published on the topic, some of which agreed with these initial conclusions and others that did not. The aim of my project was to perform a thorough experimental re-evaluation of the data by establishing more robust assays with which to test the prevailing hypotheses. By establishing a single-cell assay to simultaneously monitor spindle pole body and kinetochore position, I have demonstrated that spindle orientation is not monitored in this organism, nor does the angle of the spindle influence the timing of anaphase onset. In short, there is no SOC operating in fission yeast.

I have also re-examined the mechanisms controlling spindle orientation in fission yeast as it was unclear whether this was governed by intra-nuclear or astral microtubules and if so, at what cell cycle phase. I have found firstly that there is no corrective orientation during either pro-metaphase or metaphase thus intra-nuclear spindle microtubules cannot direct spindle orientation. Secondly, I have shown that astral microtubules are only nucleated after anaphase onset and thereafter play only a minor role in aligning the mitotic spindle along the longitudinal axis of the cell. Instead I have demonstrated that orientation is dependent on the initial positioning of the duplicated but unseparated interphase SPBs prior to mitosis, which in turn are positioned by cytoplasmic microtubules.

It was previously thought that treatment of fission yeast cells with Latrunculin A (Lat A) delayed anaphase onset by causing spindle mis-orientation. I found that this is not the case and that instead, Lat A delays anaphase onset by influencing mitotic spindle stability. This effect is abolished in *act1-R183A,D184A* cells, which express an actin mutant specifically insensitive to

Lat A, showing for the first time that actin contributes to spindle stability in fission yeast. I found that a similar pre-anaphase mitotic spindle collapse occurs in cells lacking the anti-parallel microtubule bundling protein Ase1, which binds to the spindle midzone throughout mitosis. The spindle instability of *ase1D* cells can be exacerbated by the addition of Lat A, showing that Ase1 and actin act in concert to maintain the mitotic spindle. At present, the exact mechanism by which the actin component stabilises the mitotic spindle is unknown. One appealing idea is that filamentous actin can act as an extra-spindle matrix protein as is the case in some larger cells (Fabian and Forer, 2005; figure 8.1).

In an effort to shed more light on the actin-dependent pathway controlling bipolar spindle stability I have identified two proteins, Mal3 and a novel kinesin, Klp9, which are essential for cell viability in the absence of Ase1. Interestingly, cells lacking Klp9 have a slower anaphase B but also exhibit pre-anaphase spindle collapse, a phenotype which is not exacerbated by the addition of Lat A. For this reason I tentatively place Klp9 on an actin-dependent pathway controlling bipolar spindle stability.

8.2 Why do spindles collapse in only a proportion of cells?

The incidence of spindle collapse is approximately 50% in cells treated with Lat A or lacking either Ase1 or Klp9. In the presence of drug, this collapse frequency could be a result of cell-to-cell variation due to sub-maximal concentration of Lat A. However, in the deletion strains it is harder to understand why only approximately half the cells undergo a collapse event. Phototoxicity can be discounted since cells in the same visual field undergo different fates despite being exposed to the same amount of light. However, other strains that have a delay over anaphase onset, such as *mal3D* cells, do not undergo any collapses. Furthermore, control cells monitored at a lower temperature, which have a significantly extended phase 2, do not undergo collapse despite increased light exposure.

One intriguing explanation could be that two populations of cells exist in an *S.pombe* culture with different inherent spindle properties. A precedent for this is described in the work of Grallert *et al.* (2004). These authors show that the

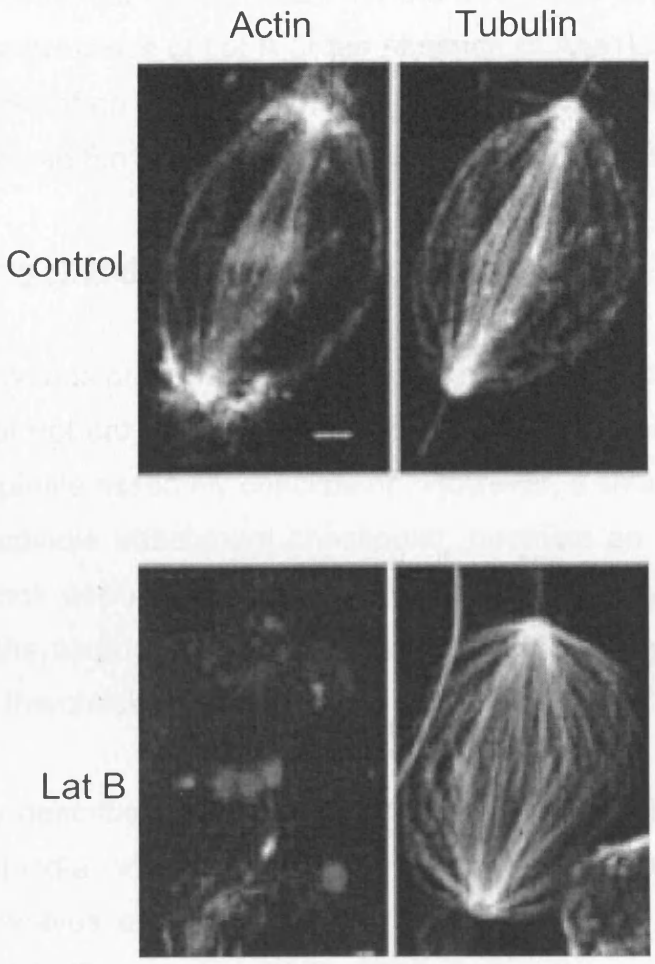

Figure 8.1 Actin acts as a spindle matrix protein in another organism

Actin acts as a spindle matrix protein in crane fly spermatocytes. Notice the more dispersed conformation of tubulin in the presence of Lat B. Reproduced from Fabian and Forer (2005).

NIMA-related kinase Fin1, an inhibitor of SIN activation, is always found bound to the "old" SPB but only on the "new" SPB in 50% of cells. It follows that two types of cell exist, one with Fin1 symmetrically bound to both poles and another with an asymmetrical distribution of Fin1 (figure 8.2). It is possible that mature, Fin1-marked poles behave differently to naïve unmarked poles, perhaps nucleating more pole-to-pole microtubules. This could increase the stability of the spindle in cells that contain two Fin1-marked poles and therefore prevent collapses in the presence of Lat A or the absence of Ase1 or Klp9. Observing if there is a correlation between those cells that collapse and those that asymmetrically load Fin1 to the poles could test this hypothesis.

8.3 Spindle checkpoint(s) affecting mitotic progression in fission yeast

In light of the findings presented in this thesis and summarised above, I propose a redefinition of not only the SOC but also the SAC. At present the SAC is an acronym for "spindle assembly checkpoint". However, it should more accurately be named a "spindle attachment checkpoint" because an element of spindle assembly is not dependent on all SAC genes, namely spindle stability. Conveniently the acronym remains unchanged but crucially the description of what activates the checkpoint is refined.

The previously described SOC, a "spindle orientation checkpoint", does not in fact monitor spindle orientation in *S.pombe* and so the name is erroneous. However, it involves a specific branch of the SAC that is activated in the presence of Lat A (Gachet *et al.*, 2001, 2004; Rajagopalan *et al.*, 2004; Tournier *et al.*, 2004) or in absence of Mal3 (Asakawa *et al.*, 2005). This branch consists of a subset of SAC proteins that include Bub1, Bub3, Mph1 and Mad3 (implicated in tension and attachment sensing) but not Mad1 or Mad2 (implicated in attachment sensing only). Since I have shown that the addition of Lat A causes not only anaphase delays but also frequent spindle collapses the specific subset of SAC components in question may in fact monitor spindle stability or integrity, perhaps through correct tension across the poles. In this way the SOC is really part of a more complex "spindle assembly checkpoint". To avoid confusion I propose renaming this checkpoint element as the "spindle integrity checkpoint" (SIC) (figure 8.3). Importantly, it is not yet known whether

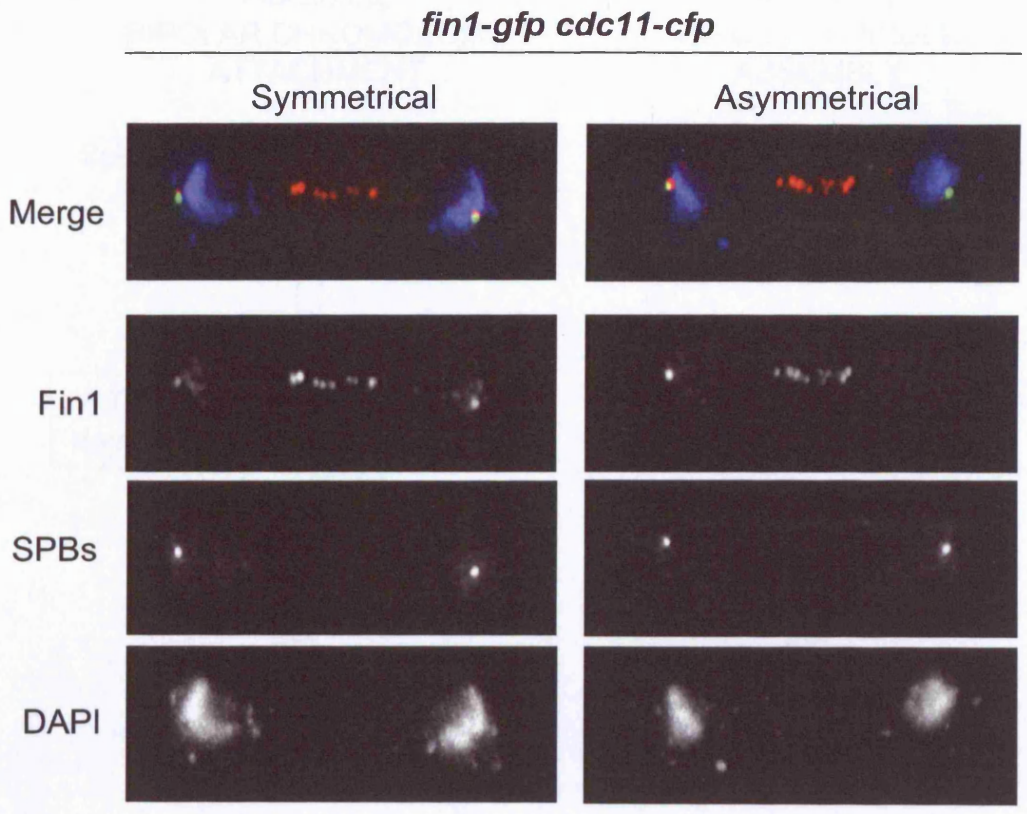

Figure 8.2 The localisation of Fin1 reveals two distinct lineage-dependent populations of fission yeast cells

Images of two log phase cells expressing Fin1-GFP (red) and Cdc11-CFP (SPBs, green). DNA (blue) is stained with DAPI. Fin1 localises to SPBs (either symmetrically (left column) or asymmetrically (right column)) and the spindle midzone, as described by Grallert *et al.* (2004).

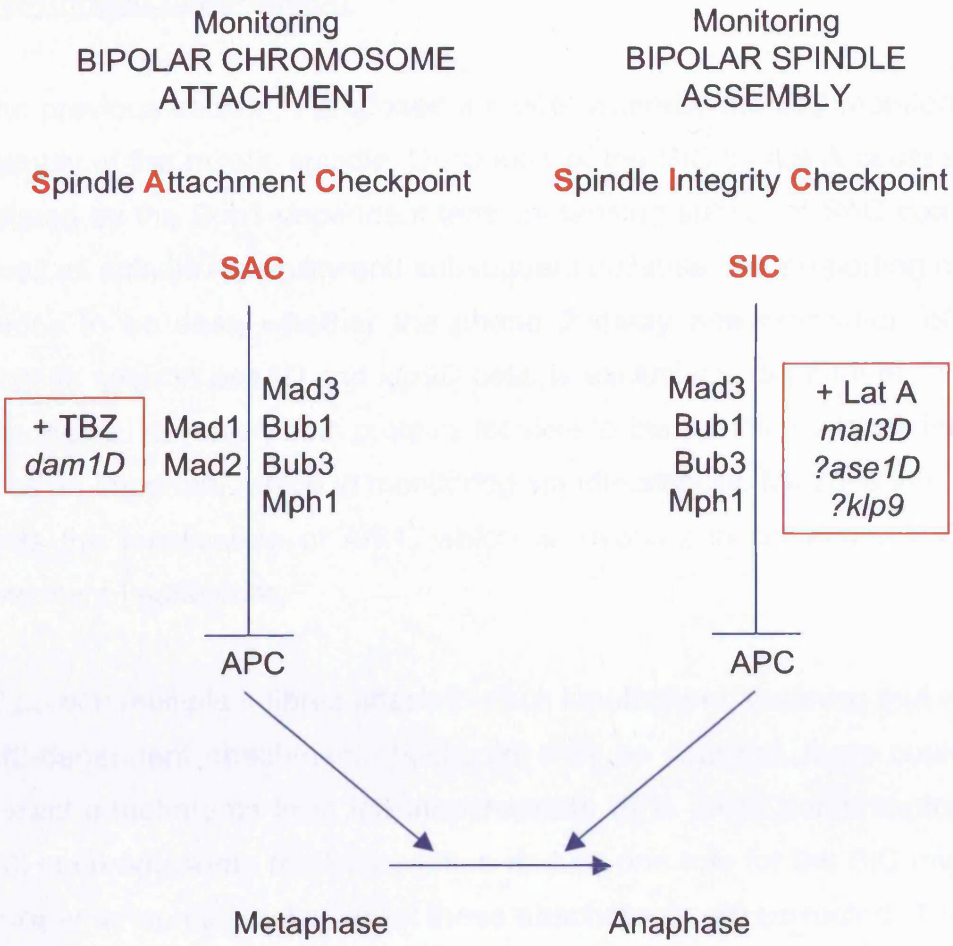

Figure 8.3 Re-defining the checkpoints acting over mitotic progression in fission yeast

Data from this and other work suggests that there are two branches of the classical spindle assembly checkpoint functioning in fission yeast. The first, which monitors kinetochore occupancy, requires all 6 SAC components and can be activated by microtubule depolymerisation. This is referred to here as the spindle attachment checkpoint (SAC). The second branch, that appears to monitor the fidelity of the spindle, requires a subset of SAC components and can be activated by actin depolymerisation. This is shown here as the spindle integrity checkpoint (SIC).

spindle assembly checkpoint proteins are required to delay anaphase onset in cells lacking either Ase1 or Klp9 and, if so, which ones.

8.4 The spindle integrity checkpoint: a spatial model monitoring tension *via* chromatid congression

In the previous section, I proposed a model whereby the SIC monitors correct assembly of the mitotic spindle. Disruption of the SIC by Lat A causes a delay mediated by the Bub1-dependent tension-sensing subset of SAC components as well as spindle instability and subsequent collapse in a proportion of cells. It remains to be seen whether the phase 2 delay and proportion of spindle collapses seen in *ase1D* and *klp9D* cells is exclusively dependent on the SIC components. However, both proteins localise to the spindle midzone implicating this as an important region in monitoring spindle stability. Midzone integrity also affects the localisation of Ark1, which is involved in correcting k-fibre and kinetochore interactions.

In *S.pombe* multiple k-fibres attach to each kinetochore, meaning that whilst the Mad2-dependent attachment checkpoint may be satisfied, there could still be incorrect attachments from the inappropriate SPB. Such conformations could result in chromosome mis-segregation and so one role for the SIC might be to ensure an anaphase delay whilst these attachments are corrected. The correct conformation, termed amphitelic attachment, is where an equal number of k-fibres from each SPB are attached to opposing kinetochores. This arrangement causes balanced tension across the kinetochores prior to anaphase and results in the sister chromatids aligning at the spindle midzone equidistant from the poles. In the proposed model, only when all three chromatid pairs reach this conformation, termed the metaphase plate, would the SIC be satisfied and anaphase initiated (figure 8.4). A metaphase plate was described in fission yeast involving chromosome congression (Tournier *et al.*, 2004). Importantly, these authors note that in the presence of Lat A when the SIC is activated, this congression is not observed, which could be due to midzone destabilisation. Similarly, loss of the proteins Ase1 and Klp9 could impair the ability of the midzone to determine the location, and therefore correct attachment, of sister

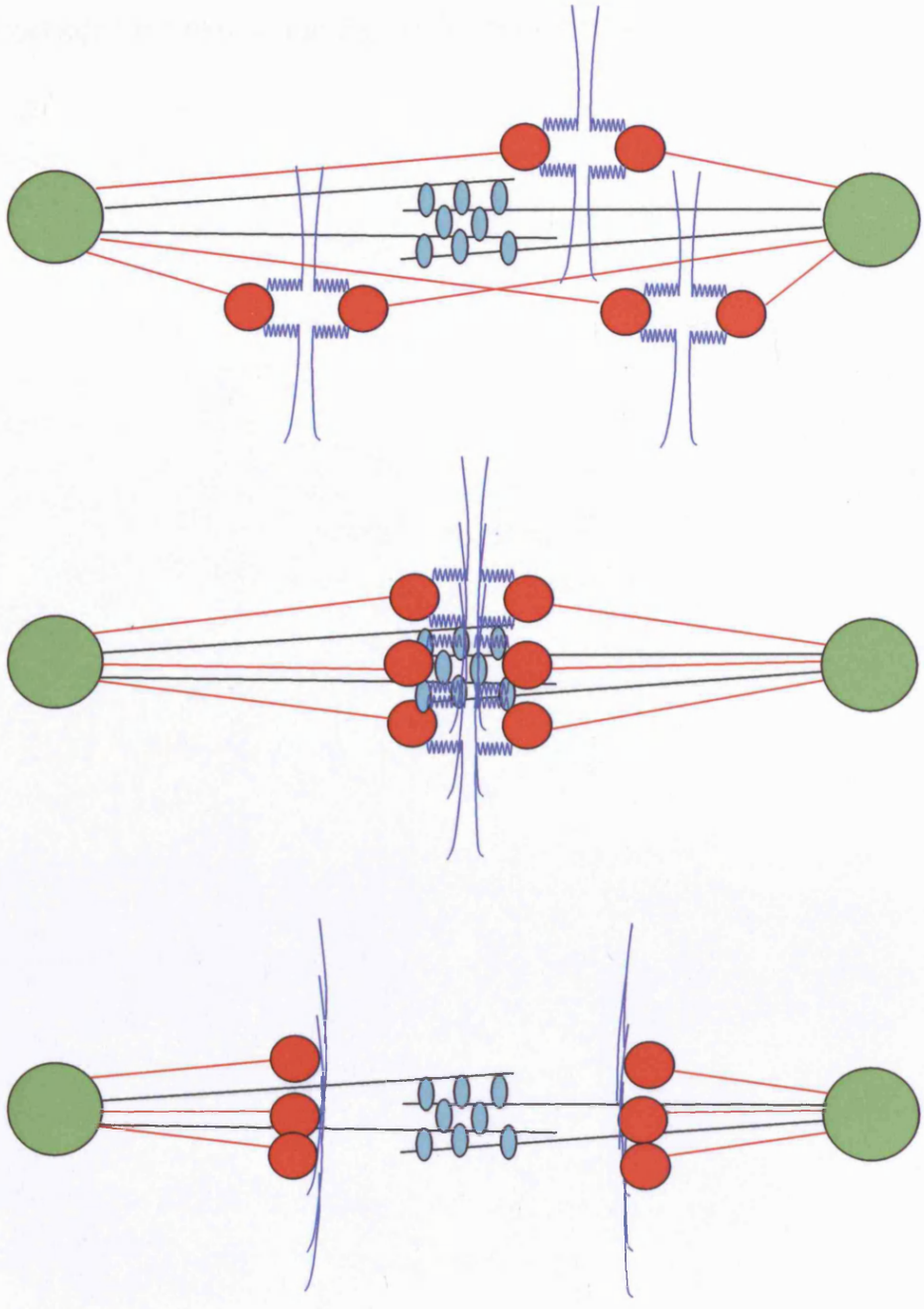

Figure 8.4 Is the midzone involved in a tension-sensing pathway that ensures spindle integrity?

A model proposing that balanced tension across the kinetochores is sensed at the spindle midzone, allowing anaphase to occur only after the metaphase plate conformation is attained. SPBs are represented in green, kinetochores and k-fibres as red circles and lines respectively, pole-to-pole microtubules in black, ase1 in cyan and chromatids in blue.

chromatids. The method of communication between the midzone and kinetochores is unknown and provides a rich area for future study.

REFERENCES

Adames, N. R., Oberle, J. R. & Cooper, J. A. (2001). The surveillance mechanism of the spindle position checkpoint in yeast. *J Cell Biol* **153**, 159-168.

Adams, R. R., Tavares, A. A., Salzberg, A., Bellen, H. J. & Glover, D. M. (1998). pavarotti encodes a kinesin-like protein required to organize the central spindle and contractile ring for cytokinesis. *Genes Dev* **12**, 1483-1494.

Adams, R. R., Wheatley, S. P., Gouldsworthy, A. M., Kandels-Lewis, S. E., Carmena, M., Smythe, C., Gerloff, D. L. & Earnshaw, W. C. (2000). INCENP binds the Aurora-related kinase AIRK2 and is required to target it to chromosomes, the central spindle and cleavage furrow. *Curr Biol* **10**, 1075-1078.

Alfa, C. E., Ducommun, B., Beach, D. & Hyams, J. S. (1990). Distinct nuclear and spindle pole body population of cyclin-cdc2 in fission yeast. *Nature* **347**, 680-682.

Arai, R., Nakano, K. & Mabuchi, I. (1998). Subcellular localization and possible function of actin, tropomyosin and actin-related protein 3 (Arp3) in the fission yeast Schizosaccharomyces pombe. *Eur J Cell Biol* **76**, 288-295.

Arai, R. & Mabuchi, I. (2002). F-actin ring formation and the role of F-actin cables in the fission yeast Schizosaccharomyces pombe. *J Cell Sci* **115**, 887-898.

Asakawa, K., Toya, M., Sato, M., Kanai, M., Kume, K., Goshima, T., Garcia, M. A., Hirata, D. & Toda, T. (2005). Mal3, the fission yeast EB1 homologue, cooperates with Bub1 spindle checkpoint to prevent monopolar attachment. *EMBO Rep* **6**, 1194-1200.

Asbury, C. L., Gestaut, D. R., Powers, A. F., Franck, A. D. & Davis, T. N. (2006). The Dam1 kinetochore complex harnesses microtubule dynamics to produce force and movement. *Proc Natl Acad Sci U S A* **103**, 9873-9878.

Ayscough, K. R., Stryker, J., Pokala, N., Sanders, M., Crews, P. & Drubin, D. G. (1997). High rates of actin filament turnover in budding yeast and roles for actin in establishment and maintenance of cell polarity revealed using the actin inhibitor latrunculin-A. *J Cell Biol* **137**, 399-416.

Bahler, J. & Pringle, J. R. (1998). Pom1p, a fission yeast protein kinase that provides positional information for both polarized growth and cytokinesis. *Genes Dev* **12**, 1356-1370.

Bahler, J., Steever, A. B., Wheatley, S., Wang, Y., Pringle, J. R., Gould, K. L. & McCollum, D. (1998a). Role of polo kinase and Mid1p in determining the site of cell division in fission yeast. *J Cell Biol* **143**, 1603-1616.

Bahler, J., Wu, J. Q., Longtine, M. S., Shah, N. G., McKenzie, A., 3rd, Steever, A. B., Wach, A., Philippsen, P. & Pringle, J. R. (1998b). Heterologous modules for efficient and versatile PCR-based gene targeting in Schizosaccharomyces pombe. *Yeast* **14**, 943-951.

Barbet, N., Muriel, W. J. & Carr, A. M. (1992). Versatile shuttle vectors and genomic libraries for use with Schizosaccharomyces pombe. *Gene* **114**, 59-66.

Bardin, A. J., Visintin, R. & Amon, A. (2000). A mechanism for coupling exit from mitosis to partitioning of the nucleus. *Cell* **102**, 21-31.

Bardin, A. J. & Amon, A. (2001). Men and sin: what's the difference? *Nat Rev Mol Cell Biol* **2**, 815-826.

Beach, D. L., Thibodeaux, J., Maddox, P., Yeh, E. & Bloom, K. (2000). The role of the proteins Kar9 and Myo2 in orienting the mitotic spindle of budding yeast. *Curr Biol* **10**, 1497-1506.

Beinhauer, J. D., Hagan, I. M., Hegemann, J. H. & Fleig, U. (1997). Mal3, the fission yeast homologue of the human APC-interacting protein EB-1 is required for microtubule integrity and the maintenance of cell form. *J Cell Biol* **139**, 717-728.

Belmont, L. D., Patterson, G. M. & Drubin, D. G. (1999). New actin mutants allow further characterization of the nucleotide binding cleft and drug binding sites. *J Cell Sci* **112** (Pt 9), 1325-1336.

Bernard, P., Hardwick, K. & Javerzat, J. P. (1998). Fission yeast bub1 is a mitotic centromere protein essential for the spindle checkpoint and the preservation of correct ploidy through mitosis. *J Cell Biol* **143**, 1775-1787.

Biggins, S., Severin, F. F., Bhalla, N., Sassoon, I., Hyman, A. A. & Murray, A. W. (1999). The conserved protein kinase Ipl1 regulates microtubule binding to kinetochores in budding yeast. *Genes Dev* **13**, 532-544.

Birkenbihl, R. P. & Subramani, S. (1992). Cloning and characterization of rad21 an essential gene of Schizosaccharomyces pombe involved in DNA double-strand-break repair. *Nucleic Acids Res* **20**, 6605-6611.

Birkenbihl, R. P. & Subramani, S. (1995). The rad21 gene product of Schizosaccharomyces pombe is a nuclear, cell cycle-regulated phosphoprotein. *J Biol Chem* **270**, 7703-7711.

Blanco, M. A., Sanchez-Diaz, A., de Prada, J. M. & Moreno, S. (2000). APC(ste9/srw1) promotes degradation of mitotic cyclins in G(1) and is inhibited by cdc2 phosphorylation. *Embo J* **19**, 3945-3955.

Blessing, C. A., Ugrinova, G. T. & Goodson, H. V. (2004). Actin and ARPs: action in the nucleus. *Trends Cell Biol* **14**, 435-442.

Bolton, M. A., Lan, W., Powers, S. E., McCleland, M. L., Kuang, J. & Stukenberg, P. T. (2002). Aurora B kinase exists in a complex with survivin and INCENP and its kinase activity is stimulated by survivin binding and phosphorylation. *Mol Biol Cell* **13**, 3064-3077.

Brazer, S. C., Williams, H. P., Chappell, T. G. & Cande, W. Z. (2000). A fission yeast kinesin affects Golgi membrane recycling. *Yeast* **16**, 149-166.

Bridge, A. J., Morphew, M., Bartlett, R. & Hagan, I. M. (1998). The fission yeast SPB component Cut12 links bipolar spindle formation to mitotic control. *Genes Dev* **12**, 927-942.

Browning, H., Hayles, J., Mata, J., Aveline, L., Nurse, P. & McIntosh, J. R. (2000). Tea2p is a kinesin-like protein required to generate polarized growth in fission yeast. *J Cell Biol* **151**, 15-28.

Brunner, D. & Nurse, P. (2000). CLIP170-like tip1p spatially organizes microtubular dynamics in fission yeast. *Cell* **102**, 695-704.

Busch, K. E. & Brunner, D. (2004). The microtubule plus end-tracking proteins mal3p and tip1p cooperate for cell-end targeting of interphase microtubules. *Curr Biol* **14**, 548-559.

Byers, B. & Goetsch, L. (1975). Behavior of spindles and spindle plaques in the cell cycle and conjugation of Saccharomyces cerevisiae. *J Bacteriol* **124**, 511-523.

Carazo-Salas, R. & Nurse, P. (2007). Sorting out interphase microtubules. *Mol Syst Biol* **3**, 95.

Carazo-Salas, R. E., Antony, C. & Nurse, P. (2005). The kinesin Klp2 mediates polarization of interphase microtubules in fission yeast. *Science* **309**, 297-300.

Carazo-Salas, R. E. & Nurse, P. (2006). Self-organization of interphase microtubule arrays in fission yeast. *Nat Cell Biol* **8**, 1102-1107.

Carnahan, R. H. & Gould, K. L. (2003). The PCH family protein, Cdc15p, recruits two F-actin nucleation pathways to coordinate cytokinetic actin ring formation in Schizosaccharomyces pombe. *J Cell Biol* **162**, 851-862.

Cassimeris, L., Rieder, C. L., Rupp, G. & Salmon, E. D. (1990). Stability of microtubule attachment to metaphase kinetochores in PtK1 cells. *J Cell Sci* **96** (Pt 1), 9-15.

Chang, F. & Nurse, P. (1996). How fission yeast fission in the middle. *Cell* **84**, 191-194.

Cheeseman, I. M., Brew, C., Wolyniak, M., Desai, A., Anderson, S., Muster, N., Yates, J. R., Huffaker, T. C., Drubin, D. G. & Barnes, G. (2001a). Implication of a novel multiprotein Dam1p complex in outer kinetochore function. *J Cell Biol* **155**, 1137-1145.

Cheeseman, I. M., Enquist-Newman, M., Muller-Reichert, T., Drubin, D. G. & Barnes, G. (2001b). Mitotic spindle integrity and kinetochore function linked by the Duo1p/Dam1p complex. *J Cell Biol* **152**, 197-212.

Cheeseman, I. M., Anderson, S., Jwa, M., Green, E. M., Kang, J., Yates, J. R., 3rd, Chan, C. S., Drubin, D. G. & Barnes, G. (2002). Phospho-regulation of kinetochore-microtubule attachments by the Aurora kinase Ipl1p. *Cell* **111**, 163-172.

Chen, R. H., Shevchenko, A., Mann, M. & Murray, A. W. (1998). Spindle checkpoint protein Xmad1 recruits Xmad2 to unattached kinetochores. *J Cell Biol* **143**, 283-295.

Ciosk, R., Zachariae, W., Michaelis, C., Shevchenko, A., Mann, M. & Nasmyth, K. (1998). An ESP1/PDS1 complex regulates loss of sister chromatid cohesion at the metaphase to anaphase transition in yeast. *Cell* **93**, 1067-1076.

Courtheoux, T., Gay, G., Reyes, C., Goldstone, S., Gachet, Y. & Tournier, S. (2007). Dynein participates in chromosome segregation in fission yeast. *Biol Cell* **99**, 627-637.

Creanor, J. & Mitchison, J. M. (1996). The kinetics of the B cyclin p56cdc13 and the phosphatase p80cdc25 during the cell cycle of the fission yeast Schizosaccharomyces pombe. *J Cell Sci* **109** (Pt 6), 1647-1653.

D'Aquino, K. E., Monje-Casas, F., Paulson, J., Reiser, V., Charles, G. M., Lai, L., Shokat, K. M. & Amon, A. (2005). The protein kinase Kin4 inhibits exit from mitosis in response to spindle position defects. *Mol Cell* **19**, 223-234.

Daga, R. R. & Chang, F. (2005). Dynamic positioning of the fission yeast cell division plane. *Proc Natl Acad Sci U S A* **102**, 8228-8232.

Daga, R. R., Lee, K. G., Bratman, S., Salas-Pino, S. & Chang, F. (2006a). Self-organization of microtubule bundles in anucleate fission yeast cells. *Nat Cell Biol* **8**, 1108-1113.

Daga, R. R., Yonetani, A. & Chang, F. (2006b). Asymmetric microtubule pushing forces in nuclear centering. *Curr Biol* **16**, 1544-1550.

Decottignies, A., Zarzov, P. & Nurse, P. (2001). In vivo localisation of fission yeast cyclin-dependent kinase cdc2p and cyclin B cdc13p during mitosis and meiosis. *J Cell Sci* **114**, 2627-2640.

Desai, A. & Mitchison, T. J. (1997). Microtubule polymerization dynamics. *Annu Rev Cell Dev Biol* **13**, 83-117.

Ding, R., McDonald, K. L. & McIntosh, J. R. (1993). Three-dimensional reconstruction and analysis of mitotic spindles from the yeast, Schizosaccharomyces pombe. *J Cell Biol* **120**, 141-151.

Ding, R., West, R. R., Morphew, D. M., Oakley, B. R. & McIntosh, J. R. (1997). The spindle pole body of Schizosaccharomyces pombe enters and leaves the nuclear envelope as the cell cycle proceeds. *Mol Biol Cell* **8**, 1461-1479.

Drummond, D. R. & Cross, R. A. (2000). Dynamics of interphase microtubules in Schizosaccharomyces pombe. *Curr Biol* **10**, 766-775.

Fabian, L. & Forer, A. (2005). Redundant mechanisms for anaphase chromosome movements: crane-fly spermatocyte spindles normally use actin filaments but also can function without them. *Protoplasma* **225**, 169-184.

Fantes, P. (1979). Epistatic gene interactions in the control of division in fission yeast. *Nature* **279**, 428-430.

Fantes, P. A. & Nurse, P. (1978). Control of the timing of cell division in fission yeast. Cell size mutants reveal a second control pathway. *Exp Cell Res* **115**, 317-329.

Feierbach, B. & Chang, F. (2001). Roles of the fission yeast formin for3p in cell polarity, actin cable formation and symmetric cell division. *Curr Biol* **11**, 1656-1665.

Feierbach, B., Verde, F. & Chang, F. (2004). Regulation of a formin complex by the microtubule plus end protein tea1p. *J Cell Biol* **165**, 697-707.

Flory, M. R., Morphew, M., Joseph, J. D., Means, A. R. & Davis, T. N. (2002). Pcp1p, an Spc110p-related calmodulin target at the centrosome of the fission yeast Schizosaccharomyces pombe. *Cell Growth Differ* **13**, 47-58.

Franco, A., Meadows, J. C. & Millar, J. B. (2007). The Dam1/DASH complex is required for the retrieval of unclustered kinetochores in fission yeast. *J Cell Sci* **120**, 3345-3351.

Fujita, M., Ichinose, S., Kiyono, T., Tsurumi, T. & Omori, A. (2003). Establishment of latrunculin-A resistance in HeLa cells by expression of R183A D184A mutant beta-actin. *Oncogene* **22**, 627-631.

Funabiki, H., Kumada, K. & Yanagida, M. (1996a). Fission yeast Cut1 and Cut2 are essential for sister chromatid separation, concentrate along the metaphase spindle and form large complexes. *Embo J* **15**, 6617-6628.

Funabiki, H., Yamano, H., Kumada, K., Nagao, K., Hunt, T. & Yanagida, M. (1996b). Cut2 proteolysis required for sister-chromatid seperation in fission yeast. *Nature* **381**, 438-441.

Funabiki, H., Yamano, H., Nagao, K., Tanaka, H., Yasuda, H., Hunt, T. & Yanagida, M. (1997). Fission yeast Cut2 required for anaphase has two destruction boxes. *Embo J* **16**, 5977-5987.

Gachet, Y., Tournier, S., Millar, J. B. & Hyams, J. S. (2001). A MAP kinase-dependent actin checkpoint ensures proper spindle orientation in fission yeast. *Nature* **412**, 352-355.

Gachet, Y., Tournier, S., Millar, J. B. & Hyams, J. S. (2004). Mechanism controlling perpendicular alignment of the spindle to the axis of cell division in fission yeast. *Embo J* **23**, 1289-1300.

Gachet, Y., Reyes, C., Goldstone, S. & Tournier, S. (2006). The fission yeast spindle orientation checkpoint: a model that generates tension? *Yeast* **23**, 1015-1029.

Garcia, M. A., Vardy, L., Koonrugsa, N. & Toda, T. (2001). Fission yeast ch-TOG/XMAP215 homologue Alp14 connects mitotic spindles with the kinetochore and is a component of the Mad2-dependent spindle checkpoint. *Embo J* **20**, 3389-3401.

Garcia, M. A., Koonrugsa, N. & Toda, T. (2002). Two kinesin-like Kin I family proteins in fission yeast regulate the establishment of metaphase and the onset of anaphase A. *Curr Biol* **12**, 610-621.

Glynn, J. M., Lustig, R. J., Berlin, A. & Chang, F. (2001). Role of bud6p and tea1p in the interaction between actin and microtubules for the establishment of cell polarity in fission yeast. *Curr Biol* **11**, 836-845.

Gonsior, S. M., Platz, S., Buchmeier, S., Scheer, U., Jockusch, B. M. & Hinssen, H. (1999). Conformational difference between nuclear and cytoplasmic actin as detected by a monoclonal antibody. *J Cell Sci* **112** (Pt 6), 797-809.

Gorbsky, G. J., Sammak, P. J. & Borisy, G. G. (1987). Chromosomes move poleward in anaphase along stationary microtubules that coordinately disassemble from their kinetochore ends. *J Cell Biol* **104**, 9-18.

Gorbsky, G. J., Sammak, P. J. & Borisy, G. G. (1988). Microtubule dynamics and chromosome motion visualized in living anaphase cells. *J Cell Biol* **106**, 1185-1192.

Gould, K. L. & Nurse, P. (1989). Tyrosine phosphorylation of the fission yeast *cdc2+* protein kinase regulates entry into mitosis. *Nature* **342**, 39-45.

Grallert, A. & Hagan, I. M. (2002). Schizosaccharomyces pombe NIMA-related kinase, Fin1, regulates spindle formation and an affinity of Polo for the SPB. *Embo J* **21**, 3096-3107.

Grallert, A., Krapp, A., Bagley, S., Simanis, V. & Hagan, I. M. (2004). Recruitment of NIMA kinase shows that maturation of the S. pombe spindle-pole body occurs over consecutive cell cycles and reveals a role for NIMA in modulating SIN activity. *Genes Dev* **18**, 1007-1021.

Grallert, A., Beuter, C., Craven, R. A., Bagley, S., Wilks, D., Fleig, U. & Hagan, I. M. (2006). S. pombe CLASP needs dynein, not EB1 or CLIP170, to induce microtubule instability and slows polymerization rates at cell tips in a dynein-dependent manner. *Genes Dev* **20**, 2421-2436.

Grishchuk, E. L., Molodtsov, M. I., Ataullakhanov, F. I. & McIntosh, J. R. (2005). Force production by disassembling microtubules. *Nature* **438**, 384-388.

Grishchuk, E. L. & McIntosh, J. R. (2006). Microtubule depolymerization can drive poleward chromosome motion in fission yeast. *Embo J* **25**, 4888-4896.

Guacci, V., Koshland, D. & Strunnikov, A. (1997). A direct link between sister chromatid cohesion and chromosome condensation revealed through the analysis of MCD1 in S. cerevisiae. *Cell* **91**, 47-57.

Hagan, I., Hayles, J. & Nurse, P. (1988). Cloning and sequencing of the cyclin-related cdc13+ gene and a cytological study of its role in fission yeast mitosis. *J Cell Sci* **91** (Pt 4), 587-595.

Hagan, I. & Yanagida, M. (1990). Novel potential mitotic motor protein encoded by the fission yeast cut7+ gene. *Nature* **347**, 563-566.

Hagan, I. & Yanagida, M. (1992). Kinesin-related cut7 protein associates with mitotic and meiotic spindles in fission yeast. *Nature* **356**, 74-76.

Hagan, I. & Yanagida, M. (1997). Evidence for cell cycle-specific, spindle pole body-mediated, nuclear positioning in the fission yeast Schizosaccharomyces pombe. *J Cell Sci* **110** (Pt 16), 1851-1866.

Hagan, I. M. & Hyams, J. S. (1988). The use of cell division cycle mutants to investigate the control of microtubule distribution in the fission yeast Schizosaccharomyces pombe. *J Cell Sci* **89** (Pt 3), 343-357.

Hagan, I. M. (1998). The fission yeast microtubule cytoskeleton. *J Cell Sci* **111** (Pt 12), 1603-1612.

Hardwick, K. G. & Murray, A. W. (1995). Mad1p, a phosphoprotein component of the spindle assembly checkpoint in budding yeast. *J Cell Biol* **131**, 709-720.

Hardwick, K. G., Johnston, R. C., Smith, D. L. & Murray, A. W. (2000). MAD3 encodes a novel component of the spindle checkpoint which interacts with Bub3p, Cdc20p, and Mad2p. *J Cell Biol* **148**, 871-882.

Hartwell, L. H. & Weinert, T. A. (1989). Checkpoints: controls that ensure the order of cell cycle events. *Science* **246**, 629-634.

Heitz, M. J., Petersen, J., Valovin, S. & Hagan, I. M. (2001). MTOC formation during mitotic exit in fission yeast. *J Cell Sci* **114**, 4521-4532.

Hentges, P., Van Driessche, B., Tafforeau, L., Vandenhaute, J. & Carr, A. M. (2005). Three novel antibiotic marker cassettes for gene disruption and marker switching in Schizosaccharomyces pombe. *Yeast* **22**, 1013-1019.

Higuchi, T. & Uhlmann, F. (2005). Stabilization of microtubule dynamics at anaphase onset promotes chromosome segregation. *Nature* **433**, 171-176.

Hilioti, Z., Chung, Y. S., Mochizuki, Y., Hardy, C. F. & Cohen-Fix, O. (2001). The anaphase inhibitor Pds1 binds to the APC/C-associated protein Cdc20 in a destruction box-dependent manner. *Curr Biol* **11**, 1347-1352.

Horio, T., Uzawa, S., Jung, M. K., Oakley, B. R., Tanaka, K. & Yanagida, M. (1991). The fission yeast gamma-tubulin is essential for mitosis and is localized at microtubule organizing centers. *J Cell Sci* **99** (Pt 4), 693-700.

Hoyt, M. A., Totis, L. & Roberts, B. T. (1991). S. cerevisiae genes required for cell cycle arrest in response to loss of microtubule function. *Cell* **66**, 507-517.

Hwang, L. H., Lau, L. F., Smith, D. L., Mistrot, C. A., Hardwick, K. G., Hwang, E. S., Amon, A. & Murray, A. W. (1998). Budding yeast Cdc20: a target of the spindle checkpoint. *Science* **279**, 1041-1044.

Ikui, A. E., Furuya, K., Yanagida, M. & Matsumoto, T. (2002). Control of localization of a spindle checkpoint protein, Mad2, in fission yeast. *J Cell Sci* **115**, 1603-1610.

Janke, C., Ortiz, J., Tanaka, T. U., Lechner, J. & Schiebel, E. (2002). Four new subunits of the Dam1-Duo1 complex reveal novel functions in sister kinetochore biorientation. *Embo J* **21**, 181-193.

Janson, M. E., Setty, T. G., Paoletti, A. & Tran, P. T. (2005). Efficient formation of bipolar microtubule bundles requires microtubule-bound gamma-tubulin complexes. *J Cell Biol* **169**, 297-308.

Janson, M. E., Loughlin, R., Loiodice, I., Fu, C., Brunner, D., Nedelec, F. J. & Tran, P. T. (2007). Crosslinkers and motors organize dynamic microtubules to form stable bipolar arrays in fission yeast. *Cell* **128**, 357-368.

Jensen, S., Geymonat, M. & Johnston, L. H. (2002). Mitotic exit: delaying the end without FEAR. *Curr Biol* **12**, R221-223.

Kadura, S. & Sazer, S. (2005). SAC-ing mitotic errors: how the spindle assembly checkpoint (SAC) plays defense against chromosome mis-segregation. *Cell Motil Cytoskeleton* **61**, 145-160.

Kamasaki, T., Arai, R., Osumi, M. & Mabuchi, I. (2005). Directionality of F-actin cables changes during the fission yeast cell cycle. *Nat Cell Biol* **7**, 916-917.

Kang, J., Cheeseman, I. M., Kallstrom, G., Velmurugan, S., Barnes, G. & Chan, C. S. (2001). Functional cooperation of Dam1, Ipl1, and the inner centromere protein (INCENP)-related protein Sli15 during chromosome segregation. *J Cell Biol* **155**, 763-774.

Kawashima, S. A., Tsukahara, T., Langegger, M., Hauf, S., Kitajima, T. S. & Watanabe, Y. (2007). Shugoshin enables tension-generating attachment of kinetochores by loading Aurora to centromeres. *Genes Dev* **21**, 420-435.

Keeney, J. B. & Boeke, J. D. (1994). Efficient targeted integration at leu1-32 and ura4-294 in Schizosaccharomyces pombe. *Genetics* **136**, 849-856.

Kilmartin, J. V. (2003). Sfi1p has conserved centrin-binding sites and an essential function in budding yeast spindle pole body duplication. *J Cell Biol* **162**, 1211-1221.

Kim, S. H., Lin, D. P., Matsumoto, S., Kitazono, A. & Matsumoto, T. (1998). Fission yeast Slp1: an effector of the Mad2-dependent spindle checkpoint. *Science* **279**, 1045-1047.

Kitamura, K., Maekawa, H. & Shimoda, C. (1998). Fission yeast Ste9, a homolog of Hct1/Cdh1 and Fizzy-related, is a novel negative regulator of cell cycle progression during G1-phase. *Mol Biol Cell* **9**, 1065-1080.

Kominami, K., Seth-Smith, H. & Toda, T. (1998). Apc10 and Ste9/Srw1, two regulators of the APC-cyclosome, as well as the CDK inhibitor Rum1 are required for G1 cell-cycle arrest in fission yeast. *Embo J* **17**, 5388-5399.

Krapp, A., Gulli, M. P. & Simanis, V. (2004). SIN and the art of splitting the fission yeast cell. *Curr Biol* **14**, R722-730.

Krawchuk, M. D. & Wahls, W. P. (1999). High-efficiency gene targeting in Schizosaccharomyces pombe using a modular, PCR-based approach with long tracts of flanking homology. *Yeast* **15**, 1419-1427.

Kumada, K., Nakamura, T., Nagao, K., Funabiki, H., Nakagawa, T. & Yanagida, M. (1998). Cut1 is loaded onto the spindle by binding to Cut2 and promotes anaphase spindle movement upon Cut2 proteolysis. *Curr Biol* **8**, 633-641.

Kumagai, A. & Dunphy, W. G. (1996). Purification and molecular cloning of Plx1, a Cdc25-regulatory kinase from Xenopus egg extracts. *Science* **273**, 1377-1380.

La Carbona, S., Le Goff, C. & Le Goff, X. (2006). Fission yeast cytoskeletons and cell polarity factors: connecting at the cortex. *Biol Cell* 98, 619-631.

Lee, M. G. & Nurse, P. (1987). Complementation used to clone a human homologue of the fission yeast cell cycle control gene *cdc2. Nature* **327**, 31-35.

Lenart, P., Bacher, C. P., Daigle, N., Hand, A. R., Eils, R., Terasaki, M. & Ellenberg, J. (2005). A contractile nuclear actin network drives chromosome congression in oocytes. *Nature* **436**, 812-818.

Leverson, J. D., Huang, H. K., Forsburg, S. L. & Hunter, T. (2002). The Schizosaccharomyces pombe aurora-related kinase Ark1 interacts with the inner centromere protein Pic1 and mediates chromosome segregation and cytokinesis. *Mol Biol Cell* **13**, 1132-1143.

Lew, D. J. & Burke, D. J. (2003). The spindle assembly and spindle position checkpoints. *Annu Rev Genet* **37**, 251-282.

Li, R. & Murray, A. W. (1991). Feedback control of mitosis in budding yeast. *Cell* **66**, 519-531.

Li, X. & Nicklas, R. B. (1995). Mitotic forces control a cell-cycle checkpoint. *Nature* **373**, 630-632.

Li, Y., Bachant, J., Alcasabas, A. A., Wang, Y., Qin, J. & Elledge, S. J. (2002). The mitotic spindle is required for loading of the DASH complex onto the kinetochore. *Genes Dev* **16**, 183-197.

Loiodice, I., Staub, J., Setty, T. G., Nguyen, N. P., Paoletti, A. & Tran, P. T. (2005). Ase1p organizes antiparallel microtubule arrays during interphase and mitosis in fission yeast. *Mol Biol Cell* **16**, 1756-1768.

Lundgren, K., Walworth, N., Booher, R., Dembski, M., Kirschner, M. & Beach, D. (1991). mik1 and wee1 cooperate in the inhibitory tyrosine phosphorylation of cdc2. *Cell* **64**, 1111-1122.

Luo, X., Fang, G., Coldiron, M., Lin, Y., Yu, H., Kirschner, M. W. & Wagner, G. (2000). Structure of the Mad2 spindle assembly checkpoint protein and its interaction with Cdc20. *Nat Struct Biol* **7**, 224-229.

Luo, X., Tang, Z., Rizo, J. & Yu, H. (2002). The Mad2 spindle checkpoint protein undergoes similar major conformational changes upon binding to either Mad1 or Cdc20. *Mol Cell* **9**, 59-71.

Luo, X., Tang, Z., Xia, G., Wassmann, K., Matsumoto, T., Rizo, J. & Yu, H. (2004). The Mad2 spindle checkpoint protein has two distinct natively folded states. *Nat Struct Mol Biol* **11**, 338-345.

Mallavarapu, A., Sawin, K. & Mitchison, T. (1999). A switch in microtubule dynamics at the onset of anaphase B in the mitotic spindle of Schizosaccharomyces pombe. *Curr Biol* **9**, 1423-1426.

Margolis, R. L. & Wilson, L. (1981). Microtubule treadmills--possible molecular machinery. *Nature* **293**, 705-711.

Marks, J., Hagan, I. M. & Hyams, J. S. (1986). Growth polarity and cytokinesis in fission yeast: the role of the cytoskeleton. *J Cell Sci Suppl* **5**, 229-241.

Mata, J. & Nurse, P. (1997). tea1 and the microtubular cytoskeleton are important for generating global spatial order within the fission yeast cell. *Cell* **89**, 939-949.

Matsumoto, T. (1997). A fission yeast homolog of CDC20/p55CDC/Fizzy is required for recovery from DNA damage and genetically interacts with p34cdc2. *Mol Cell Biol* **17**, 742-750.

Matuliene, J. & Kuriyama, R. (2002). Kinesin-like protein CHO1 is required for the formation of midbody matrix and the completion of cytokinesis in mammalian cells. *Mol Biol Cell* **13**, 1832-1845.

McCollum, D. & Gould, K. L. (2001). Timing is everything: regulation of mitotic exit and cytokinesis by the MEN and SIN. *Trends Cell Biol* **11**, 89-95.

Michaelis, C., Ciosk, R. & Nasmyth, K. (1997). Cohesins: chromosomal proteins that prevent premature separation of sister chromatids. *Cell* **91**, 35-45.

Miki, H., Okada, Y. & Hirokawa, N. (2005). Analysis of the kinesin superfamily: insights into structure and function. *Trends Cell Biol* **15**, 467-476.

Millband, D. N. & Hardwick, K. G. (2002). Fission yeast Mad3p is required for Mad2p to inhibit the anaphase-promoting complex and localizes to kinetochores in a Bub1p-, Bub3p-, and Mph1p-dependent manner. *Mol Cell Biol* **22**, 2728-2742.

Minestrini, G., Harley, A. S. & Glover, D. M. (2003). Localization of Pavarotti-KLP in living Drosophila embryos suggests roles in reorganizing the

cortical cytoskeleton during the mitotic cycle. *Mol Biol Cell* **14**, 4028-4038.

Miranda, J. J., De Wulf, P., Sorger, P. K. & Harrison, S. C. (2005). The yeast DASH complex forms closed rings on microtubules. *Nat Struct Mol Biol* **12**, 138-143.

Mishima, M., Pavicic, V., Gruneberg, U., Nigg, E. A. & Glotzer, M. (2004). Cell cycle regulation of central spindle assembly. *Nature* **430**, 908-913.

Mitchison, J. M. & Nurse, P. (1985). Growth in cell length in the fission yeast Schizosaccharomyces pombe. *J Cell Sci* **75**, 357-376.

Mitchison, T. & Kirschner, M. (1984). Dynamic instability of microtubule growth. *Nature* **312**, 237-242.

Mitchison, T. J. (1989). Polewards microtubule flux in the mitotic spindle: evidence from photoactivation of fluorescence. *J Cell Biol* **109**, 637-652.

Mitchison, T. J. & Salmon, E. D. (1992). Poleward kinetochore fiber movement occurs during both metaphase and anaphase-A in newt lung cell mitosis. *J Cell Biol* **119**, 569-582.

Mollinari, C., Kleman, J. P., Jiang, W., Schoehn, G., Hunter, T. & Margolis, R. L. (2002). PRC1 is a microtubule binding and bundling protein essential to maintain the mitotic spindle midzone. *J Cell Biol* **157**, 1175-1186.

Moreno, S., Nurse, P. & Russell, P. (1990). Regulation of mitosis by cyclic accumulation of p80cdc25 mitotic inducer in fission yeast. *Nature* **344**, 549-552.

Moreno, S., Klar, A. & Nurse, P. (1991). Molecular genetic analysis of fission yeast Schizosaccharomyces pombe. *Methods Enzymol* **194**, 795-823.

Morishita, J., Matsusaka, T., Goshima, G., Nakamura, T., Tatebe, H. & Yanagida, M. (2001). Bir1/Cut17 moving from chromosome to spindle upon the loss of cohesion is required for condensation, spindle elongation and repair. *Genes Cells* **6**, 743-763.

Moritz, M. & Agard, D. A. (2001). Gamma-tubulin complexes and microtubule nucleation. *Curr Opin Struct Biol* **11**, 174-181.

Morton, W. M., Ayscough, K. R. & McLaughlin, P. J. (2000). Latrunculin alters the actin-monomer subunit interface to prevent polymerization. *Nat Cell Biol* **2**, 376-378.

Motegi, F., Mishra, M., Balasubramanian, M. K. & Mabuchi, I. (2004). Myosin-II reorganization during mitosis is controlled temporally by its

dephosphorylation and spatially by Mid1 in fission yeast. *J Cell Biol* **165**, 685-695.

Mulvihill, D. P., Petersen, J., Ohkura, H., Glover, D. M. & Hagan, I. M. (1999). Plo1 kinase recruitment to the spindle pole body and its role in cell division in Schizosaccharomyces pombe. *Mol Biol Cell* **10**, 2771-2785.

Nabeshima, K., Nakagawa, T., Straight, A. F., Murray, A., Chikashige, Y., Yamashita, Y. M., Hiraoka, Y. & Yanagida, M. (1998). Dynamics of centromeres during metaphase-anaphase transition in fission yeast: Dis1 is implicated in force balance in metaphase bipolar spindle. *Mol Biol Cell* **9**, 3211-3225.

Nasmyth, K. (2005). How do so few control so many? *Cell* 120, 739-746.

Neef, R., Klein, U. R., Kopajtich, R. & Barr, F. A. (2006). Cooperation between mitotic kinesins controls the late stages of cytokinesis. *Curr Biol* **16**, 301-307.

Nislow, C., Lombillo, V. A., Kuriyama, R. & McIntosh, J. R. (1992). A plus-end-directed motor enzyme that moves antiparallel microtubules in vitro localizes to the interzone of mitotic spindles. *Nature* **359**, 543-547.

Nurse, P. (1975). Genetic control of cell size at cell division in yeast. *Nature* **256**, 547-551.

Nurse, P. & Thuriaux, P. (1980). Regulatory genes controlling mitosis in the fission yeast *Schizosaccharomyces pombe. Genetics* **96**, 627-637.

Nurse, P. (1990). Universal control mechanism regulating onset of M-phase. *Nature* **344**, 503-508.

Ohkura, H., Hagan, I. M. & Glover, D. M. (1995). The conserved Schizosaccharomyces pombe kinase plo1, required to form a bipolar spindle, the actin ring, and septum, can drive septum formation in G1 and G2 cells. *Genes Dev* **9**, 1059-1073.

Oliferenko, S. & Balasubramanian, M. K. (2002). Astral microtubules monitor metaphase spindle alignment in fission yeast. *Nat Cell Biol* **4**, 816-820.

Palmer, R. E., Sullivan, D. S., Huffaker, T. & Koshland, D. (1992). Role of astral microtubules and actin in spindle orientation and migration in the budding yeast, Saccharomyces cerevisiae. *J Cell Biol* **119**, 583-593.

Paoletti, A. & Chang, F. (2000). Analysis of mid1p, a protein required for placement of the cell division site, reveals a link between the nucleus and the cell surface in fission yeast. *Mol Biol Cell* **11**, 2757-2773.

Pardo, M. & Nurse, P. (2003). Equatorial retention of the contractile actin ring by microtubules during cytokinesis. *Science* **300**, 1569-1574.

Pederson, T. & Aebi, U. (2005). Nuclear actin extends, with no contraction in sight. *Mol Biol Cell* **16**, 5055-5060.

Pellman, D., Bagget, M., Tu, Y. H., Fink, G. R. & Tu, H. (1995). Two microtubule-associated proteins required for anaphase spindle movement in Saccharomyces cerevisiae. *J Cell Biol* **130**, 1373-1385.

Pereira, G., Hofken, T., Grindlay, J., Manson, C. & Schiebel, E. (2000). The Bub2p spindle checkpoint links nuclear migration with mitotic exit. *Mol Cell* **6**, 1-10.

Pereira, G., Tanaka, T. U., Nasmyth, K. & Schiebel, E. (2001). Modes of spindle pole body inheritance and segregation of the Bfa1p-Bub2p checkpoint protein complex. *Embo J* **20**, 6359-6370.

Pereira, G. & Schiebel, E. (2005). Kin4 kinase delays mitotic exit in response to spindle alignment defects. *Mol Cell* **19**, 209-221.

Petersen, J., Heitz, M. J. & Hagan, I. M. (1998). Conjugation in S. pombe: identification of a microtubule-organising centre, a requirement for microtubules and a role for Mad2. *Curr Biol* **8**, 963-966.

Petersen, J., Paris, J., Willer, M., Philippe, M. & Hagan, I. M. (2001). The S. pombe aurora-related kinase Ark1 associates with mitotic structures in a stage dependent manner and is required for chromosome segregation. *J Cell Sci* **114**, 4371-4384.

Petersen, J. & Hagan, I. M. (2003). S. pombe aurora kinase/survivin is required for chromosome condensation and the spindle checkpoint attachment response. *Curr Biol* **13**, 590-597.

Peterson, J. B. & Ris, H. (1976). Electron-microscopic study of the spindle and chromosome movement in the yeast Saccharomyces cerevisiae. *J Cell Sci* **22**, 219-242.

Pfleger, C. M., Lee, E. & Kirschner, M. W. (2001). Substrate recognition by the Cdc20 and Cdh1 components of the anaphase-promoting complex. *Genes Dev* **15**, 2396-2407.

Pinsky, B. A., Kotwaliwale, C. V., Tatsutani, S. Y., Breed, C. A. & Biggins, S. (2006). Glc7/protein phosphatase 1 regulatory subunits can oppose the Ipl1/aurora protein kinase by redistributing Glc7. *Mol Cell Biol* **26**, 2648-2660.

Pollard, T. D. (2007). Regulation of actin filament assembly by arp2/3 complex and formins. *Annu Rev Biophys Biomol Struct* **36**, 451-477.

Qi, H., Rath, U., Wang, D., Xu, Y. Z., Ding, Y., Zhang, W., Blacketer, M. J., Paddy, M. R., Girton, J., Johansen, J. & Johansen, K. M. (2004). Megator, an essential coiled-coil protein that localizes to the putative spindle matrix during mitosis in Drosophila. *Mol Biol Cell* **15**, 4854-4865.

Rajagopalan, S. & Balasubramanian, M. K. (1999). S. pombe Pbh1p: an inhibitor of apoptosis domain containing protein is essential for chromosome segregation. *FEBS Lett* **460**, 187-190.

Rajagopalan, S. & Balasubramanian, M. K. (2002). Schizosaccharomyces pombe Bir1p, a nuclear protein that localizes to kinetochores and the spindle midzone, is essential for chromosome condensation and spindle elongation during mitosis. *Genetics* **160**, 445-456.

Rajagopalan, S., Bimbo, A., Balasubramanian, M. K. & Oliferenko, S. (2004). A potential tension-sensing mechanism that ensures timely anaphase onset upon metaphase spindle orientation. *Curr Biol* **14**, 69-74.

Rajagopalan, S., Mishra, M. & Balasubramanian, M. K. (2006). Schizosaccharomyces pombe homolog of Survivin, Bir1p, exhibits a novel dynamic behavior at the spindle mid-zone. *Genes Cells* **11**, 815-827.

Rath, U., Wang, D., Ding, Y., Xu, Y. Z., Qi, H., Blacketer, M. J., Girton, J., Johansen, J. & Johansen, K. M. (2004). Chromator, a novel and essential chromodomain protein interacts directly with the putative spindle matrix protein skeletor. *J Cell Biochem* **93**, 1033-1047.

Riedel, C. G., Gregan, J., Gruber, S. & Nasmyth, K. (2004). Is chromatin remodeling required to build sister-chromatid cohesion? *Trends Biochem Sci* **29**, 389-392.

Rieder, C. L., Schultz, A., Cole, R. & Sluder, G. (1994). Anaphase onset in vertebrate somatic cells is controlled by a checkpoint that monitors sister kinetochore attachment to the spindle. *J Cell Biol* **127**, 1301-1310.

Rupes, I., Webb, B. A., Mak, A. & Young, P. G. (2001). G2/M arrest caused by actin disruption is a manifestation of the cell size checkpoint in fission yeast. *Mol Biol Cell* **12**, 3892-3903.

Russell, P. & Nurse, P. (1986). cdc25+ functions as an inducer in the mitotic control of fission yeast. *Cell* **45**, 145-153.

Russell, P. & Nurse, P. (1987). Negative regulation of mitosis by *wee1+*, a gene encoding a protein kinase homolog. *Cell* **49**, 559-567.

Sanchez-Perez, I., Renwick, S. J., Crawley, K., Karig, I., Buck, V., Meadows, J. C., Franco-Sanchez, A., Fleig, U., Toda, T. & Millar, J. B. (2005). The DASH complex and Klp5/Klp6 kinesin coordinate bipolar chromosome attachment in fission yeast. *Embo J* **24**, 2931-2943.

Sandblad, L., Busch, K. E., Tittmann, P., Gross, H., Brunner, D. & Hoenger, A. (2006). The Schizosaccharomyces pombe EB1 homolog Mal3p binds and stabilizes the microtubule lattice seam. *Cell* **127**, 1415-1424.

Sasabe, M. & Machida, Y. (2006). MAP65: a bridge linking a MAP kinase to microtubule turnover. *Curr Opin Plant Biol* 9, 563-570.

Sato, M., Koonrugsa, N., Toda, T., Vardy, L., Tournier, S. & Millar, J. B. (2003). Deletion of Mia1/Alp7 activates Mad2-dependent spindle assembly checkpoint in fission yeast. *Nat Cell Biol* **5**, 764-766; author reply 766.

Sato, M., Vardy, L., Angel Garcia, M., Koonrugsa, N. & Toda, T. (2004). Interdependency of fission yeast Alp14/TOG and coiled coil protein Alp7 in microtubule localization and bipolar spindle formation. *Mol Biol Cell* **15**, 1609-1622.

Sawin, K. E. & Nurse, P. (1998). Regulation of cell polarity by microtubules in fission yeast. *J Cell Biol* **142**, 457-471.

Sawin, K. E., Lourenco, P. C. & Snaith, H. A. (2004). Microtubule nucleation at non-spindle pole body microtubule-organizing centers requires fission yeast centrosomin-related protein mod20p. *Curr Biol* **14**, 763-775.

Schoenenberger, C. A., Buchmeier, S., Boerries, M., Sutterlin, R., Aebi, U. & Jockusch, B. M. (2005). Conformation-specific antibodies reveal distinct actin structures in the nucleus and the cytoplasm. *J Struct Biol* **152**, 157-168.

Schuyler, S. C. & Pellman, D. (2001). Search, capture and signal: games microtubules and centrosomes play. *J Cell Sci* **114**, 247-255.

Schuyler, S. C., Liu, J. Y. & Pellman, D. (2003). The molecular function of Ase1p: evidence for a MAP-dependent midzone-specific spindle matrix. Microtubule-associated proteins. *J Cell Biol* **160**, 517-528.

Schwab, M., Neutzner, M., Mocker, D. & Seufert, W. (2001). Yeast Hct1 recognizes the mitotic cyclin Clb2 and other substrates of the ubiquitin ligase APC. *Embo J* **20**, 5165-5175.

Segal, M. & Bloom, K. (2001). Control of spindle polarity and orientation in Saccharomyces cerevisiae. *Trends Cell Biol* **11**, 160-166.

Sellitto, C. & Kuriyama, R. (1988). Distribution of a matrix component of the midbody during the cell cycle in Chinese hamster ovary cells. *J Cell Biol* **106**, 431-439.

Seshan, A. & Amon, A. (2005). Ras and the Rho effector Cla4 collaborate to target and anchor Lte1 at the bud cortex. *Cell Cycle* **4**, 940-946.

Sethi, N., Monteagudo, M. C., Koshland, D., Hogan, E. & Burke, D. J. (1991). The CDC20 gene product of Saccharomyces cerevisiae, a beta-transducin homolog, is required for a subset of microtubule-dependent cellular processes. *Mol Cell Biol* **11**, 5592-5602.

Simanis, V. & Nurse, P. (1986). The cell cycle control gene *cdc2+* of fission yeast encodes a protein kinase potentially regulated by phosphorylation. *Cell* **45**, 261-268.

Simanis, V. (2003). The mitotic exit and septation initiation networks. *J Cell Sci* **116**, 4261-4262.

Sironi, L., Mapelli, M., Knapp, S., De Antoni, A., Jeang, K. T. & Musacchio, A. (2002). Crystal structure of the tetrameric Mad1-Mad2 core complex: implications of a 'safety belt' binding mechanism for the spindle checkpoint. *Embo J* **21**, 2496-2506.

Skoufias, D. A., Andreassen, P. R., Lacroix, F. B., Wilson, L. & Margolis, R. L. (2001). Mammalian mad2 and bub1/bubR1 recognize distinct spindle-attachment and kinetochore-tension checkpoints. *Proc Natl Acad Sci U S A* **98**, 4492-4497.

Snaith, H. A., Samejima, I. & Sawin, K. E. (2005). Multistep and multimode cortical anchoring of tea1p at cell tips in fission yeast. *Embo J* **24**, 3690-3699.

Sohrmann, M., Fankhauser, C., Brodbeck, C. & Simanis, V. (1996). The dmf1/mid1 gene is essential for correct positioning of the division septum in fission yeast. *Genes Dev* **10**, 2707-2719.

Sohrmann, M., Schmidt, S., Hagan, I. & Simanis, V. (1998). Asymmetric segregation on spindle poles of the Schizosaccharomyces pombe septum-inducing protein kinase Cdc7p. *Genes Dev* **12**, 84-94.

Sparks, C. A., Morphew, M. & McCollum, D. (1999). Sid2p, a spindle pole body kinase that regulates the onset of cytokinesis. *J Cell Biol* **146**, 777-790.

Spector, I., Shochet, N. R., Blasberger, D. & Kashman, Y. (1989). Latrunculins--novel marine macrolides that disrupt microfilament organization and affect cell growth: I. Comparison with cytochalasin D. *Cell Motil Cytoskeleton* **13**, 127-144.

Stearns, T., Evans, L. & Kirschner, M. (1991). Gamma-tubulin is a highly conserved component of the centrosome. *Cell* **65**, 825-836.

Strunnikov, A. V. (2003). Condensin and biological role of chromosome condensation. *Prog Cell Cycle Res* **5**, 361-367.

Sudakin, V., Chan, G. K. & Yen, T. J. (2001). Checkpoint inhibition of the APC/C in HeLa cells is mediated by a complex of BUBR1, BUB3, CDC20, and MAD2. *J Cell Biol* **154**, 925-936.

Tanaka, K., Mukae, N., Dewar, H., van Breugel, M., James, E. K., Prescott, A. R., Antony, C. & Tanaka, T. U. (2005). Molecular mechanisms of kinetochore capture by spindle microtubules. *Nature* **434**, 987-994.

Tanaka, K., Kitamura, E., Kitamura, Y. & Tanaka, T. U. (2007). Molecular mechanisms of microtubule-dependent kinetochore transport toward spindle poles. *J Cell Biol* **178**, 269-281.

Tanaka, T. U., Rachidi, N., Janke, C., Pereira, G., Galova, M., Schiebel, E., Stark, M. J. & Nasmyth, K. (2002). Evidence that the Ipl1-Sli15 (Aurora kinase-INCENP) complex promotes chromosome bi-orientation by altering kinetochore-spindle pole connections. *Cell* **108**, 317-329.

Tatebayashi, K., Kato, J. & Ikeda, H. (1998). Isolation of a Schizosaccharomyces pombe rad21ts mutant that is aberrant in chromosome segregation, microtubule function, DNA repair and sensitive to hydroxyurea: possible involvement of Rad21 in ubiquitin-mediated proteolysis. *Genetics* **148**, 49-57.

Tatebe, H., Goshima, G., Takeda, K., Nakagawa, T., Kinoshita, K. & Yanagida, M. (2001). Fission yeast living mitosis visualized by GFP-tagged gene products. *Micron* **32**, 67-74.

Taylor, S. S. & McKeon, F. (1997). Kinetochore localization of murine Bub1 is required for normal mitotic timing and checkpoint response to spindle damage. *Cell* **89**, 727-735.

Thanbichler, M. & Shapiro, L. (2006). Chromosome organization and segregation in bacteria. *J Struct Biol* **156**, 292-303.

Tolic-Norrelykke, I. M., Sacconi, L., Thon, G. & Pavone, F. S. (2004). Positioning and elongation of the fission yeast spindle by microtubule-based pushing. *Curr Biol* **14**, 1181-1186.

Tolic-Norrelykke, I. M., Sacconi, L., Stringari, C., Raabe, I. & Pavone, F. S. (2005). Nuclear and division-plane positioning revealed by optical micromanipulation. *Curr Biol* **15**, 1212-1216.

Tomonaga, T., Nagao, K., Kawasaki, Y., Furuya, K., Murakami, A., Morishita, J., Yuasa, T., Sutani, T., Kearsey, S. E., Uhlmann, F., Nasmyth, K. & Yanagida, M. (2000). Characterization of fission yeast cohesin: essential anaphase proteolysis of Rad21 phosphorylated in the S phase. *Genes Dev* **14**, 2757-2770.

Toth, A., Ciosk, R., Uhlmann, F., Galova, M., Schleiffer, A. & Nasmyth, K. (1999). Yeast cohesin complex requires a conserved protein, Eco1p(Ctf7), to establish cohesion between sister chromatids during DNA replication. *Genes Dev* **13**, 320-333.

Tournier, S., Gachet, Y., Buck, V., Hyams, J. S. & Millar, J. B. (2004). Disruption of astral microtubule contact with the cell cortex activates a Bub1, Bub3, and Mad3-dependent checkpoint in fission yeast. *Mol Biol Cell* **15**, 3345-3356.

Tran, P. T., Marsh, L., Doye, V., Inoue, S. & Chang, F. (2001). A mechanism for nuclear positioning in fission yeast based on microtubule pushing. *J Cell Biol* **153**, 397-411.

Trautmann, S., Wolfe, B. A., Jorgensen, P., Tyers, M., Gould, K. L. & McCollum, D. (2001). Fission yeast Clp1p phosphatase regulates G2/M transition and coordination of cytokinesis with cell cycle progression. *Curr Biol* **11**, 931-940.

Troxell, C. L., Sweezy, M. A., West, R. R., Reed, K. D., Carson, B. D., Pidoux, A. L., Cande, W. Z. & McIntosh, J. R. (2001). pkl1(+)and klp2(+): Two kinesins of the Kar3 subfamily in fission yeast perform different functions in both mitosis and meiosis. *Mol Biol Cell* **12**, 3476-3488.

Uhlmann, F., Lottspeich, F. & Nasmyth, K. (1999). Sister-chromatid separation at anaphase onset is promoted by cleavage of the cohesin subunit Scc1. *Nature* **400**, 37-42.

van Hemert, M. J., Deelder, A. M., Molenaar, C., Steensma, H. Y. & van Heusden, G. P. (2003). Self-association of the spindle pole body-related

intermediate filament protein Fin1p and its phosphorylation-dependent interaction with 14-3-3 proteins in yeast. *J Biol Chem* **278**, 15049-15055.

Vanoosthuyse, V., Valsdottir, R., Javerzat, J. P. & Hardwick, K. G. (2004). Kinetochore targeting of fission yeast Mad and Bub proteins is essential for spindle checkpoint function but not for all chromosome segregation roles of Bub1p. *Mol Cell Biol* **24**, 9786-9801.

Vanoosthuyse, V., Prykhozhij, S. & Hardwick, K. G. (2007). Shugoshin 2 regulates localization of the chromosomal passenger proteins in fission yeast mitosis. *Mol Biol Cell* **18**, 1657-1669.

Venkatram, S., Tasto, J. J., Feoktistova, A., Jennings, J. L., Link, A. J. & Gould, K. L. (2004). Identification and characterization of two novel proteins affecting fission yeast gamma-tubulin complex function. *Mol Biol Cell* **15**, 2287-2301.

Verde, F., Mata, J. & Nurse, P. (1995). Fission yeast cell morphogenesis: identification of new genes and analysis of their role during the cell cycle. *J Cell Biol* **131**, 1529-1538.

Visintin, R., Prinz, S. & Amon, A. (1997). CDC20 and CDH1: a family of substrate-specific activators of APC-dependent proteolysis. *Science* **278**, 460-463.

Vogel, S. K., Raabe, I., Dereli, A., Maghelli, N. & Tolic-Norrelykke, I. (2007). Interphase microtubules determine the initial alignment of the mitotic spindle. *Curr Biol* **17**, 438-444.

Walker, D. L., Wang, D., Jin, Y., Rath, U., Wang, Y., Johansen, J. & Johansen, K. M. (2000). Skeletor, a novel chromosomal protein that redistributes during mitosis provides evidence for the formation of a spindle matrix. *J Cell Biol* **151**, 1401-1412.

Waters, J. C., Chen, R. H., Murray, A. W. & Salmon, E. D. (1998). Localization of Mad2 to kinetochores depends on microtubule attachment, not tension. *J Cell Biol* **141**, 1181-1191.

Weisenberg, R. C., Deery, W. J. & Dickinson, P. J. (1976). Tubulin-nucleotide interactions during the polymerization and depolymerization of microtubules. *Biochemistry* **15**, 4248-4254.

Weiss, E. & Winey, M. (1996). The Saccharomyces cerevisiae spindle pole body duplication gene MPS1 is part of a mitotic checkpoint. *J Cell Biol* **132**, 111-123.

Wertman, K. F., Drubin, D. G. & Botstein, D. (1992). Systematic mutational analysis of the yeast ACT1 gene. *Genetics* **132**, 337-350.

West, R. R., Vaisberg, E. V., Ding, R., Nurse, P. & McIntosh, J. R. (1998). cut11(+): A gene required for cell cycle-dependent spindle pole body anchoring in the nuclear envelope and bipolar spindle formation in Schizosaccharomyces pombe. *Mol Biol Cell* **9**, 2839-2855.

West, R. R., Malmstrom, T. & McIntosh, J. R. (2002). Kinesins klp5(+) and klp6(+) are required for normal chromosome movement in mitosis. *J Cell Sci* **115**, 931-940.

Westermann, S., Avila-Sakar, A., Wang, H. W., Niederstrasser, H., Wong, J., Drubin, D. G., Nogales, E. & Barnes, G. (2005). Formation of a dynamic kinetochore- microtubule interface through assembly of the Dam1 ring complex. *Mol Cell* **17**, 277-290.

Wheatley, S. P., Carvalho, A., Vagnarelli, P. & Earnshaw, W. C. (2001). INCENP is required for proper targeting of Survivin to the centromeres and the anaphase spindle during mitosis. *Curr Biol* **11**, 886-890.

Wilkinson, C. R., Penney, M., McGurk, G., Wallace, M. & Gordon, C. (1999). The 26S proteasome of the fission yeast Schizosaccharomyces pombe. *Philos Trans R Soc Lond B Biol Sci* **354**, 1523-1532.

Winey, M., Mamay, C. L., O'Toole, E. T., Mastronarde, D. N., Giddings, T. H., Jr., McDonald, K. L. & McIntosh, J. R. (1995). Three-dimensional ultrastructural analysis of the Saccharomyces cerevisiae mitotic spindle. *J Cell Biol* **129**, 1601-1615.

Wood, V., Gwilliam, R., Rajandream, M. A., Lyne, M., Lyne, R., Stewart, A., Sgouros, J., Peat, N., Hayles, J., Baker, S., Basham, D., Bowman, S., Brooks, K., Brown, D., Brown, S., Chillingworth, T., Churcher, C., Collins, M., Connor, R., Cronin, A., Davis, P., Feltwell, T., Fraser, A., Gentles, S., Goble, A., Hamlin, N., Harris, D., Hidalgo, J., Hodgson, G., Holroyd, S., Hornsby, T., Howarth, S., Huckle, E. J., Hunt, S., Jagels, K., James, K., Jones, L., Jones, M., Leather, S., McDonald, S., McLean, J., Mooney, P., Moule, S., Mungall, K., Murphy, L., Niblett, D., Odell, C., Oliver, K., O'Neil, S., Pearson, D., Quail, M. A., Rabbinowitsch, E., Rutherford, K., Rutter, S., Saunders, D., Seeger, K., Sharp, S., Skelton, J., Simmonds, M., Squares, R., Squares, S., Stevens, K., Taylor, K., Taylor, R. G., Tivey, A., Walsh, S., Warren, T., Whitehead, S., Woodward, J.,

Volckaert, G., Aert, R., Robben, J., Grymonprez, B., Weltjens, I., Vanstreels, E., Rieger, M., Schafer, M., Muller-Auer, S., Gabel, C., Fuchs, M., Dusterhoft, A., Fritzc, C., Holzer, E., Moestl, D., Hilbert, H., Borzym, K., Langer, I., Beck, A., Lehrach, H., Reinhardt, R., Pohl, T. M., Eger, P., Zimmermann, W., Wedler, H., Wambutt, R., Purnelle, B., Goffeau, A., Cadieu, E., Dreano, S., Gloux, S., Lelaure, V., Mottier, S., Galibert, F., Aves, S. J., Xiang, Z., Hunt, C., Moore, K., Hurst, S. M., Lucas, M., Rochet, M., Gaillardin, C., Tallada, V. A., Garzon, A., Thode, G., Daga, R. R., Cruzado, L., Jimenez, J., Sanchez, M., del Rey, F., Benito, J., Dominguez, A., Revuelta, J. L., Moreno, S., Armstrong, J., Forsburg, S. L., Cerutti, L., Lowe, T., McCombie, W. R., Paulsen, I., Potashkin, J., Shpakovski, G. V., Ussery, D., Barrell, B. G. & Nurse, P. (2002). The genome sequence of Schizosaccharomyces pombe. *Nature* **415**, 871-880.

Woodbury, E. L. & Morgan, D. O. (2007). Cdk and APC activities limit the spindle-stabilizing function of Fin1 to anaphase. *Nat Cell Biol* **9**, 106-112.

Wu, J. Q., Kuhn, J. R., Kovar, D. R. & Pollard, T. D. (2003). Spatial and temporal pathway for assembly and constriction of the contractile ring in fission yeast cytokinesis. *Dev Cell* **5**, 723-734.

Wu, J. Q., Sirotkin, V., Kovar, D. R., Lord, M., Beltzner, C. C., Kuhn, J. R. & Pollard, T. D. (2006). Assembly of the cytokinetic contractile ring from a broad band of nodes in fission yeast. *J Cell Biol* **174**, 391-402.

Yamada, H. Y., Matsumoto, S. & Matsumoto, T. (2000). High dosage expression of a zinc finger protein, Grt1, suppresses a mutant of fission yeast slp1(+), a homolog of CDC20/p55CDC/Fizzy. *J Cell Sci* **113** (Pt 22), 3989-3999.

Yamano, H., Gannon, J. & Hunt, T. (1996). The role of proteolysis in cell cycle progression in Schizosaccharomyces pombe. *Embo J* **15**, 5268-5279.

Yamano, H., Tsurumi, C., Gannon, J. & Hunt, T. (1998). The role of the destruction box and its neighbouring lysine residues in cyclin B for anaphase ubiquitin-dependent proteolysis in fission yeast: defining the D-box receptor. *Embo J* **17**, 5670-5678.

Yamashita, A., Sato, M., Fujita, A., Yamamoto, M. & Toda, T. (2005). The roles of fission yeast ase1 in mitotic cell division, meiotic nuclear oscillation, and cytokinesis checkpoint signaling. *Mol Biol Cell* **16**, 1378-1395.

Yanagida, M. (1987). Yeast tubulin genes. *Microbiol Sci* **4**, 115-118.

Yasuda, S., Oceguera-Yanez, F., Kato, T., Okamoto, M., Yonemura, S., Terada, Y., Ishizaki, T. & Narumiya, S. (2004). Cdc42 and mDia3 regulate microtubule attachment to kinetochores. *Nature* **428**, 767-771.

Yoshida, S., Ichihashi, R. & Toh-e, A. (2003). Ras recruits mitotic exit regulator Lte1 to the bud cortex in budding yeast. *J Cell Biol* **161**, 889-897.

Zhu, C., Bossy-Wetzel, E. & Jiang, W. (2005). Recruitment of MKLP1 to the spindle midzone/midbody by INCENP is essential for midbody formation and completion of cytokinesis in human cells. *Biochem J* **389**, 373-381.

Zimmerman, S., Daga, R. R. & Chang, F. (2004). Intra-nuclear microtubules and a mitotic spindle orientation checkpoint. *Nat Cell Biol* **6**, 1245-1246.

Zimmerman, S. & Chang, F. (2005). Effects of {gamma}-tubulin complex proteins on microtubule nucleation and catastrophe in fission yeast. *Mol Biol Cell* **16**, 2719-2733.

Appendix

Movie legends

Movie 3.1 Kinetochore and spindle pole body dynamics in a mitotic control cell

A cell expressing Ndc80-GFP (marking the kinetochores, red) and Cdc11-CFP (marking the spindle pole bodies, green). Images acquired every 30 seconds.

Movie 3.2 Kinetochore and spindle pole body dynamics in a mitotic *mto1D* cell

An *mto1D* cell expressing Ndc80-GFP (marking the kinetochores, red) and Cdc11-CFP (marking the spindle pole bodies, green). Images acquired every 30 seconds.

Movie 3.3 Retrieval of unclustered kinetochores in an *mto1D* cell

An *mto1D* cell expressing Ndc80-GFP (marking the kinetochores, red) and Cdc11-CFP (marking the spindle pole bodies, green). Images acquired every 30 seconds.

Movie 5.1 Pre-anaphase spindle collapse in a control cell in the presence of Lat A

A cell expressing Ndc80-GFP (marking the kinetochores, red) and Cdc11-CFP (marking the spindle pole bodies, green) in the presence of 1.25μM Lat A. Images acquired every 30 seconds.

Movie 6.1 Mitotic localisation of Ase1

A cell expressing Ase1-GFP (green) and Cdc11-CFP (spindle pole bodies, red). Images acquired every minute.

Movie 6.2 Kinetochore and spindle pole body dynamics in a mitotic *ase1D* cell

An *ase1D* cell expressing Ndc80-GFP (marking the kinetochores, red) and Cdc11-CFP (marking the spindle pole bodies, green). Images acquired every 30 seconds.

Movie 6.3 Mitotic spindle fates in *ase1D* cells are independent of light exposure

Three *ase1D* cells expressing Ndc80-GFP (marking the kinetochores, red) and Cdc11-CFP (marking the spindle pole bodies, green) labelled (a), (b) and (c). Images acquired every 30 seconds.

Movie 7.1 Mitotic localisation of Klp9

A cell expressing Klp9-GFP. Images acquired every 30 seconds.